The University Of Sheffield

Daniel Leocadio-Victoria

Post-Translational Modification And Nuclear Targeting Of Beta-Dystroglycan

Thesis submitted in partial fulfilment of
the requirements for the degree of
Doctor of Philosophy

2015

Post-Translational Modification And Nuclear Targeting Of Beta-Dystroglycan

Daniel Leocadio-Victoria

Thesis submitted in partial fulfilment of
the requirements for the degree of
Doctor of Philosophy

Department of Biomedical Science
The University of Sheffield
Sheffield, UK.

June, 2015

To my parents, my brothers and my family with love!

Acknowledgements

I would like to express my sincere thanks to Professor Steve J. Winder for his invaluable support and mentorship since much time before starting this adventure. I am indeed grateful for all the advice, encouragement, patience and enthusiasm he has always provided throughout my project.

Thanks to professor Kathryn R. Ayscough, for her critical advice all along my PhD studies.

To past and present members of the Winder and Ayscough labs: Grinu Mathew, Chris Moore, Robert Piggot, Bernardo Chapa, Oliver Thompson, Leanne Lipscomb, Adam Smith, Andrew Mitchel, Gaynor Miller, Laura Jacobs, Sarah Palmer, Agnieszka Urbanek, Chris Marklew, Iwona Smaczynska-de Rooi, Emma Hoffman, Tracy Emmerson, Kate Collins, Joe Tyler, Katja Vogt, Ellen Allwood, Wesley Booth, Lemya Abugharsa and Laila Moushtaq, you made my time in the U.K. so enjoyable, thanks a lot.

Also, I would like to extend my gratitude to Professor Carl Smythe and Dr. Penny Rashbass for their invaluable advice during my PhD project. Thanks to Dr. Mark Collins and Dr. Richard Beniston for their technical support and advice during the mass-spectrometry analysis.

Thanks a lot to people within the BMS department who were always there providing me with technical advice and material whenever required.

I am grateful to Consejo Nacional de Ciencia y Tecnología (CONACYT) and Consejo Mexiquense de Ciencia y Tecnología (COMECYT) for awarding me the fellowship for my PhD studies.

To my friends who were always there cheering me up...thanks a lot!

To you all.. thank you very much, your support is indeed appreciated!

Abstract

Cellular communication and the link between the extracellular and intracellular environments are in part mediated by signalling events from plasma membrane proteins. Their tight regulation by a diverse array of post-translational modifications (PTM) is essential to maintain the cellular integrity. Understanding these modifications would help with understanding cancer cell progression.

Dystroglycan is one of the plasma membrane proteins with both structural and signalling properties, and is a core component of the dystrophin associated protein complex (DAPC). The nuclear localisation of dystroglycan and some DAPC members suggests similar roles to those observed in the plasma membrane. Dystroglycan is composed of an alpha and beta subunits that are modified by different PTM. The altered glycosylation of alpha and the phosphorylation of Y890 in beta, are triggering factors for the instability of dystroglycan leading to the disruption of the DAP complex. In cancer studies, it has recently been indicated that in addition to the above-mentioned PTM, other signalling events such as additional phosphorylation sites and ubiquitination, could mediate the rapid turnover of dystroglycan from the plasma membrane and from the nucleus.

Here we show that beta-dystroglycan is susceptible to additional phosphorylation, and we were able to demonstrate its multiple ubiquitination. Further experiments revealed that beta-dystroglycan is subject to intramembrane pro-

teolytic events induced by increased cellular density and PDBu treatment. Interestingly, we observed the translocation of beta- dystroglycan to the nucleus due to high cell density growth. By enzymatic inhibition studies we were able to identify gamma-secretase and furin as the enzymes responsible for the shedding of beta-dystroglycan from both the plasma membrane and nuclear envelope. Interestingly, we observed the preferential nuclear translocation and degradation by the proteasome of the cytoplasmic fragment of beta-dystroglycan. An interactome analysis by mass spectrometry techniques revealed that beta-dystroglycan interacts with components of the ubiquitin-proteasome system, the cell-cycle, and the nucleus.

This all together suggests that, the regulated intramembrane proteolysis mediated by ubiquitination and phosphorylation PTM of beta-dystroglycan triggers downstream nuclear signalling events. These findings provide more ideas of the mechanisms implicated in the regulation of beta-dystroglycan and importantly, of some nuclear processes wherein beta-dystroglycan is involved. These insights may have further implications in the understanding of the progression of cancer and the development of useful therapies.

Contents

List of Figures

List of Tables

Abbreviations

ACN ..... Acetonitrile

AR ..... Androgen Receptor

CD ..... Cytoplasmic domain of beta-dystroglycan

CIP ..... Calf Intestinal Phosphatase

DAPC ..... Dystrophin Associated Protein Complex

DMD ..... Duchenne Muscular Dystrophy

EMT ..... Epithelial-Mesenchymal Transition

EpCAM ..... Epithelial Cell Adhesion Molecule

ERAD ..... Endoplasmic Reticulum Associated Degradation

ERK ..... Extracellular-signal-Regulated Kinase

ERM ..... Ezrin, Radixin, Moesin proteins

ETV1 ..... ETS Translocation Variant 1

Full ..... Full-length beta-dystroglycan

GAPDH ..... Glyceraldehyde 3-phosphate deshydrogenase

Grb2 ..... Growth Factor Receptor-bound Protein 2

HDG ..... Slow migrating species of dystroglycan

HECT ..... Homologous to the E6-AP Carboxyl Terminus

HpDG ..... Slow migrating species of phosphorylated dystroglycan

HuDG ..... Slow migrating species of ubiquitinated dystroglycan

HUWE1 ..... E3 ubiquitin-protein ligase HUWE1

INM ..... Inner Nuclear Membrane

KASH ..... Klarsicht, ANC-1, Syne homology

LARGE ..... Like-acetylglucosaminyltransferase

LDG ..... Fast migrating species of dystroglycan

LEF ..... Lymphoid Enhancer-binding Factor 1

LINC ..... Linker of Nucleoskeleton and Cytoskeleton

MCM ..... Mini-chromosome maintenance complex

MET ..... Mesenchymal-Epithelial Transition

MMP ..... Matrix Metalloproteinase

NEED4L ..... E3 ubiquitin-protein ligase NEDD4-like

NEM ..... N-Ethylmaleimide

NES ..... Nuclear Export Signal

NLS ..... Nuclear Localization Signal

nNOS ..... neuronal Nitric Oxide Synthase

NPC ..... Nuclear Pore Complex

ONM ..... Outer Nuclear Membrane

PDZ ..... Post synaptic density protein (PSD95), Drosophila disc large tumour suppressor (Dlg1), and zona occludens-1 (ZO-1) domain

PEST ..... Proline (P), glutamic aspartic (E), Serine (S), and Threonine (T) motif

PI3K Phosphatidylinositol-3-kinase

PKC ..... Protein Kinase C

PNGaseF ..... Peptide-N-Glycosidase F

PSA ..... Prostate Specific Antigen

PSMA ..... Prostate-Specific Membrane Antigen

PTEN ..... Phosphatase and TENsin homologue

PTM ..... Post-translational modification

RIP ..... Regulated Intramembrane Proteolysis

SH2 ..... Src-Homology 2 domain

SMC ..... Structural Maintenance of Chromosome

SUN ..... Sad and UNC-84

TCF ..... Transcription Factor 1

TGFβ ..... Tumour Growth Factor β

TM ..... Transmembrane domain

TP53 ..... Tumour Promoter 53

WW ..... WWP repeating motif

1 Generalities

1.1 Introduction

Humans are able to develop their daily activities thanks to the concerted functions of their organs and systems. Within each organ, the activity performed by every single cell is pivotal for maintaining a healthy status in the human body, the so called, homeostasis. Furthermore, cellular integrity is dictated by the correct synthesis, processing and interaction of its bio-molecules into a complex network of signalling pathways in space and time. Although cells are provided with specialized mechanisms to cope with possible alterations of these pathways, sometimes these alterations are not detected by cells, leading to detrimental effects which result in serious outcomes such as cancer.

1.2 Cancer

Normal cells are able to perform different activities throughout their lifespan, but are always restricted by certain biological boundaries. Generally, normal cells are able to reproduce themselves at the right place and time and, once their normal activities are culminated, they programme their own death. Healthy cells are also coordinated by other cells and stop growing once they touch another cell.

Cancer cells, on the other hand, do not exhibit the same characteristics as

those present in normal cells. The main definition of cancer is the uncontrolled growth of the cells, and this growth leads to the formation of tumours. The increase in the tumour size can have different consequences: the deprivation of nutrients to normal adjacent cells, the invasion and alteration of normal functions of adjacent or distant tissues (metastasis), or the damage of adjacent tissues by interfering in their physical space. Cancers are named according to the source where the original deregulated cell comes from and therefore, there are as many cancers as cells type in the human body. Cancers are complex diseases, as multiple factors can contribute to their development including a person's environment and genetic background. These factors are usually strong enough to damage critical biomolecules, such as DNA, which in turn disrupts the normal functions of the cells ((Blanpain, 2013; Boland, 2003; Merlo, Pepper, Reid, & Maley, 2006) and `http://www.cancer.gov`, `http://www.cancerresearchuk.org`, `http://www.who.int/cancer/en/`).

Cancer cells have inherent features that distinguish them from normal cells, termed "hallmarks". Hanahan and Weinberg classified these "hallmarks" into 6 groups, plus two "emerging hallmarks". The "hallmarks" of cancer are: sustained proliferative signalling, evasion of growth suppressors, resisting cell death, replicative immortality, induction of angiogenesis, and activation of invasion and metastasis. Deregulating cellular energetics and avoiding immune destruction account for the emerging hallmarks, and genome instability and mutation, as well as tumour-promoting inflammation are enabling characteristics of cancer (Hanahan & Weinberg, 2011; Lazebnik, 2010). The acquisition of these characteristics may be a gradual process, involving multiple steps. However, in the end, all these characteristics may be present within malignant cells (Hainaut & Plymoth, 2013).

The growth of normal cells is restricted by their own and extracellular signals. In the case of **growth signals**, cancer cells may develop two mechanisms to sustain proliferation, one dependent and one independent of growth factors, in addition to the disruption of factors that control the cell cycle. In malignant cells the production of growth factors may act in an autocrine or paracrine way

to stimulate themselves or to stimulate neighbouring cells, or increase the concentration of growth factor receptors present at the cell membrane. Alterations to the DNA, which lead to the constant activation of growth receptors and the disruption of the mechanisms that decrease the signals of proliferation, account for the mechanisms involved in sustaining proliferative signalling through the growth factor independent mechanism (Hanahan & Weinberg, 2011).

Once cancerous cells have gained the ability to sustain proliferation, they have to develop mechanisms in order to **avoid growth suppressors**. Although there are many, retinoblastoma associated (RB) and TP53 are the two canonical tumour suppressors. In cancer cells, as the RB and TP53 functions are damaged, the cells are able to have a continued cell proliferation and to escape apoptosis respectively. Additionally, cells are able to evade contact inhibition of growth and the antiproliferative effects of tumour growth factor β (TGFβ) (Hanahan & Weinberg, 2011).

Apoptosis (programmed cell death) is one of the main characteristics that differentiate normal cells from cancerous counterparts. In the case of malignant cells, they develop mechanisms to bypass apoptotic events mediated by TP53. Also, they are able to up-regulate or down-regulate the expression of antiapoptotic or proapoptotic agents respectively. Autophagy and necrosis are two mechanisms that can be advantageous to cancer cells. Autophagy can provide metabolites to the fast growing cells, which require of a large amount of nutrients, and necrosis, by releasing the cellular components to the exterior, can have proinflammatory and tumour-promoting potentials (Fernald & Kurokawa, 2013; Hanahan & Weinberg, 2011).

Whilst a normal cell is destined to programmed cell death upon completion of its functions, a malignant cell has the potential of **replicative immortality**. This mechanism is sustained mainly by taking control of the enzyme telomerase and up-regulating its functions. In this way, telomerases maintain elongated telomeres, which in turn allow the cells to avoid senescence and escape apoptosis (Hanahan & Weinberg, 2011).

The formation of new tumours requires a sustained supply of nutrients and

also a way to dispose of metabolic waste. This is achieved by the formation of **new vessels (vasculogenesis) and the branching of the pre-existing ones (sprouting)**, which remain active as the tumour grows and develops. Additionally, pericytes and bone marrow-derived cells are important players in tumour angiogenesis (Hanahan & Weinberg, 2011).

The progression of tumours into more malignant stages is in part achieved by **regional invasion and distant metastasis**. The characteristic step into this hallmark is the loss of cell-cell and cell-extracellular matrix contacts. Upon the downregulation of cell adhesion proteins, among them E-cadherin, cancerous cells are able to change their morphology and adhesive properties. This series of events in turn leads to the up-regulation of adhesion proteins involved in cell migration. The "invasion-metastasis cascade" is a gradual event characterised by regional invasion, intravasation into local blood and lymphatic vessels, travelling through the lymphatic-haematic stream, exiting of cancerous cells from vessels into new sites under colonisation (extravasation), formation of micrometastasis and the colonisation of a new environment (growth of the new tumour).

This cascade is regulated by a process called epithelial-mesenchymal transition (EMT). This mechanism is characterised by the loss of cell adhesions at the adherens junctions with a consequent change in cellular morphology, synthesis of enzymes in charge of degrading extracellular matrix, gain of mobility, and the ability to evade apoptosis. EMT is commonly supported by neighbour cells, such as macrophages, which are in charge of secreting enzymes to help in the remodelling of the extracellular matrix. Once malignant cells have colonised a new site, they can change their morphology to an epithelial-like shape through a process called mesenchymal-epithelial transition (MET). Following this, malignant cells will be required to adapt to the new environmental conditions, "or colonization" (Bogenrieder & Herlyn, 2003; Hanahan & Weinberg, 2011; Lu, Weaver, & Werb, 2012; Yilmaz, Christofori, & Lehembre, 2007).

Additional hallmarks include the alteration of the energetic balance in or-

der to support the continuing growth of the tumour, and escape of immune system destruction, characteristics facilitated by two main mechanisms: the alteration to the DNA (genomic instability) and tissue inflammation (Hanahan & Weinberg, 2011).

1.3 Prostate cancer

The prostate is a small gland, part of the men's reproductive system that helps in the production of semen (`http://www.cancer.org/index`). Prostate cancer is a very heterogeneous and complex disease, and is the second most common malignancy in men. During the year 2012, approximately 1.1 million male patients were diagnosed with prostate cancer around the world, which represented 15% of all the cancers affecting men. In the same year, the 307,000 deaths attributed to prostate cancer, represented the 5th main cause of death from cancer in men (`http://globocan.iarc.fr/Default.aspx`). According to Cancer Research UK, older men have a higher probability of being diagnosed with prostate cancer, with a median age of diagnosis above 70 years (`http://www.cancerresearchuk.org`).

Prostate cancer tumours have particular characteristics. Prostate cancer cells can be divided into two main groups, androgen dependent and androgen independent, based on their capacity to respond to 5α-dihydrotestosterone. Prostate tumours have a predilection to form metastases to skeletal bone, lymph nodes, lung and liver. Prostate cancer cells express the antigen markers prostate specific antigen (PSA) and prostate-specific membrane antigen (PSMA). Additionally, the interaction of the tumour with its microenvironment seems to be of particular importance for the colonisation of new metastatic sites (Morrissey & Vessella, 2007; Russell & Kingsley, 2003).

Hormone therapy, radical prostatectomy and radiation therapy are the first choice therapies in prostate cancer. However, recurrence and resistance towards hormone treatment, or invasion and metastasis are the main factors

associated with the advanced stages of prostate cancer, and these factors usually subvert the previous therapies resulting in death (Balk & Knudsen, 2008; Collins & Maitland, 2006; Morrissey & Vessella, 2007).

An understanding of the molecular mechanisms associated with the origin, development and progression of prostate cancer is therefore required in order to develop efficient therapies. The best way to explore the mechanisms associated with prostate cancer progression is by using models that represent the human body in order to mimic the same processes in prostate cancer progression. Animal models represent a good option, however, the ethical issues and the cost of their handling make them difficult models in the study of prostate cancer and in the design of therapies (Sobel & Sadar, 2005).

Cell culture models have been developed to surpass this problem. The best representative models of prostate cancer are the DU145, PC3 and LNCaP cell lines. DU145 cells were derived from a central nervous system metastasis, are not androgen responsive, do not express PSA and androgen receptor (AR) and have a mutated p53. PC3 cells, were derived from a lumbar metastasis, have a deletion in p53 and similar to DU145, are not androgen sensitive and do not express PSA and AR (Russell & Kingsley, 2003; Sobel & Sadar, 2005).

LNCaP cells are a cell line that is androgen sensitive, expresses acid phosphatase, PSA and AR and have a silent mutation in p53. This metastatic cell line was derived from a supraclavicular lymph node from a Caucasian 50-year-old male patient with prostatic adenocarcinoma and was first isolated by Horoszewicz and colleagues (Horoszewicz et al., 1983; Russell & Kingsley, 2003; Sobel & Sadar, 2005).

Additional characteristics of this cell line include: an *in vitro* doubling time of approximately 60 hours, an ability to develop tumours in athymic nude mice, an ability to undergo functional differentiation, loose attachment to a substrate unless poly-L-lysine is used, and once they reach high densities, they detach forming clumps (Horoszewicz et al., 1983; Russell & Kingsley, 2003; Sobel & Sadar, 2005).

The invasive potential of these cells suggests that some proteins involved in

attaching them to the cell surface in order to restrict their uncontrolled growth may be damaged. Integrins are good candidates, however, components of the dystrophin associated protein complex (DAPC) also play an important role as "potential tumours suppressors" (Lu et al., 2012; Sgambato & Brancaccio, 2005).

1.4 The dystrophin associated protein complex

The dystrophin associated protein complex (DAPC) is a group of proteins associated with dystrophin (Ervasti, Ohlendieck, Kahl, Gaver, & Campbell, 1990; Ervasti & Campbell, 1991). DAPC components can be divided into extracellular, transmembrane and cytoplasmic proteins. The main components are: dystrophin/utrophin, dystroglycan, sarcoglycans, sarcospan, syntrophins, dystrobrevin, syncoilin, nNOS (Figure 1.1) (Allikian & McNally, 2007; Constantin, 2014; Ehmsen, Poon, & Davies, 2002).

In striated muscle the DAPC confers protection to the sarcolemma during muscle contraction and relaxation, and serves as a physical connection between the cytokeleton and the extracellular matrix (Petrof, Shrager, Stedman, Kelly, & Sweeney, 1993), the lack of which leads to necrosis of the muscle fibres (Ibraghimov-Beskrovnaya et al., 1992), a triggering molecular factor in the pathogenesis of muscular dystrophy (Ervasti et al., 1990). Some of the proteins within the DAPC have signalling properties and for this reason it is believed that the DAPC also plays a role in signalling events. Importantly, some proteins can harbour motifs such as SH2, SH3, WW, PDZ binding targets, which are implicated in protein-protein interactions, conferring the DAPC with scaffolding properties (Constantin, 2014). Each component within the DAPC has critical roles, as the alteration of any of these can lead to varying and severe outcomes: some resulting in embryonic lethality, others, in muscular dystrophy-like phenotypes (Ehmsen et al., 2002; Whitmore & Morgan, 2014).

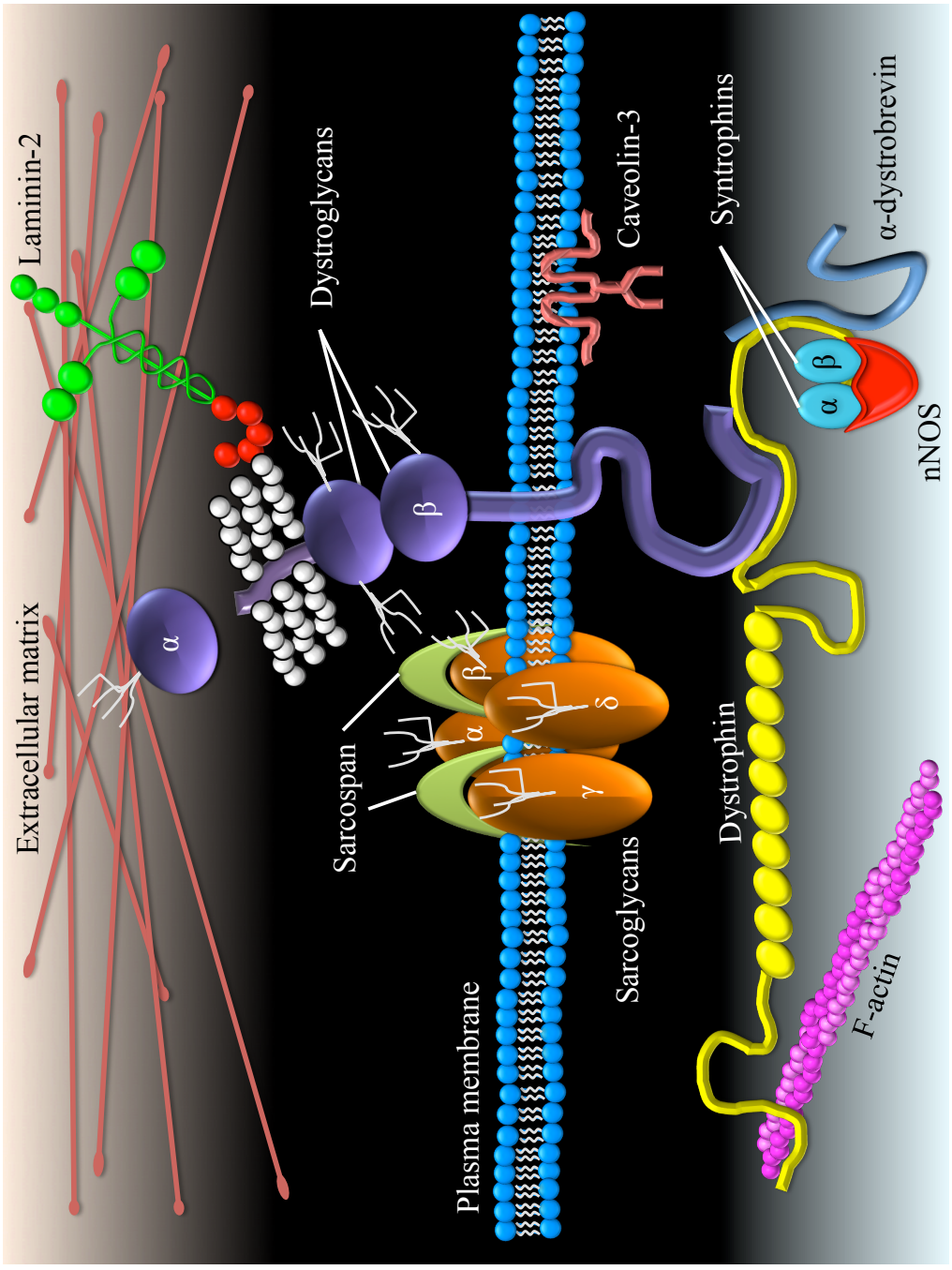

Figure 1.1: The dystrophin associated protein complex (DAPC). The DAPC is composed of extracellular (alpha-dystroglycan), transmembrane (sarcoglycans, sarcospan and beta-dystroglycan), and intracellular proteins (dystrophin, dystrobrevin, caveolin-3, syntrophins and nNOS). Laminin G-like (LG) domains in laminin are shown in red. Components are not drawn to scale and the relative localisation of each component in the schematic is simply to represent the central components of the DAPC.

1.5 Dystroglycan

1.5.1 Biosynthesis and structure of dystroglycan

Although later confirmed to be the same proteins (Smalheiser & Kim, 1995), dystroglycan was originally termed cranin (Smalheiser & Schwartz, 1987), and was first isolated from neural cells, and described as a 120 kDa glycoprotein with laminin binding properties (Douville, Harvey, & Carbonetto, 1988; Smalheiser & Schwartz, 1987; Gee et al., 1993).

Human dystroglycan (dystrophin associated glycoprotein) is encoded by the DAG1 gene, and was mapped to band 21 of the short arms of chromosome 3 (locus 3p21.1-21.31) by using skeletal muscle cDNA. The DAG1 gene has two exons separated by an intronic region (Ibraghimov-Beskrovnaya et al., 1993). In mice, Dag1 is located on chromosome 9 (Górecki, Derry, & Barnard, 1994). Pre-mRNA splicing of human DAG1 generates a transcript with the coding sequence for an immature protein of 895 amino acids. The 97 kDa translated immature protein is further cleaved after amino acid 653 (Holt, Crosbie, Venzke, & Campbell, 2000), to generate the 56 kDa core alpha- and 43 kDa beta-subunits of dystroglycan. Although these subunits remain together on the plasma membrane, they are not covalently attached. The primary structure of mature dystroglycan, commencing on the extreme N-terminus, can be divided in to three main sequences: 1) a hydrophobic fragment corresponding to a signal peptide; 2) alpha-dystroglycan, which harbours many amino acids prone to post-translational modifications (PTM) such as N- and O-glycosylation; and 3) beta-dystroglycan, which has a potential residue that can be subject to N-glycosylation, a transmembrane domain and a cytoplasmic fragment rich in proline residues (Ibraghimov-Beskrovnaya et al., 1992) (Figure 1.2).

Depending on the tissue, mature alpha-dystroglycan is glycosylated to differing extents, leading to a variation in its size from approximately 120 kDa to near 160 kDa (Ibraghimov-Beskrovnaya et al., 1992). Its structure consists of N- and C-terminal globular domains separated by a central rod or mucin-like domain (Brancaccio, Schulthess, Gesemann, & Engel, 1995, 1997). In com-

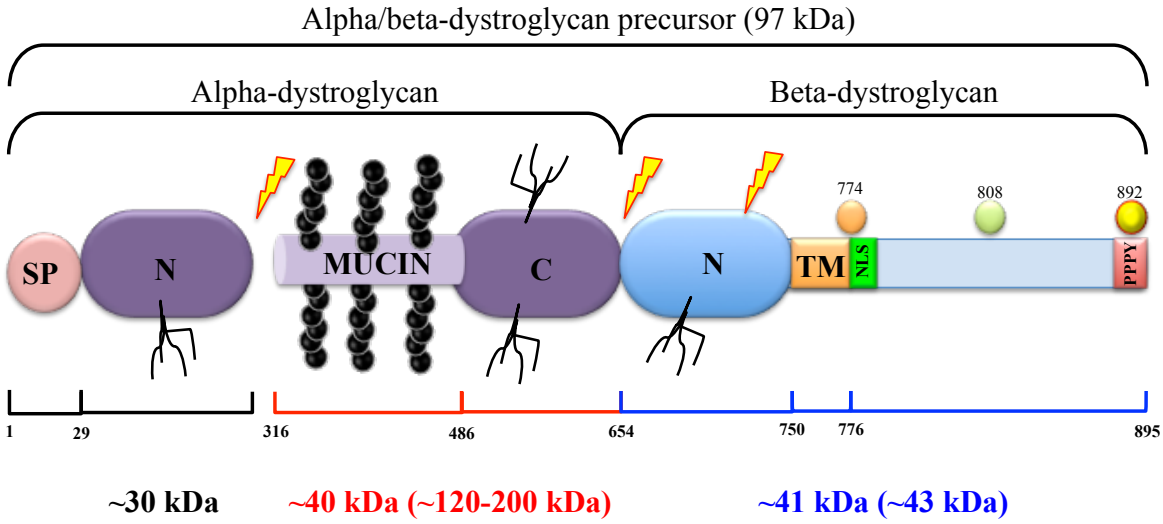

(a)

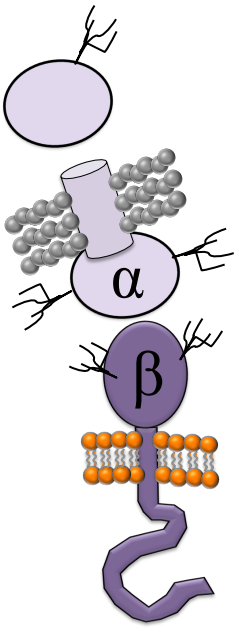

(b)

Figure 1.2: Biosynthesis of dystroglycan. (a) The schematic shows the structural organization of human dystroglycan. Alpha-dystroglycan harbours many potential sites for N-glycosylation (branches) and O-glycosylation (black circles), beta-dystroglycan on the other hand is glycosylated to a lesser extent. The transmembrane domain (TM), nuclear localisation signal (NLS) and the PPXY motif are shown. Lightnings represent the approximate location of the proteolytic cleavages by furin, autolysis and MMP. The known sites for palmitoylation, ubiquitination and phosphorylation are shown in orange, green and yellow circles respectively. Numbers in parentheses represent the molecular weight of mature proteins. (b) The mature protein is embedded in the plasma membrane with alpha-dystroglycan facing the extracellular environment.

parison, beta-dystroglycan has an unfolded N-terminal domain, followed by a transmembrane fragment and a highly disordered C-terminal cytoplasmic domain (Akhavan, Crivelli, Singh, Lingappa, & Muschler, 2008; Boffi et al., 2001; Di Stasio et al., 1999) (Figure 1.2a).

Human dystroglycan functions may be diverse as it is highly expressed in skeletal and heart tissues, and to a lesser extent in brain, placenta, lung, liver, kidney, pancreas tissues (Ibraghimov-Beskrovnaya et al., 1993).

Dystroglycan has a high degree of homology and is expressed amongst different species including human (Ibraghimov-Beskrovnaya et al., 1993), mouse (Górecki et al., 1994), rabbit (Ibraghimov-Beskrovnaya et al., 1993, 1992), zebrafish (Parsons, Campos, Hirst, & Stemple, 2002), *Drosophila* (Deng et al., 2003), dog (Leeb, Neumann, Deppe, Breen, & Brenig, 2000) and *C. elegans* (Grisoni, Martin, Gieseler, Mariol, & Ségalat, 2002).

1.5.2 Dystroglycan, multiple signalling and protein-protein interactions

Dystroglycan is on first inspection a passive protein whose function is to serve as a bridge between the basal lamina and the dynamic cytoskeleton. However, there are some internal characteristics within the structure of dystroglycan that enable it to change from a static to a very dynamic status.

In the extracellular environment, alpha-dystroglycan is highly glycosylated. This property allows its interaction with members of the extracellular matrix such as laminin, agrin, neurexin, perlecan and pikachurin via LG domains (Montanaro, Lindenbaum, & Carbonetto, 1999; Winder, 2001). The disruption of this interaction, due to hypo-glycosylation, can lead to deleterious effects such as muscular dystrophies.

Alpha-dystroglycan is also a receptor for *Mycobacterium leprae* (Rambukkana et al., 1998) and Lassa fever and lymphocytic choromeningitis viruses (Cao et al., 1998). Again, glycan groups on its surface are important for its interac-

tion with the viruses (Kunz et al., 2005) (Figure 1.3). Importantly, a recent hypothesis states that low levels of glycosylation on alpha-dystroglycan and the proteolysis of beta-dystroglycan by MMPs could be a protective mechanism against pathogenic infection (Emery, 2008; Sciandra et al., 2003). In this regard, it should not be forgotten that alpha-dystroglycan is susceptible to a proteolytic cleavage by furin (Singh et al., 2004). Then, it may be that all these mechanisms, which affect the stability of dystroglycan, modulate the susceptibility of cells to bacterial and viral infection. Furthermore, invasive processes not only involve an interaction between dystroglycan and the pathogen, but also downstream signalling events. Moraz and colleagues demonstrated that the internalisation of Lassa virus triggered the phosphorylation of tyrosine residues on beta-dystroglycan (other than Y892) and the disruption of the interaction between dystroglycan and utrophin (Moraz et al., 2013).

From these examples, it is clear that the alteration of alpha-dystroglycan can have consequences involving the beta subunit and other intracellular proteins. Importantly, the same mechanism seems to be applicable to other situations, for example, in cancer.

Beta-dystroglycan is also a very enigmatic protein. This protein is particularly promiscuous because it has been found interacting with different proteins within different complexes. Additionally it is subject to a wide range of post-translational modifications: it can be phosphorylated (Sotgia et al., 2001), ubiquitinated (K. A. Lee et al., 2011), glycosylated (Ibraghimov-Beskrovnaya et al., 1992), sumoylated (Steve J. Winder, personal communication), palmitoylated (Kang et al., 2008) and proteolytically cleaved (Yamada et al., 2001). The cytoplasmic region has different motifs such as SH2, SH3 and WW (Figure 1.5). Furthermore, its localisation in compartments other than the plasma membrane such as the nucleus and its expression in different cell types and species, confer additional properties on beta-dystroglycan beyond those already known in skeletal muscle (Figure 1.4).

The extracellular domain of beta-dystroglycan mediates the interaction with its partner alpha. This domain is also important because it is the site

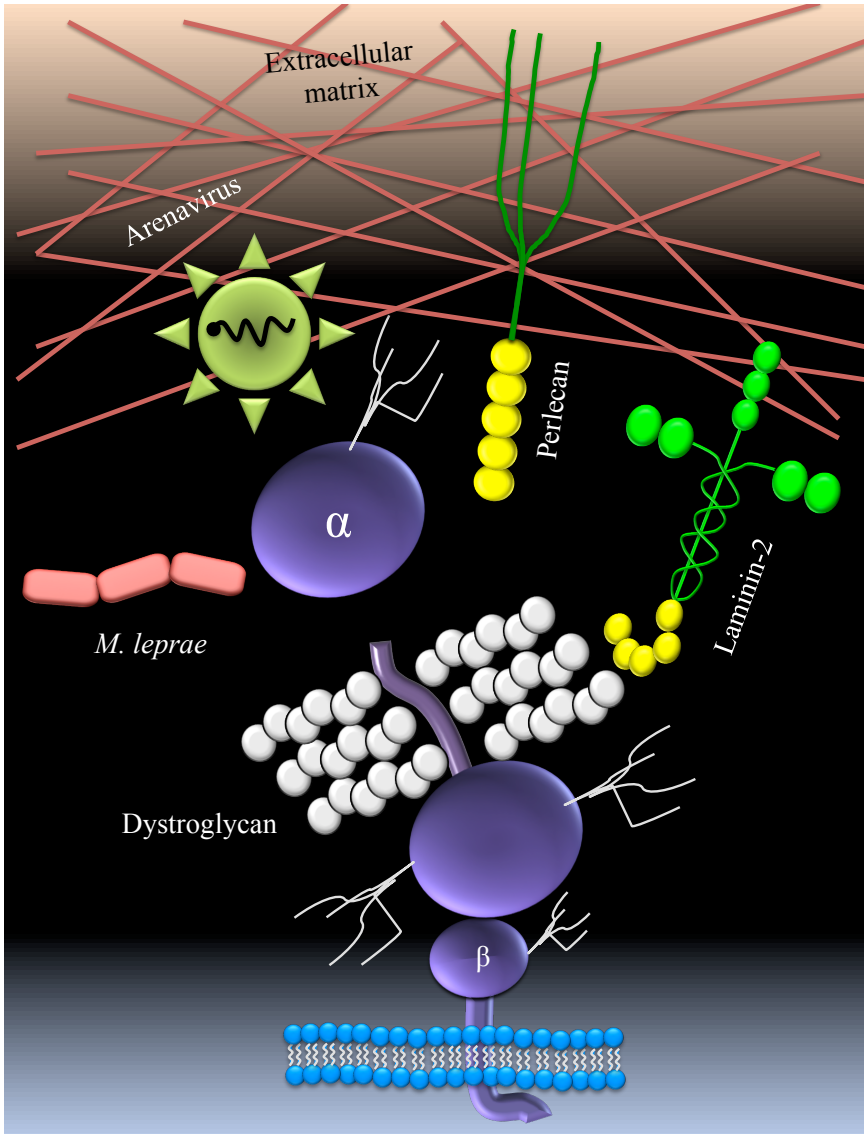

Figure 1.3: Alpha-dystroglycan binding partners. Alpha-dystroglycan is an extracellular protein that interacts with components of the extracellular matrix (laminin-2, agrin, neurexin, perlecan and pikachurin). It is also an important receptor for mycobacterias and arenaviruses. Alpha-dystroglycan binds through its carboxy terminus to the N-terminal side of beta-dystroglycan. Laminin G-like (LG) domains in laminin are shown in yellow.

where MMP-2 and -9 perform a proteolytic cleavage resulting in the generation of a 31 kDa transmembrane anchored fragment (Yamada et al., 2001).

The transmembrane domain, which could seem to be immune to any modifications, has been suggested as the site where gamma-secretase could further cleave the 31 kDa fragment of beta-dystroglycan to generate another, smaller, 26 kDa fragment presumably in a regulated intramembrane proteolysis (RIP)

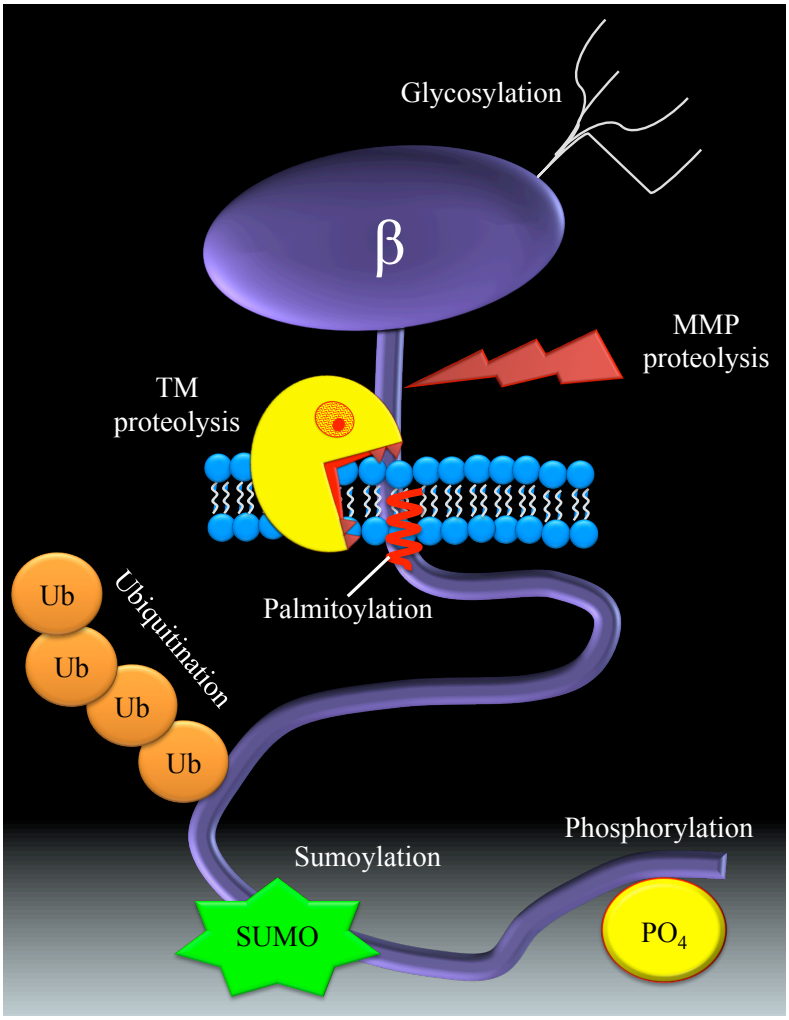

Figure 1.4: Beta-dystroglycan is subject to different PTM. Beta-dystroglycan is glycosylated and cleaved by MMPs on its extracellular domain. In the TM region, it is further cleaved and subject to palmitoylation. The cytoplasmic fragment on the other hand is modified by ubiquitination, sumoylation and phosphorylation.

manner (Hemming, Elias, Gygi, & Selkoe, 2008) (Figure 1.4).

The plasma membrane contains proteins with different topologies that depending on their orientation are classified into two main groups, type-I and type-II proteins. Type-I proteins display their N-terminus towards the extracellular environment and their C-terminus faces the cytosol; type-II proteins, on the other hand, have an opposite orientation. The cleavage of these proteins for particular cellular purposes, such as turnover or signalling, is performed by a process termed RIP. This mechanism is achieved within the hydrophobic environment of the plasma membrane by three main families of proteases:

metalloproteases, aspartyl proteases and serine proteases. Within each family there are subgroups of proteases that have a specific affinity for type-I or type-II substrates. Type-I proteins are cleaved by gamma-secretase and rhomboid, whereas type-II proteins can be cleaved by S2P, SPP/SPPL and PARL (Kopan & Ilagan, 2004; Lemberg, 2011).

The proteolysis performed by gamma-secretase, a GXGD-type aspartyl protease, is usually initiated by the cleavage of proteins on their N-terminal extracellular domain by extracellular proteases (e.g. MMP), which renders truncated anchored plasma membrane proteins that are efficiently processed by gamma-secretase. Gamma-secretase refers to a group of integral plasma membrane proteins, and is composed of Nicastrin, presenilin, Aph-1 and Pen-2. The mechanism starts with the recognition of the truncated cleaved protein by Nicastrin. Following this, Aph-1 which functions as a central platform, brings together Nicastrin, presenilin and Pen-2. In the core of this complex, the proteolytic cleavage of the substrate is performed by presenilin. Given the fact that the substrates for gamma-secretase are very diverse, there is still not a consensus sequence where gamma-secretase exerts its proteolytic action. RIP mediated by gamma-secretase has many biological implications, such as in protein turnover and cellular signalling, the deregulation of which can lead to disease, such as cancer and neurological problems (Kopan & Ilagan, 2004; Lemberg, 2011; Selkoe & Wolfe, 2007; Steiner, Fluhrer, & Haass, 2008; Wakabayashi & De Strooper, 2008)

The primary sequence of the 26 kDa fragment of beta-dystroglycan is flanked by a cysteine residue in its amino-terminus (C774) (`http://www.ncbi.nlm.nih.gov/protein/Q14118.2`). A recent report, aimed to investigate palmitoylated proteins in neurons, identified C774 below the transmembrane domain as a potential site for palmitoylation (Kang et al., 2008). Palmitoyl modification is usually associated with the retention of proteins in the plasma membrane (Aicart-Ramos, Valero, & Rodriguez-Crespo, 2011). So far, no more investigations have been carried out to investigate the role of this PTM in beta-dystroglycan (Figure 1.4).

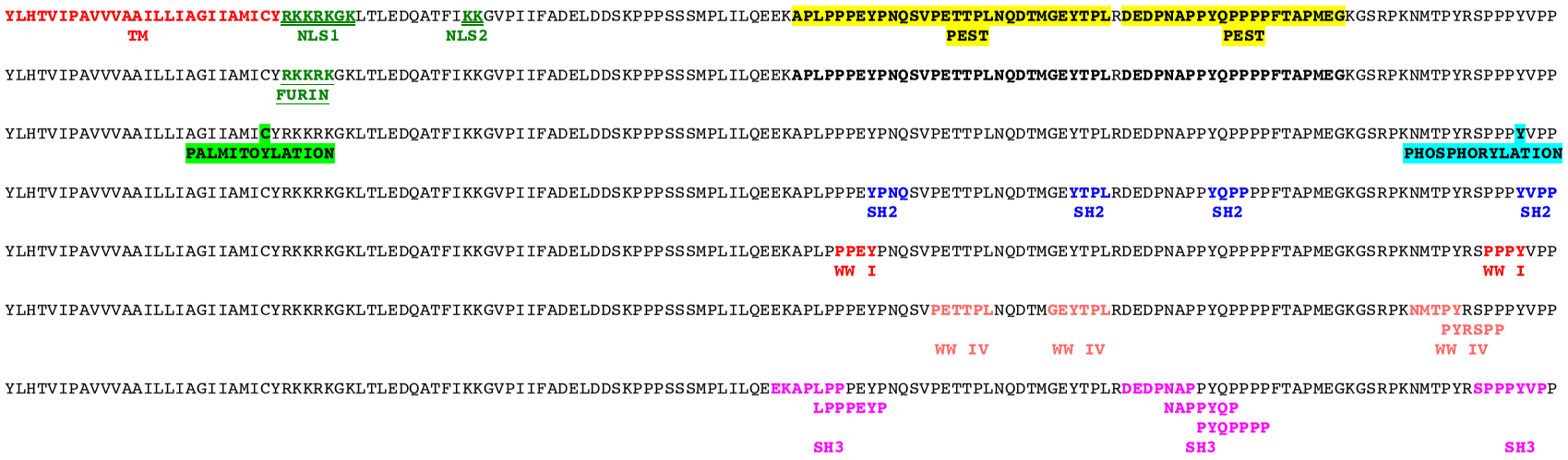

Figure 1.5: Structural organisation of the cytoplasmic region of beta-dystroglycan. The transmembrane domain (TM), nuclear localisation signal (NLS) and PEST motifs (Proline (P), glutamic aspartic (E), Serine (S), and Threonine (T) motif and Figure 6.1) are shown. Known residues subject to palmitoylation and phosphorylation are highlighted in green and turquoise. Interaction motifs for SH2, WWI, WWIV and SH3 domains are highlighted in blue, red, light red and magenta. Motifs were predicted using the ELM resource (`http://elm.eu.org`).

After the C774 residue, there is a stretch of basic amino acids with some known reported functions. Through this group of lysine and arginine residues, beta-dystroglycan interacts with the cytoskeletal protein ezrin, a member of the adaptor ERM (ezrin, radixin, moesin) group of proteins. The implications of this interaction were related to the formation of microvilli and fillopodia-like structures, due to the remodelling of the F-actin cytoskeleton (Spence, Chen, et al., 2004). Additionally, it was observed that the activity of Cdc42 was required for the targeting of beta-dystroglycan-ezrin in complex with Dbl to the plasma membrane, and the consequences were the same as the ones described above (Figures 1.5 and 1.6) (Batchelor et al., 2007).

This group of amino acids seems to be a kind of 'hot spot' within the sequence of beta-dystroglycan. In addition to the previous interactions, it was demonstrated that this domain functions as a nuclear localisation signal (NLS) as it was required for the nuclear translocation of beta-dystroglycan (Lara-Chacón et al., 2010; Oppizzi, Akhavan, Singh, Fata, & Muschler, 2008). Then, this domain seems to have dual functions, as it is important for the formation of beta-dystroglycan-ezrin complex, which in turn leads to the formation of cellular protrusions, and also, it is important for the nuclear translocation of this complex in an ezrin-dependent manner (Figures 1.5 and 1.6) (Vásquez-Limeta et al., 2014).

An additional function of this domain in neuromuscular junctions was demonstrated. It was observed that rapsyn functioned as a bridge between the acethylcholine receptor and beta-dystroglycan, and again, the stretch of basic amino acids in beta-dystroglycan was found mediating the interaction (Apel, Roberds, Campbell, & Merlie, 1995; Cartaud, Coutant, Petrucci, & Cartaud, 1998). This group of basic residues is also a point of convergence for the ERK MAPK-dystroglycan-integrin signalling pathways. The interaction between beta-dystroglycan and ERK is mediated by the same stretch of basic amino acids that function as an NLS. Interestingly, the sequestering of ERK and MAPK by beta-dystroglycan is performed in different compartments within the cell (Figure 1.6) (Bao et al., 2009; Ferletta et al., 2003; Moore &

Winder, 2010; Spence, Dhillon, James, & Winder, 2004).

The cytoplasmic region of beta-dystroglycan harbours other motifs that could potentially mediate interactions with other proteins. It contains sites for interactions with proteins containing PDZ, WW, SH2 and SH3 domains (`http://www.elm.eu.org`) (Moore & Winder, 2010) (Figure 1.5).

A tyrosine (Y892 in humans) within the PPXY motif located in the very carboxy terminus of beta-dystroglycan has gained special attention, because (depending on its phosphorylated status) this tyrosine can interact with WW or SH2 domains. An initial characterization showed that it is phosphorylated by Src and that, upon phosphorylation, it was able to interact with c-Src, Fyn, Csk, NCK and SHC SH2 domains (Sotgia et al., 2001). On the other hand, the phosphorylation of Y892 prevents the interaction between the carboxy terminus of beta-dystroglycan and the WW domain in utrophin (James et al., 2000) or dystrophin (Ilsley, Sudol, & Winder, 2001; Rentschler et al., 1999). Importantly, the disruption of this interaction by phosphorylated tyrosine was reported to render an unstable beta-dystroglycan, which is susceptible to proteasomal degradation However, when prevented, components of the DAPC were restored to the plasma membrane, and the dystrophic phenotype of the mdx mouse was improved (Miller et al., 2012). In a similar form as with dystrophin/utrophin, caveolin-3 has been shown to bind to the non-phosphorylated tyrosine within the PPXY motif; however, caveolin-3 competes with dystrophin for this interaction (Figure 1.6) (Ilsley, Sudol, & Winder, 2002; Sotgia et al., 2000).

Another motif, with the consensus sequence RXXXPXXP, is found in the very carboxy terminus of beta-dystroglycan and overlaps with the PPXY mentioned previously (Moore & Winder, 2010) (Figure 1.5). This motif in beta-dystroglycan was reported to be required for the interaction with the SH3 motif of the protein Grb2 (Cavaldesi et al., 1999; Russo et al., 2000; Yang et al., 1995). An additional interaction mediated by this motif is that between beta-dystroglycan and the third SH3 domain in vinexin in focal adhesions. Vinculin was also found in the focal adhesion complex, however, the associ-

ation with beta-dystroglycan was attributed to the interaction of vinculin to the first and second SH3 motifs in vinexin (Thompson et al., 2010). It was not conclusively demonstrated, but this motif may mediate the interaction of beta-dystroglycan to the SH3 domain in the adaptor protein TKS5, in complex with Src during the formation of podosomes (Figure 1.6) (Thompson et al., 2008).

In *Drosophila*, the WW-domain binding motifs in beta-dystroglycan have been suggested to have redundant functions towards their interaction to dystrophin (Yatsenko et al., 2009). However it has to be remembered that beta-dystroglycan not only binds dystrophin, but several other proteins. Therefore, whilst one WW-domain binding motif interacts with dystrophin, the other may mediate an interaction with another protein (Figure 1.5).

Dystroglycan may be subject to ubiquitination (it has not been defined if both subunits or only one subunit of dystroglycan is subject to ubiquitination), however, the limited evidence regarding this PTM is introduced here.

As explained in this chapter, in muscular dystrophies and cancer diseases, a reduction in the protein levels of beta-dystroglycan is frequently observed. Of the different hypotheses explaining this reduction, ubiquitination within the ubiquitin-proteasome system stands as the most plausible.

The evidence of a potential ubiquitination on dystroglycan comes from experiments performed with the proteasome inhibitor MG-132. The local and systemic treatment of mdx mice, a mouse model of Duchenne muscular dystrophy with MG-132 led to the restoration of components of the DAPC (alpha- and beta-dystroglycan and alpha-sarcoglycan) to the plasma membrane. Importantly, this restoration was able to improve the dystrophic phenotype of the mdx mice (Bonuccelli et al., 2003). A similar approach using muscle explants from patients with Becker and Duchenne muscular dystrophy showed comparable results (Assereto et al., 2006). By employing the FDA-approved drug velcade (also a proteasomal inhibitor), later experiments with the same objective demonstrated a restoration of the DAPC members to the plasma membrane, further confirming the involvement of the ubiquitin proteasome system

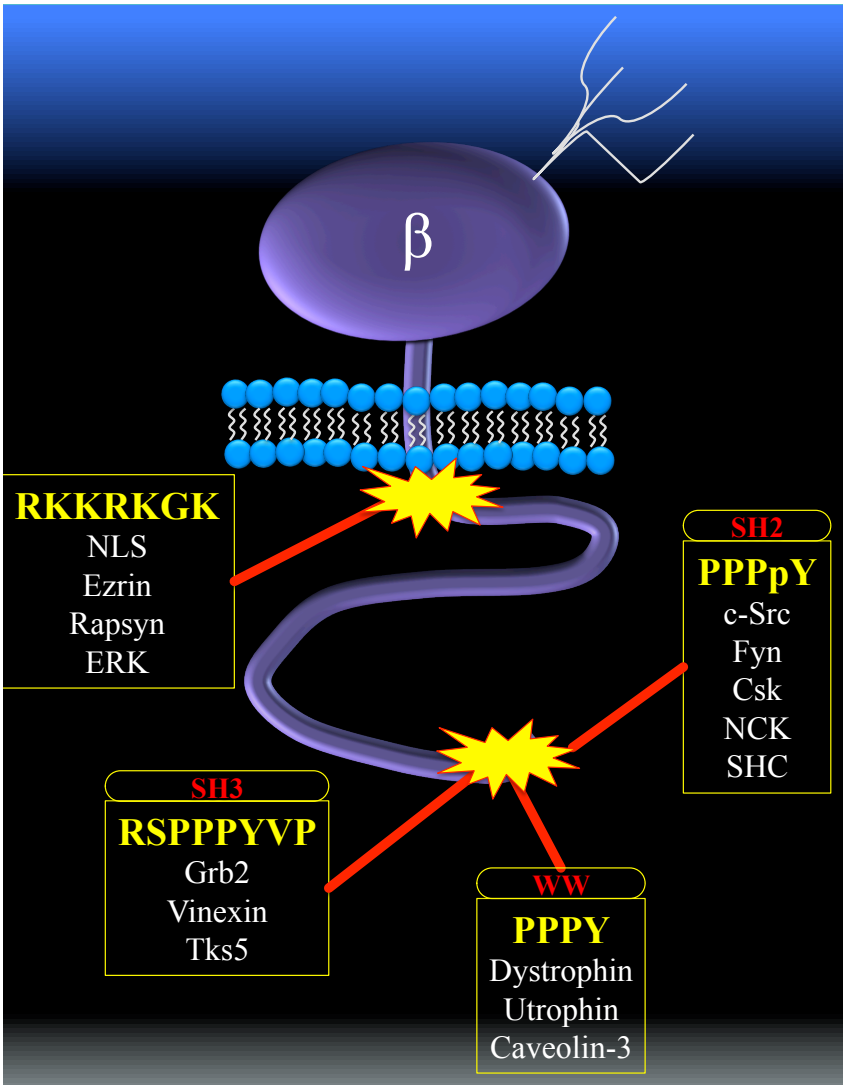

Figure 1.6: Binding partners of beta-dystroglycan. Beta-dystroglycan interacts with multiple proteins through its stretch of basic amino acids and its SH2, SH3 and WW protein binding domains. Other proteins were omitted, however, they are further mentioned in the following chapters.

in their degradation (Bonuccelli et al., 2007; Gazzerro et al., 2010). This set of results, although not showing the direct ubiquitination of beta-dystroglycan, clearly suggest that beta-dystroglycan is subject to ubiquitination.

There are some research groups reporting ubiquitinated dystroglycan (K. A. Lee et al., 2011; W. Kim et al., 2011). However, the significance of this PTM in the turnover of dystroglycan is still unknown. Additionally, it is still not known how this PTM regulates the interaction of dystroglycan with other proteins, or what its potential implication is in muscular dystrophies and cancer. Sumoy-

lation, a PTM with some homology to ubiquitination, is thought to modify dystroglycan, however the data supporting this is limited (Steve J. Winder, personal communication).

The combination of all the post-translational modifications, the motifs and the disordered structure of the cytoplasmic fragment, make beta-dystroglycan an enigmatic protein with still more roles to discover. In order to understand how the alterations of dystroglycan can lead to disease, it is necessary first fully understand its regulation in space and time. A major caveat of previous research has been the focus on dystroglycan and its functions as isolated events at the protein level. However, it has to be understood that there may be many pools of dystroglycan within a cell that have different forms of PTMs at the same time: whilst one form bridges the cytoskeleton to the plasma membrane, the other regulates transcription, cell cycle progression, development or neural transmission, as shown below (Bello et al., 2015; Bozzi, Morlacchi, Bigotti, Sciandra, & Brancaccio, 2009; Moore & Winder, 2010; Winder, 2001).

1.5.3 Dystroglycan in human disease

Dystroglycan is indeed an enigmatic protein. It takes part in a multitude of pathways due to its ability to interact with other proteins and to its flexibility to adopt different post-translational modifications (Barresi & Campbell, 2006; Winder, 2001). Its critical role is supported by the fact that alterations in its synthesis, in its primary structure, and in its modifications lead to very dramatic effects in the organism, as first described by Williamson and colleagues. In that study, in contrast to the heterozygous mice which had an apparently normal phenotype, the ablation of the *Dag1* gene led to peri-implantation lethality, which were characterised by alteration of Reichert's membrane and in the localisation of laminin and collagen extracellular matrix components (Williamson et al., 1997).

Dystroglycan was mapped to the short arms of human chromosome 3 in a locus that spans the region 3p21.1-3p21.31. An early report suggested a

potential role for dystroglycan as a tumour suppressor, because of its ability to facilitate the communication between the surrounding extracellular matrix and the cytoskeleton (Sgambato & Brancaccio, 2005). Interestingly, there are reports indicating that the region 3p21.3 harbours many genes with tumour suppressor properties (Hesson, Cooper, & Latif, 2007) and furthermore this region seems to be susceptible to different chromosomal rearrangements in epithelial tumours, such as breast, lung, cervical, ovarian and others (Angeloni, 2007; Ji, Minna, & Roth, 2005; Lerman & Minna, 2000). It is also reported that the same locus is involved in Crohn's disease (Morgan, Han, Lam, Fraser, & Ferguson, 2010). These findings indicate a potential role of dystroglycan in cancer and Crohn's disease.

Over time, subsequent reports have further highlighted the detrimental effects of the alteration of dystroglycan at its genomic level, named primary dystroglycanopathies; and that of the enzymes in charge of the glycosylation of alpha dystroglycan, termed secondary dystroglycanopathies (see section 1.5.3.1). However, the role of dystroglycan seems not to be only limited to dystroglycanopathies, as a new role in cancer has emerged, as described later (see section 1.5.3.2).

1.5.3.1 Dystroglycan in muscular dystrophies

The disease field involving dystroglycan that is most studied is that concerning the muscular dystrophies. As understanding the effects of dystroglycan's alterations in muscular diseases could provides us with clues about its alterations in cancer and vice versa, the impact of beta-dystroglycan in the muscular dystrophies will be briefly discussed.

Muscular dystrophies are a group of gradually progressive inherited diseases. At the cellular level, some of the main characteristics of these diseases are the alteration in proteins levels of members of the DAPC and their glycosylases, proteins associated to the nuclear membrane, and others (Mercuri & Muntoni, 2013).

A few studies of primary dystroglycanopathies have shown how important dystroglycan is. Following the description by Williamson about the severe effects of dystroglycan loss (Williamson et al., 1997), another report relating the deficiency of beta-dystroglycan to a mild form of muscular dystrophy phenotype, further highlighted the consequences of the alteration of dystroglycan in humans (the other components of the DAPC were normal) (Salih et al., 1996). Later, although not confirmed that the phenotype was due to DAG1's alteration, the heterozygous deletion of a locus comprising the DAG1 gene in a young female, resulted in a phenotype that resembled that of Walker-Warbur syndrome and muscle-eye-brain disease (Frost et al., 2010).

The breakthrough to the critical role of dystroglycan was provided by Kevin Campbell's group. His group described the first known primary dystroglycanopathy. This was caused by the mutation Thr192Met located in the N-terminal side of alpha-dystroglycan. This mutation, which prevented the O-glycosylation performed by LARGE, led to a reduction in the binding of dystroglycan to laminin. Thus, the critical role of dystroglycan is highlighted by the fact that a single mutation was able to cause limb-girdle muscular dystrophy, despite the fact that alpha-dystroglycan has many potential O-glycosylation sites, other than those described here (Hara et al., 2011).

Additional mutations in the DAG1 gene leading muscular dystrophy phenotypes have been identified (Dong et al., 2015; Geis et al., 2013) and recently, the first mutation leading to a complete absence of dystroglycan has been reported (Riemersma et al., 2015).

Compared to the mouse, the ablation of dystroglycan in zebrafish was not lethal, although a dystrophic phenotype was observed (Parsons et al., 2002). Interestingly, the mutation V567D in *Patchytail* fish was able to cause a muscular dystrophy-like phenotype (Gupta et al., 2011).

Secondary dystroglycanopathies are characterised by defects in glycosyltransferases that attach sugar groups to alpha-dystroglycan, which in turn prevent the interaction of alpha-dystroglycan with laminin, neurexin, agrin and perlecan, leading to the disruption of the connection between cytoskeleton

and the extracellular matrix (Michele & Campbell, 2003). There are different genes (enzymes) whose disruption have been shown to affect dystroglycan's glycosylation: they include LARGE (like glycosyltransferase), FKTN (fukutin), FKRP (fukutin related protein), POMGNT1 (protein-O-linked mannose beta 1,2-N-acetylglucosaminyltransferase), POMT2 (protein-omannosyltranferase 2), POMT1 (protein-O-mannosyltransferase 1), DPM2 (dolichyl-phosphate mannosyltranferase polypeptide 2), DPM3 (dolichyl-phosphate mannosyltranferase polypeptide 3), and many others which were recently reported by Jae and colleagues (Brown & Winder, 2012; Jae et al., 2013; Godfrey, Foley, Clement, & Muntoni, 2011). The phenotypes associated with these alterations are diverse, but they usually involve the damage to the skeletal muscle, cardiac problems, ocular problems and mental retardation. The differential combination of these defects leads to distinct forms of muscular dystrophies, such as Fukuyama congenital muscular dystrophy (FCMD), muscle-eye-brain disease (MEB), Walker-Warburg Syndrome (WWS) and limb girdle muscular dystrophy (LGMD) which can also be divided in various sub-types (Brown & Winder, 2012; Godfrey et al., 2011; Mercuri & Muntoni, 2013; Michele & Campbell, 2003).

Current research is aimed to gain a better understanding of dystroglycan glycosylation. This PTM is so critical that there are numerous genetically modified mouse models for many of the enzymes implicated in the glycosylation of dystroglycan; in addition, other mouse models that are deficient for constituent proteins of the DAPC other than dystroglycan have been generated (Whitmore & Morgan, 2014). Additional research aims to understand the glycosylome of alpha-dystroglycan, which includes the way dystroglycan is structurally modified, and additional players involved in its glycosylation (Harrison et al., 2012; Jae et al., 2013; Nilsson, Larson, & Grahn, 2010; Stalnaker et al., 2010, 2011)

Altogether, these findings demonstrate that dystroglycan is important and that small changes in its primary structure or post-translational modifications can lead to severe effects in humans. From the examples so far, the prevail-

ing factor as a cause of disease is the hypo-glycosylation of alpha-dystroglycan. Therefore, finding a way of producing normal, glycosylated alpha-dystroglycan will be a breakthrough in muscular dystrophies. However, dystroglycan is a protein not only expressed on the sarcolemma in skeletal muscle, but a protein that is also expressed in nervous and epithelial tissues. In epithelial tissues, dystroglycan maintains the cellular integrity and restricts the uncontrolled growth of the cells by its interaction with components of the extracellular matrix. This lead us to question, what do dystroglycan's roles in cellular environments other than those of skeletal muscle tell us about its role in disease?

1.5.3.2 Dystroglycan in cancer

In the previous section it was highlighted how important the role of dystroglycan is at the plasma membrane. In skeletal muscle, through its association with other members of the DAPC, dystroglycan provides structural roles, and functions as a kind of bridge, facilitating communication between the exterior and interior environments of the cells. Interestingly, in epithelial cells these same mechanisms seem to be governing dystroglycan and, importantly, the disruption of those mechanisms are an important part in the development of cancer (Sgambato & Brancaccio, 2005).

The cross-linked extracellular matrix, the basement membrane, surrounds epithelial and endothelial tissues as a form of protection. The communication of the cell with its extracellular environment is mediated by the interaction between components in the extracellular matrix, such as laminin, agrin, collagen, perlecan and nidogens, and receptor proteins found on the plasma membrane of the cells, which can include integrins, dystroglycan, sarcoglycan, the Lutheran glycoprotein and sulfatides. This interaction is important in order to regulate the behaviour of the cell, and importantly, the disruption of the integrity of the basement membrane favours the invasion and migration of metastatic cells. Thus, a cell can be modulated from the outside, and vice versa, by changing the activation of genes responsible for producing components of the

extracellular matrix and the adhesion proteins that interact with it, the cell can modulate its interaction with the surrounding tissue environment (Kelley, Lohmer, Hagedorn, & Sherwood, 2014; Yurchenco, 2011).

In this regard, integrins are a group of proteins that confer adhesion to cells during migration and invasion, as well as participating in signalling between the interior and exterior environments. By adhering to the extracellular matrix, integrins are able to trigger downstream signalling pathways involved in the remodelling of the cytoskeleton which in turn lead to the formation of cellular structures, like lamellipodia (outside-in signalling). The processes mediated by integrins are important not only at the front of the cells but also at the rear. Here, in order to migrate, the cell has to detach from the substrate, a process that involves the degradation or internalization of integrins (Hood & Cheresh, 2002). Hence, integrins can also respond to intracellular signals to change their extracellular binding capabilities (inside-out signalling).

Dystroglycan, a topologically similar protein to the integrins, shares a similar functionality. Glycosylated dystroglycan interacts with laminin (or other components of the extracellular matrix) (Matsumura et al., 1997), which in turn is able to trigger the assembly of the basement membrane (Yurchenco, 2011). In cancer, the interactions that dependend on the glycosylation state of alpha-dystroglycan, are also implicated in cell migration and invasion. Bao and colleagues observed that the formation of prostate tumours and metastasis was dependent on the degree of glycosylation on alpha-dystroglycan; hyper-glycosylation alpha-dystroglycan lead to the formation of small tumours and fewer metastatic events compared with hypo-glycosylated alpha-dystroglycan. They concluded that the glycosylation on alpha-dystroglycan mediated by β3GnT1 allowed the interaction with laminin, in turn attenuating downstream events of the integrin pathway such as the sequestering of ERK (Bao et al., 2009).

Changes to the glycosylation of alpha-dystroglycan seem to be common in the development of cancer, as a similar phenomenon was observed by another group in metastatic prostate cancer. However, high rates of invasion

and proliferation were only detected with reduced levels of LARGE2 (Esser et al., 2013). This phenomenon of the interaction between glycosylated alpha-dystroglycan and laminin in tumorigenicity is also reported for breast cancers (Akhavan et al., 2012). Although the enzyme responsible for the altered glycosylation of alpha-dystroglycan (which in turn leads to the interaction with laminin) is not reported by the studies, it is clear that the altered glycosylation of alpha-dsytroglycan is a triggering event in the development of malignancies such as: oesophageal (Parberry-Clark, Bury, Cross, & Winder, 2011), prostate (Shimojo et al., 2011), pediatric solid tumours (alveolar rhabdomyosarcoma, embryonal rabdomyosarcoma, neuroblastoma and medulloblastoma) (Martin, Glass, Dosunmu, & Martin, 2007), cervical and vulvar (Sgambato, Tarquini, et al., 2006).

In addition, glycosylation appears to confer protection to alpha-dystroglycan and the other members of the DAPC. In other words, not only alpha-dystroglycan is affected by the absence of this PTM: beta-dystroglycan is affected as well. Upon hypo-glycosylation of alpha-dystroglycan, beta-dystroglycan is susceptible to proteolysis by proteases found in the extracellular environment. Previous studies have shown that the cleavage between residues His-715 and Leu-716 on the extracellular globular domain of beta-dystroglycan (Bozzi, Inzitari, et al., 2009) by matrix metalloproteases-2 and -9, results in a 31 kDa plasma membrane attached fragment (Jing et al., 2004; Michaluk et al., 2007; Shang, Ethunandan, Górecki, & Brennan, 2008; Yamada et al., 2001; Zhong et al., 2006).

Importantly, the presence of this fragment seems to be associated with disease. In the case of muscular dystrophies, the 31 kDa transmembrane fragment was observed to be increased in sarcoglycanopathies and DMD (Matsumura et al., 2005). In cancer, increases in the 31 kDa fragment were observed in squamous cell carcinoma (Jing et al., 2004; Shang et al., 2008), breast (Losasso et al., 2000), colon (Losasso et al., 2000), cervical (Losasso et al., 2000) and prostate tumour cells (Losasso et al., 2000). Furthermore, this small 31 kDa fragment was also observed in stroke and heart attack (Armstrong, Latham,

& Ganote, 2003).

Additionally, and although the causes of the reduction were not determined, full-length dystroglycan was found to be greatly decreased or absent at the plasma membrane in most types of cancer studied including: breast (Cross et al., 2008; Henry, Cohen, & Campbell, 2001; Muschler et al., 2002; Sgambato et al., 2003), prostate (Henry et al., 2001; Sgambato et al., 2007), colon (Cross et al., 2008; Sgambato et al., 2003), oesophageal (Cross et al., 2008; Parberry-Clark et al., 2011) and transitional cell carcinomas of the urothelium (Cross et al., 2008).

Therefore, it seems that the mechanism by which dystroglycan is reduced from the plasma membrane starts with problems in the glycosylation of alpha-dystroglycan. This in turn renders an exposed beta-dystroglycan that is susceptible to cleavage by matrix metalloproteases, which confers an advantage in the mestastatic process of cancerous cells.

1.5.4 The nuclear translocation of beta-dystroglycan

The initial characterization of dystroglycan clearly established its important role within the DAPC in order to confer stability to muscle fibres during contraction and relaxation. Throughout the years, further discoveries correlated the alteration of dystroglycan as an important cause of muscular dystrophies. More recently, research into dystroglycan has extended to cancer, where many studies have correlated the reduced expression of dystroglycan with cancer progression. Although it was not completely understood, the general idea was that dystroglycan was the anchor of the cell to the extracellular matrix, providing integrity to the sarcolemma or, in the case of cancer, restricting the uncontrolled growth of cells.

The puzzle became more complicated with the description by the Cisneros group of the dystrophin variant Dp71 in the nucleus of cervical (HeLa), muscle (C2C12), neuroblast (N1E-115) (González et al., 2000) and pheochromocytoma (PC12) cells (Marquez et al., 2003). The initial observation of the

co-localization between beta-dystroglycan and Dp71 prompted the question as to whether other members of the DAPC were also present in the nucleus of the cell. Later research performed by the same group revealed the localisation of beta-dystroglycan and other members of the DAPC such as Dp71, sarcoglycan, dystrobrevin, syntrophin and nNOS in the nucleus of cervical cancer cells. It was then thought that the functions of the new nuclear complex were related to scaffolding-related activities (Fuentes-Mera et al., 2006).

A further logic step was to determine the way that this complex, in particular beta-dystroglycan, was travelling to the nucleus.

The nuclear membrane is an important structure that divides the interior of the cell into two spatial compartments, the nucleoplasm and the cytosol. This compartmentalisation separates the machinery involved in the synthesis of mRNA (transcription) in the nucleoplasm, from that involved in the production of proteins (translation) in the cytosol. The communication between both compartments is enabled by the presence of macromolecular structures embedded in the nuclear membrane called nuclear pore complexes (NPC). These complexes allow the regulated transport of proteins between the cytosol and the nucleoplasm through a mechanism known as the nuclear import pathway, and involves the protein to be transported (cargo) and adaptor proteins (carriers) known as importins (karyopherins) or exportins (Kau, Way, & Silver, 2004; Stewart, 2007; Wente & Rout, 2010).

For proteins with a molecular weight (MW) below 40 kDa it is believed that the mechanism of nuclear import through the NPC is by protein diffusion and does not require carriers. On the other hand, proteins with a MW equal or higher than 40 kDa require the presence of the importin system in order to be translocated to the nucleus. Furthermore, high MW cargoes require signals within their primary sequence in order to be recognised by the importin system. These signals, known as nuclear localisation sequences (NLS), can consist of a single stretch of basic amino acids composed of $\sim 4-5$ amino acids (monopartite), or two stretches separated by $\sim 10-12$ amino acids (bipartite). The NLS of SV40 large-T antigen and nucleophosmin are examples of mono

and bipartite NLS respectively (Kau et al., 2004; Stewart, 2007; Wente & Rout, 2010).

The mechanism starts in the cytosol with the formation of the cargo-carrier complex. The formation of the importin-alpha-importin-beta dimer through an importin-beta binding domain exposes a domain in importin-alpha, which is able to recognise the NLS in the protein cargo. The complex is directed to the NPC, where importin-beta mediates the interaction with nucleoporins via phenylalanine-glycine-nucleoporin (FG-nucleoporin) repeats, and is then translocated to the nucleoplasm. Once in the nucleus, high concentrations of RanGTP disassemble the complex. The protein cargo is released, and importin-alpha in complex with RanGTP, and importin-beta combined with RanGTP, and nuclear export factor CAS are recycled back to the cytoplasm. In the cytoplasm RanGAP helps in the disassembly of the complex, rendering importins free for another round of transport. High concentrations of RanGDP in the cytoplasm or RanGTP in the nucleoplasm are maintained by RanGAP (Ran GTPase activating protein) and RanGEF (Ran guanine nucleotide-exchange factor) respectively (Figure 1.7) (Kau et al., 2004; Stewart, 2007; Wente & Rout, 2010).

The nuclear export of proteins is mediated by the counterparts transportin, CRM1, exportin-5 and exportin-t and the sequences that mediate the recognition of the protein cargo to the exportin complex are named nuclear export signals (NES), which are a cluster of leucine-rich amino acids. In the classic nuclear export pathway, importin-beta complexed with RanGTP is transported back to the cytoplasm. Importin-alpha on the other hand, forms a complex with RanGTP and CAS. Both complexes containing importin-alpha and importin-beta are transported to the cytoplasm through the NPC. Once in the cytoplasm by the action of RanGAP, both importins are released, leaving them free for another round of transport. By a similar mechanism, cargo proteins to be transported back to the cytoplasm are recognised by exportins through their NES (Kau et al., 2004; Stewart, 2007; Wente & Rout, 2010).

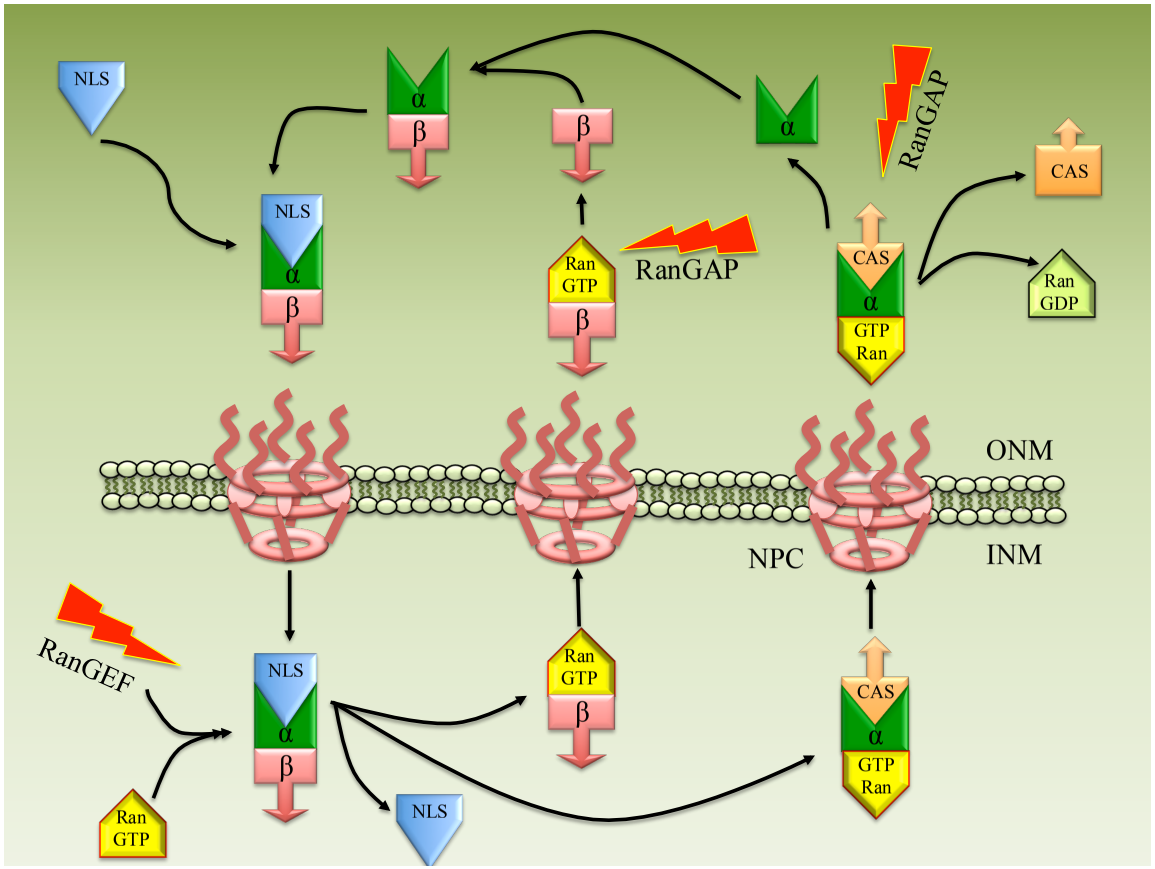

Figure 1.7: Nucleo-cytoplasmic transport of proteins. Proteins harbouring an NLS are recognised by the dimer of importins alpha-beta in the cytosol. The trimeric complex is transported to the nucleus through the nuclear pore complex. In the nucleus the high concentrations of RanGTP by means of RanGEF dissociate the complex. The cargo is released in the nucleoplasm and the carriers alpha and beta importins are transported back to the cytoplasm complexed with RanGTP-CRM1 (exportin) or RanGTP respectively. In the cytosol, RanGAP liberates the carrier proteins leaving them ready for another round of transport.

The import of proteins through the nuclear import pathway seems to be the preferred mechanism by proteins with functions other than cytosolic roles, as is the case of dystroglycan and other DAPC components.

Oppizzi and colleagues determined that, in breast carcinoma cell lines, the nuclear translocation of beta-dystroglycan was mediated by the presence of a bipartite NLS located after the sequence that encodes the transmembrane domain. The interesting observation of a dynamic beta-dystroglycan in the nucleoplasm directly questioned the previous static model proposed by the Cisneros group (Fuentes-Mera et al., 2006; Oppizzi et al., 2008). Further studies confirmed that, in addition to the transport mediated by a nuclear localisation signal, beta-dystroglycan travels to the nucleus in an importin-alpha/beta regulated pathway. In that study, it was suggested that Y892, a tyrosine that has been implicated in other signalling processes, could be influencing the transport of beta-dystroglycan to the nucleus (Lara-Chacón et al., 2010). Parallel studies showed that the assembly of the DAPC complex could be regulated by the differentiated status of myoblasts (González-Ramírez, Morales-Lázaro, Tapia-Ramírez, Mornet, & Cisneros, 2008) and that in pheochromocytoma cells, Dp71 was important for the assembly of the DAPC in the nucleus (Villarreal-Silva, Suárez-Sánchez, Rodríguez-Muñoz, Mornet, & Cisneros, 2010).

These previous studies clearly showed the presence of a new pool of DAPC components in the nucleus of different cell lines. The debate about the static (by its immersion in the nuclear membrane), or dynamic (by its unrestricted movement in the nucleoplasm) functions of beta-dystroglycan persisted, but new observations suggested that both hypothesis were plausible.

Two papers published almost simultaneously provided more important clues. In muscle derived cells, the C2C12 cell line, in addition to its previously described association with lamin B, beta-dystroglycan was found associated with nuclear organelles such as the nucleolus, splicing speckles, emerin and cajal bodies. The interaction between beta-dystroglycan and these organelles (verified by immunoprecipitation, immunofluorescence and pull-down)

was slightly altered by the downregulation of beta-dystroglycan compared to the dramatic effect observed with lamin B. Additional alterations observed were the miss-localisation of the centrosomes, which raised the hypothesis of beta-dystroglycan and its possible involvement in the cell cycle (Martínez-Vieyra et al., 2013).

The second work took a step forward in providing clues to the activities of beta-dystroglycan in the nucleus. In healthy prostate human tissue, there was a strong expression of beta-dystroglycan on the basal side and baso-lateral junctions of the epithelial cells. However, the intensity of the staining pattern was greatly reduced in prostate carcinoma tissue. After cell fractionation the nuclear distribution of beta-dystroglycan was confirmed. The most striking result to emerge from that work was that the overexpression of the cytoplasmic fragment of beta-dystroglycan had a preferential nuclear accumulation, which in turn led to the expression of transcription factors such as ETV1, which the authors confirmed by microarray analysis (Mathew et al., 2013).

From this set of results it appears that beta-dystroglycan is an important player in the organisation of the nuclear architecture (Tadayoni, Rendon, Soria-Jasso, & Cisneros, 2012), but is also an important modulator of other nuclear processes, such as gene-transcription. The interplay between both mechanisms is still not completely understood, nor the mechanisms triggering the nuclear translocation of cytosolic beta-dystroglycan, although ezrin is implicated (Vásquez-Limeta et al., 2014). Importantly, it is still not known what the role of nuclear beta-dystroglycan is, nor how this enigmatic protein mediates those new nuclear events, despite it being clear that beta-dystroglycan does not bind to the nuclear DNA (Bozzi, Morlacchi, et al., 2009; Brancaccio, 2012; Moore & Winder, 2010; Tadayoni et al., 2012).

1.5.5 Dystroglycan and the cell cycle

The conservation of life can be achieved by one simple, yet complex, process. It consists of the division of a 'mother' cell to give raise to two identical 'daughter'

cells. This mechanism can be divided into two main phases, the interphase (a kind of "resting" phase) and mitosis (the process wherein one cell generates two cells). These two phases are separated by two main intervals named 'gaps', G1 and G2.

The interphase, the phase of apparent resting, is instead a period of intense activity in the cell. This phase can be sub-divided into G1-phase, S-phase and G2-phase. During G1-phase, the phase that separates mitosis from the S-phase, the cell senses the surrounding environment and, under favourable conditions, the cells proceeds into S-phase. If the conditions are not favourable, the cell enters into a phase of resting for an undefined time. In S-phase, the cell is able to synthesize (S) two identical copies of DNA (replication). The cell progress into G2 phase once replication has concluded. In this phase, the cell verifies the proper replication of DNA and prepares all the material required in order for the cell to enter into mitosis.

Mitosis comprises two important events during cell division, the segregation of the nucleus (mitosis) and the segregation of the cytoplasm (cytokinesis). Mitosis is divided into different stages, all of them characterised by specific episodes during the separation of chromosomes: prophase, pro-metaphase, metaphase, anaphase and telophase. Once the chromosomes are completely separated, the cell specifies a site of division, the cleavage furrow, as a mark that dictates the place where the cell has to be separated. This leads to the constriction of the cell and the formation of the midbody, which functions until the cells are completely separated (Alberts et al., 2008).

The evidence gathered so far indicates that beta-dystroglycan may be implicated in the cell cycle at different stages: as a regulator, but also as a subject of regulation.

The different events that are apparently regulated by beta-dystroglycan are evident from by the following observations.

During the cytokinesis of REF52 and Swiss 3T3 fibroblasts, and cervical HeLa cells, beta-dystroglycan is targeted to the cleavage furrow and midbody. The possibility of the requirement of its cytoplasmic fragment was confirmed

because a truncated form of beta-dystroglycan lacking this region was not able to localise to these structures (Higginson, Thompson, & Winder, 2008). This observation was further supported by a later report indicating that, in pheochromocytoma cells (PC12), beta-dystroglycan (in association with Dp71) was co-localised to the same structures and additionally, was observed to be co-localised with the mitotic spindle. By decreasing Dp71 expression, the role of Dp71 in organising this complex was established; furthermore, the authors observed defects in the structure of the nuclear membrane (Villarreal-Silva, Centeno-Cruz, Suárez-Sánchez, Garrido, & Cisneros, 2011). This last observation led the authors to hypothesize that beta-dystroglycan, together with lamin B and Dp71, are able to organise the mitotic spindle poles during cell division (Tadayoni et al., 2012). From these findings it is clear that beta-dystroglycan modulates events in the final stages of mitosis.

Other characteristics that have been associated with beta-dystroglycan within the cell cycle are abnormalities during the transition of the S- and M-phases.

Following down-regulation of beta-dystroglycan it was reported that mammary epithelial cells accumulated in the S-phase of the cell cycle (Sgambato, Di Salvatore, et al., 2006). On the other hand, reduced levels of dystroglycan have also been reported to cause a lag in a G2/M transition of fibroblats cells, a phenomenon presumably attributable to reduced levels of ERK (Higginson et al., 2008). A different study reported similar findings, but in the transition of G0 to G1 (Villarreal-Silva et al., 2011). Although the results from the last group can not be compared to the other papers cited above, because the targeted reduced protein was Dp71, it points out the fact that the alteration of the DAPC members may lead to alterations in the transition of the cell cycle.

Dystroglycan is subject to regulation throughout the cell cycle. In bovine aortic entothelial cells (BAE) increased levels of beta-dystroglycan in S-phase were associated with angiogenesis (Hosokawa, Ninomiya, Kitamura, Fujiwara, & Masaki, 2002). Later on, in synchronised HC11 murine mammary epithelial cells, dystroglycan mRNA levels were observed up-regulated during S-

phase, a mechanism mirrored at protein level (Sgambato, Di Salvatore, et al., 2006). Current research indicates that the observed up-regulation of beta-dystroglycan during the S-phase of the cell cycle is extended to prostate LNCaP cancer cells (Laura A. Jacobs, personal communication).

Finally, the role of dystroglycan (and that of the other DAPC members) in cell survival is highlighted once more by the fact that reduced expression has been linked to apoptosis (Higginson et al., 2008; Sgambato, Di Salvatore, et al., 2006; Villarreal-Silva et al., 2011).

1.6 Project outline

The presence of dystroglycan at the plasma membrane is important to control the unrestricted growth of cells. In different carcinomas the reduced expression of beta-dystroglycan has been frequently observed (Cross et al., 2008; Henry et al., 2001). Previous evidence indicates that proteolytic events (Mitchell et al., 2013) and post-translational modifications (Miller et al., 2012) may be involved in this reduction. Additionally, the nuclear localisation of beta-dystroglycan and its association with nuclear organelles (Martínez-Vieyra et al., 2013), as well as the regulation of transcription factors (Mathew et al., 2013), indicate that both mechanisms may be linked. However, the mechanisms behind these events are still unknown.

The main motivations of this project are to understand: i) how post-translational modifications, such as phosphorylation and ubiquitination, affect the integrity of beta-dystroglycan; ii) the mechanisms that trigger the proteolysis of beta-dystroglycan from the plasma membrane and its downstream consequences; and iii) possible functions of beta-dystroglycan in the nucleus of LNCaP cells by means of its interaction with nuclear proteins.

1.7 Hypothesis

In LNCaP cells, beta-dystroglycan is subject to the proteolytic cleavage by gamma-secretase in a Regulated Intramembrane Proteolysis dependent manner to release a 26 kDa cytoplasmic fragment which is transported to the nucleus where it regulates nuclear functions.

1.8 Aims

1. To identify post-translational modifications on beta-dystroglycan regulating its stability and function.

2. To identify the mechanisms and proteases involved in the generation of the 26 kDa cytoplasmic fragment of beta-dystroglycan.

3. To perform a mass spectrometry analysis to identify candidate proteins interacting with beta-dystroglycan that could explain its functions in: the nucleus, the cell cycle, the ubiquitin proteasome system and others.

4. To perform mass spectrometry analysis to identify post-translational modifications on beta-dystroglycan.

2 Materials & methods

2.1 Materials and methods

The formulation of the solutions and the gels, the sequences of the primers, the characteristics of the plasmids and the antibodies referred in the text are fully described in the corresponding appendixes.

2.1.1 Bacterial techniques

2.1.1.1 Preparation of calcium competent *Escherichia coli* DH5α

A colony of fresh plated *E. coli* DH5α bacteria were used to inoculate 10 ml of 2x YT medium (starting culture) (see Appendix A) and then incubated at 37°C overnight in a shaking incubator. Next day, 0.5 ml of the starting culture was used to inoculate 100 ml of 2x YT medium and left at 37°C in a shaking incubator until the optical density at 600 nm was 0.6 (OD_{600}=0.6), as determined by use of a 7315 spectrophotomer (Jenway). Cellular growth was stopped by incubating the bacterial culture on ice for 10 minutes followed by centrifugation at 5000 x *g* for 10 minutes at 4°C. The supernatant was discarded and the pellet was resuspended in 50 ml of chilled sterile 100 mM $CaCl_2$ solution and then incubated on ice for 4 hours. Following a second centrifugation at 5000 x *g* for 10 minutes at 4°C, the supernatant was discarded and the pellet was resuspended in 5 ml of 100 mM $CaCl_2$. To prepare stocks

of competent cells, the resuspended pellet was mixed with sterile glycerol to a final concentration of 15% (v/v), and then frozen and stored at -80°C.

2.1.1.2 Transformation of competent bacteria

Frozen bacteria were thawed on ice before mixing with the required amount of DNA (usually 500 ng), and subsequent incubation on ice for 30 minutes. Bacteria were transformed by heat shock at 42°C for 2 minutes in a water bath. Thereafter, 1 ml of pre-warmed 2x YT medium without antibiotic was added and the culture was incubated at 37°C for 30 minutes in a water bath. 200 μl of this recovering culture were spread on to plates of 2x YT agar containing the appropriate selective antibiotic. Plates were incubated overnight at 37°C.

2.1.1.3 Bacterial protein induction

E. coli BL21(DE3) transformed with the plasmids pGST (GST) or pGST-MD (MultiDsk) (M. D. Wilson, Saponaro, Leidl, & Svejstrup, 2012) and grown on 2x YT agar with Ampicillin (100 μg/ml) were used to inoculate 600 ml LB medium with ampicillin (100 μg/ml). Inoculated medium was incubated in a rotating incubator at 37°C until it reached an optical density of 0.6 (OD_{600}=0.6). Once the OD was reached, protein expression was induced by the addition of Isopropyl β-D-1-thiogalactopyranoside (IPTG) to a final concentration of 1 mM. A good protein expression was obtained by incubating the culture for a further 4 hours at 37°C in a rotating incubator after induction (Figure 2.1). Following this, bacteria were pelleted by centrifugation at 6000 x g for 15 minutes, the supernatant was discarded and the pellet was washed once with PBS pH 7.4. The bacterial pellet was used immediately or stored at −20°C.

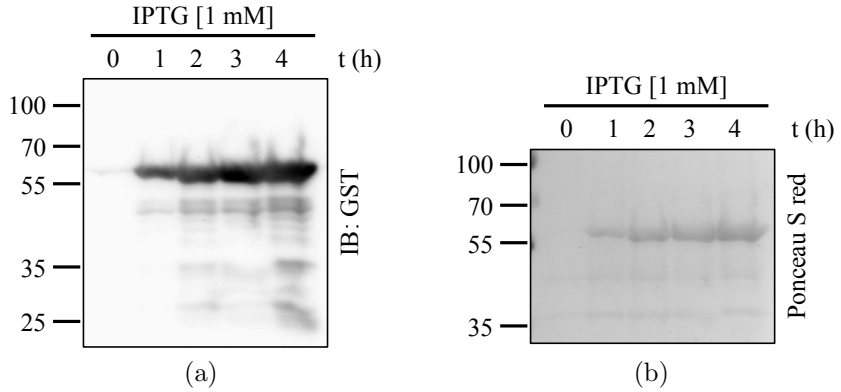

Figure 2.1: Transformed bacteria with the plasmid pGST-MD were inoculated in 2x YT medium and the expression of GST-MD was induced by the addition of IPTG. Samples of the induced culture were taken at the various time points shown and boiled with an equal volume of 2x Laemmli loading buffer, prior to gel electrophoresis and electroblotting. (a) Western blot analysis with an anti-GST antibody shows an increase in the amount of GST-MD protein (60 kDa) expressed over the time. (b) The membrane stained with Ponceau S red staining solution reveals total proteins in samples.

2.1.1.4 GST and MultiDsk protein purification

GST and GST-MD were purified according to the method described by Wilson and colleagues (M. D. Wilson et al., 2012). An induced bacterial pellet, produced as described above, was resuspended in 20 ml of STE buffer (Sodium Chloride-Tris-EDTA) supplemented with lysozyme to a final concentration of 100 μg/ml and incubated on ice for 15 minutes. Dithiothreitol (DTT) and sarcosyl (N-lauryl sarcosine) were added to the resuspended pellet to final concentrations of 5 mM and 1.5% (v/v) respectively (DTT was added before sarcosyl). Samples were mixed, gently sonicated and then centrifuged at 10000 x g for 5 minutes at 4°C. After filtration through a 0.45 μm filter to get rid of viscous material, the filtrate was combined with Triton X-100 to a final concentration of 3% (v/v) followed by a 5 minute incubation on ice.

500 μl of pre-equilibrated glutathione agarose beads in STE buffer were incubated with the filtrate for 4 hours at 4°C on a tube roller. Following incubation and by sequential centrifugation, the beads were washed with 50 ml of chilled wash buffer 1 (450 mM NaCl, 10% glycerol (v/v), 0.1 mM EDTA, 0.1% Triton X-100 (v/v), 2 mM DTT and protease inhibitors in PBS), followed

by washing with 25 ml of buffer 2 (50 mM NaCl, 10% glycerol (v/v), 1 mM 2-mercaptoethanol, 0.2% Triton X-100 (v/v) in 50 mM potassium phosphate buffer (40.1 mM K2HPO4, 9.9 mM KH_2PO_4, pH 7.4)). Following washing, beads were equilibrated with PBS pH 7.4, and then resuspended in PBS pH 7.4 supplemented with 1 mM sodium azide. Resuspended beads were stored at 4°C (M. D. Wilson et al., 2012) (Figure 2.2).

2.1.2 Molecular biology techniques

2.1.2.1 Agarose gel electrophoresis

All agarose gels used in this project were prepared at a final concentration of 1% (w/v). Agarose was melted in 1x TAE buffer (Tris-acetate-EDTA) (see Appendix A) and combined with ethidium bromide to a final concentration of 0.5 μg/ml. The solidified gel was placed in a tank containing 1x TAE and then DNA, which had been mixed with DNA loading buffer (see Appendix A), was loaded into the gel. Samples were separated at a constant voltage of 140 V for 40 minutes. DNA was visualized using the UV source in the ChemiDoc XRS+ system from Bio-Rad.

2.1.2.2 Small (miniprep) and large (maxiprep) scale DNA purification and DNA concentration determination

Purification of DNA was performed according to manufacturer's guidelines. For small and large scale DNA purification, the Plasmid Mini Kit (Bioline) and the QIAGEN Plasmid Maxi Kit were used respectively. DNA pellets were resuspended in sterile 10 mM Tris-Cl pH 8.5. The concentration of the DNA was determined by measuring the absorbance at 260 nm using a quartz 1 cm path-length cuvette (Unico) in a 7315 spectrophotometer (Jenway). DNA was stored at 4^{o}C for immediate use or at -20°C for long-term storage.

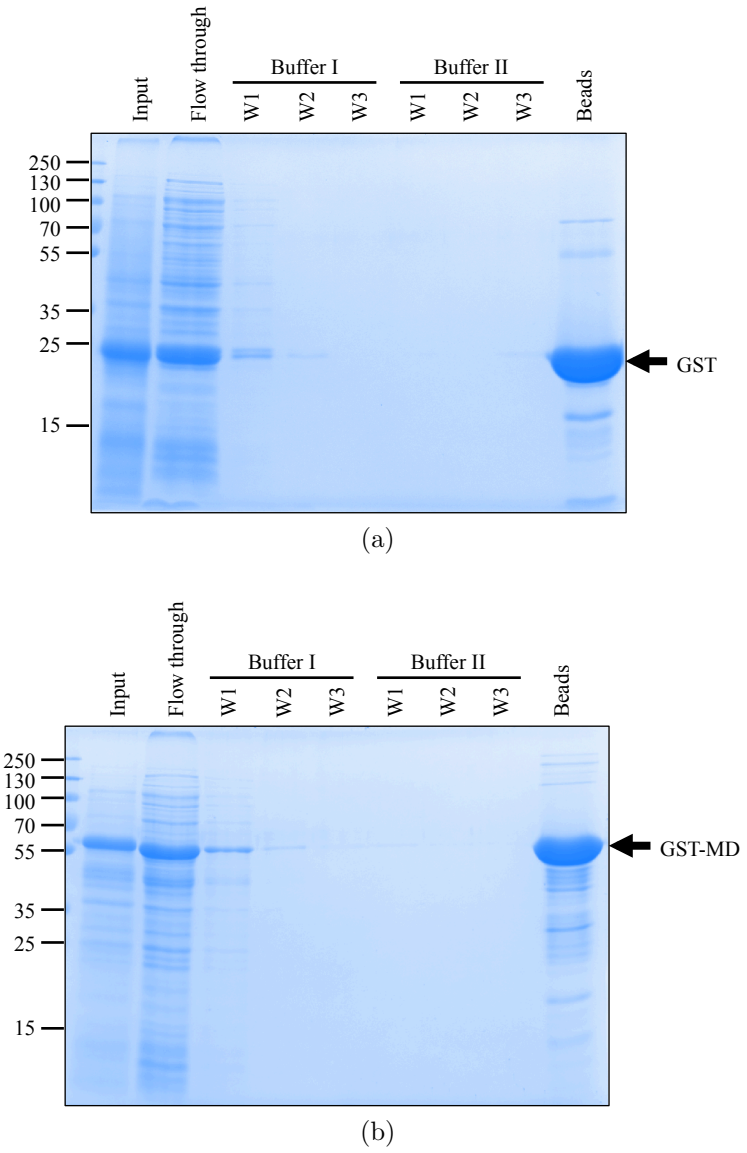

Figure 2.2: Purification of GST and GST-MD proteins. Proteins were purified as described in materials and methods. An aliquot of the input, the flow through, the washes and the beads was mixed with 2x sample loading buffer and resolved by SDS PAGE. Gels were stained with Coomassie blue safe staining. Shown are the bands corresponding to GST(25 kDa) (a) and GST-MD (60 kDa) (b) recombinant proteins.

2.1.2.3 Generation of a Flag tag in the primary sequence of mouse-$\alpha\beta$DgFlag by site directed mutagenesis

A Flag tag was introduced into the coding sequence of mouse $\alpha\beta$Dg (plasmid pcDNA2-$\alpha\beta$Dg, see Appendix C) through a complementary pair of primers (see Appendix B) designed to insert and to mutate the amino acids shown in

Figure 3.6. The design of the primers and the protocol followed were performed according to the instructions provided by the QuikChange XL Site-Directed Mutagenesis Kit (Agilent Technologies). The primers were designed to incorporate the desired changes with minimal modifications in the primary structure of the protein.

XL10-Gold Ultracompetent cells (Agilent technologies) were transformed with mutated construct and then incubated with NZY+ broth as indicated in the manufacturer's protocol. Transformed bacteria were plated on 2x YT agar with ampicillin (100 μg/ml) and then incubated at 37°C for >16 hours.

Candidate transformed colonies were used for purification of DNA using the Plasmid Mini Kit (Bioline). Purified DNA was characterized by DNA sequencing (Source BioScience). Working stocks of DNA containing $\alpha\beta$DgFlag were prepared by maxi-prep.

2.1.2.4 Cloning of coding sequences of mouse-$\alpha\beta$DgFlag (full) and mouse-cβDgFlag (cyto) into the plasmid pcDNA3.1(+)

A pair of oligonucleotides containing the restriction sites for the enzymes EcoRI (5') and XhoI (3') were used to amplify the coding sequence of full-length mouse $\alpha\beta$-dystroglycan by PCR. For the cytoplasmic domain, which corresponds to residues 773 to 892 of the full-length sequence, the forward primer was designed to contain an additional methionine after the restriction site for EcoRI and before the tyrosine 773 (the reverse primer was the same used in the amplification of full dystroglycan) (see Appendix B). The PCR was carried out using the 2x Phusion Master mix according to manufacturer's guidelines (New England Biolabs Inc) (Table 2.1).

The amplicons were verified by agarose gel electrophoresis. The plasmid pcDNA3.1(+) and the amplicons from the full-length and cyto-βdystroglycan PCRs were digested with the restrictions enzymes EcoRI-HF and XhoI in EcoRI buffer (New England Bio-labs) for 2 hours at 37°C.

Cycle step	Temp (°C)	Time (s)	Cycles
Initial denaturation	98	30	1
Denaturation	98	10	30
Annealing	60	30	30
Extension	72	75	30
Final extension	72	600	1
	4	∞	

Table 2.1: PCR conditions

The digested products were characterized by agarose gel electrophoresis and then purified from the agarose gel using the QIAquick gel extraction kit (QIAGEN). The purified digested amplicons were ligated into the pcDNA3.1(+) vector using the Quick Ligation kit (New England Bio labs). Ligated DNA was used for transformation. Candidate colonies were expanded in 2x YT with ampicillin (100 μg/ml) and DNA purified by mini-prep. Correct ligation of the construct was validated by sequencing.

2.1.2.5 Generation of the mutations Y890F and K806R in the primary sequence of mouse $\alpha\beta$DgFlag by site directed mutagenesis

The mutations Y890F and K806R were introduced into the coding sequence of mouse $\alpha\beta$DgFlag (see Appendix C) by PCR using the primers listed in Appendix B following the instructions provided in the QuikChange Lightning Site-Directed Mutagenesis kit (Agilent Technologies). Transformed candidate bacteria were used for small scale DNA purification. Purified DNA was characterized by DNA sequencing, and DNA carrying either of the desired mutations was used to prepare working stocks by maxi-prep.

2.1.3 Tissue culture techniques

2.1.3.1 Growth and passaging of LNCaP cells

LNCaP cells were maintained in RPMI medium (Gibco, Life technologies) [+]-L-glutamine supplemented with 10% (v/v) Fetal Bovine Serum (Gibco, Life technologies). Cells were incubated at 37°C in an incubator with a 5% CO2 atmosphere (Galaxy S, Biohit). Before each experiment, cells were allowed to grow for a minimum of 24 hours. For cell passaging, cells were dissociated using 1% (v/v) Trypsin-EDTA (Sigma) and reseeded at a final cell density according to the requirements of each experiment. Growth medium was replaced with fresh medium every 2 days.

2.1.3.2 Preparation of LNCaP cell stocks

LNCaP cells were grown in RMPI medium [+]-L-glutamine supplemented with 10% (v/v) of Fetal Bovine Serum and allowed to reach a high cell density in large flasks (175 cm^2). Following trypsinization, cells were pelleted at 600 x g for 3 minutes and gently resuspended in freezing medium (RPMI medium, 20% DMSO, 20% FBS). Resuspended cells were aliquoted into cryovials and stored in a container with isopropanol at -80°C for 24 hours.

Long-term storage was carried out by storing the tubes in liquid nitrogen. Cells were thawed by placing the vial in a water bath at 37°C for 3 minutes and then resuspended in complete warm medium. Medium was replaced after the complete attachment of the cells to the flask in order to minimize exposure to DMSO.

2.1.3.3 Cell counting using a Neubauer chamber

10 μl of trypsinized pelleted cells resuspended in RPMI medium (usually 10 ml) were mixed with 90 μl of Trypan Blue Solution 0.4% (Sigma, T8154). An aliquot of 10 μl was used to load the Neubauer chamber. Cells were counted

according to the manufacturer's instructions. The total number of cells was calculated according to the following formula:

Total cells = $(\frac{cell\ counted}{4\ (to\ average\ for\ one\ square)})$ x (dilution factor used) x10^4(to convert the volume into ml)

2.1.3.4 Transfection of LNCaP cells using the Neon Transfection System

LNCaP cells were grown for a minimum of 48 hours before transfection. On the day of transfection cells were trypsinized as described above, before resuspension in growth medium. Cells were pelleted by centrifugation at 600 x *g* for 3 minutes at RT. The pellets were resuspended in growth medium and an aliquot was used to determine the cellular density with a Neubauer chamber. The number of cells was adapted to the conditions of each individual experiment according to the table 2.2.

Tip	**10 μl**		**100 μl**			
Scale	***6 well scale***		***6 well scale***		***60 mm or 100 mm disch scale***	
Well number	1 well/6 well	6 well/6 well	1 well/6 well	6 well/6 well	60 mm dish	100 mm dish
Cell number	0.6 x 10^6	4 x 10^6	1.2 x 10^6	8 x 10^6	3.6 x 10^6	7.2 x 10^6
DNA	2.4 μg	16 μg	2.4 μg	16 μg	7.2 μg	14.4 μg
Solution R	12 μl	64 μl	120 μl	784 μl	120 μl	120 μl

Table 2.2: Transfection conditions

The required number of cells were centrifuged at 600 x *g* for 3 minutes at RT and the pellets were resuspended in the recommended amount of Solution R (Life technologies). Resuspended cells were combined with the appropriate amount of DNA as shown on the table above and then loaded into an appropriate Neon Pipette Tip (Life technologies). The pipette was assembled into a Neon Pipette Station containing 3 ml of solution E2 (Life technologies). The

cells were microporated according to the conditions in the table 2.3.

Pulse voltage (v)	Pulse width (ms)	Pulse number	Tip type
1200	20	2	10 μl
1200	20	2	100 μl

Table 2.3: Microporation conditions

Once microporated, the cells were seeded onto poly-L-lysine pre-coated petri dishes containing pre-warmed growth medium. Cells were grown for a minimum of 24 hours before starting further experiments.

2.1.3.5 Stimulation of LNCaP cells with phorbol 12,13-dibutyrate (PDBu)

Cells were grown at a low cell density for 24 hours on petri dishes coated with poly-L-Lysine in RPMI growth medium. PKC activation was induced with RPMI medium containing PDBu [2.5 μM] (Sigma, prod. no. P1269) or DMSO (control) and incubated for different times protected from the light. After the specified times, cells were rinsed gently with cold 1x PBS.

2.1.3.6 Treatment of LNCaP cells with DAPT or Furin Inhibitor I

Confluent LNCaP cells were seeded on petri dishes coated with poly-L-lysine. Cells were allowed to attach and to grow for a minimum of 24 hours before starting treatment. The inhibition of gamma-secretase or furin activities, was performed by treating the cells with DAPT (N-[N-(3,5-Difluorophenacetyl-L-alanyl)]-S-phenylglycine t-Butyl Ester) (Calbiochem, cat. no. 565770) or Furin Inhibitor I (Decanoyl-RVKR-CMK) (Calbiochem Millipore, prod. no. 344930) respectively. DAPT or Furin Inhibitor I prepared in DMSO, were dissolved

in complete RPMI medium and then added to the cells. The treatment, performed at different concentrations as shown on the respective figures, was performed for 24 hours for both compounds. Cells were treated with the same volume of DMSO alone as a control.

2.1.3.7 Treatment of LNCaP cells with resveratrol

Non-confluent LNCaP cells (15000 cells/cm^2) were seeded on petri dishes coated with poly-L-lysine. Cells were grown for 24 hours and then treated with resveratrol (Enzo Life Sciences, prod. no. BML-FR104) to a final concentration of 100 μM for different times in order to induce the activation of NOTCH. For each time point, the same volume of DMSO was used for control treatments.

2.1.3.8 Treatment of LNCaP cells with MG132

Confluent LNCaP cells were grown on petri dishes coated with poly-L-lysine for 24 hours. The proteasome activity inhibition was performed by replacing the medium with full medium supplemented with MG132 [15 μM] (Calbiochem, cat. no. 474790) and then incubated for 4 hours at 37°C. The experiment was also performed using different concentrations of MG132 or using one concentration of MG132 for different times as shown in the respective figures. Cells treated with the same volume of DMSO were used as a control.

2.1.3.9 Treatment of LNCaP cells with cycloheximide

LNCaP cells, either WT or transfected, were grown for 24 hours and then treated with the protein synthesis inhibitor cycloheximide (Sigma, C7698) to a final concentration of 100 μg/ml for different times. Cells were washed with 1x PBS before further analysis.

2.1.3.10 Treatment of LNCaP cells with calyculin A and sodium peroxovanadate

24 hours post-transfection, LNCaP cells were washed with pre-warmed RPMI medium without serum and phenol red. The inhibition of serine and threonine phosphatases was performed by treating the cells with calyculin (Cell Signaling Technology, prod no. 9902), and of tyrosine phosphatases by treatment with sodium peroxovanadate.

Calyculin (prepared in DMSO) was used at a final concentration of 0.1 μM dissolved in RMPI medium without serum.

For peroxovanadate treatment, hydrogen peroxide and sodium orthovanadate were dissolved in RPMI medium without serum to final concentrations of 2 mM and 1 mM respectively.

These treatments were performed alone or together, and DMSO was used as the control. Following the addition of treatment, cells were incubated for 15 minutes at 37°C. Afterwards, LNCaP cells were washed with 1x PBS before further analysis (Ruff, Chen, & Cohen, 1997; Resjö, Oknianska, Zolnierowicz, Manganiello, & Degerman, 1999).

2.1.4 Microscopy techniques

2.1.4.1 Immunofluorescence staining

Cells were seeded on glass 13 mm coverslips pre-coated with poly-L-Lysine. After each individual experiment, cells were washed twice with 1x PBS. Cells were immediately fixed using paraformaldehyde 3.7% (v/v) in PBS for 10 minutes at RT, washed once with 1x PBS, and then permeabilized using 0.1% (v/v) Triton X-100 in PBS for 5 minutes at RT. Cells were gently washed twice with cold PBS. To block non-specific binding, coverslips were inverted on to blocking buffer (see Appendix A) on parafilm. Blocking was carried out at room temperature for 10 minutes in a humidified chamber in the dark. After blocking, cells were incubated with the required concentration of primary

antibodies (see Appendix E), dissolved in blocking buffer for 2 hours in the same way as in the blocking step. Gentle washing of the coverslips in PBS reduced low affinity primary antibody binding. Coverslips were incubated with fluorophore-labelled secondary antibodies, dissolved in blocking buffer, in a similar manner to the primary antibodies (see Appendix E). Multiple washes of coverslips in PBS reduced the excess of secondary antibody binding. Coverslips were allowed to dry and mounted on to a glass slide using a preservative antifade mounting medium (see Appendix A) and stored overnight at 4°C in the dark, prior to microscopy analysis (Fincham, James, Frame, & Winder, 2000).

2.1.4.2 Epifluorescence microscopy

Epifluorescent images were taken using a Leica DMIRE2 inverted fluorescence microscope powered by a Leica CTRMIC controller. Images were taken using a Leica HCX PL 63x immersion oil objective lens and a Leica DC350F CCD camera and acquired using Leica QFluoro software.

2.1.4.3 DeltaVision microscopy

Widefield deconvolution microscopy was performed using a DeltaVision RT system (Applied Precision, Issaquah, WA, USA).

Samples were analyzed with an Olympus 60x/1.40, PlanApo oil objective. The excitation bandwidths were 340-380 nm, 480-500 nm, and 541-569 nm for the blue, green and red channels, respectively. The emission filters had bandwidths of 432-482 nm, 541-569 nm and 581-654 nm for the blue, green and red channels respectively. Images were captured using a Photometrics COOLSNAPHQ CCD camera. Image data was deconvolved using the SoftWorx constrained iterative deconvolution algorithm.

2.1.5 Protein biochemistry techniques

2.1.5.1 Protein extraction from mammalian cells

Cells on petri dishes were washed twice with cold 1x PBS, followed by direct cell lysis with 1x RIPA or mild cell lysis buffer supplemented with protease and phosphatase inhibitors (see Appendix A) at 4°C for 15 minutes. Cell extracts were collected using a cell scraper, and then transferred to a micro-centrifuge tube. Lysates were briefly sonicated to shear the DNA and clarified by centrifugation at 18000 x *g* for 15 minutes at 4°C to pellet cell debris. The supernatant was then transferred into a new tube and stored at -20°C.

2.1.5.2 Cell fractionation

Cells were washed twice with cold 1x PBS and then scraped in a minimum volume of cold hypotonic Buffer I (see Appendix A). Plasma membrane was then further disrupted using a cold glass Dounce homogenizer. The homogenate was spun down at 600 x *g* for 10 minutes at 4°C. Pellet (nuclei) and supernatant (non-nuclear) were retained for further purification. Nuclear contaminants were removed from the non-nuclear fraction by centrifuging the supernatant twice at 9300 x *g* for 10 minutes at 4°C. The pellet was discarded and the final supernatant was saved as the purified non-nuclear fraction.

The nuclear fraction was further purified by resuspending the nuclear pellet in equal volumes of Buffers II and I (see Appendix A). This mixture was carefully overlayed on an equal volume of a 1.8 M sucrose cushion and then spun down at 30000 x *g* for 1 hour at 4°C. The supernatant was discarded and the pellet was recovered as the purified nuclear fraction. The pellet was resuspended in a small amount of either RIPA or lysis buffer according to the requirements of each particular experiment and clarified as in section 2.1.5.1. Non-nuclear and nuclear fractions were stored at -20°C (Mathew et al., 2013).

2.1.5.3 Protein quantification using the Micro BCA Protein Assay Kit

The concentration of protein in cell lysates was determined following the recommendations of the manufacturer (Thermo scientific, product no. 23235). Briefly, proteins were diluted 1/125 using RIPA buffer to a final volume of 500 μl and then mixed with 500 μl of working reagent. The mixture was incubated at 60°C for 1 hour and then allowed to cool to RT. The absorbance of the samples was determined at 562 nm against a blank composed of a mixture of RIPA and working reagent. The total amount of protein was determined by interpolating the absorbance of the samples against a standard curve (0-200 μg/ml) prepared using dilutions of BSA as a standard.

2.1.5.4 Immunoprecipitation with protein A

30 μl of 50% protein A slurry (Amintra, expedeon) were transferred to a 1.5 ml tube and washed three times with cold RIPA buffer. To pre-clear the sample, beads were combined with protein lysates and incubated at 4°C on a tube roller for 1 hour at 4°C. Beads were pelleted by centrifugation at 15000 x g for 30 seconds at 4°C.

A small aliquot of pre-cleared lysate was saved as the input sample. The remaining pre-cleared lysate was divided in two. One half was combined with the desired antibody according to the dilutions shown in Appendix E and the other half was left without antibody (control). Samples were incubated on a tube roller for 2 hours at 4°C. Thereafter, samples with and without antibody were incubated for an additional hour with 30 μl of pre-equilibrated protein A on a tube roller at 4°C followed by centrifugation at 15000 x g for 30 seconds. The supernatant was kept on ice and the beads were washed three times with cold RIPA buffer. A small aliquot of input, supernatants and beads were combined with the respective amount of 2x Laemmli loading buffer and boiled at 100°C for 5 minutes.

2.1.5.5 Immunoprecipitation of Flag tagged proteins with anti-Flag M2-agarose affinity gel

The protocol followed was that provided by the manufacturer (Sigma, cat. no. A2220). Flag M2 resin was thoroughly resuspended and transferred to a clean tube. The resin was washed five times with 1x TBS buffer (20x gel volume) at 7000 x *g* for 30 seconds. After removing the supernatant, the resin was combined with the required amount of lysate (total lysates, cell fraction lysates, etc.) and adjusted to a final volume of 1000 μl with lysis buffer.

Samples were left incubating on a tube roller at 4°C for 2 hours to overnight. After the incubation period, the resin was recovered by centrifugation at 7000 x *g* for 30 seconds, and the supernatant was removed by pipetting using a narrow-end pipette tip. Beads were then washed 3 times with chilled 1x TBS.

Protein elution was performed by competition with 100 μl of the 3x Flag peptide (Sigma, cat. no. F4799) to a final concentration 300 ng/μl. Samples were incubated on a tube roller for 30 minutes to 1 hour at 4°C and centrifuged at 7000 x *g* for 30 seconds. The supernatant was transferred to a new tube for immediate use or stored at -20°C.

2.1.5.6 Ubiquitin enrichment from LNCaP whole cell lysates

The total lysates used for this experimental approach were obtained as described in the section 2.1.5.1 using RIPA buffer supplemented with 10 mM NEM. 500 μg of clarified extracts were then diluted with RIPA buffer (without any Triton X-100) to a final concentration of 0.25% Triton X-100 and incubated with 40 μl or agarose-GST or agarose-MD beads on a tube roller at 4°C for 3 hours. Supernatants and beads were collected by centrifugation at 700 x *g* for 2 minutes. Beads were subjected to two washes with high salt buffer (RIPA buffer 0% Triton X-100 supplemented with 500 mM potassium acetate), two washes with low salt buffer (RIPA buffer 0% Triton X-100 plus 50 mM potassium acetate) and one wash with RIPA buffer 0% Triton X-100. Beads were finally resuspended in an equal amount of 2x Laemmli loading

buffer and boiled at 100°C for 5 minutes (M. D. Wilson et al., 2012).

2.1.5.7 Sodium orthovanadate activation

In order to achieve a maximal inhibition of protein phosphotyrosyl-phosphatases, sodium orthovanadate 200 mM was adjusted to pH 10.0 using 1 N NaOH or 1 N HCl. The solution was boiled until turned colorless. The pH was readjusted and stabilized to 10, through different rounds of boiling-cooling (Gordon, 1991).

2.1.5.8 In vitro protein dephosphorylation assay using Calf Intestinal Phosphatase (CIP)

Dephosphorylation of proteins was carried out by combining a volume of lysate containing 40 μg of protein with 40 U of CIP and NEBuffer 3 (New England Biolabs, prod. no. M0290S). The mixture was adjusted to the desired final volume using distilled water. The mixture was incubated at 37°C for 1 hour and then stopped by the addition of an equal volume of 2x Laemmli loading buffer.

2.1.5.9 Sodium Dodecyl Sulphate Polyacrylamide Gel Electrophoresis (SDS-PAGE) (single concentration and gradient gels)

Pre-clarified protein samples were mixed with the required amount of 5x Laemmli loading buffer, boiled at 100°C for 5 minutes and then cooled to RT. Mini-gels (10 cm x 10 cm x 1 mm) were run using the BioRad mini-gel system. Resolving gels were prepared at 7.5%, 10% or 12.5% concentration and the stacking gels at 5% concentration (see Table D.1). Samples were separated at 150 volts while running in the stacking gel and resolved at 200 volts while running in the resolving gel.

For gradient gels, the concentrations of resolving and stacking gels are given in Appendix D (Laemmli, 1970).

2.1.5.10 Tricine-SDS-PAGE discontinuous gels

The preparation of these gels was performed employing the setup used for multiple gradient gels and the protocol described by Schägger and Von Jagow, (1987) (Schägger & von Jagow, 1987).

For the preparation of resolving 11%T, 0.67% gels (see Table D.3), the amounts of acrylamide and bisacrylamide were calculated using the following formulas (`http://www.carlroth.com/media/_en-com/usage/3039.pdf`).

$$V_a = (T \text{ x } (100\text{-}C) \text{ x } V_t)/4000^*$$

$$V_b = (T \text{ x } C \text{ x } V_t)/200$$

Where:

V_t=Total volume of gel casting solution (ml)
T = Gel concentration in % = % acrylamide + % bisacrylamide
C = % crosslinking =(% bisacrylamide x 100)/T
V_a = volume gel A (acrylamide) in ml
V_b = volume gel B (bisacrylamide) in ml
* The concentration of acrylamide was 40%, hence the factor 4000.

2.1.5.11 Electrotransfer

Proteins were electroblotted to polyvinylidene fluoride (PVDF) membranes activated in methanol (Immobilon-PSQ, 0.2 μm, Merck Millipore) using a Mini Trans-Blot electrophoretic transfer cell (Bio-Rad). After electrophoresis, the gel, together with the fiber pads and the filter papers, was soaked in Towbin buffer supplemented with 20% (v/v) methanol and 0.02% (w/v) SDS for 10

minutes (see Appendix A). Following this, all components were assembled in a gel sandwich as required by the Mini Trans Blot electrophoretic transfer system. The chamber was filled with Towbin transfer buffer supplemented with 20% methanol and 0.02% SDS. An even buffer temperature (generated by the Bio-Ice cooling unit) and ion distribution were maintained by stirring (Towbin, Staehelin, & Gordon, 1979).

2.1.5.12 Western blotting

After electroblotting of proteins to PVDF membranes, membranes were soaked in TBST to eliminate the excess SDS. Membranes were then incubated with blocking buffer (5% skimmed milk (w/v) in TBST) for 30 minutes at RT. The membrane was then incubated overnight at 4°C with the primary antibody diluted in blocking buffer according to the required dilution of each specific antibody (see Appendix E). The following day, membranes were washed three times with TBST for 10 minutes each at RT in order to eliminate the excess primary antibody. Following this, membranes were incubated with a secondary antibody (see Appendix E) diluted in blocking buffer for 1 hour at RT. Antibodies not bound to the membrane were reduced by washing the membrane 3x with TBST for 10 minutes each. The presence of specific proteins on the membrane was revealed by the chemiluminescent signal generated by the mixture and addition of equal volumes of ECL I and II solutions to the membrane (see Appendix A) (Miller et al., 2012). Chemiluminescent signal was recorded using a BioRad Chemidoc XRS+ system.

2.1.5.13 Membrane stripping

The removal of primary and secondary antibodies from PVDF membranes was achieved by incubating the membranes with mild stripping buffer (see Appendix A). Membranes were incubated at RT twice with mild stripping buffer for 15 minutes, then twice with 1x PBS pH 7.4 for 15 minutes and,

finally twice with TBST for 10 minutes. After blocking with milk 5% (w/v) in TBST, membranes were ready for incubation with another desired antibody.

2.1.5.14 Coomassie blue safe staining of SDS-PAGE gels

After SDS electrophoresis, gels were rinsed briefly with distilled water. Coomassie blue safe stain (see Appendix A) was poured on the gels and microwaved for 10 seconds. Following incubation on a moving platform at RT for 1 hour, staining solution was discarded. Further washing of the gel with distilled water, usually overnight, removed non-specific staining and revealed protein bands (`http://www.labtimes.org/labtimes/issues/lt2008/lt06/lt_2008_06_53_53.pdf`). Gels were imaged in the ChemiDoc XRS+ using the image Lab software (BioRad).

2.1.6 Imaging techniques

2.1.6.1 Western blot band quantification and data analysis

Chemiluminescent signal was imaged using the ChemiDoc XRS+ (BioRad) and the quantification of band intensity was performed using image Lab software (BioRad). Images with saturated pixels were not considered for quantification. The values obtained from the bands were then exported and analyzed with GraphPad Prism 6. In all the cases the mean calculated was the average of a minimum of three independent experiments. The average and standard error of the mean (SEM) were plotted and used to distinguish changes between controls and treatments.

2.1.7 Proteomic techniques

Solutions were prepared using MilliQ water at 18.2MΩcm^{-1} and the chemicals/solvents used were LC-MS grade.

2.1.7.1 Reduction and alkylation of proteins

To reduce proteins, DTT (dithiothreitol) prepared fresh to a final concentration of 1mM was mixed with sample loading buffer. The mixture was incubated at 70° for 10 minutes and then allowed to cool down before alkylation. The sample was alkylated with fresh prepared IAA (iodoacetamide) to a final concentration of 2 mM. The mixture was further incubated for 30 minutes at room temperature in the dark.

2.1.7.2 In gel protein di-methyl labeling

Gel slices were completely destained with 50% ACN (acetonitrile) and shrunk with 100% ACN. The excess of ACN was eliminated by evaporation and the gel slices were incubated with labeling solution (0.4% formaldehyde (v/v) (Sigma, prod. no. F1635), 60 mM cyanoborohydrade (Aldrich, prod. no. 156159) in 0.25 M MES buffer pH 5.5 (prepared fresh)) in a thermomixer at RT for 30 minutes. The labeling solution was removed and the gel pieces were washed 5 times with 50% ACN/100 mM ammonium bicarbonate. The gel slices were shrunk once more with 100% ACN before proceeding with tryptic digestion.

2.1.7.3 Brilliant blue G-colloidal staining compatible with mass spectrometry

After SDS electrophoresis, gels were rinsed with Milli-Q water. Proteins were fixed in a solution containing 40% methanol / 2% acetic acid (v/v) for 1 hour. Following this, gels were stained for 2 hours with brilliant blue G-colloidal according to the instructions provided by the company (Sigma, prod. no. B-2025).

Gels were destained with 25% methanol for 2 hours and then left in Milli-Q water until further processed.

2.1.7.4 Tryptic digestion and peptide extraction from gel slices

All the solutions used for tryptic digestion were prepared fresh before use.

Excised gel slices were placed in Protein LoBind tubes (Eppendorf, cat. no. 0030108116) and fully destained by the addition of 50% ACN /50 mM ammonium bicarbonate pH 8.5 followed by incubation at RT for 30 minutes. The liquid was removed by centrifugation at 600 x g; this step was repeated until gel slices were colorless (from hours to overnight). To secure the complete destaining, the gel slices were incubated once more with 100% ACN for 15 minutes at RT. Once the liquid was discarded the gel slices were stored at 4°C until tryptic digestion.

Before digestion, Sequencing Grade Trypsin from bovine pancreas (Roche, cat. no. 11418475001) was prepared as follows:

Stock solution: Trypsin was prepared at a concentration of 0.1 μg/μl using 0.1% TFA.

Working solution: Trypsin was prepared at a final concentration of 1 ng/μl using 50 mM Ambic.

To perform digestion, dried gel slices were incubated with trypsin (working solution) in a thermomixer (600 rpm) for 1 hour at 37°C. Samples were then left incubating at 25°C overnight.

Next day, after centrifugation at 600 x g for 1 minute, the supernatants were collected into a new tube SCT (supernatant collection tube). Further extraction of peptides was performed by incubating the gel slices with 100% ACN at 37°C for 20 minutes followed by collection of supernatants as before.

Gel slices were further incubated with 0.5% formic acid at 37°C for 20 minutes and then 100% ACN for the same time and temperature followed by the collection of supernatants into SCT as stated before. After a further repetition of this step, gel slices were incubated with 100% ACN at 37°C for 15 minutes followed by the collection of supernatants into the SCT.

Extracted peptides were dried down using a SpeedVac concentrator and then stored at 4°C.

Before the analysis by LC-MS the peptides were resuspended in 0.5% formic

acid at RT for 10 minutes with gentle shaking.

2.1.7.5 HPLC-Mass spectrometry settings

100% of resuspended peptides was injected, using a Dionex Ultimate 3000 uHPLC, onto a PepMap100 C18 2 cm x 75 μm I.D. trap column (ThermoFisher Scientific) at 5μl/min in 0.1% formic acid, 2% acetonitrile and 45°C in the column oven and 6°C in the autosampler. The sample was separated, over a 60-minute gradient of increasing acetonitrile from 2.4% up to 72%, in 0.1% formic acid, using a 15 cm PepMap100 C18 analytical column (2 μm particle size, 100 Åpore size 75 μm I.D.) (ThermoFisher Scientific) at 300 nl/min and 45°C.

The mass spectrometer analyzer used was an ETD (electron transfer dissociation) enabled ThermoFisher-Scientific Orbitrap Elite, equipped with a Nanospray Flex Ion ESI source (ThermoFisher Scientific). Nanospray ionization was carried out at 2.3 kV, with the ion transfer capillary at 250°C, and S-lens setting of 60%. MS1 spectra were acquired at a resolving power of 60,000 with an AGC (automatic gain control) target value of $1x10^6$ ions by the Orbitrap detector, with a range of 350-1850 m/z. Following MS1 analysis the top 15 most abundant precursors were selected for data dependant activation (MS^2 analysis) using CID (collision induced dissociation), with a 10 ms activation time, and an AGC setting of 10,000 ions in the dual cell linear ion trap on normal scan rate resolution. Precursor ions of single charge were rejected, and a 30 second dynamic exclusion window setting was used after a single occurrence of an ion.

2.1.7.6 Data analysis

Data analysis from 4 biological replicates was performed using the MaxQuant and Perseus v 1.4 databases. For protein identification, false discovery rates (FDRs) at both the protein and peptide levels were set at 1% by decoy database

searching. Proteins with 3 valid intensity values in the Flag-βDG immunoprecipitations were considered for quantification. Missing values for proteins with 2 or more missing values in the control IP were impute from a down shifted normal distribution. The statistical analysis was then performed by t-testing with correction for multiple hypothesis testing at two thresholds, 0.05 (5% FDR) and 0.01 (1% FDR). A fold enrichment (S0) = 2 for both, non-nuclear and nuclear fractions was included in the statistical analysis. Proteins required a minimum of two peptides or above in order to be reported.

3 Beta-dystroglycan protein modifications

3.1 Introduction

The human body can develop its activities thanks to the precise and coordinated action of its organs and systems, which is dictated by the homeostatic status of its cells. The vast collection of proteins within cells orchestrates most of the cellular functions such as perception of the extracellular environment, inter and intra cellular communication, cellular shape, internal organization, structural integrity and several other functions.

The functional regulation of proteins, from integral membrane proteins to metabolic enzymes and transcription factors, is achieved by an array of post-translational modifications (PTM). The concerted regulation in space and time of PTM such as acetylation, phosphorylation, glycosylation, sumoylation, methylation, proteolysis, ubiquitination and others, dictate the functional activity of the proteins. Under certain conditions, these PTM either individually or as combinatorial sequence of events, affect the stability, concentration, conformational changes, interactions, cellular location and other functions, of specific target proteins as shown in Figure 3.1 (Deribe, Pawson, & Dikic, 2010; Filtz, Vogel, & Leid, 2014; Jensen, 2006).

Plasma membrane proteins have to be subject to dynamic and strict quality control mechanisms through different post-translational modifications in order to regulate a vast array of signalling pathways. Also, these mechanisms have the function of detecting and removing proteins from this environment that

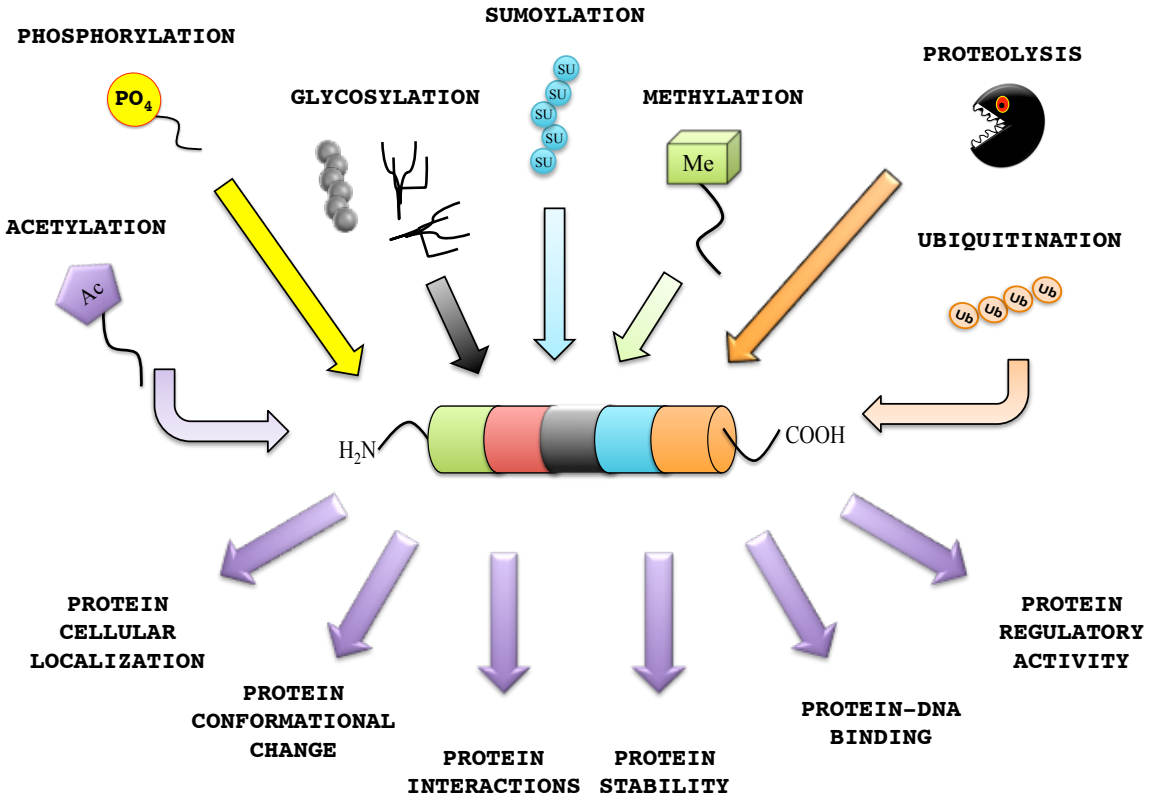

Figure 3.1: Protein post-translational modifications. Proteins are subject to a vast array of modifications affecting key cellular functions.

otherwise could damage the cellular integrity (Babst, 2014). In these instances, PTM functions as a form of quality control.

The dystrophin glycoprotein complex spans the plasma membrane providing structural integrity to muscle cells during processes of contraction and relaxation. Also, due to its ability to interact with signalling molecules, this complex is thought to be an important modulator of signalling events from the extra to the intracellular environment (Constantin, 2014; Moore & Winder, 2012).

Dystroglycan, an important core protein within this complex, performs both mechanical and signalling functions. By interacting with the laminin, agrin, perlecan and neurexin extracellular matrix components, and cytoskeletal linker proteins (e.g., dystrophin/utrophin) in the intracellular environment, dystroglycan provides a structural link, which is important for the adhesion and communication of the cell with the surrounding environment and vice

versa (Barresi & Campbell, 2006; Henry & Campbell, 1999; Sgambato & Brancaccio, 2005).

Besides its structural activities, dystroglycan is an important modulator of a multitude of signalling events. The presence of a structurally disordered cytoplasmic domain seems to confer an advantage to beta-dystroglycan for its interaction with a great variety of signalling molecules in specific cellular situations. Importantly, the phosphorylation of a tyrosine in its C-terminal motif PPXY seems to be an important master switch modulating these protein interactions (Bozzi, Morlacchi, et al., 2009; Moore & Winder, 2010).

Given the important and dynamic functions of this type I transmembrane protein, its quality control, turnover and remodelling, all have to be under tight control in order to avoid the impairment of the plasma membrane. Such impairments are linked to severe outcomes, such as defects during development, muscular dystrophies and cancer (Godfrey et al., 2011; Sgambato & Brancaccio, 2005; Williamson et al., 1997).

Phosphorylation, glycosylation, proteolysis and ubiquitination, are the PTM most commonly studied with beta-dystroglycan. Regarding phosphorylation, it has been shown that the presence of a phosphate group on Y892 (of human dystroglycan) is able to regulate the structural interaction of beta-dystroglycan with dystrophin or utrophin, and the stability of the other associated proteins, rendering beta-dystroglycan, presumably, susceptible to targeting for proteasomal degradation (Ilsley et al., 2001; James et al., 2000; Miller et al., 2012; Sotgia et al., 2001). Additionally, the same Y892, is thought to be a potential regulator of signalling events by virtue of its proposed interaction with signalling molecules (Sotgia et al., 2001). Recently, it was hypothesized that in addition to Y892, other phosphorylated tyrosines in beta-dystroglycan could have potential roles in key cellular events, such as the processes of arenavirus infection (Moraz et al., 2013). In addition to tyrosines, the cytoplasmic domain of beta-dystroglycan is particularly rich in serine/threonine residues, which may also be the target of phosphorylation.

Ubiquitination seems to be another PTM modulating key events on dystro-

glycan. Indirect experimental evidence suggests that not only dystroglycan, but also other members of the dystrophin associated protein complex (DAPC) axis could be subject to ubiquitination. In laminin alpha2 chain deficient mice, an up-regulation of components of the ubiquitin proteasome system was observed (Carmignac, Quéré, & Durbeej, 2011). Similarly, an up-regulation of the E3 ubiquitin ligases Atrogin-1/MAFbf and MuRF1, was observed in cancer induced *mdx* mice (these ligases were subsequently reduced upon the restoration of the dystrophin glycoprotein complex (DGC)) (Acharyya et al., 2005). Furthermore, although not directly investigated here, the restoration of components of the DAPC upon treatment with MG132 in dystrophic mice models suggest their modification by ubiquitination in proteolytic mediated events (Assereto et al., 2006; Bonuccelli et al., 2003; Kumamoto et al., 2000).

Together, these studies provide important evidence that phosphorylation events on dystroglycan, as well as ubiquitination, regulate dystroglycan and may regulate cellular processes as a result. The studies presented thus far support the hypothesis of additional phosphorylation events carried out on phosphorylatable amino acids other than Y890 and the modification of dystroglycan by ubiquitination.

In this chapter, the characterisation of the LNCaP cell line for the localisation of endogenous dystroglycan will be described. The characterisation of the recombinant dystroglycan proteins used to study the phosphorylation-ubiquitination post-translational modifications will also be presented. Additionally, it will be shown that dystroglycan is modified with phosphates and ubiquitin groups.

3.2 Cellular distribution

Beta-dystroglycan is a ubiquitous protein expressed in all vertebrate cells and tissues (`http://www.genecards.org`). Its expression, post-translational modifications such as glycosylation and proteolysis, effects in epithelial to mes-

enchymal transition (a process linked to development and cancer progression), migration and metastasis and its nuclear translocation have been characterized using the LNCaP cell line, a widely used model of prostate cancer (Mathew et al., 2013; Mitchell et al., 2013; Sgambato et al., 2007).

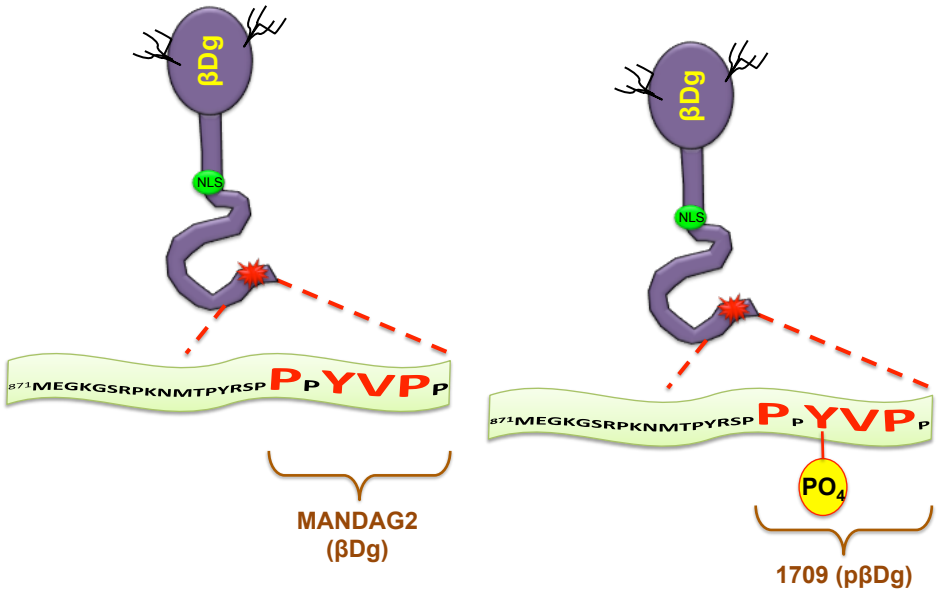

(a) (b)

Figure 3.2: Binding epitopes of Mandag2 and 1709 antibodies. The schematic shows the residues 871-893 on the carboxy-terminus domain of beta-dystroglycan. In (a), Mandag2 antibody detects the non-phosphorylated form of the PXYVP epitope (amino acids highlighted in red), while 1709 antibody (b) binds a phosphorylated tyrosine within the same epitope (residues highlighted in red).

A basic cellular characterisation for the localisation of dystroglycan in LNCaP cells was carried out. Lysates of wild type LNCaP cells were collected and either used directly or processed by biochemical fractionation. Lysates and fractions were then analysed by western blot using antibodies raised against non-phospho- and phospho-βDg, herein referred to as βDg and pβDg respectively. Given the critical role of the phosphorylated tyrosine 892, it was important to differentiate the cellular distribution of βDg and pβDg. In order to achieve this, it was decided to use the Mandag2 and pYβDG (1709) antibodies. These antibodies were produced in the Morris and Winder labs respectively (Helliwell, Nguyen, & Morris, 1994; Ilsley et al., 2001). The subsequent characterisation by peptide spot assays showed that, Mandag2 binds

the PxYVP epitope located in the C-terminus of βDg, while pYβDG binds a phosphorylated tyrosine within the same epitope (James et al., 2000; Miller et al., 2012) (Figure 3.2).

By using both antibodies, it was possible to detect the full-length 43 kDa beta-dystroglycan (Full) in total lysates and in non-nuclear and nuclear fractions. Additionally, in total lysates, other smaller species with sizes of 36 (herein referred to as 31) and 26 kDa were observed (Figure 3.3). Previous reports have pointed out that these species belong to the transmembrane anchored domain (TM) and to the cytoplasmic fragment (Cyto) of beta-dystroglycan respectively (Mitchell et al., 2013; Yamada et al., 2001). Importantly, the cytoplasmic fragment was distributed between the non-nuclear and nuclear fractions (Figure 3.3).

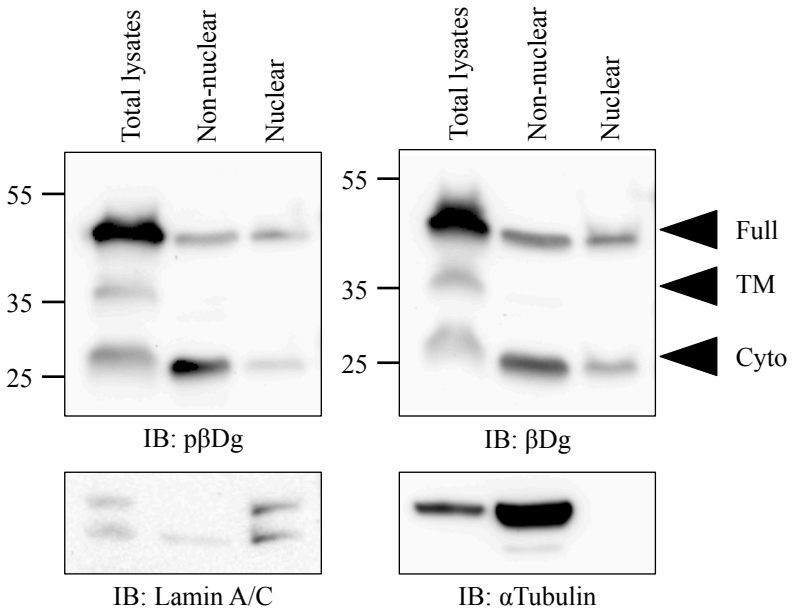

Figure 3.3: Cellular distribution of beta-dystroglycan in LNCaP cells. LNCaP WT cells were collected for total lysates or for biochemical fractionation. Western blot analysis of the lysates using Mandag2 and pYβDG antibodies shows the non-nuclear and nuclear localisation the 43 (Full) and 26 (Cyto) kDa forms of non-phospho-(βDg) and phospho-beta-dystroglycan (pβDg). Lamin A/C and alpha-tubulin are shown as the loading controls of the nuclear and non-nuclear fractions respectively.

The results obtained from the biochemical fractionation were corroborated by immunocytochemistry analysis through the use of organelle-specific protein

markers such as lamin A/C and Fibrillarin, and alpha-tubulin and GAPDH, for nuclear and non-nuclear fractions respectively. The presence and quantification of these protein markers provided an idea about the purity of the cellular fractions (Lodish et al., 2008). With Mandag2 the signal is distributed throughout the cell. Filopodia structures were well stained in addition to the plasma membrane and parts of the cytoplasm. Interestingly, βDg also had a nuclear distribution along the nuclear envelope-like structure (white arrowhead) and nucleoplasm. The signal around the nuclear envelope is not an experimental artefact (the signal generated by secondary antibodies was observed to be at very low levels in control immunofluorescences) as most of the cells analysed in middle stack sections of confocal microscopy images showed a similar pattern (Figure 3.4, left). The phosphorylated form of beta-dystroglycan had a more cytoplasmic and nucleoplasmic distribution (it was also found distributed along the nuclear envelope-like structure, white arrowhead). It is interesting to note that pβDg is found surrounding the DNA of metaphase cells (white arrow) (Figure 3.4, bottom right). The potential nuclear functions of beta-dystroglycan, such as in the cell cycle or nuclear regulation, are discussed later in this work.

Taken together, these results show that in LNCaP WT cells both βDg and pβDg are distributed throughout non-nuclear and nuclear fractions as shown by biochemical and immunocytochemistry analysis. Importantly, the nuclear distribution of beta-dystroglycan supports use of the LNCaP cell line as a good model to study the hypothesis that this protein has nuclear functions.

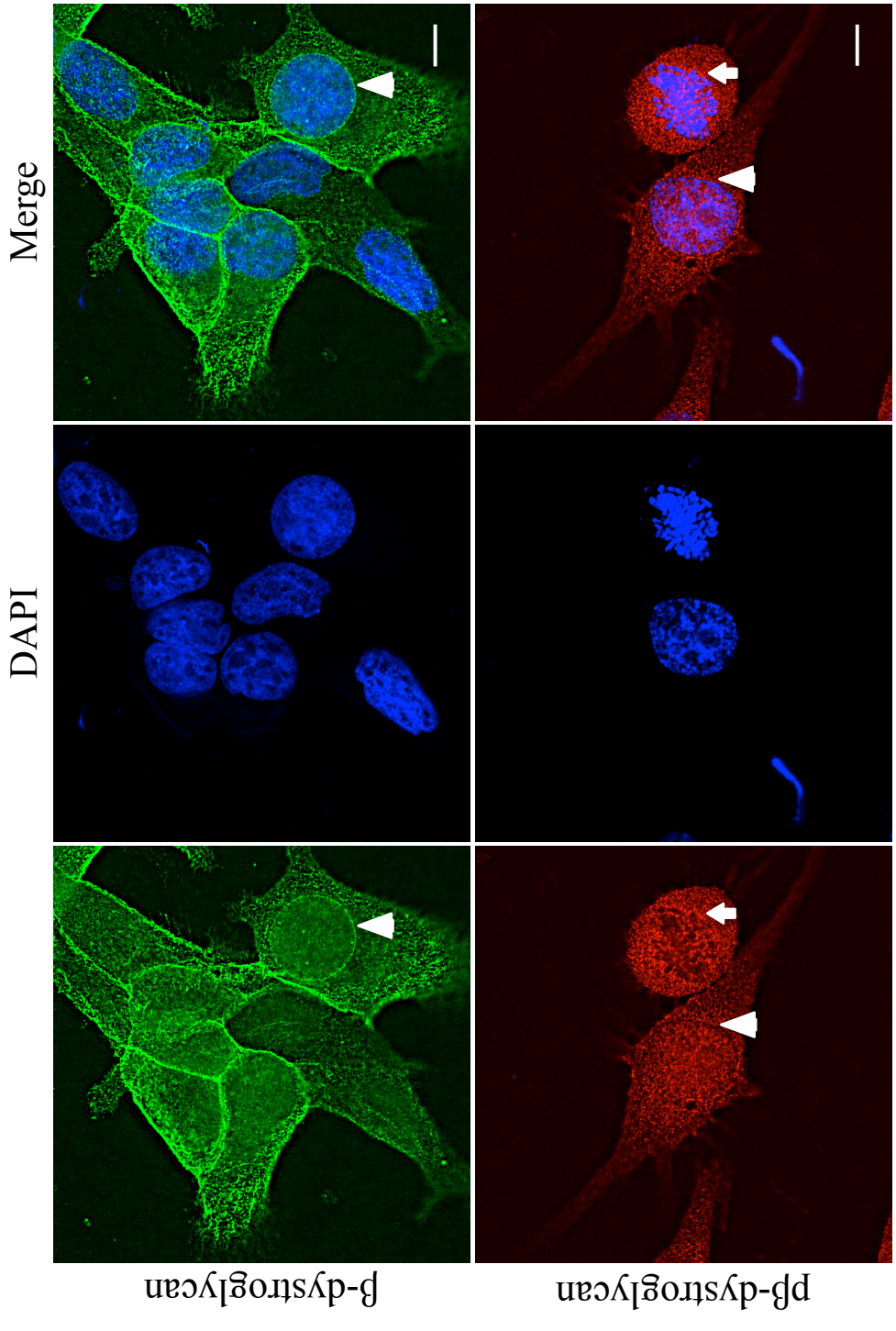

Figure 3.4: Cellular localisation of beta-dystroglycan in LNCaP cells. LNCaP cells were immunostained with antibodies anti-βDg (green) and anti-pβDg (red). A middle stack section of deconvolved confocal microscopy images shows the localisation of βDg in the cytoplasmic and nuclear compartments of the cells. Nuclei were counterstained with DAPI. Scale bar = 10 μm.

3.3 A C-ter tag affects the phosphorylation of Y890

The insertion of tags such as myc/his or GFP, in the C-terminus of beta-dystroglycan could be a good strategy for its isolation, purification and localisation, but on the other hand, these tags could affect the PTM of neighbouring amino acids and the interaction of beta-dystroglycan with other proteins.

Dystroglycan is an important cell adhesion molecule subject to PTM such as phosphorylation and tags that alter PTM may have a profound effect on normal processing. For example, the phosphorylation of Y890 in the C-terminal of mouse beta-dystroglycan, has been reported to be an important PTM regulating both stability (Miller et al., 2012) and the interaction with other proteins such as dystrophin/utrophin and other proteins containing SH2 domains (Ilsley et al., 2001; James et al., 2000; Sotgia et al., 2001).

To verify if the presence of a myc/his tag in the C-terminus of mouse βDg affects its phosphorylation (Figure 3.5a), lysates of LNCaP cells transfected with a plasmid encoding $\alpha\beta$Dg-myc/his were subjected to immunoprecipitation with an anti-myc antibody. Figure 3.5b shows that the pYβDG antibody is able to detect phosphorylated beta-dystroglycan in the supernatant fraction but not in the pellet fraction of the immunoprecipitation performed with the anti-myc antibodies. The presence of an additional faint band in the pellet fraction is suggestive of beta-dystroglycan being phosphorylated on an amino-acid other than Y890. The immunoblot of the same lysates with anti-myc antibodies shows that there was a strong enrichment of βDg immunoprecipitating with anti-myc antibodies, but this was not subject to phosphorylation as it was not detected by the pYβDG antibody (at least the band that belongs to the 43 kDa βDg) (Figure 3.5b). Overall, through immunoprecipitation assay, it has been shown that the insertion of a myc tag in the C-terminus of beta-dystroglycan affects its phosphorylation, making it a non-suitable recombinant protein for downstream analysis, such as those dependent on the phosphorylation of Y890.

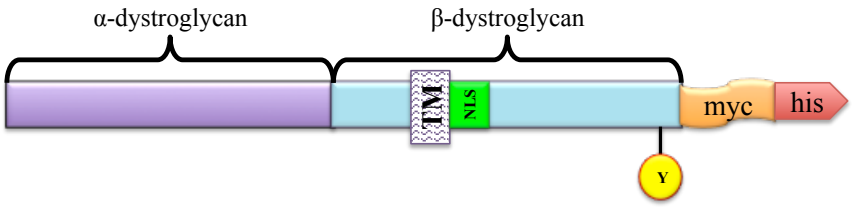

(a)

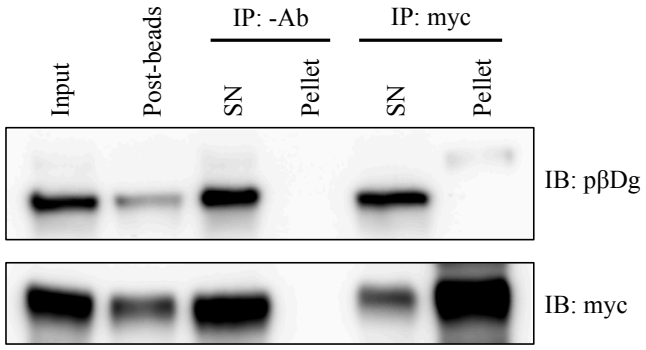

(b)

Figure 3.5: The myc/his tag inhibits the phosphorylation of Y890 in beta-dystroglycan. (a) Schematic showing the structure of dystroglycan and the position of the myc/his tag in its C-terminus. (b) LNCaP cells were transfected with the plasmid pcDNA3.1(+)-$\alpha\beta$Dg-myc/his and allowed to grow for 24 hours. Cells were collected with RIPA buffer and subjected to immunoprecipitation with anti-myc antibodies. Input, eluates and pellets were resolved by SDS-PAGE. Immunoblot analysis with antibodies anti-pβDg shows the absence of immuno-reactivity.

3.4 The transgenic LNCaP-$\alpha\beta$DgFlag cell line

Having shown that the insertion of a tag in the C-terminus of βDg affects an important PTM, such as the phosphorylation of Y890, we were prompted to generate a new plasmid encoding full-length dystroglycan (alpha and beta) with the insertion of tag in a position with minimum deleterious effects. Flag tags are hydrophilic 8 amino acid peptides proven to be detected by high specific antibodies such as M1, M2 and M5. Due to its hydrophilic nature, this tag has a high probability of being located on the surface of the proteins, allowing a better detection by antibodies and having a minimum effect in the functionality of the protein (reviewed in (Einhauer & Jungbauer, 2001)). By using the ELM server (`http://elm.eu.org`) which predicts functional sites in proteins, a region near amino acid 800 was identified with minimal interactions.

Also, the alignment of the sequence of the Flag tag with the primary sequence of βDg showed that there were some amino acids shared between the two sequences, requiring minimal changes to generate the Flag tag (Figure 3.6a). Taking into account these characteristics, the Flag tag was inserted around residue 800, and downstream the proposed NLS of βDg (Lara-Chacón et al., 2010) (Figure 3.6b).

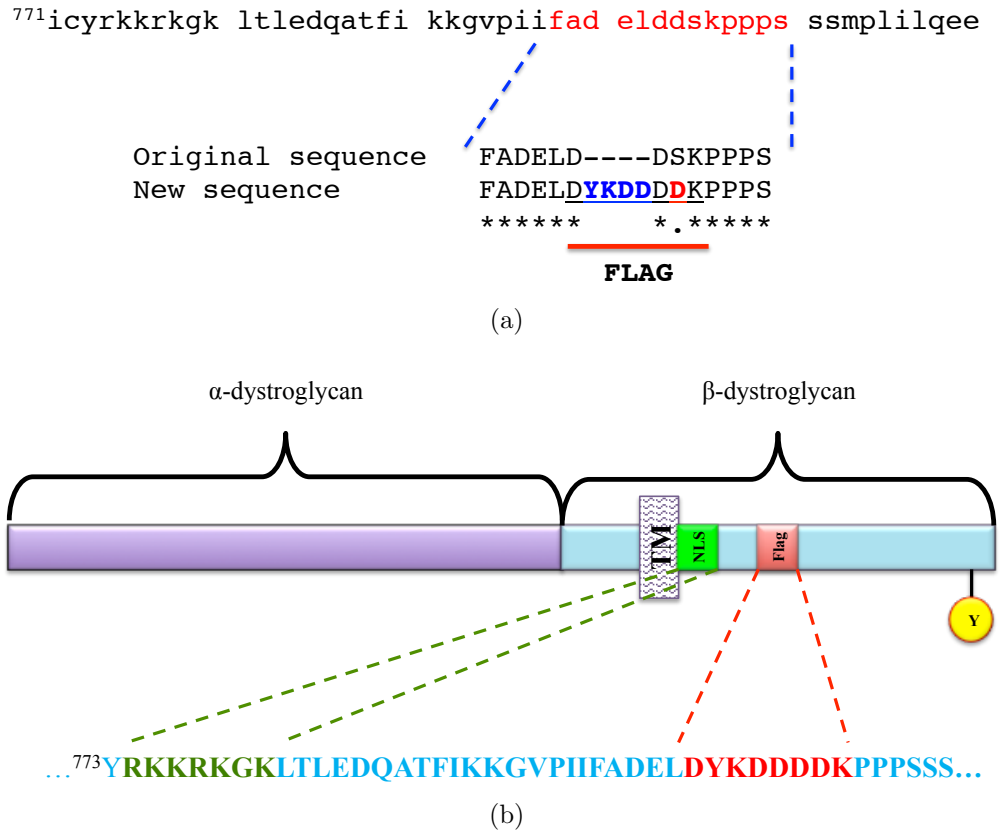

Figure 3.6: Insertion of the Flag tag in the coding sequence of mouse αβDg. (a) To generate the Flag tag in the primary sequence of mαβDgFlag, a pair of oligonucleotides was designed to insert the residues YKDD (blue) and to change the amino acid S to D (red) (see Appendix B). These changes were made in order to avoid major changes in the structure of βDg while inserting the whole sequence of Flag (underlined). Also, according to the Eukaryotic Linear Motif resource (`http://elm.eu.org`), the area used to insert the Flag tag is an area with no predicted interactions in βDg. (b) The schematic shows the final position of some key elements in the primary sequence of mαβDgFlag such as its TM domain, its NLS (green) and its Flag tag (red).

The generation of the Flag tag in mouse dystroglycan was confirmed by DNA sequencing and then subjected to DNA purification for the characterisation of the recombinant protein by western blot. LNCaP cells were transiently

transfected with the plasmid $\alpha\beta$DgFlag, allowed to grow for 24 hours and then collected for total lysates. The immunoblot analysis using anti-Flag M2 antibodies shows the presence of a strong band of approximately 43 kDa in the total lysates. Additionally, the antibody was able to detect bands above and below the 43 kDa form (Figure 3.7).

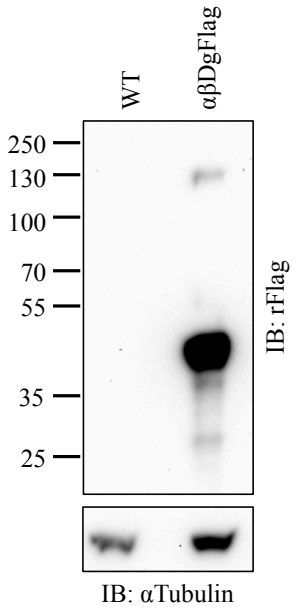

Figure 3.7: Characterisation of the recombinant DgFlag. The plasmid pcDNA3.1(+)-$\alpha\beta$DgFlag was used for transient transfection of LNCaP cells. Cells were collected for total lysates and subjected to immunoblot analysis with antibodies anti-Flag. Western blot analysis of total lysates shows a band of approximately 43 kDa and other bands in lysates of cells transfected. These bands were absent in lysates of cells not transfected indicating a high specificity of the antibody.

By immunoprecipitation it can be observed that, in addition to Flag antibodies (Figure 3.8a), pYβDG and Mandag2 antibodies had immunoreactivity with Flag-tagged βDg. There was a clear difference in the signal generated by pYβDG (Figure 3.8b) and Mandag (Figure 3.8c) indicating that the most abundant species of βDg is the phosphorylated form. Additionally, Flag antibodies were able to immunoprecipitate species of βDg of high (HDG_A and HDG_B) and low molecular weight (TM and Cyto). The origin of high molecular weight bands (HDG_B) is due to, presumably, PTM such as ubiquitination and phosphorylation (amongst others); and the band detected between 130-

250 kDa (HDG_A) could represent the propeptide of dystroglycan or perhaps, oligomerization of beta-dystroglycan, all of them a matter of discussion in the following sections.

By biochemical fractionation, there was a clear distribution of βDgFlag in non-nuclear and nuclear fractions of LNCaP cells (Figure 3.13).

By immunofluorescence, the distribution of βDgFlag was throughout the cell, presenting a clear signal on the plasma membrane, the cytoplasm and the nucleus. The Flag antibodies clearly co-localized with pYβDG and Mandag2 antibodies. Transfected LNCaP cells had an increased number of longer filopodia-like structures, microvilli and an increased number of branches compared with the wild type cells, a similar phenotype to that previously observed in myoblast, fibroblat, HeLa and other cell types (Batchelor et al., 2007; Y. J. Chen et al., 2003; Spence, Chen, et al., 2004; Thompson, 2007; Thompson et al., 2008). Also, beta-dystroglycan was observed around the cell body, with accumulation at the leading edges of the new filopodia and growth cone-like structures (Figure 3.9).

The branching and filopodia formation upon the overexpression of dystroglycan clearly resembled the observations previously reported by Eyermann and colleagues, in differentiating oligodendroglia (Eyermann, Czaplinski, & Colognato, 2012). Furthermore, some transfected LNCaP cells displayed neuronal-like morphologies.

Taken together, the biochemical and immunocytochemical analysis show that exogenous dystroglycan expressing the Flag tag has similar characteristics to the endogenous counterpart, making it a better candidate for localisation and interaction experiments than a carboxyl-terminal tag.

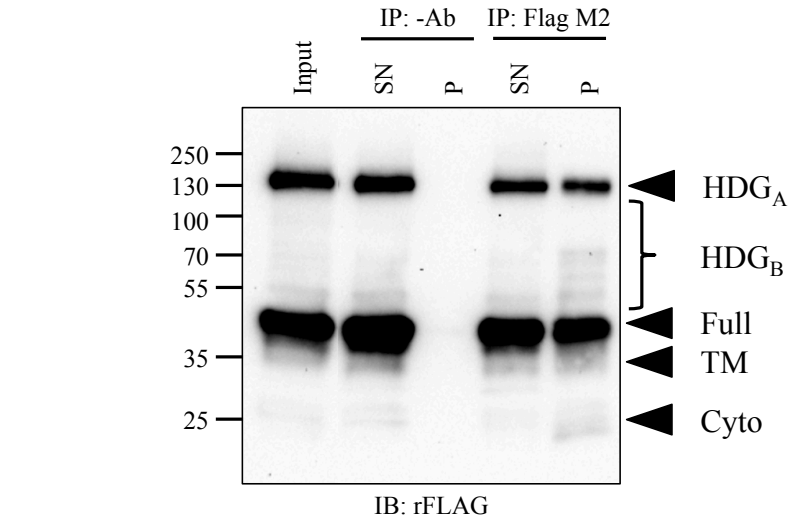

(a)

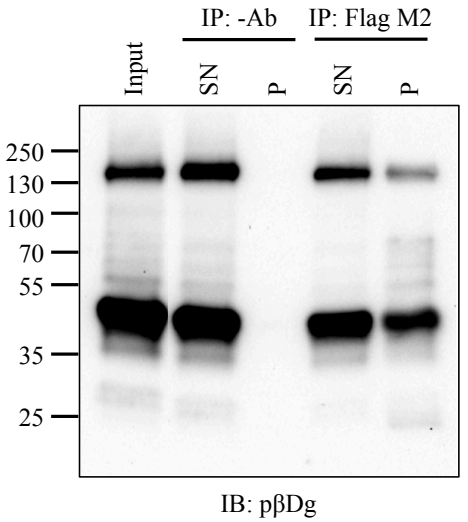

(b)

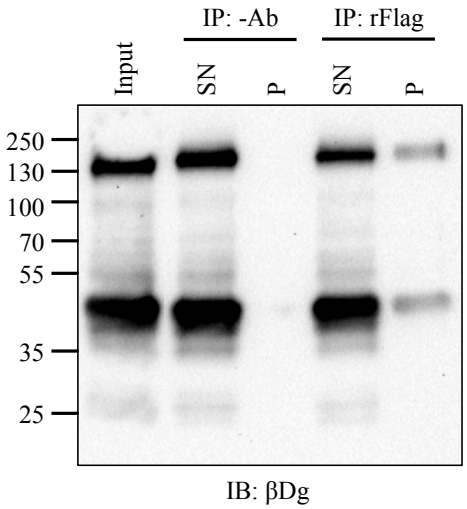

(c)

Figure 3.8: Immunoprecipitation of the recombinant $\alpha\beta$DgFlag. Total lysates of LNCaP transfected with the plasmid $\alpha\beta$DgFlag were used for a detailed characterisation by immunoprecipitation. Immunoprecipitations were prepared by combining the total lysates with anti-Flag M2 (raised in mouse) (a and b), anti-rFlag (c) (raised in rabbit) antibodies or left without antibody. Inputs, recovered supernatants after immunoprecipitation (SN) and the beads (P) were resolved by SDS-PAGE. Lysates immunoprecipitated with antibodies raised in mouse were used for immunoblotting with antibodies raised in rabbit and vice versa in order to avoid the signal produced by the light and heavy chains of the immunoglobulins. This immunoprecipitation permitted to confirm that $\alpha\beta$Dg with the Flag tag is recognized by antibodies against Flag and against phospho- and non-phospho-βDg (1709 and Mandag2 respectively).

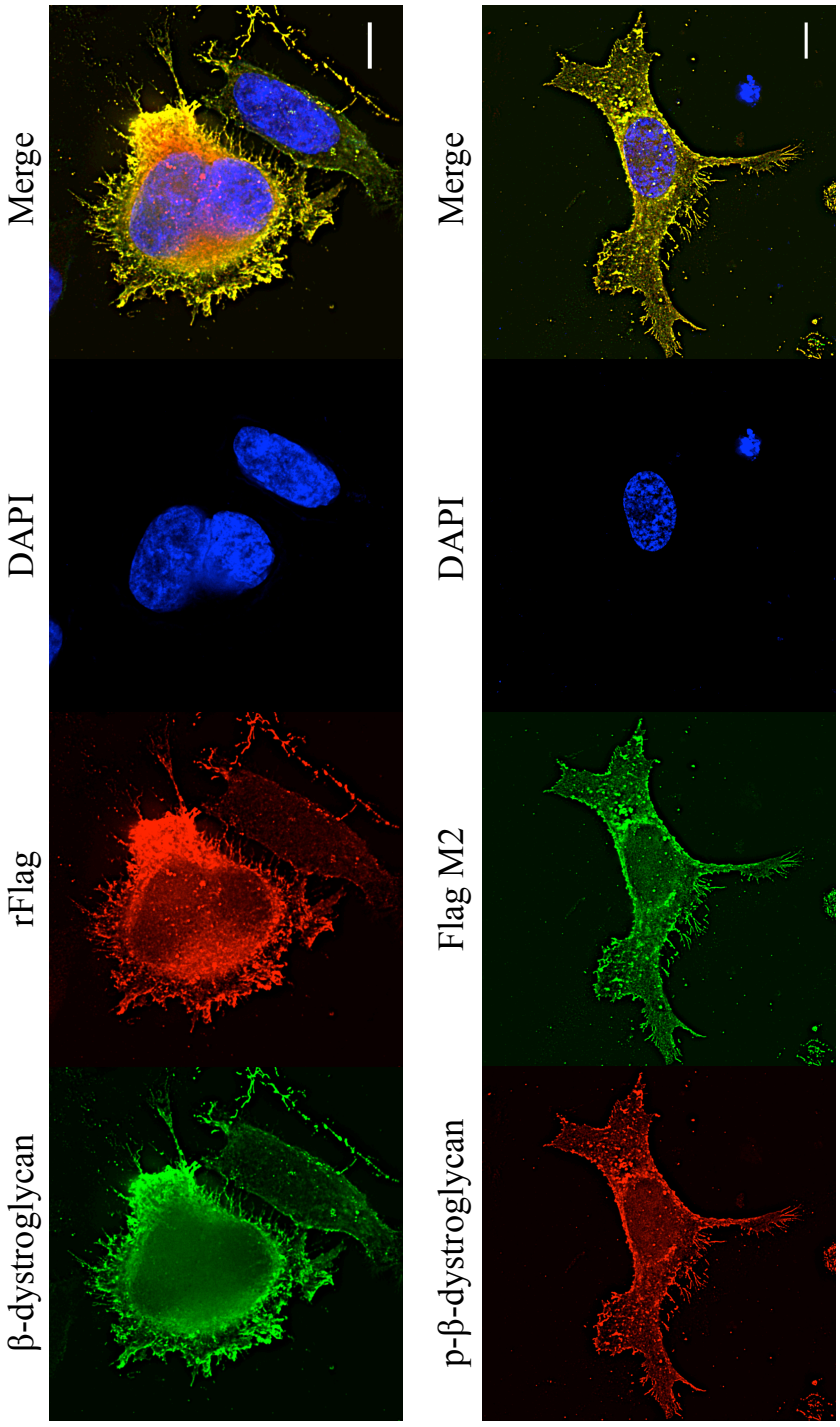

Figure 3.9: Localisation of βDgFlag in LNCaP cells. Transfected LNCaP cells were washed with PBS, fixed and co-immunostained with anti-βDg (green) and anti-rFlag (red) or anti-p-βDg (red) and anti-Flag M2 (green) antibodies. A stack section of deconvolved confocal microscopy images, shows the co-localisation of βDg and p-βDg with βDgFlag throughout LNCaP cells. Nuclei were counterstained with DAPI. Scale bar = 10 μm.

3.5 Localisation of alpha-dystroglycan in LNCaP cells

As pointed out in the previous section, the antibodies Flag, pYβDG and Mandag2, were able to detect an additional band between 130 and 250 kDa. So far, from previous studies and judging by electrophoretic mobility, one can hypothesize that the slow migrating band belongs to the dystroglycan propeptide. As reviewed by Barresi and Campbell in 2006, αDg can have a size that ranges from 120-156 kDa, although the estimated size of the core protein is approximately 70 kDa (Barresi & Campbell, 2006). It has been suggested that the big changes in size are in part due to the tissue under study, although other parameters such as glycosylation may also affect mobility.

In order to determine how the expression of alpha-dystroglycan in LNCaP cells is and its possible relationship with the 130-250 kDa band, it was decided to express exogenous αDg harbouring a myc/his tag (see appendix C.1). LNCaP cells transfected with the plasmid αDg-myc/his were collected for total lysates or cell fractionation.

Surprisingly, the band detected in whole cell lysates with anti-myc antibodies, presumably alpha-dystroglycan, did not correspond in size to the previously observed 130-250 kDa band (Figure 3.10).

The band of alpha-dystroglycan observed had a size of approximately 50 kDa with a smearing that extended far beyond the 70 kDa marker. Moreover, αDg had a non-nuclear and nuclear distribution. The smearing could be indicative of some variable PTM such as glycosylation. These observations obtained from at least three independent replicates and the fact that the nuclear fractions were not contaminated with non-nuclear fractions give also a strong support of a new pool of nuclear alpha-dystroglycan.

As will be discussed later, the lack of expression of enzymes in charge of the glycosylation of αDg (like LARGE), could be a potential explanation of the very reduced size of αDg in LNCaP cells. Interestingly, the identity of the 130-250 kDa remains a mystery and more deep analysis will be required to

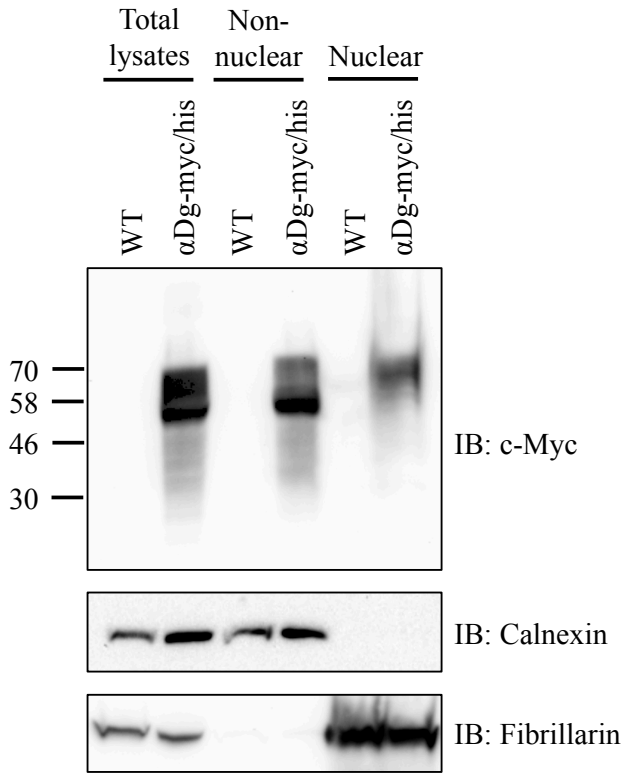

Figure 3.10: Nuclear localisation of alpha-dystroglycan. LNCaP cells WT or transfected with the plasmid αDg-myc/his were fractionated in non-nuclear and nuclear fractions. Western blot analysis with anti-c-Myc and anti-his (not shown) antibodies showed immunoreactivity in the non-nuclear and nuclear fraction of the cells transfected (shown is a representative image of three independent experiments). Membranes were stripped and reprobed with anti-calnexin (ER marker) and anti-fibrillarin (nuclear marker) antibodies as controls of purity and protein loading.

discard the different running hypotheses. In conclusion, an alpha-dystroglycan-like protein is expressed in non-nuclear and nuclear fractions of LNCaP cells and based on the size, the band observed does not seem to correspond to the previously seen 130-250 kDa band.

3.6 Phosphorylation and ubiquitination of dystroglycan

3.6.1 The transgenic LNCaP-Y890F and K806R cell lines

The residues Y890 and K806 in beta-dystroglycan have been shown to be subject to phosphorylation and ubiquitination respectively (Miller et al., 2012; K. A. Lee et al., 2011). In order to determine their effects in the stability of dystroglycan, it was decided to engineer coding sequences of dystroglycan carrying the mutations Y890F and K806R and transfect them into LNCaP cells. The absence of the hydroxyl group in phenylalanine keeps a structural similar amino acid to tyrosine and prevents the addition of phosphate groups, rendering a protein with minimal structural changes; similarly, the blocked amino group in arginine, prevents the additional modification with ubiquitin groups (Figures 3.11).

Western blot analysis with anti-Flag antibodies of total lysates of LNCaP cells WT or transfected with the parental or mutated plasmids, show that the mutants had a similar expression to the unmodified exogenous dystroglycan. It is interesting to note that the mutant K806R had a slightly faster migration when compared to the mutant Y890F and parental exogenous dystroglycan (Figure 3.12).

Turning now to the cellular distribution of exogenous $\alpha\beta$DgFlag and its mutants, LNCaP cells transfected with the 3 plasmids were subjected to cell fractionation followed by immunoblot analysis. Both plasmids, Y890F and K806R, had a similar distribution in the nucleus compared to the unmodified $\alpha\beta$DgFlag. Apparently, both mutations neither affect the synthesis nor their nuclear translocation (Figures 3.13a and 3.13b).

By immunofluorescence, the staining of cells expressing the mutant Y890F with Mandag2 was distributed along the plasma membrane and mostly excluded from the cytoplasm and nucleus (Figure 3.14, left, green). Interestingly, the signal generated by Flag (red) was distributed all along the cell

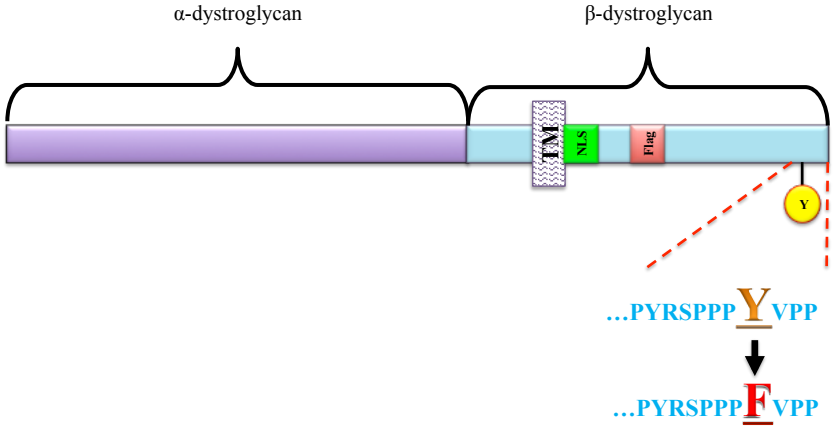

(a)

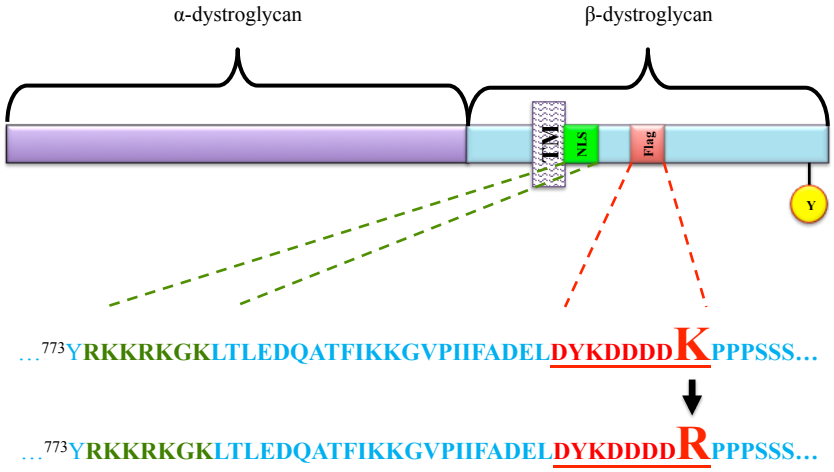

(b)

Figure 3.11: Generation of the mutants Y890F- and K806R-$\alpha\beta$DgFlag. The schematics show the amino acids that were changed to introduce the mutations Y890F (a) and K806R (b) by site directed mutagenesis. After corroborating the proper introduction of the mutations by DNA sequencing, the plasmids were purified and used for transient transfection of LNCaP cells.

(Figure 3.14, left, red). It is worth noting that both antibodies, Flag and Mandag2, showed a clear localisation all around the cells, but the signal generated by Mandag2 was excluded from the cytoplasm (Figure 3.14, left, merge).

Regarding the co-localisation between pYβDG and Flag antibodies, both antibodies were distributed throughout the cell. The signal generated by pYβDG was more cytoplasmic (Figure 3.14, right, red). Flag, on the other hand, had a strong signal at the plasma membrane and in the cytoplasm (Figure 3.14, right, green). Both antibodies showed some co-localisation but the

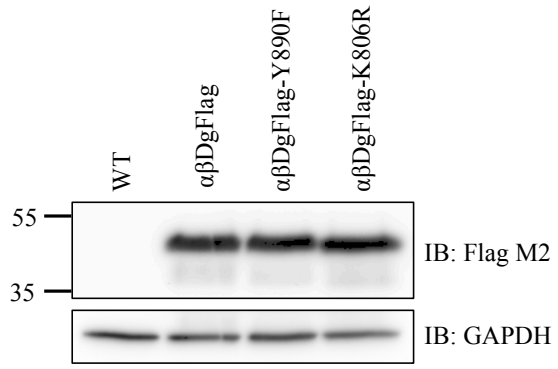

Figure 3.12: Characterisation of the mutants Y890F- and K806R-$\alpha\beta$DgFlag. By western blot analysis, the anti-Flag M2 antibody is able to detect specific bands in the lysates of the cells transfected with the plasmid $\alpha\beta$DgFlag and the ones harbouring the mutations Y890F and K806R. Lysates of LNCaP WT were included as a control of specificity of the anti-Flag antibody. GAPDH is shown as the loading control.

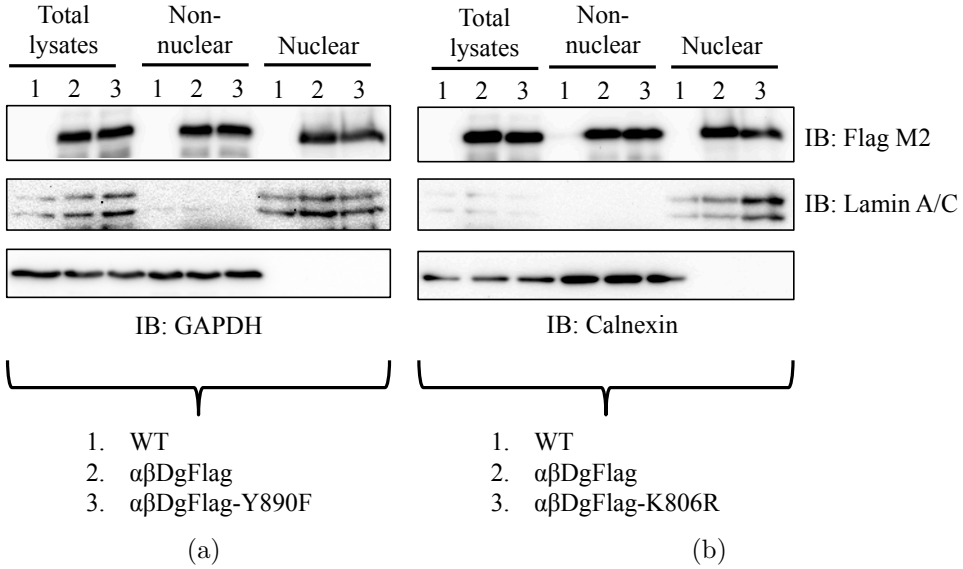

Figure 3.13: Cellular distribution of the mutants Y890F- and K806R-$\alpha\beta$DgFlag in LNCaP cells. LNCaP cells WT or transfected with the plasmids $\alpha\beta$DgFlag, $\alpha\beta$DgFlag-Y890F (a) and $\alpha\beta$DgFlag-K806R (b) were collected for total lysates or cell fractionation. The analysis by western blot with anti-Flag antibodies shows that both mutants have a cytoplasmic and nuclear distribution. Lamin A/C, GAPDH and Calnexin are shown as the loading controls.

co-localized signals were restricted to some areas of strong signal on the plasma membrane and was reduced towards more central areas near the nucleus (Figure 3.14, right, merge).

Turning now to the mutant K806R, it was observed that there was a good

co-localisation between Mandag2 and Flag (raised in rabbit), and pYβDG and Flag (raised in mouse) antibodies compared with the mutant Y890F. The distribution of the protein was all along the plasma membrane to the cytoplasm. There were some areas of non co-localisation that could be explained by the fact that some species that harbour the mutation K806R could be either subject to phosphorylation or left unmodified (Figure 3.15).

Overall, these results show that dystroglycan harbouring the mutations Y890F and K806R is expressed in LNCaP cells. They are distributed from the plasma membrane to the nucleus and apparently, these two modifications do not interfere in their nuclear transport.

3.6.2 Beta-dystroglycan is extensively phosphorylated

Beta-dystroglycan is a transmembrane protein with many serine (S), threonine (T) and tyrosine (Y) amino acids predicted to be phosphorylated. Due to its critical localisation, Y890 (in mouse) is the amino acid that has been most deeply studied. As mentioned before, its phosphorylated state (maintained by Src) is critical for interactions with other proteins, and to keep the stability of other dystrophin associated proteins on the plasma membrane. By site directed mutagenesis and mass spectrometry analysis, other amino acids in addition to the Y890 have been identified as potential residues subject to phosphorylation (`http://www.phosphosite.org/homeAction.do`).

So far, in the experiments performed with WT or overexpressed dystroglycan, there were some bands appearing above the 43 kDa species. The shift in the migration of the bands could be due to the presence of post-translational modifications on dystroglycan such as phosphorylation, ubiquitination or sumoylation. In 2000, James and colleagues observed that upon treatment of HeLa cells with peroxovanadate, beta-dystroglycan had a retardation in its electrophoretic migration. Immunoprecipitation analysis with anti-p-tyrosine antibodies confirmed that the slow migrating band was due to dystroglycan phosphorylation (James et al., 2000).

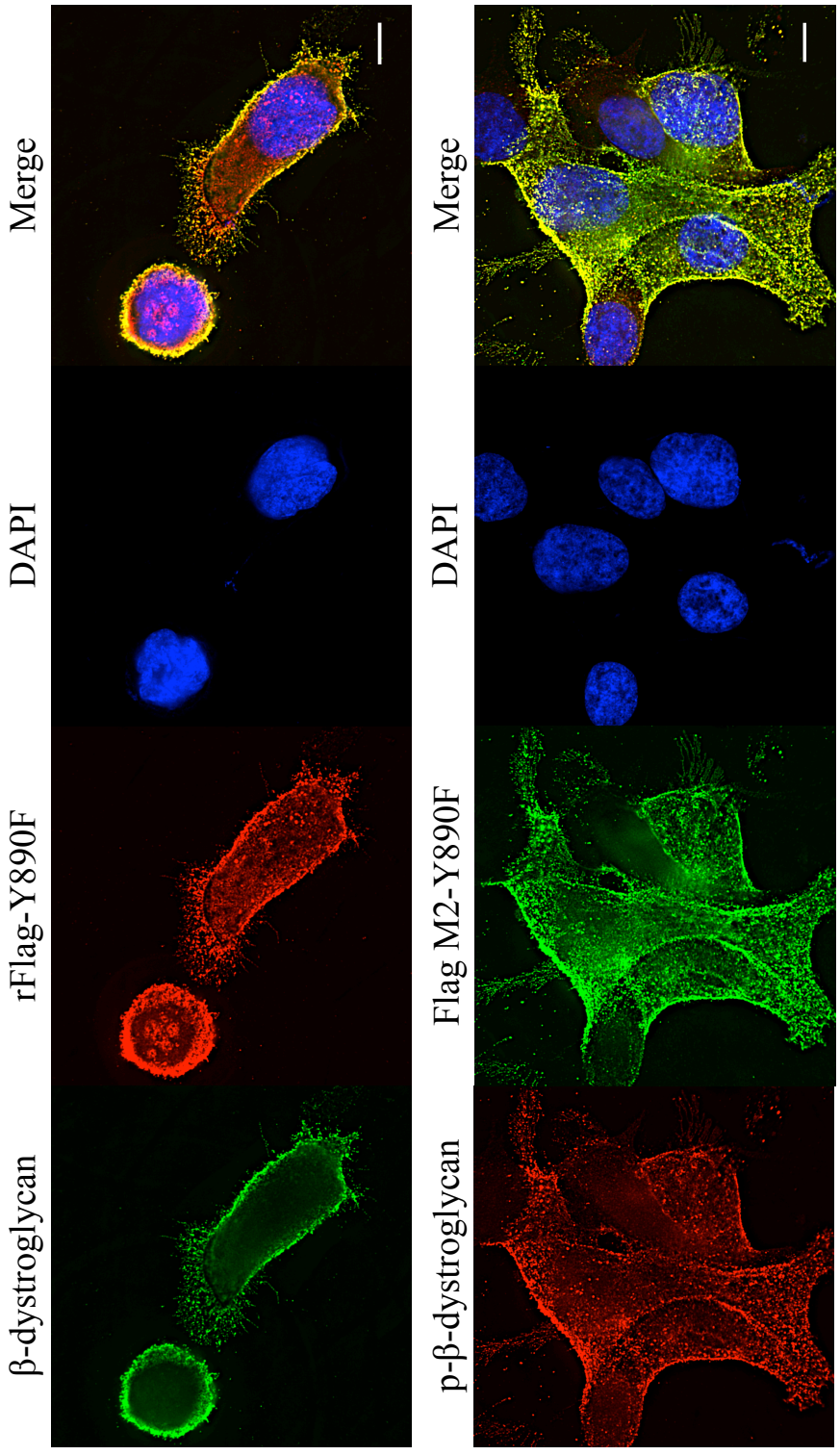

Figure 3.14: Immunocytochemical characterisation of the mutant Y890F-$\alpha\beta$DgFlag in LNCaP cells. LNCaP cells transiently transfected with the plasmid $\alpha\beta$DgFlag-Y890F were co-immunostained with anti-Flag (Flag (rabbit)=red, Flag M2 (mouse)=green) and anti-βDg (βDg (mouse)=green, pYβDG (rabbit)=red). Shown are stack sections of deconvolved confocal microscopy images. DAPI was used to counterstain the DNA. Scale bar = 10 μM.

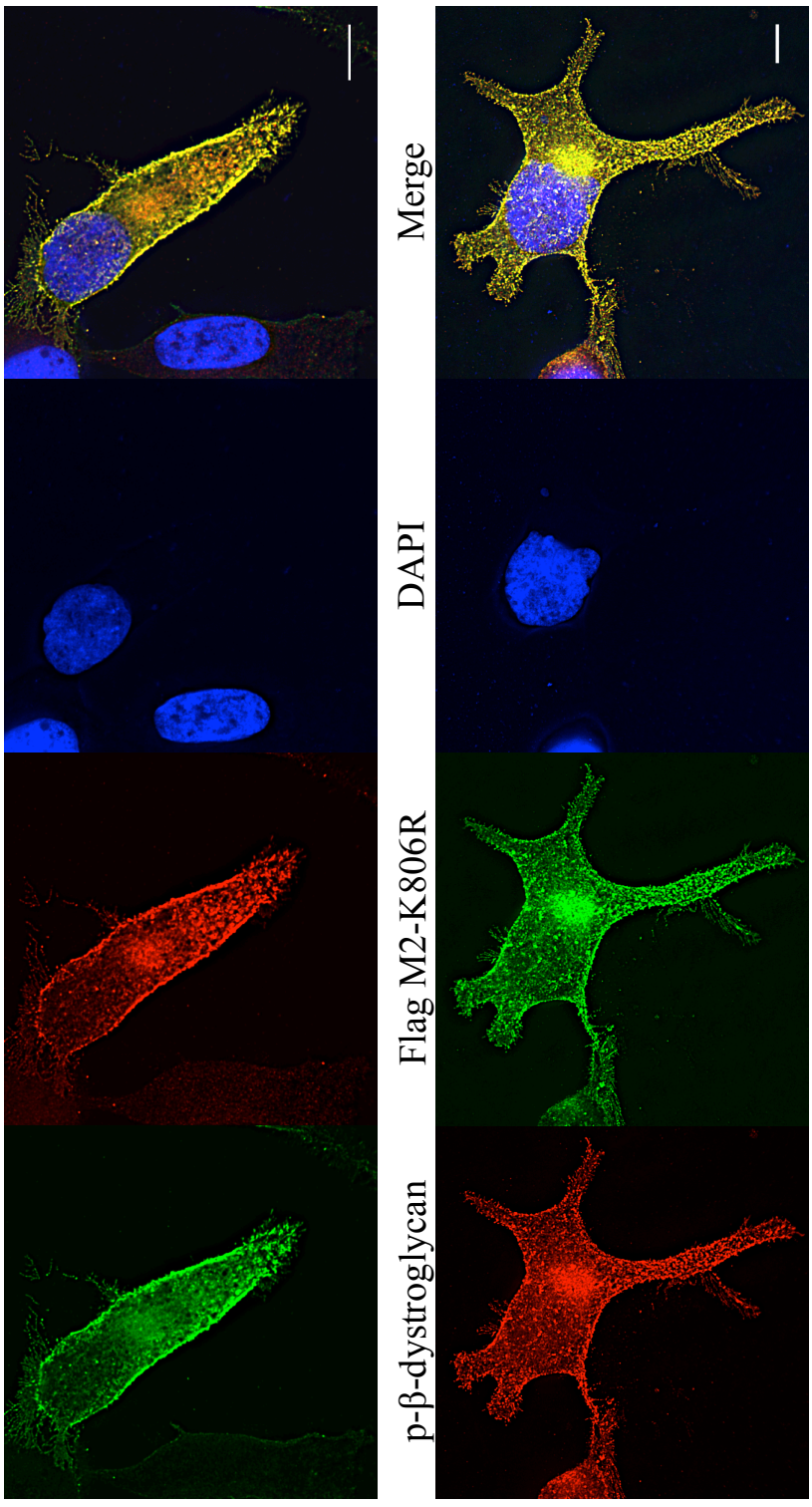

Figure 3.15: Immunocytochemical characterisation of the mutant K806R-$\alpha\beta$DgFlag in LNCaP cells. LNCaP cells transiently transfected with the plasmid $\alpha\beta$DgFlag-K806R were co-immunostained with anti-Flag (Flag (rabbit)=red, Flag M2 (mouse)=green) and anti-βDg (βDg (mouse)=green, pβDg (rabbit)=red). Shown are stack sections of deconvolved confocal microscopy images. DAPI was used to counterstain the DNA. Scale bar = 10 μM.

In order to test the hypothesis that the slower migrating bands observed on immunoblots during the course of this project, are due to phosphorylation, it was decided to inhibit the activity of serine, threonine and tyrosine phosphatases in LNCaP cells. Sodium peroxovanadate (Ruff et al., 1997) and calyculin (Resjö et al., 1999) have been shown to be potent inhibitors of tyrosine, and serine/threonine phosphatases respectively. To determine the effects of both compounds on the phosphorylated status of beta-dystroglycan, LNCaP cells transfected with the plasmid $\alpha\beta$DgFlag were treated with calyculin A, sodium peroxovanadate, a combination of both, or DMSO. Total lysates resolved in a Tricine-SDS-PAGE gels (see section 2.1.5.10) followed by western blot analysis with anti-Flag antibodies showed no apparent changes in the electrophoretic migration in lysates of cells exposed to individual treatments compared with the control (DMSO). However, the combination of both treatments led to a dramatic increase in the abundance of the 26, 35, 43 kDa forms of beta-dystroglycan and, most importantly, in slow migrating bands of a higher molecular weight (HDG_B) (Figure 3.16).

Blotting of the same lysates with antibodies anti-p-MAPK revealed the protective effects against protein phosphatases provided by both inhibitors (Figure 3.16, top figure on the right).

Another approach to test the phosphorylated status of proteins is by *in vitro* analysis, such as dephosphorylation with Calf Intestinal Phosphatase (CIP), which has the ability to remove phosphate groups from S, T and Y amino acids. Changes in electrophoretic mobility upon treatment with CIP could indicate the presence of phosphorylated amino acids. Therefore, lysates of cells transfected with the plasmid $\alpha\beta$DgFlag were treated with CIP. Additionally, lysates of cells transfected with the $\alpha\beta$DgFlag-Y890F mutant were included in the analysis in order to highlight some changes not associated with the phosphorylation of the Y890.

The transfection of the mutant $\alpha\beta$DgFlag-Y890F in LNCaP cells followed by immunoblot analysis with anti-Flag antibodies revealed two exciting results. First, the banding pattern of the mutant Y890F was not the same

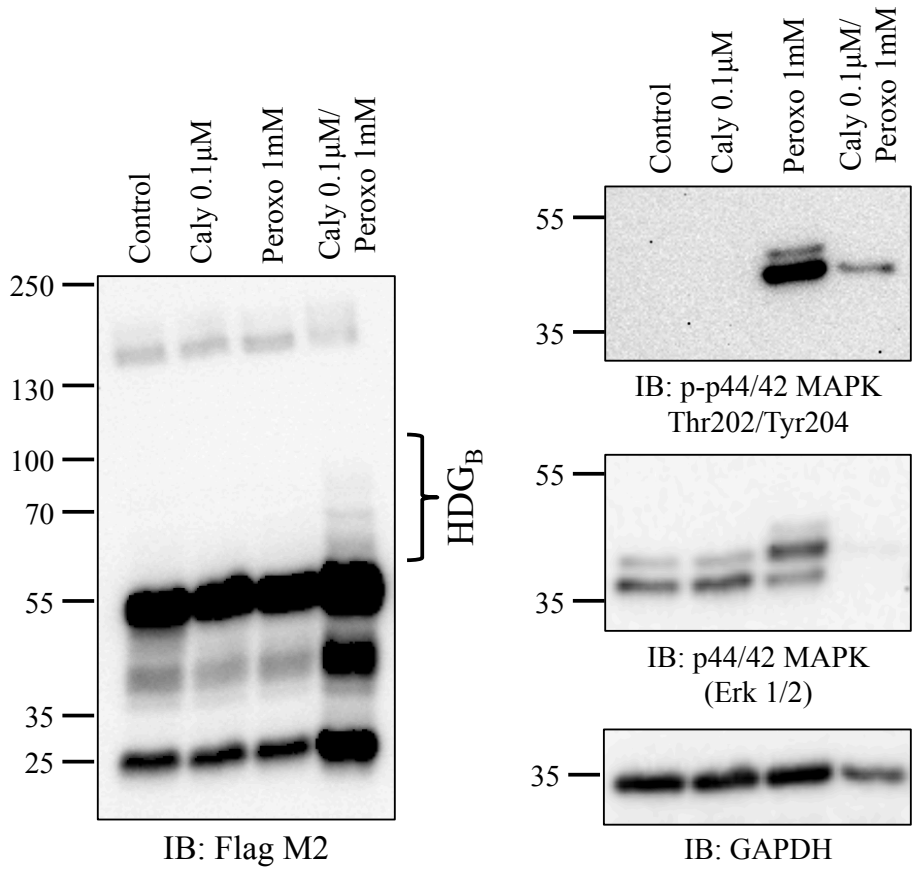

Figure 3.16: Calyculin and peroxovanadate lead to increased levels of phosphorylation of beta-dystroglycan. LNCaP transiently transfected with the plasmid $\alpha\beta$DgFlag were grown for 24 hours. Cells were then treated with DMSO, calyculin, peroxovanadate or a combination of calyculin/peroxovanadate for 15 minutes. Lysates were immunoblotted with anti-Flag antibodies. The treatment of the cells with peroxovanadate and calyculin led to the appearance of slower migrating bands (HDG$_B$) when using a 11%T, 0.67% Tricine-SDS PAGE gels. Membranes were incubated with an anti-p-MAPK antibody to show the efficacy of calyculin and peroxovanadate treatments. Reprobed membranes with anti-MAPK and anti-GAPDH are shown as the loading controls.

compared with the non-mutated form of exogenous beta-dystroglycan. There was a slight delay in the migration of the Y890F mutant which was more evident in non-nuclear fractions of transfected cells (dashed line in Figure 3.17a). This resembled a similar pattern in the mobility of the recombinant protein beta-dystroglycan fused to an alkaline phosphatase tag harbouring the same mutation (Sotgia et al., 2003). Second, the western blot analysis of total lysates showed that some migrating bands above (-HDG) and below (-LDG)

full-length beta-dystroglycan (43 kDa) were absent compared to the parental protein $\alpha\beta$DgFlag (Figure 3.17b).

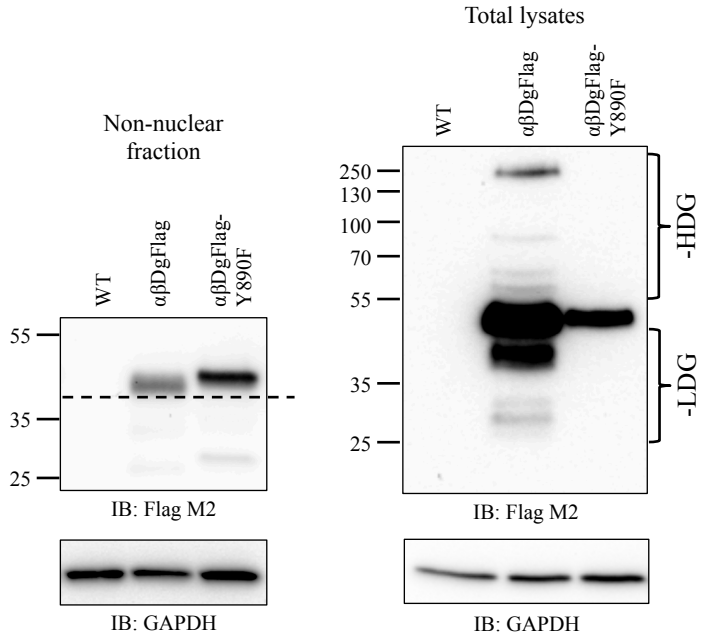

Figure 3.17: The mutation Y890F affects other PTM on beta-dystroglycan. (a) Western blot analysis of non-nuclear fractions of cells transfected with the plasmids $\alpha\beta$DgFlag and $\alpha\beta$DgFlag-Y890F reveals a retardation in the migration of the mutant Y890F compared with normal $\alpha\beta$DgFlag (dashed line). (b) The mutation Y890F affects other PTM on βDg. Lysates of LNCaP cells transfected with the plasmids $\alpha\beta$DgFlag and $\alpha\beta$DgFlag-Y890F were subjected to immunoblot analysis with antibodies anti-Flag. The introduction of the mutation in Y890 abolished other PTM on beta-dystroglycan (-HDG and -LDG)

Following this, the treatment with CIP revealed interesting findings. Lysates containing $\alpha\beta$DgFlag had a multiple banding pattern above the main band of βDg in the absence of CIP treatment. However, upon treatment with CIP, there was a reduction in band intensity generated by anti-Flag antibody around bands 100-130 (-HpDGa) and the signal was at very reduced levels on bands near 60 kDa (-HpDGb). If we now turn to mutant Y890F, it is possible to see that lysates not treated with CIP still lack some slower migrating bands and the ones present were at a lower abundance (-HpDGa). When the same lysates were subjected to treatment with CIP, the remnant doublet observed at approximately 60 kDa (-HpDGb) was completely abolished (Figure 3.18a).

The resolution of the same lysates in a 10%T, 3%C tricine-SDS-PAGE system (see Table D.3), followed by immunoblotting with Mandag2 antibodies gave unexpected outcomes. Lysates of cells transfected with the parental plasmid $\alpha\beta$DgFlag and left untreated, showed many slower migrating bands. Some of those bands disappeared when the same lysates were subjected to treatment with CIP. On the other hand, in lysates with mutant Y890F the presence of bands above 43 kDa were considerably reduced under the two conditions (HpDG in Figure 3.18b).

The disappearance of bands in lysates treated with CIP suggests the presence of additional phosphorylatable amino acids, and importantly, the phosphorylation of Y890 seems to be a triggering factor for additional post-translational modifications in beta-dystroglycan. The use of anti-phosphotyrosine antibodies in order to further show the presence of additional phosphorylatable amino acids in beta-dystroglycan will be required.

3.6.3 Beta-dystroglycan is ubiquitinated

Immunoblotting of beta-dystroglycan, either endogenous or exogenous, with the antibodies anti-pYβDG, Mandag2 or Flag, usually revealed some bands of high molecular weight in addition to the unmodified 43 kDa species. The experiments performed with the inhibitors of phosphatases calyculin A and sodium peroxovanadate, and the treatment of total lysates with CIP, suggested that the retardation in the migration of some bands was due to phosphorylation. These changes occurred mainly between the range of the 43 and 80 kDa, which does not explain the presence of other bands usually observed above 80 kDa. The speed of their migration was suggestive of two important PTM, ubiquitination or sumoylation.

Ubiquitination could be a potential candidate to explain the presence of high molecular weight migrating bands. This dynamic PTM can control many cellular processes depending on very specific situations. The classic pathway is the labelling with ubiquitin groups of proteins targeted for degradation,

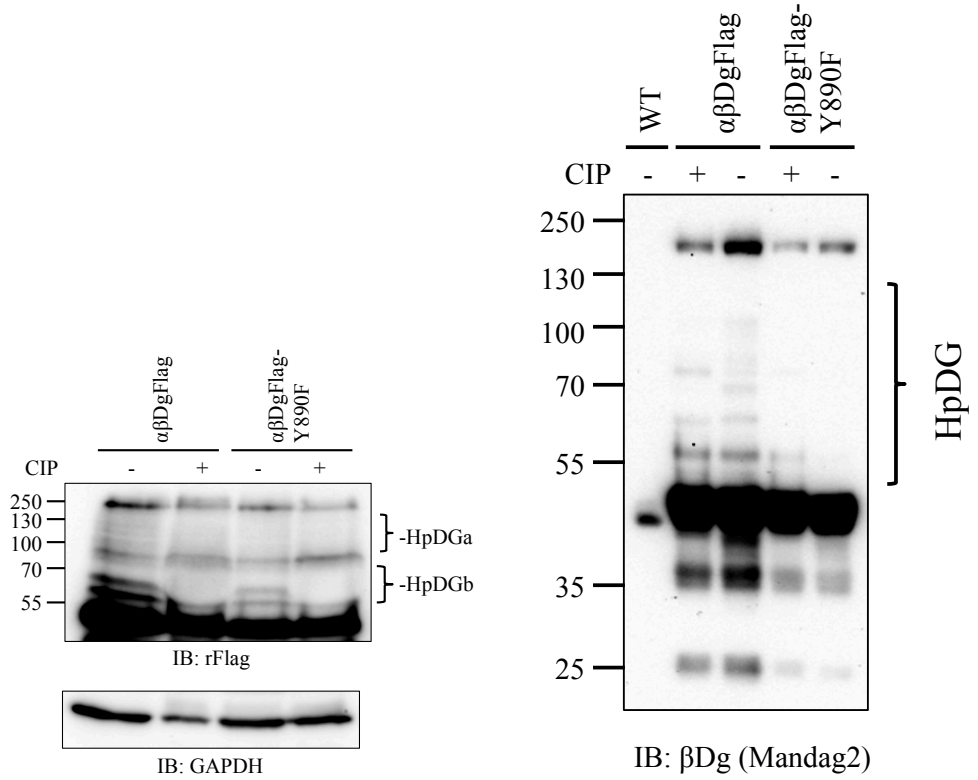

Figure 3.18: Beta-dystroglycan is extensively phosphorylated. (a) Total lysates of LNCaP transfected with the plasmid $\alpha\beta$DgFlag or $\alpha\beta$DgFlag-Y890F were subject to dephosphorylation with CIP (+). The analysis by western blot using anti-M2 Flag antibodies shows the absence of some slow migrating bands in samples treated with CIP (-HpDGa and -HpDGb). GAPDH is shown as the loading control. (b) The electrophoretic separation of the same samples using a 10%T, 3%C tricine-SDS PAGE gels gave a better resolution of phosphorylated beta-dystroglycan (HpDG).

although other non-proteolytic activities have been attributed to ubiquitination, such as the modification of specific proteins for a better interaction with other proteins or for protection against their degradation by the proteasome (K. P. Bhat & Greer, 2011).

The inhibition of proteasome activity usually leads to an electrophoretic retardation in the migration of proteins subject to ubiquitination. To probe whether the bands above 80 kDa were ubiquitinated beta-dystroglycan, LNCaP cells expressing exogenous $\alpha\beta$DgFlag were subjected to treatment with MG132, a proteasomal inhibitor. Total lysates obtained in the presence of N-ethylmaleimide

(NEM), a deubiquitinase inhibitor, were then resolved by SDS-PAGE gradient gels and western blotted with anti-Flag antibodies. When cells were treated with DMSO and then lysed in the absence or presence of NEM, no significant changes were observed in the migration of the bands above 43 kDa. However, treatment with MG132 still produced the bands between 55 and 70 kDa (HuDGc), but reduced the density of the approximately 80 kDa band (HuDGb) and led to the appearance of bands between the 90-120 kDa (HuDGa). The band above 130 kDa was also altered. Upon treatment with MG132 this band was reduced but present as a doublet (HuDGp) (Figure 3.19a).

It is well known that the concentration of acrylamide affects the good transfer of proteins. The higher the concentration, the more difficult is to transfer high molecular weight proteins. To determine if the reduced amount of the 130 kDa band was due to the generation of other slower migrating species above 200 kDa, the same lysates of Figure 3.19a, were resolved in a 11%T 0.67%C Tricine-SDS-PAGE gel (see section 2.1.5.10). The most impressive result to emerge from this second immunoblot analysis with anti-Flag antibodies is the presence of other species of an even high molecular weight but only in the presence of NEM (Figure 3.19b).

Taken together, these results support the hypothesis of beta-dystroglycan being modified by ubiquitin groups. Although the high molecular weight species of beta-dystroglycan were only present when cells were treated with MG132, or collected in lysis buffer containing NEM, this does not completely confirm that the shifts were due to ubiquitination.

The development of technologies for the isolation and protection of ubiquitinated proteins has been of great advantage in the study of functional and degradative processes in which ubiquitination is implicated. MultiDsk (MD), a high affinity ubiquitin binding protein developed by Wilson and colleagues in 2012, has been shown to be an important approach for the enrichment and protection of mono- and poly-ubiquitinated proteins (M. D. Wilson et al., 2012). This construct cloned into a GST expression vector consists of a tandem of 5 repeats of the yeast Dsk2 ubiquitin binding domain flanked by

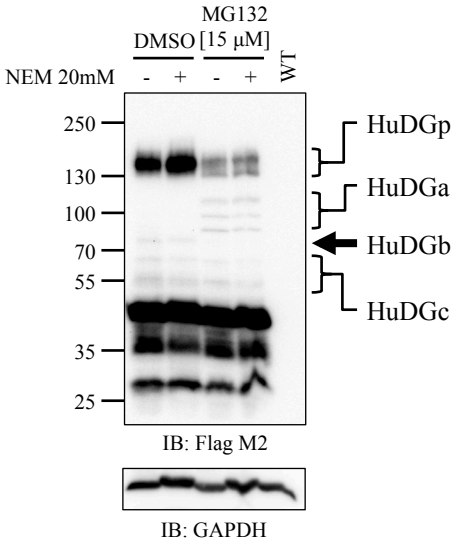

(a)

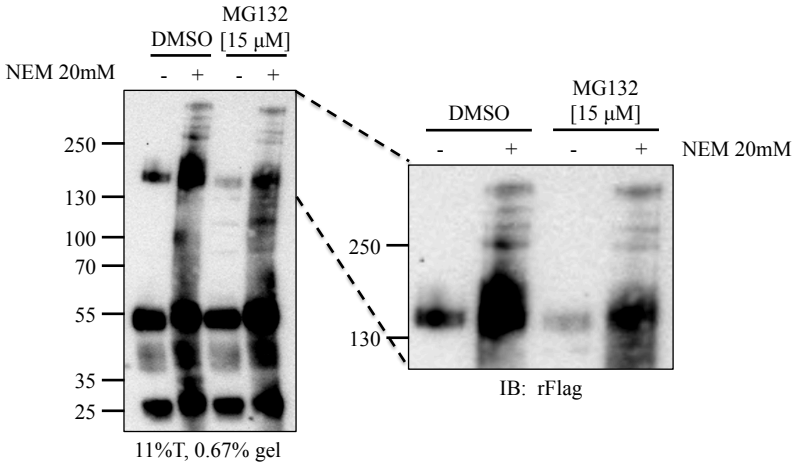

(b)

Figure 3.19: Potential ubiquitination of beta-dystroglycan. (a) LNCaP cells transiently transfected with the plasmid $\alpha\beta$DgFlag were subjected to treatment with MG132 for 4 hours. Cells lysed with RIPA buffer (supplemented with NEM) were resolved by gradient SDS-PAGE gels (7.5-15%) and immunoblotted with primary antibodies anti-Flag. The treatment with MG132 leads to the appearance of slower migrating bands around 100 kDa (HuDGa). (b) The loading of the same lysates in a 11%T 0.67%C Tricine SDS PAGE gel, allowed a better resolution of bands migrating above 150 kDa. Lysates of LNCaP WT were loaded as a control for specificity of Flag antibodies. Stripped membranes were reprobed with anti-GAPDH antibody as a loading control. The difference in the banding patter between the blots (a) and (b) may be due to the different species of antibodies used.

two 6x His tags (Figure 3.20a). In order to determine the specificity of this novel protein, LNCaP cells transfected with the plasmid $\alpha\beta$DgFlag were lysed

in the presence of NEM. Lysates were then incubated with agarose, agarose-GST or agarose-MD beads. The separation of supernatant and pellets on a SDS-PAGE gel followed by immunoblot analysis with anti-ubiquitin antibodies showed that a great amount of ubiquitinated protein was recovered interacting with MultiDsk (pellet). As no protein was observed in the pellet of agarose or agarose-GST it can be concluded that MultiDsk is highly specific to bind ubiquitinated proteins (Figures 3.20b and 3.20c).

Having corroborated the specificity of the resin, the next step was to determine the profile of ubiquitinated beta-dystroglycan. For that, LNCaP cells overexpressing $\alpha\beta$DgFlag were treated with DMSO or MG132 and then lysed in the presence of NEM. Untreated and treated lysates were incubated with agarose-GST or MultiDsk, resolved by SDS-PAGE and immunoblotted using anti-Flag antibodies.

As expected, many high molecular weight proteins in the range of 60-300 kDa precipitated with MultiDsk and were absent in pellets of GST alone (HuDG). Interestingly, the recovery of ubiquitinated proteins with MultiDsk was the same for cells treated or not treated with MG132 indicating that MultiDsk is sufficient to protect ubiquitinated substrates from degradation (Figure 3.21b) (M. D. Wilson et al., 2012). Another interesting observation is that the 55 and 60 kDa species, although present, were not precipitated with the MultiDsk resin (HpDG). Despite the fact that this experiment suggests that beta-dystroglycan is ubiquitinated, there is still the question of whether βDg is being mono-ubiquitinated on multiple residues, modified in one critical residue with a poly-ubiquitin chain, or a combination of both.

The next obvious question was to determine if beta-dystroglycan subjected to ubiquitination was also subject to phosphorylation on Y890. As stated before, pYβDG and Mandag2 are two antibodies that detect phosphorylated and non-phosphorylated tyrosines in a stretch of amino acids located in the C-terminus of beta-dystroglycan respectively. The immunoblot analysis with these two antibodies detected the presence of two bands above 70 kDa (HuDG*), suggesting that ubiquitination of beta-dystroglycan in LNCaP

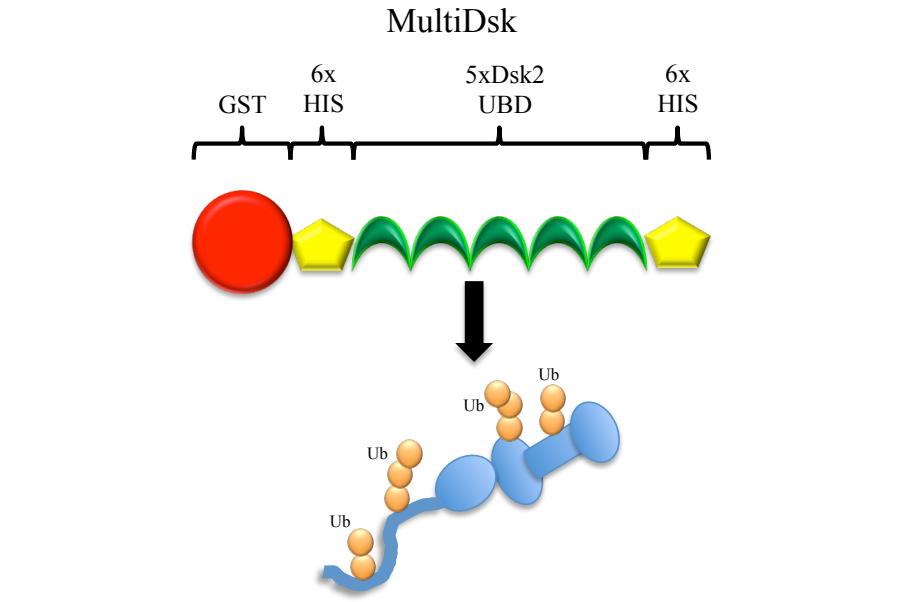

(a)

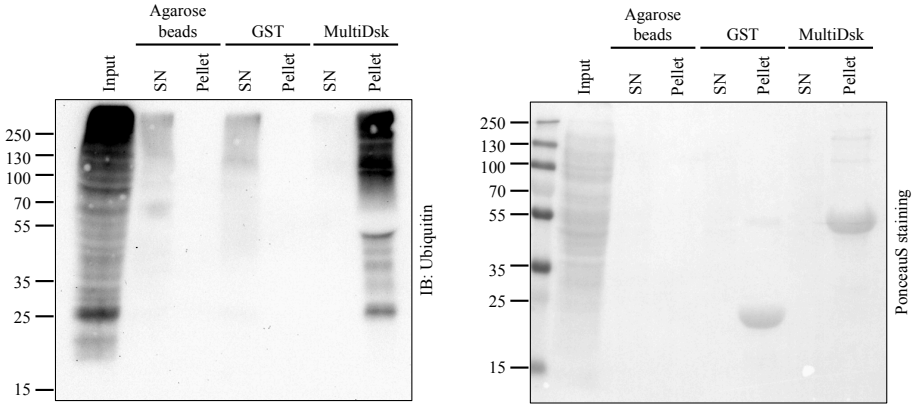

(b) (c)

Figure 3.20: Purification of ubiquitinated proteins with MultiDsk affinity resin. (a) Schematic structure of GST-MultiDsk (reproduced and modified with permission of Jesper Q. Svejstrup.) (b) LNCaP cells were transfected with the plasmid $\alpha\beta$DgFlag and lysed with RIPA buffer supplemented with 10 mM NEM. Lysates were incubated with agarose, agarose-GST or agarose-GST-MD beads. After washing the beads as indicated in material and methods, pulled down proteins were resolved by SDS PAGE. Western blot analysis with an anti-ubiquitin antibody shows that most of the ubiquitinated proteins were recovered in the MultiDsk pellet compared with the controls (agarose and agarose-GST beads). (c) The membrane was stained with Ponceau S red staining solution to show the equal loading of the recombinant proteins GST and GST-MD.

cells is not dependent of the phosphorylated tyrosine Y890 in its C-terminus (Figures 3.21c and 3.21d).

To have a deeper insight into ubiquitinated dystroglycan, LNCaP cells transfected with the plasmid $\alpha\beta$DgFlag were used for imunocytochemical analysis. Co-immunostaining of the transfected cells with antibodies anti-Flag and anti-ubiquitin shows some areas of clear co-localisation of ubiquitin and Flag (Figure 3.22).

As shown in the section related to phosphorylation of βDg, the introduction of the mutation Y890F led to a dramatic reduction of high molecular weight migrating bands. Additionally, as stated in the introduction, the K806 seems to be a critical residue in the ubiquitination for beta-dystroglycan. To determine if both mutants are affecting the generation of slow migrating species in the range of 70-300 kDa, LNCaP cells transfected with the parental plasmid $\alpha\beta$DgFlag and those harbouring the mutations Y890F and K806R were treated with MG132 or DMSO. Lysates of cells treated with MG132 or left untreated (DMSO) were obtained with RIPA buffer supplemented with NEM or normal RIPA buffer respectively. As revealed by the anti-Flag antibodies in Figure 3.23, the pattern of bands between the 70-300 kDa (HuDG) resembled those generated by the parental plasmid (Figure 3.23). These all together support the idea that the phosphorylation of Y890 in beta-dystroglycan does not affect its ubiquitination. Additionally, the mutation K806R, although a potential amino acid predicted to be modified by ubiquitin groups (K. A. Lee et al., 2011), seems to not affect the overall pattern of higher molecular weight bands of beta-dystroglycan.

Ubiquitination is a post-translational modification that can take place either in the cytoplasm or in the nucleus. In an attempt to differentiate if ubiquitination of beta-dystroglycan takes place in both, or is restricted to one specific cellular compartment, LNCaP cells transiently expressing $\alpha\beta$DgFlag were treated with MG132. Cells were then collected for cell fractionation in the presence of NEM for those under the treatment with MG132. The analysis of non-nuclear and nuclear fractions with Flag, Mandag2, pYβDG and ubiquitin

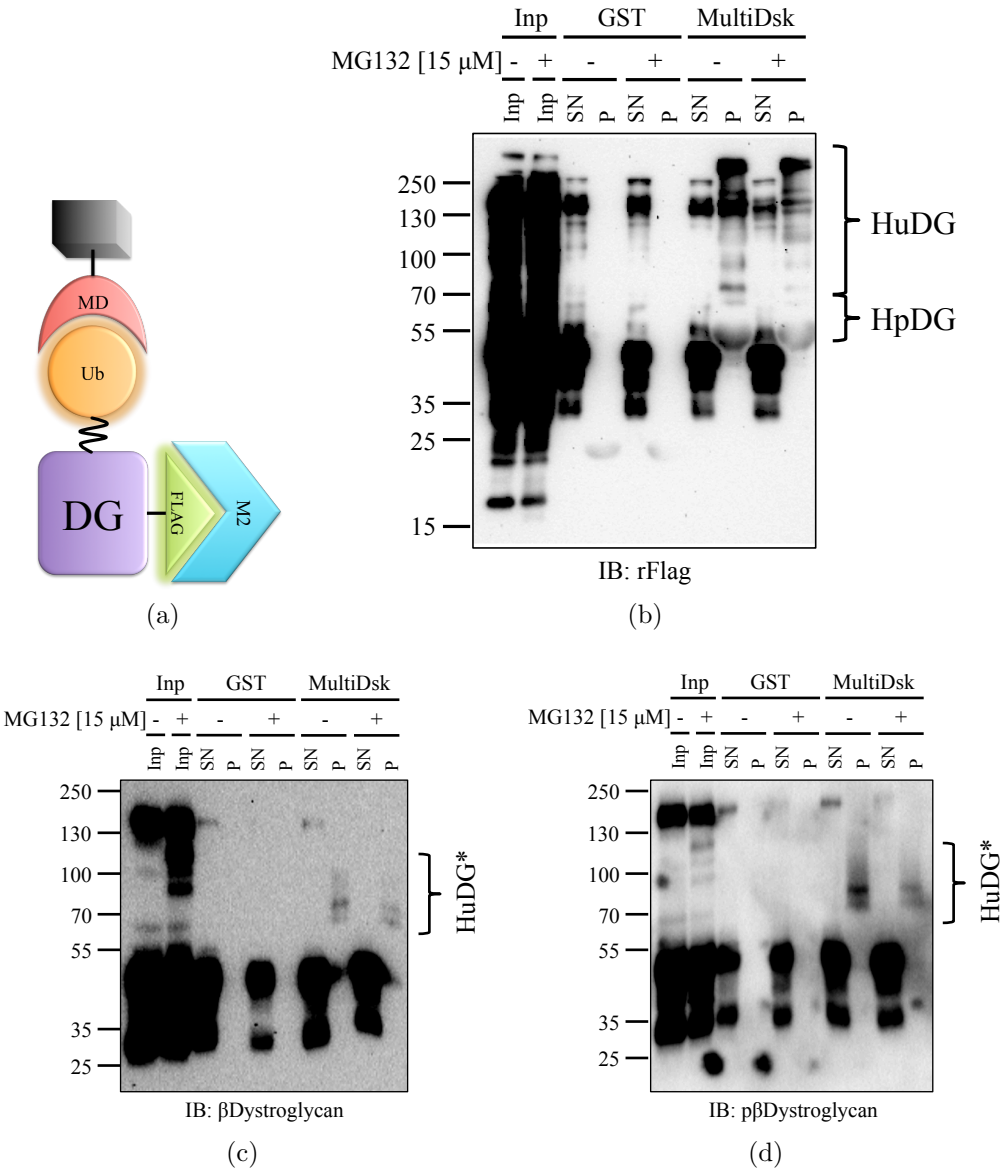

Figure 3.21: Beta-dystroglycan is multiply ubiquitinated. LNCaP cells transfected with the plasmid $\alpha\beta$DgFlag were treated with the proteasomal inhibitor MG132(+) or DMSO (-). After 4 hours treatment, cells were lysed with RIPA buffer supplemented with 10 mM NEM. Lysates were incubated with agarose-GST (control) or agarose-GST-MD beads and resolved by gradient SDS-PAGE gels (7.5-12.5%). (a) The schematic shows the molecular interactions of dystroglycan with MultiDsk and the Flag M2 Ab. (b) Immunoblot analysis using an anti-Flag antibody shows the presence of slower electrophoretic migrating bands in the pellets of lysates incubated with the MultiDsk affinity resin (HuDG). (c and d) The same lysates were immunoblotted on separate membranes with antibodies anti-βDg (Mandag2) and anti-p-βDG (pYβDG) antibodies.

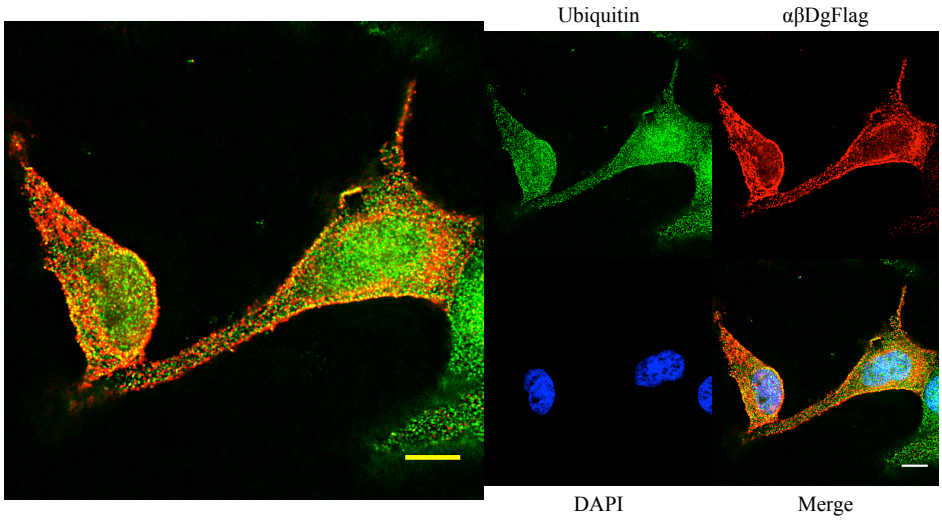

Figure 3.22: LNCaP cells transiently transfected with the plasmid $\alpha\beta$DgFlag were co-immunostained anti-Flag (red) and anti-ubiquitin (green) antibodies. A middle stack section of deconvolved confocal microscopy images shows variable co-localisation of ubiquitin and beta-dystroglycan in the cytoplasmic and nuclear fractions of the cells. Nuclei were counterstained with DAPI. Scale bar = 10 μm.

antibodies showed the classic banding pattern in the non-nuclear fraction of cells under treatment with MG132. Contrary to the expected, the abundance of ubiquitinated proteins in the nucleus was very low as was the amount of overexpressed beta-dystroglycan (Figure 3.24).

The addition of ubiquitin groups to the proteins can target them for degradation by the proteasome or other regulatory processes, as mentioned in the introduction. As shown before, beta-dystroglycan is modified by phosphorylation and ubiquitination. In addition to this, it was already shown that the mutation Y890F confers stability to beta-dystroglycan and other components of the dystrophin associated protein complex (Miller et al., 2012). Regarding the residue K806, there have been some mass spectrometry reports indicating its potential ubiquitination (K. A. Lee et al., 2011), but there is not evidence indicating how this potential ubiquitination affects the stability of beta-dystroglycan. In order to have a better idea about the way in which these two mutations, Y890F and K806R, affect the stability of beta-dystroglycan, cells transiently transfected with the corresponding plasmids were treated with the

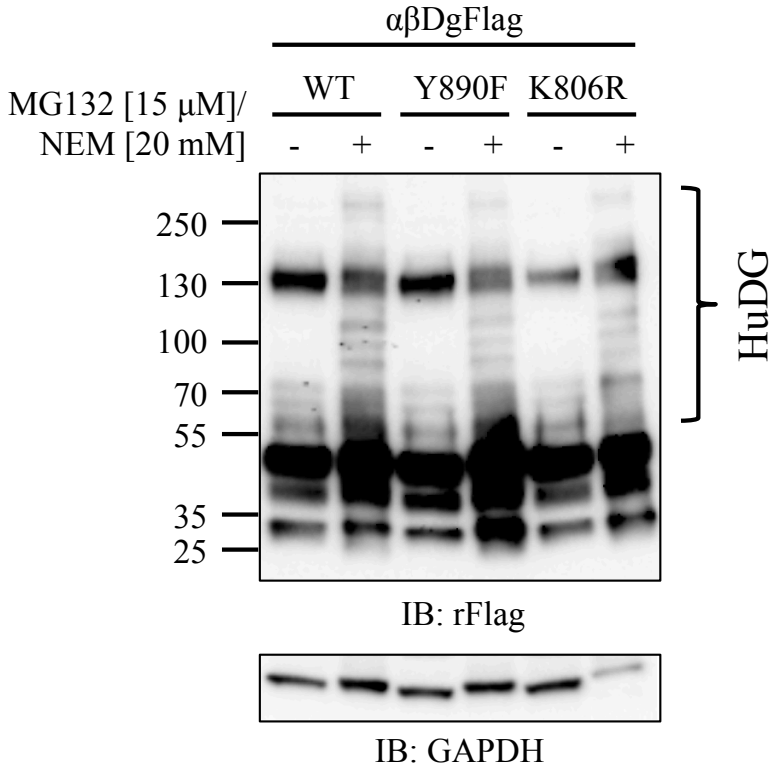

Figure 3.23: The mutations Y890F and K806R have little effects in the slower migrating bands of beta-dystroglycan. Transfected LNCaP cells with the plasmids $\alpha\beta$DgFlag and the ones with the mutants Y890F and K806R were treated with MG132 for 4 hours. Cells were washed with PBS before being collected with RIPA buffer supplemented with NEM [20 mM]. Blotted lysates with antibodies anti-Flag do not show big differences in the slow electrophoretic migrating bands (HuDG). Stripped membrane was reprobed with anti-GAPDH antibody to show the loading of the proteins.

protein synthesis inhibitor cycloheximide. After 24 h post-transfection, cells were collected for total lysates or were left growing for 12 hours more in the presence of cycloheximide and then collected for total lysates. Although it can not be completely concluded and further analyses are required, at 12 hours after stopping the synthesis of the proteins, the mutations Y890F and K806R had not any apparent changes in the amount of protein indicating the same ratio of degradation for both mutants (Figure 3.25).

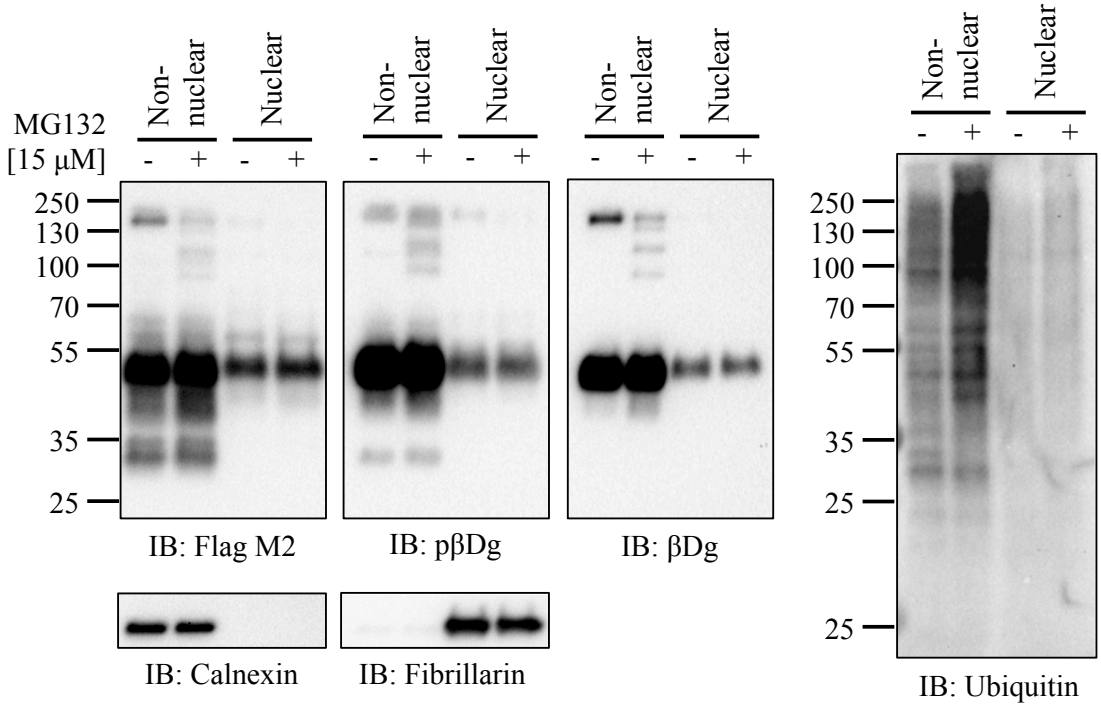

Figure 3.24: Differential ubiquitination of non-nuclear and nuclear beta-dystroglycan. LNCaP cells were transfected with the plasmid $\alpha\beta$DgFlag. After 24 hours growth, cells were further treated with MG132 [15 μM] for 4 hours. Cells were collected with buffer I for cell fractionation supplemented with NEM [10 mM]. Immunoblot analysis of both fractions shows the presence of the slower migrating bands in the non-nuclear fractions of cells treated with MG132. Membranes were stripped and reprobed with anti-βDg and anti-pβDg, anti-ubiquitin, anti-calnexin and anti-fibrillarin antibodies.

3.7 Discussion.

3.7.1 Distribution of dystroglycan in LNCaP cells

The cellular communication between the intracellular environment with neighbouring cells or the surrounding extracellular matrix is enabled by the presence of cell adhesion proteins immersed in the plasma membrane. The signal generated in the extracellular matrix is sensed by these plasma membrane proteins which in turn transmit the signal into the cell taking advantage of adaptor proteins found in the intracellular space (Alberts et al., 2008).

In addition to integrins, dystroglycan has been suggested to perform both functions. The DG complex spans the plasma membrane of many different cell

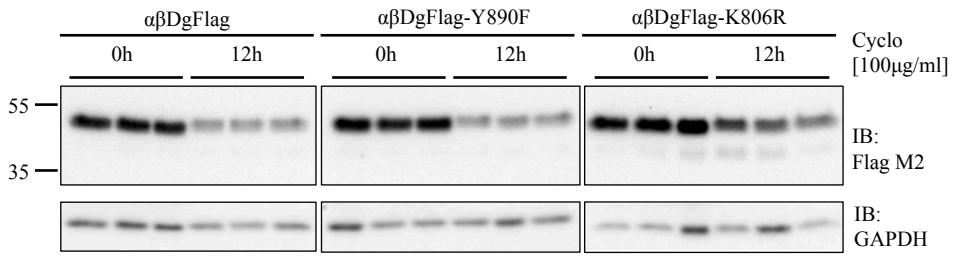

(a)

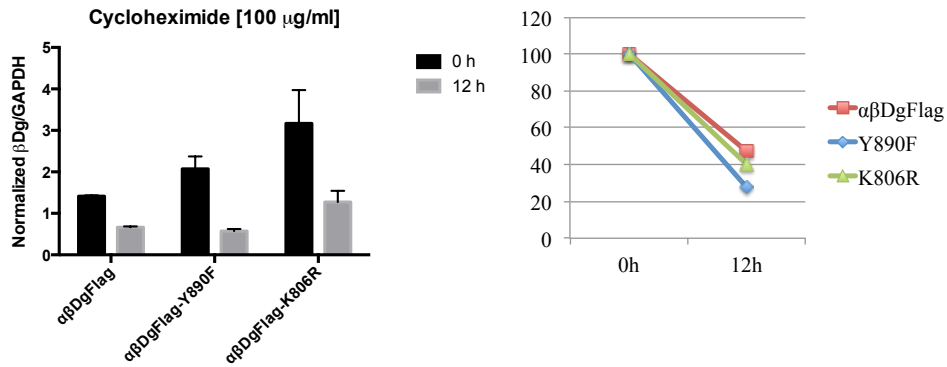

(b)

Figure 3.25: Comparison of the rate of degradation between the Flag-tagged beta-dystroglycan and the mutants Y890F and K806R. LNCaP cells transfected with the plasmid $\alpha\beta$DgFlag, $\alpha\beta$DgFlag-Y890F and $\alpha\beta$DgFlag-K806R were grown for 24 hours. Total lysates were obtained at 0 h (0 h) or after further incubation with cycloheximide [100 μg/ml] for 12 hours (12 h). Shown are the lysates of three independent experiments blotted with anti-Flag antibodies. Bands intensities of the Flag signal were normalized to GAPDH (means $\pm$ SEM, n=3).

types and tissues, performing structural and signalling activities. In prostate tissue, dystroglycan is expressed in the epithelium of basal and secretory cells but is reduced in prostate adenocarcinoma (Henry et al., 2001; Mathew et al., 2013; Sgambato et al., 2007). This prompted research to unravel the mechanisms leading to the loss of dystroglycan in prostate cancer, using the LNCaP cell line as a model system.

In this work, the biochemical fractionation and immunocytochemistry analysis of LNCaP cells showed the distribution of βDg and pβDg in the nucleus of LNCaP cells, which is in agreement with previous observations in prostate tissue and in LNCaP cells (Mathew et al., 2013). Additionally, immunofluorescence analysis showed a clear distribution of both forms of beta-dystroglycan

all along the cellular body. It is also worth noting the fact that Mandag2 showed a signal around the nuclear periphery (green channel in Figure 3.4). Although analysis of the co-localisation of beta-dystroglycan with members of the nuclear envelope were not performed, the immunocytochemistry and biochemical fractionation (Figures 3.3 and 3.4, on pages 72 and 74), are in agreement with previous reports showing the presence of dystrophin and members of the dystrophin associated protein complex, such as dystroglycan in the nucleus of different cell lines and their association with nuclear components (Fuentes-Mera et al., 2006; González et al., 2000; González-Ramírez et al., 2008; Lara-Chacón et al., 2010; Marquez et al., 2003; Martínez-Vieyra et al., 2013; Mathew et al., 2013; Oppizzi et al., 2008; Vásquez-Limeta et al., 2014; Villarreal-Silva et al., 2010). Further analyses are required to show the specific location of dystroglycan within the nucleus, and in other cellular compartments such as the Golgi apparatus or endoplasmic reticulum.

3.7.2 The myc/his tag affects the phosphorylation of Y890 in beta-dystroglycan

The critical position in the plasma membrane, the localisation in the nucleus, the diverse array of its interactions and multiple PTM, lead to the hypothesis that there are other interactions and cellular events in which dystroglycan plays a critical role that have not been unravelled. The integrity of the alpha subunit is important for linkage with extracellular components. On the other hand, its cytoplasmic domain regulates important cellular processes in the cytoplasm. In this regard, a phosphorylated tyrosine in the very C-terminus of βDg appears to be regulating a great variety of important protein interactions, such as those with dystrophin/utrophin, in addition to regulating the activation of other signalling pathways, as will be discussed later. Also, this region harbours many putative protein binding motifs such as SH2 and SH3 domains, and WW domain ligands and many additional phosphorylatable amino acids (Moore & Winder, 2010), all of which are located downstream of its nuclear localisation

signal. So, small modifications could be disadvantageous to the structure and potential interactions of the C-terminus.

The immunoprecipitation of endogenous dystroglycan for the characterisation of additional unknown interacting proteins with the antibodies Mandag2 and pYβDG has the main disadvantage that these antibodies bind the PPPY motif, the main interaction site for cytoskeletal proteins such as dystrophin/utrophin among others. Therefore, an alternative strategy could be the insertion of tags downstream the PPPY motif, however, the size and folding of such tags could alter important cellular events such as PTM and protein interactions mediated by this PPXY motif. Indeed, Figure 3.5b shows that the introduction of a myc/his tag in the carboxy-terminus affected the phosphorylation of the Y890 in mouse beta-dystroglycan.

3.7.3 The recombinant $\alpha\beta$DgFlag

Beta-dystroglycan cannot easily be expressed in the absence of alpha-dystroglycan due to the complicated co-translational modification, proteolysis and insertion in the plasma membrane. Furthermore, the extracellular domain of beta-dystroglycan is susceptible to cleavage by matrix metalloproteinases (Yamada et al., 2001). Therefore, because insertion of a tag at the C-terminus of dystroglycan prevented phosphorylation, it was necessary to look for another region in the cytoplasmic domain. An area around amino acid 800 was identified as being away from most of the putative binding motifs and suitable for the insertion of a Flag tag with minimum changes. The insertion of this Flag tag, however, does overlap with the K806 reported by Lee and colleagues to be subject to ubiquitination (K. A. Lee et al., 2011). Because of its hydrophilic characteristics, this tag seems to be always structurally exposed, which is advantageous for its detection (Figure 3.6).

The characterisation of LNCaP cells transfected with the recombinant $\alpha\beta$DgFlag showed that the Flag tag did not interfere in the detection by Mandag2 and pYβDG antibodies (Figure 3.8). Importantly, species other than

the 43 kDa beta-dystroglycan were observed on western blots and the analysis by immunofluorescence clearly resembled the visual staining phenotype observed with endogenous dystroglycan (Figure 3.9). Through cell fractionation, the nuclear distribution of recombinant beta-dystroglycan and associated species was confirmed. Therefore, through western blot and immunofluorescence analyses, the cellular localisation of $\alpha\beta$DgFlag resembles that of endogenous dystroglycan. However, it will be important to keep in mind that the solely insertion of Flag into the primary structure of dystroglycan may still affect its function, folding and some protein interactions, even the fact that it was inserted in a region with minimal interactions.

During the course of the characterisation of LNCaP WT cells and cells transfected with exogenous $\alpha\beta$DgFlag, a band between 130 and 250 kDa was commonly observed on immunoblots of total lysates, non-nuclear, or nuclear fractions (Figures 3.7, 3.8). This band usually immunoreacted with the Flag, Mandag2 and pYβDG antibodies and, intriguingly, was sometimes observed as a doublet. From the original characterisation of the dystrophin associated protein complex, the sizes ascribed to alpha- and beta-dystroglycan were 156- and 43-kDa respectively, although for core alpha dystroglycan it is much lower (Ervasti & Campbell, 1991; Ibraghimov-Beskrovnaya et al., 1992). Therefore, it was hypothesized that the band observed between 130-250 kDa could correspond to alpha-dystroglycan with some modifications.

3.7.4 Nuclear alpha-dystroglycan

The transfection of LNCaP cells with a plasmid encoding alpha-dystroglycan gave unexpected results. In total lysates, the protein detected by anti-myc and anti-6xHis antibodies had a size in the range of 50-70 kDa. What is more, it was surprising to find alpha-dystroglycan in the nucleus of LNCaP cells. The results presented in Figure 3.10 clearly show that alpha-dystroglycan was distributed in non-nuclear and nuclear fractions.

As mentioned above, one unanticipated finding was the low molecular

weight of alpha-dystroglycan. In accordance with the present results, previous studies have demonstrated that defects in the glycosylation of alpha-dystroglycan could be an explanation for its reduced size. Previous reports demonstrated that LARGE was able to recognize and modify alpha-dystroglycan but only when found in its functional form (alpha dystroglycan harbouring its N-terminal, mucin-like and C-terminal domains) (Kanagawa et al., 2004). Experiments performed in models of prostate cancer, such as the aggressive metastatic LNCaP cell line, have found that, although alpha-dystroglycan is expressed, its glycosylation is reduced. The defects in glycosylation were attributed to the reduced expression of LARGE2 in this cell line and to its concomitant reduction during prostate cancer progression (Esser et al., 2013). This phenomenon was not restricted to prostate cancer as the same defect in glycosylation was observed in cell lines derived from breast, lung and cervical cancers, presumably attributed to the silencing of LARGE (de Bernabé et al., 2009).

Thus, the defects in glycosylation could be an explanation for the reduced size of alpha-dystroglycan indicating that the species detected in this work corresponds to the core peptide. Another explanation for the reduced size of the alpha-dystroglycan species observed in this work, is the fact that other PTM, such as proteolysis could be affecting its integrity. In this regard, it has been previously reported that alpha-dystroglycan is subject to the cleavage by Furin on its N-terminal domain, liberating a ∼30kDa fragment (Kanagawa et al., 2004; Singh et al., 2004).

Together, these data lead to conclusion and future hypothesis that alpha-dystroglycan has a non-nuclear and nuclear distribution in LNCaP cells and that the great variability in its size from its counterpart in muscle could be attributed to the defects in glycosylation caused by the down-regulation of LARGE2 and to the proteolytic action of Furin in LNCaP cells. In support of this hypothesis, and although it was not clearly concluded, White and colleagues reported the nuclear localisation of alpha-dystroglycan in airway epithelial cells during wound repair using wheat germ agglutinin (WGA) (White,

Wojcik, Gruenert, Sun, & Dorscheid, 2001).

All this evidence, however, still does not explain the origins of the 130-250 kDa band. In 1996, Mummery and colleagues reported the presence of a 164 kDa and a 25 kDa species of beta-dystroglycan in post-synaptic density fractions of an adult rat forebrain. The additional *in vitro* treatment with endoglycosidase F did not show changes in the electrophoretic migration of these species of beta-dystroglycan (Mummery, Sessay, Lai, & Beesley, 1996). The observed size could be in agreement with the bands observed here in this chapter, however, in this thesis the treatment with PNGaseF did lead to a slight reduction in the size of the 130-250 kDa species of beta-dystroglycan (possibly because of the differential activities between endoglycosidase F and PNGaseF). A similar high molecular species was observed in rat retina (Ueda, Gohdo, & Ohno, 1998). Thus, if this band has immunoreactivity with antibodies used to detect the 43 kDa species, one can hypothesize that beta-dystroglycan is subject to oligomerization. In this regard, through chemical cross-linking it was shown that beta- and alpha-dystroglycan have the tendency of oligomerization in tissues such as diaphragm, skeletal muscle and heart (Finn & Ohlendieck, 1998).

A later report, however, described that the similar band of approximately 160 kDa corresponded to the precursor peptide of dystroglycan (Holt et al., 2000). This could be the explanation for the observed band in this thesis, but the reduced size of alpha-dystroglycan plus the size of beta-dystroglycan observed in these experiments do not match to the size of the high molecular weight band observed in this chapter, leading to the previous hypothesis of dystroglycan being subject to oligomerization. In support of this, a recent study reported big differences in the molarity of laminin:dystroglycan:dystrophin in a ratio of 1:41:1 in skeletal muscle (Johnson et al., 2013). Although it was concluded that the differences observed were due to the existence of complexes of dystroglycan associating with different proteins, it could be tempting to speculate that the big differences in the ratio observed are due to the formation of beta-dystroglycan multimers in the plasma membrane. This in some

way would help to explain the strong interaction with alpha-dystroglycan, as it is well know that these two subunits have a non-covalent interaction. On the other hand, the formation of multimers could help prevent the proteolysis of beta-dystroglycan. It is worth noting that cell lysates were separated in a reducing SDS-PAGE gel, which should be enough to disrupt the formation of multimers, however it has been shown that the opposite effect may happen as was observed for presenilins (De Strooper et al., 1997). Further evidence will be required to support the formation of beta-dystroglycan multimers in the plasma and nuclear membranes, and the significance of those hypothetical oligomers in cellular homeostasis.

3.7.5 Ubiquitination and phosphorylation of dystroglycan

3.7.5.1 Generation of the mutants Y890F and K806R

Given the multiple functions ascribed to dystroglycan, one would expect it to be subjected to tight regulation. From Figure 3.8 and other experiments presented in this thesis, it can be seen that beta-dystroglycan usually presents some slow migrating bands above the main 43 kDa form. Previous reports and assumptions point towards dystroglycan modification by sumoylation, ubiquitination and phosphorylation. These could be plausible hypotheses as the sequence of dystroglycan, specially the cytoplasmic domain, is rich in amino acids with a high probability of being modified by ubiquitination or phosphorylation. Growing evidence through mass spectrometry analysis confirm the previous assumption. The high sensitivity of this technique has shown that the N-terminal as well as the C-terminal domains in alpha- and beta-dystroglycan respectively, are domains subject to a broad number of modifications (most of these modifications were indirectly discovered in meta-analysis that were not aimed at dystroglycan) (`http://www.phosphosite.org/homeAction.do`).

Given the fact that Y890 is critical for protein interactions (Sotgia et al.,

2001) and for the stability of dystroglycan at the plasma membrane (Miller et al., 2012) it was decided to investigate the role of this phosphorylation in the stability of dystroglycan. Also, a lysine at position 806, K806, was identified at the peptide level as a substrate of the E3 ubiquitin ligase HDR1 by using quantitative proteomics (K. A. Lee et al., 2011). Thus, the role of this ubiquitination in the integrity of dystroglycan was investigated.

By biochemical and cytochemical analysis of LNCaP cells, similar phenotypes (expression and cellular distribution) of the mutants Y890F and K806R to the parental protein were recognized (Figures 3.11 - 3.15). Slight differences in the electrophoretic migration of the mutants compared to the parental protein were observed. The mutant K806R migrated a bit faster than the unmodified protein, however, the mutant Y890F had a retardation in its migration which will be discussed in the next section.

3.7.5.2 Dystroglycan is highly phosphorylated and ubiquitinated

The impact of phosphorylation on the regulation of beta-dystroglycan is highly debated. This PTM modifies a number of important protein-protein interactions (Ilsley et al., 2001; James et al., 2000; Sotgia et al., 2001), its protein stability (Miller et al., 2012), its vesicular transport (Sotgia et al., 2003), its virus permissibility (Moraz et al., 2013) or its adapter properties of the ERK-MAPK cascade components (Spence, Dhillon, et al., 2004). Previous research has focused the attention on tyrosine 890 located in the C-terminus of dystroglycan. This is based in the premise that the presence of pY890 is the main factor leading to the disruption of its interaction with dystrophin/utrophin, which in turn leads to the instability of the other members of the DGC leading to muscular dystrophy.

The experiments performed by Moraz and colleagues in 2013, clearly showed the existence of unknown tyrosines other than Y890 that could be subject to phosphorylation, which could be in agreement with our previous observations in Figure 3.8 (Moraz et al., 2013). Here the presence of multiple slow migrating

bands are indicative of dystroglycan being subject to either phosphorylation or ubiquitination.

Indeed, the combined effect of calyculin and peroxovanadate led to an enrichment of phosphorylated species of beta-dystroglycan, more interestingly, the appearance of slow migrating bands was suggestive of beta-dystroglycan being phosphorylated on multiple amino acids (Figure 3.16).

By immunoblot analysis the most abundant species detected were the 43 kDa species. The others were absent or at undetectable levels indicating that this mutation could be regulating other PTM like phosphorylation-ubiquitination (bands above the 43 kDa dystroglycan) or proteolysis (bands below the 43 kDa form) (Figure 3.17). Interestingly, the treatment with CIP of the parental protein and the mutant Y890F (Figure 3.18) confirmed the observations obtained with calyculin and peroxovanadate. A detailed map of amino acids subject to phosphorylation on dystroglycan will be important to determine the role of these amino acids in cellular processes such as the cell cycle and protein interactions.

In spite of the changes attributed to phosphorylation, there are still some questions about if all the observed bands above 43 kDa correspond to phosphorylated dystroglycan or other PTM such as ubiquitination. Interestingly, the treatment with MG132 and/or NEM led to the generation of bands of high molecular weight, particularly above 130 kDa. Through the use of a highly specific ubiquitin-binding resin with protective properties (M. D. Wilson et al., 2012), it was possible to see the presence of some slow migrating bands, suggestive of dystroglycan being subject to ubiquitination. Interestingly, the antibodies Mandag2 and pYβDG were able to detect some bands that were precipitated with MultiDsk indicating that dystroglycan phosphorylated or non-phosphorylated in tyrosine 890 is subject to ubiquitination (Figure 3.21).

The introduction of the mutations Y890F and K806R seems to have (if any) little effects in the ubiquitination of dystroglycan (Figure 3.23) although further characterisation with MultiDsk will be required. These small changes are not surprising since there are amino acids other than K806 that could be

modified by ubiquitination. Also, this does not discard the idea of K806 being ubiquitinated, but supports the fact that once restricted to ubiquitination other lysines are ubiquitinated instead.

The existence of the nuclear ubiquitin-proteasome system and the functionality to degrade substrates such as the transcription factor MyoD is very well established (Floyd, Trausch-Azar, Reinstein, Ciechanover, & Schwartz, 2001; Rockel, Stuhlmann, & von Mikecz, 2005; von Mikecz, 2006). So, the nuclear degradation of dystroglycan is a feasible hypothesis that has to be probed by combining inhibitors of the nuclear export/import together with MG132 and MultiDsk or by using isolated nuclei/cytoplasm cellular extracts. This could support the idea that, once translocated to the nucleus, dystroglycan exerts its structural/regulatory function before being degraded by the nuclear ubiquitin-proteasome system.

The inhibition of protein synthesis confirmed that the mutations Y890F and K806R are not enough to stop the ubiquitination and hence, the degradation of dystroglycan. This indicates that there are other underlying mechanisms playing an important role in the degradation of dystroglycan. Further research will be required to show if in addition to degradation, ubiquitinated dystroglycan has other roles in protein interactions or cell signalling regulation. It will also be important to have a complete map of the ubiquitinated amino acids in order to determine the role of these modifications in the stability of dystroglycan with therapy purposes.

The multiple ubiquitination of dystroglycan could be part of the explanation of its reduced levels in muscular dystrophies and cancer, and the reason by which its levels are restored following the inhibition of proteasomal activity (Acharyya et al., 2005; Assereto et al., 2006; Bonuccelli et al., 2003, 2007; Kumamoto et al., 2000). It will be important to determine if previously identified members of the ubiquitin-proteasome system in muscle, or their corresponding homologues in prostate cancer, are responsible for the multiple ubiquitination observed in this work (Acharyya et al., 2005; Bodine et al., 2001; Matsumoto et al., 2008). Additionally, it will be interesting to deter-

mine if other mechanisms such as proteolysis are dependent on ubiquitinated dystroglycan for its removal from the plasma membrane.

3.7.6 Summary

The results of the research presented in this chapter show that:

1. Alpha- and beta-dystroglycan are present in the nucleus of LNCaP cells.
2. The insertion of tags in the C-terminal of beta-dystroglycan affects the phosphorylation of its Y890.
3. Beta-dystroglycan may be subject to oligomerization.
4. Beta-dystroglycan is multiply phosphorylated.
5. Beta-dystroglycan is multiply ubiquitinated.

4

Regulated intramembrane proteolysis of beta-dystroglycan

4.1 Introduction

Dystroglycan is a member of the Dystrophin Associated Protein Complex (DAPC) (Ervasti & Campbell, 1991). It is a glycoprotein that mediates interactions between cytoskeletal proteins and the extracellular matrix through its alpha and beta subunits. These subunits are generated after a post-translational cleavage of a 97 kDa precursor peptide derived from a 5.8 kb mRNA transcript. The 56 kDa core alpha-dystroglycan polypeptide is subject to a high degree of O- and N-linked glycosylation, which is very variable in different tissues, rendering a mature protein with a molecular weight up to 160 kDa. On the other hand, the transmembrane beta subunit of dystroglycan has a more constant molecular mass of 43 kDa, and contrary to its counterpart alpha, it is glycosylated to a much lesser extent, although it is subject to other post-translational modifications as described in chapter 3 (Ibraghimov-Beskrovnaya et al., 1992).

The high degree of glycosylation on alpha-dystroglycan is important for its interaction with components of the basal lamina (Ervasti & Campbell, 1993; Michele et al., 2002; Saito et al., 2005) and is believed to confer protection against proteolytic activities of extracellular matrix proteases (Singh et al., 2004), the alteration of which could lead to an uncontrolled growth, as observed in cancer (Martin et al., 2007).

In muscular dystrophies and in a myriad of cancers (among them prostate cancer), the cellular levels of beta-dystroglycan are frequently observed to be reduced (Cross et al., 2008; Henry et al., 2001; Losasso et al., 2000; Muschler et al., 2002; Parberry-Clark et al., 2011; Sgambato et al., 2007). The reduction of beta-dystroglycan in these pathologies is due to proteolytic events. In this regard, a 31 kDa species separate from the 43 kDa full-length beta-dystroglycan has been frequently described in both muscular dystrophies (Matsumura et al., 2005) and cancer (Jing et al., 2004). This 31 kDa fragment is thought to comprise the transmembrane and cytoplasmic fragments of beta-dystroglycan (Losasso et al., 2000; Yamada et al., 2001), and is generated by the proteolytic action of matrix metalloproteases-2 and -9 (MMP-2 and MMP-9) in the extracellular environment (Yamada et al., 2001; Zhong et al., 2006). This cleavage is thought to be prevented by the glycosylation of alpha-dystroglycan, and so enzymes that participate in the glycosylation process can be linked to the degree of proteolysis. For example, in prostate cancer, the reduction in the expression of LARGE2 could cause hypo-glycosylated alpha-dystroglycan, leading to increased proteolysis of beta-dystroglycan, and the generation of the 31 kDa fragment (Esser et al., 2013).

Work performed in the Winder lab has demonstrated the presence of an additional cleavage product of beta-dystroglycan of approximately 26 kDa that was generated when myoblasts cells were exposed to the PKC activator, PDBu (Thompson, 2007). The same band was observed in studies of different human carcinomas, including prostate cancer(Cross et al., 2008; Mathew et al., 2013; Parberry-Clark et al., 2011). This lead us to hypothesize that MMPs have the ability to cleave beta-dystroglycan on its extracellular domain, but generate a fragment that is still anchored to the plasma membrane. This transmembrane fragment (TM), when exposed to a second cleavage by an unknown protease, releases a 26 kDa fragment to the cytoplasm to exert unknown cellular functions.

Beta-dystroglycan is a type I protein embedded in the hydrophobic environment of the plasma and nuclear membranes, and these characteristics resem-

ble other type I transmembrane proteins subject to regulated intramembrane proteolysis (RIP). RIP is mediated by intracellular proteases, and for type I membrane proteins like beta-dystroglycan, such as EpCAM, Notch, APP, Neogenin, CD44, and others (De Strooper et al., 1998, 1999; Goldschneider, Rama, Guix, & Mehlen, 2008; Lal & Caplan, 2011; H. J. Lee et al., 2002; Maetzel et al., 2009), gamma-secretase is the responsible protease. Hence, one could hypothesize that this enzyme also regulates RIP of beta-dystroglycan.

In this chapter the mechanisms triggering the cleavage of beta-dystroglycan and leading to the generation of the 26 kDa cytoplasmic fragment will be investigated. Also, some mechanisms leading to the nuclear translocation of beta-dystroglycan will be described. Additionally, an insight into the mechanisms regulating the turnover of beta-dystroglycan will be assessed. All of this is also in support of the hypothesis that, once beta-dystroglycan has performed its structural/signalling processes on the plasma and nuclear membranes, it is prone to RIP by gamma-secretase and then subjected to degradation by the nuclear proteasome system (Figure 4.1).

4.2 Triggering factors

The proteolysis of plasma membrane proteins can have several underlying effects, such as the activation of dormant domains within a protein. These proteolytic events can also generate cytoplasmic domains that exert nuclear regulatory effects, as is the case of Notch, EpCAM, Neogenin and others (De Strooper et al., 1998, 1999; Goldschneider et al., 2008; Lal & Caplan, 2011; H. J. Lee et al., 2002; Maetzel et al., 2009). Stimulation with phorbol esters and *in vitro* culturing of cells at a high density are two experimental techniques used to trigger and study these regulatory events mediated by cleaved cytoplasmic domains (Goldschneider et al., 2008; Lal & Caplan, 2011).

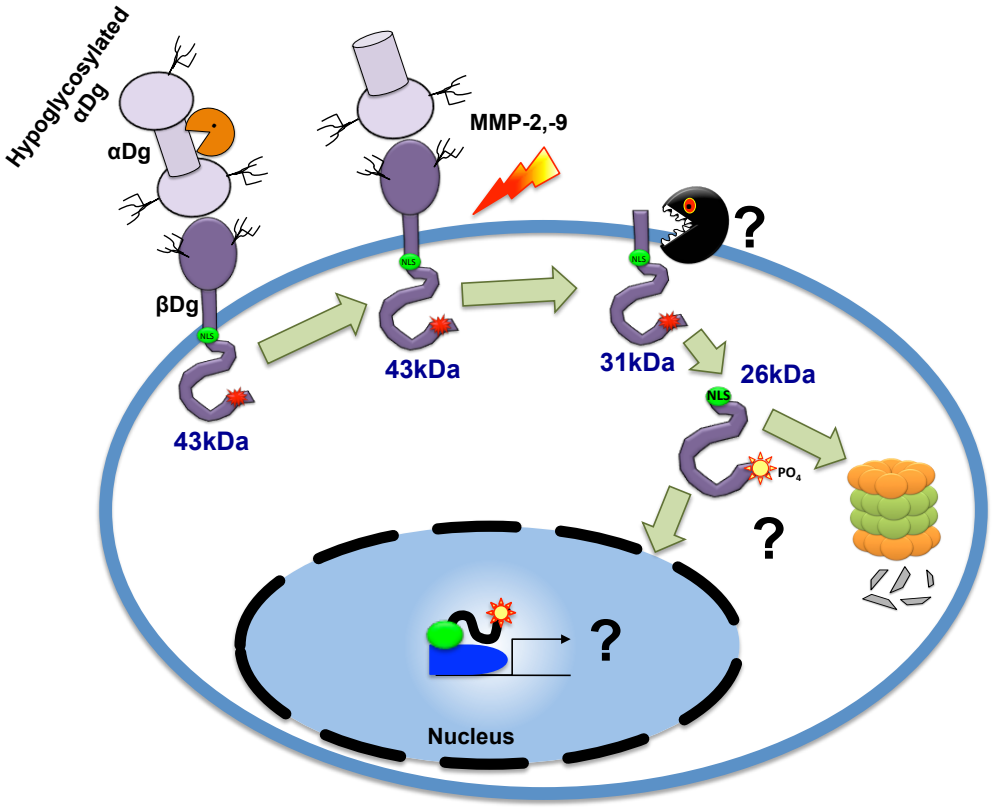

Figure 4.1: Beta-dystroglycan is subject to different proteolytic events. Beta-dystroglycan has been observed to be reduced in different pathologies including muscular dystrophies and cancer. The current hypothesis points towards proteolytic events mediated by proteases in the extracellular and intracellular environments capable of generating a 31 kDa transmembrane fragment. However, the processes governing the generation of an additional 26 kDa cytoplasmic fragment and its biological relevance remain still to be investigated.

4.2.1 PDBu stimulates the proteolysis of beta-dystroglycan

Phorbol esters, such as phorbol-12-myristate-13-acetate (PMA) and phorbol-12,13-dibutyrate (PDBu), are potent activators of the PKC pathway. In cellular models, such as the human umbilical vein endothelial cells (HUVECs), activated PKC stimulates Src, which in turn activates Cdc42, inducing the formation of podosome-like structures (Tatin, Varon, Génot, & Moreau, 2006). A similar process is observed in myoblasts where, following PDBu stimulation, Src is able to phosphorylate dystroglycan, which in turn binds the adaptor protein Tks5 leading to the formation of podosomes-like structures (Thompson et al., 2008). Podosomes are actin-rich cellular structures that degrade the

surrounding extracellular matrix components through the activation of matrix metalloproteinases such as MMP-2 (Murphy & Courtneidge, 2011; Tatin et al., 2006).

Given the reported interactions of PKC, Src, MMP-2 and dystroglycan, the activation of MMP-2 by PKC, and their recruitment to podosome-like structures upon PDBu stimulation, it was therefore decided to investigate the effects of PDBu in the proteolysis of beta-dystroglycan in LNCaP cells. Western blot analysis of phosphorylated beta-dystroglycan showed an increase in the amount of levels of phosphorylated cytoplasmic fragment (black arrowhead) compared with the full-length protein (arrow) in cells exposed to PDBu treatment. However, the levels of transmembrane fragment of beta-dystroglycan did not appear to change over the course of the treatment (empty arrowhead) (Figure 4.2). It is important to note that, cells were maintained at a low density for the PDBu experiments in order to differentiate the effects mediated by PDBu from those mediated by a high cell confluency, as will be shown later.

PDBu has been shown to stimulate the formation of podosomes-like structures in myoblasts (Thompson et al., 2008) and in LNCaP cells (unpublished Winder lab observations). To determine any possible changes produced by PDBu stimulation, including the potential nuclear translocation of beta-dystroglycan, LNCaP cells transfected with the plasmid $\alpha\beta$DgFlag were treated with PBDu and then co-immunostained with pYβDG, Mandag2 and Flag antibodies. Interestingly, upon PDBu stimulation, there is a relocalisation of beta-dystroglycan, both native and phosphorylated, to the perinuclear area. Most of the signal was lost from the plasma membrane and cells lost the classical fillopodial structures observed in cells over-expressing beta-dystroglycan, and exhibited rounded and flat lamellipodia (Figure 4.3 and 4.4).

In order to have a better idea if the visual accumulation of beta-dystroglycan observed around the nucleus represented increased levels in the nucleus, fractionation of cells treated with PDBu or without PDBu was performed. Although there was an evident increase in the amount of the 26 kDa cytoplas-

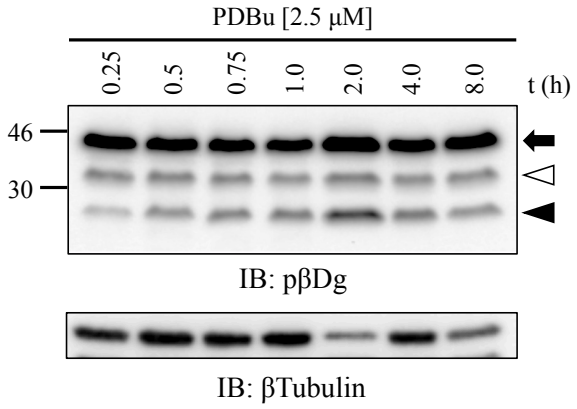

(a)

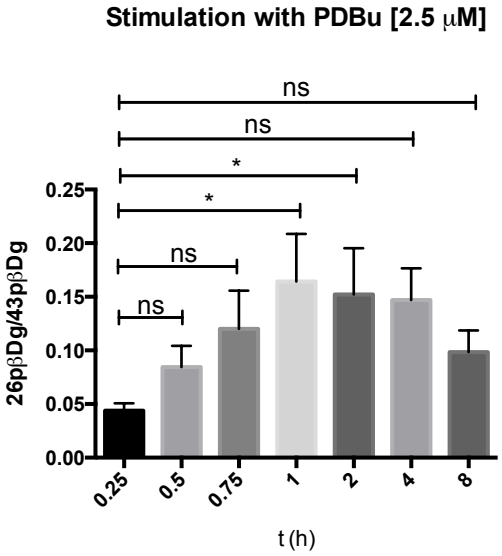

(b)

Figure 4.2: PDBu stimulates the proteolysis of phospho-beta-dystroglycan. (a) Wild type LNCaP cells seeded at a low confluency (40000 cells/cm^2) were grown for 24 hours. After the stated time, the medium was replaced with medium supplemented with PDBu [2.5 μM] and further treated for different times as shown above. Cells were collected with RIPA buffer and lysates were subjected to immunoblot analysis with antibodies to p-beta-dystroglycan. Beta-tubulin is shown as the loading control. There is a clear increase in the amount of phosphorylated cytoplasmic fragment of beta-dystroglycan over the time (black arrowhead). (b) The graph shows the ratio of the signal of the 26 kDa cytoplasmic fragment (black arrowhead) against the 43 kDa full-length (arrow) beta-dystroglycan (means ± SEM, n=3, *p=<0.05).

mic fragment of beta-dystroglycan (CD) following PDBu stimulation in the non-nuclear fraction, this increase was not observed in the nuclear fraction (Figure 4.5).

Overall, these results suggest that beta-dystroglycan is subject to proteolytic events downstream of PDBu stimulation with the consequent release of a 26 kDa cytoplasmic fragment. These events decrease the amount of beta-dystroglycan present at the plasma membrane and increase cytosolic, but not nuclear, accumulation.

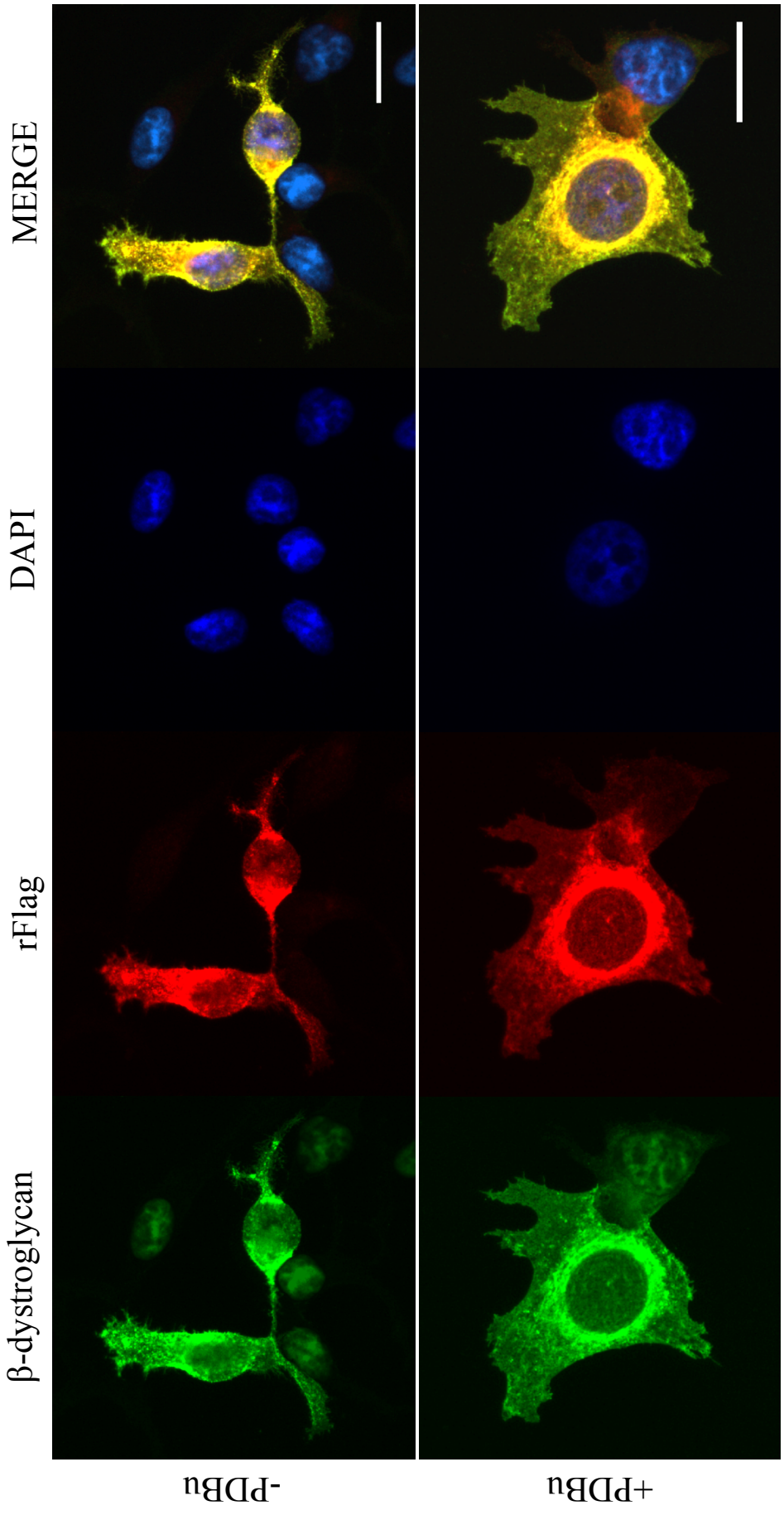

Figure 4.3: Re-localisation of beta-dystroglycan upon PDBu stimulation. LNCaP cells transfected with the plasmid $\alpha\beta$DgFlag were treated with PDBu [2.5 μM] for 2 hours. Cells were washed with PBS and then co-immunostained with anti-Flag and anti-βDg antibodies. Epi-fluorescent microscopy images show a clear co-localisation of the signal generated by both antibodies and a clear re-localisation of beta-dystroglycan from the plasma membrane to an area surrounding the nuclear compartment. Nuclei were counterstained with DAPI (Scale bar = 20 μm, objective = 63 X).

Figure 4.4: Re-localisation of p-beta-dystroglycan upon PDBu stimulation. LNCaP cells transfected with the plasmid $\alpha\beta$DgFlag were treated with PDBu [2.5 μM] for 2 hours. Cells were washed with PBS and then co-immunostained with anti-Flag and anti-p-βDg antibodies. Epi-fluorescent microscopy images show a clear co-localisation of both antibodies and a clear re-localisation of p-beta-dystroglycan to an area surrounding the nuclear compartment. Nuclei were counterstained with DAPI (Scale bar = 20 μm, objective = 63 X).

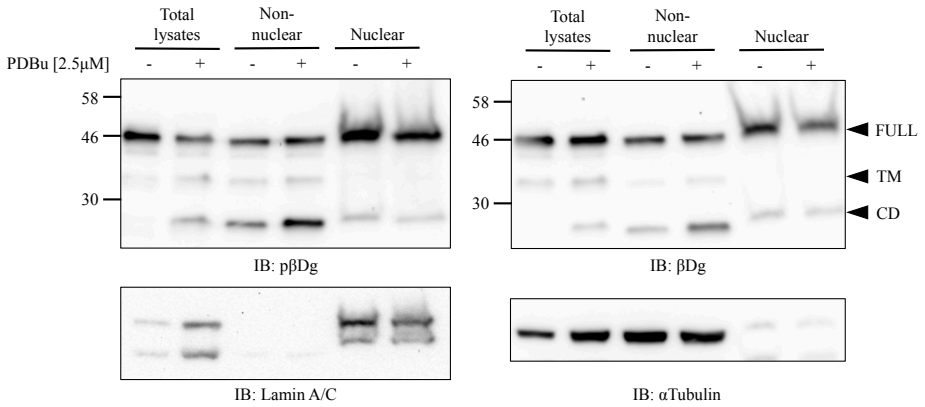

Figure 4.5: PDBu stimulates the proteolysis of beta-dystroglycan but not its nuclear translocation. LNCaP cells treated with PDBu [2.5 μM] for 2 hours were fractionated in non-nuclear and nuclear fractions. Immunoblot analysis of both fractions with antibodies anti-p-βDg and anti-βDg shows a clear increase in the amount of the 26 kDa fragment in the non-nuclear compared to the nuclear fraction. Membranes were reprobed with anti-Lamin A/C and anti-αTubulin as controls of fraction and equal loading. The images shown are representative images of three independent experiments.

4.2.2 Cellular density triggers the proteolysis and nuclear translocation of beta-dystroglycan

The partial loss of beta-dystroglycan from the basal and basolateral sides of epithelial cells has been demonstrated in cases of high grade prostate cancer (Mathew et al., 2013). Given the limitations of obtaining pure prostate tumor tissue samples, a good *in vitro* assay to mimic tumour growth is growth or culturing of cells at high densities. Through these assays, Mitchell and colleagues were able to demonstrate the cell density-dependent proteolysis of beta-dystroglycan (Mitchell et al., 2013).

In this regard, LNCaP cells were plated at different densities (20, 50, 80 and 110 x $10^6/cm^2$) representing the range from low to high cell density (Figure 4.6a) and then the total lysates were analysed by western blotting using the antibodies Mandag2 and pYβDG. With successive increases in cell density an increase in the amount of the cytoplasmic fragment of beta-dystroglycan

(CD) was observed. Interestingly, the increase in the cellular density led to an increase in the synthesis of full-length beta-dystroglycan (Full). Apparently, non-phospho and phospho-beta-dystroglycan were subject to the same rate of proteolytic events (Figure 4.6b).

After corroborating that cell density is a mechanism triggering the proteolysis of beta-dystroglycan it was decided to investigate if changes in cell density where linked to an alteration in the levels of proteolysed beta-dystroglycan in the nucleus. LNCaP cells under the same conditions as those described above (see Figure 4.6) were subjected to cell fractionation. Surprisingly, through cell fractionation it was possible to differentiate mechanisms regulating the fate of beta-dystroglycan. First, increases in the cell density led to an increase in the proteolysis of beta-dystroglycan observed by the reduction of full-length protein (FULL) and an increase of the 26 kDa fragment (CD) in the non-nuclear fraction. Second, increasing the cellular density led to an increase in the amount of full (FULL) and cytoplasmic (CD) forms of beta-dystroglycan in the nucleus (Figure 4.7).

Together these results provide important insights into the proteolysis of beta-dystroglycan: upon PDBu stimulation and in high cell density conditions, beta-dystroglycan is cleaved generating a 26 kDa fragment. Both, the full-length and cytoplasmic forms of beta-dystroglycan are translocated to the nucleus when cells reach a high cell density, but not upon PDBu stimulation, suggesting an overlap of both mechanisms in proteolysis but not in nuclear transport. The next section, therefore, reports on the proteases involved in the cleavage of beta-dystroglycan that generates the 26 kDa cytoplasmic fragment.

4.3 Dystroglycan-cleaving proteases

Beta-dystroglycan is a type I transmembrane protein. From previous reports it is known that matrix-metalloproteases are able to exert a proteolytic cleavage on the extracellular domain of beta-dystroglycan (Yamada et al., 2001). This

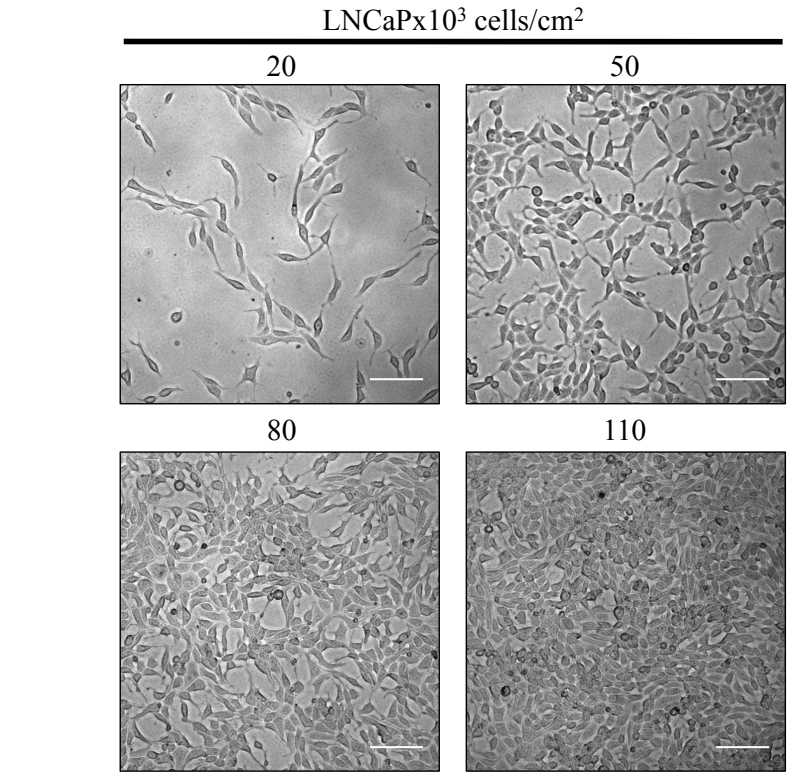

(a)

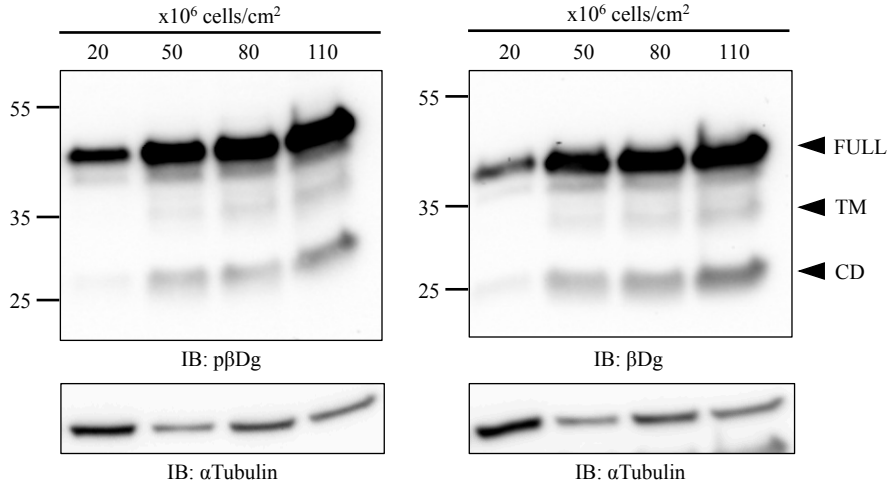

(b)

Figure 4.6: Cell density dependent proteolysis of beta-dystroglycan. (a) LNCaP cells were seeded at different densities (20, 50, 80, 111 x 106 cells/cm^2 representing the ranges from low to high cell density) (bright field microscopy, objective 10X, scale bar = 100 μm) and lysed after 48 hours growth. (b) Lysates were immunoblotted with antibodies anti β-dystroglycan (Mandag2) and anti p-β-dystroglycan (pYβDG) antibodies. The increase in the cell density leads to an increase in the proteolysis of beta-dystroglycan. Alpha-tubulin is shown as the loading control.

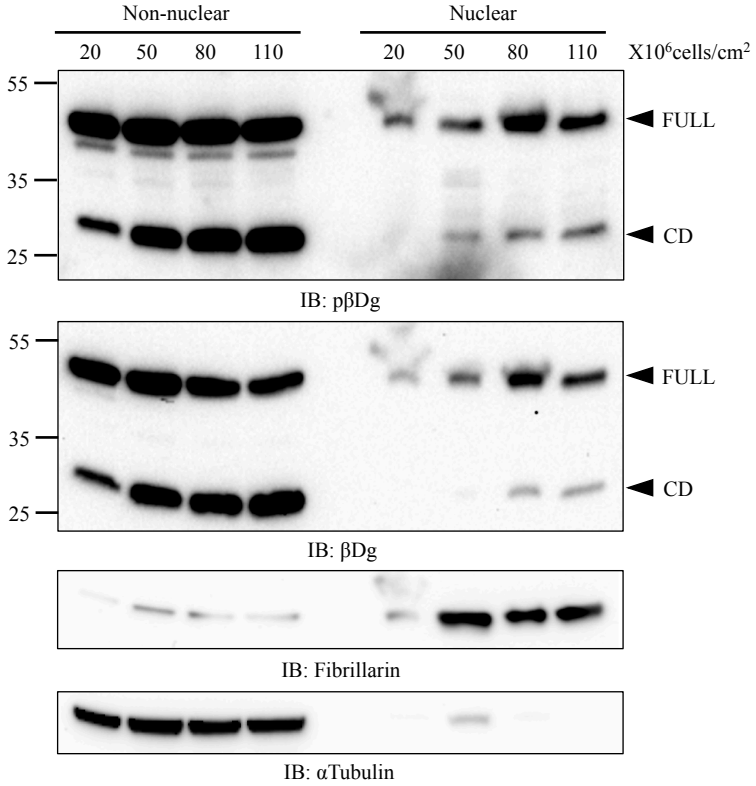

Figure 4.7: Full-length and cd-βDg are translocated to the nucleus in a cell density dependent manner. LNCaP cells were seeded as in Figure 4.6. After 48 hours, cells were collected for cell fractionation. Non-nuclear and nuclear fractions were incubated with primary antibodies Mandag2 and pYβDG. Representative images of three independent experiments show the nuclear accumulation of the 43 kDa and 26 kDa forms of non-phospho- and phospho-beta-dystroglycan. Fibrillarin and alpha-tubulin are shown as the loading controls.

cleavage generates a 31 kDa fragment of beta-dystroglycan that is still anchored to the plasma membrane. So, there may be other proteases responsible for additional cleavages and generation of the 26 kDa cytoplasmic fragment. The plasma membrane is a hydrophobic environment wherein most cellular enzymes have a restricted function, because of their main requirement for water. Of the proteases known to exert proteolytic functions in hydrophobic environments, gamma-secretase is the best candidate enzyme for the cleavage of beta-dystroglycan and the generation of the cytoplasmic fragment.

4.3.1 Gamma-secretase and furin

It was observed previously that at high LNCaP cell density the amount of the 26 kDa fragment of beta-dystroglycan increased. To replicate this, LNCaP cells were plated at a high confluency. Following growth for a further 24 hours, cells were treated with DAPT (N-[N-(3,5-Difluorophenacetyl-L-alanyl)]-S-phenylglycine t-Butyl Ester), which has been shown to be an inhibitor of gamma-secretase (Dovey et al., 2001). Cells that were treated with different concentrations of DAPT (although not significant) showed a tendency to reduction in the ratio of cytoplasmic fragment to full-length beta-dystroglycan compared with the control, however this reduction was not significant. Although this was expected to be partnered with an increase in the levels of the transmembrane fragment of beta-dystroglycan, this did not happen (Figure 4.8). It could be that, if increased, the transmembrane fragment is not detected because it is subjected to a rapid turnover by mechanisms such as the proteasomal activity, as will be shown later.

From experiments involving cell fractionation under high cell density conditions, a large amount of cleaved beta-dystroglycan was observed and also an increase in the amount of full and cytoplasmic forms of beta-dystroglycan within the nucleus (Figure 4.7). To determine if the same effects observed in whole cell lysates of cells treated with DAPT were also observed in nuclear beta-dystroglycan it was decided to fractionate cells under DAPT treatment and compare non-nuclear and nuclear beta-dystroglycan with untreated controls. This time the reduction in the amount of the cytoplasmic fragment (CD) was not very evident, however, an increase in the amount of the transmembrane (TM) fragment of beta-dystroglycan in cells under pharmacological treatment in total cell lysates was observed (Figure 4.9). Although faint, the same effect was observed in non-nuclear and nuclear fractions. The increase in the amount of the transmembrane fragment of beta-dystroglycan was accompanied by an increase in the amount of the full-length form (FULL) in the nucleus (Figure 4.9).

Beta-dystroglycan harbours a nuclear localisation signal immediately down-

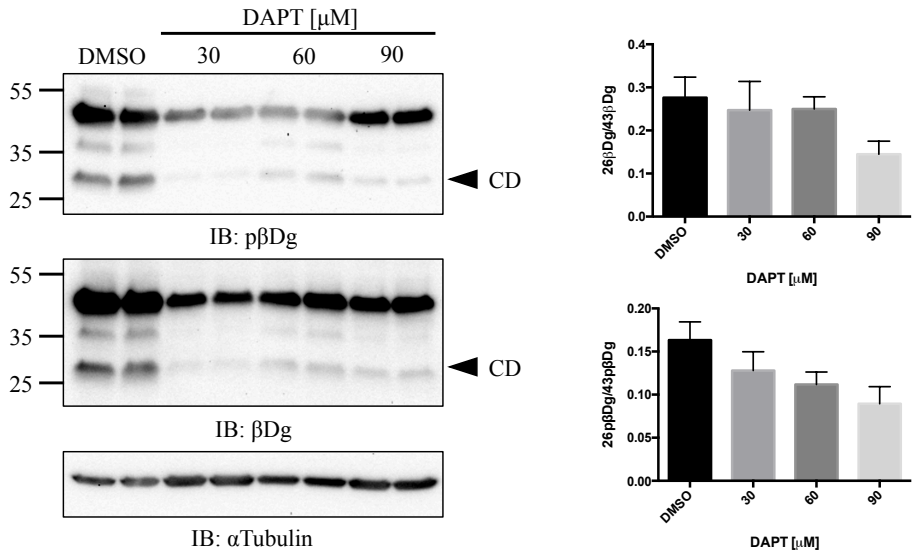

(a) (b)

Figure 4.8: The generation of the 26 kDa fragment of beta-dystroglycan is gamma-secretase dependent. (a) LNCaP WT were grown for 24 hours before being treated with different concentrations of DAPT or DMSO (control) for further 24 hours. Cells were washed with PBS and then lysed with RIPA buffer. Lysates were immunoblotted with anti-p-βDg and anti-βDg antibodies. The increase in the concentration of DAPT leads to a reduction in the amount of the cytoplasmic fragment of beta-dystroglycan. Alpha-tubulin is shown as the loading control. (b) The graphs show the normalization of the 26 kDa fragment to the full-length 43 kDa beta-dystroglycan (means ± SEM, n=3).

stream of the transmembrane domain (see Figure 3.6b). This domain is a motif rich in basic R and K amino acids. An in-depth analysis of this motif using the Eukaryotic Linear Motif resource (`http://elm.eu.org`), highlighted its susceptibility to further proteolytic events mediated by furin. In order to exclude the possibility of furin cleaving beta-dystroglycan, LNCaP cells were treated with increasing concentrations of the peptidyl chloromethylketone, furin inhibitor I. Increasing concentrations of the inhibitor reduced the level of the 26 kDa fragment of beta-dystroglycan (Figure 4.10). Although there were reduced levels of the cytoplasmic fragment of beta-dystroglycan as a consequence of the treatment with furin inhibitor I, additional experiments are required to further show the role of furin in the cleavage of dystroglycan downstream its transmembrane domain.

In summary, the experiments shown in this section provide evidence of

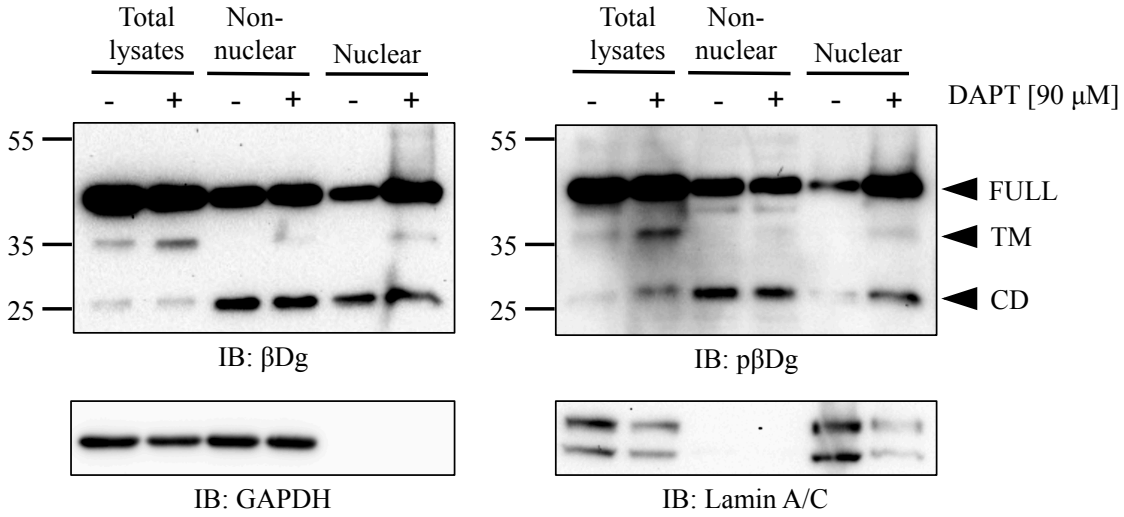

Figure 4.9: Gamma-secretase has a potential role in the proteolysis of nuclear beta-dystroglycan. LNCaP cells treated under the same conditions as for whole cell lysates were collected for cell fractionation. Immunoblot analysis with anti-p-βDg and anti-βDg of total lysates, non-nuclear and nuclear fractions show an increase in the amount of the transmembrane fragment of beta-dystroglycan in the cells treated. Membranes were stripped and reprobed with anti-GAPDH and anti-Lamin A/C antibodies to show the loading controls for the non-nuclear and nuclear fractions respectively.

gamma-secretase and furin as the enzymes involved in the generation of the cytoplasmic fragment of beta-dystroglycan. Regulated intramembrane proteolysis is a process that usually involves the generation of a cytoplasmic fragment that is then translocated to the nucleus to exert regulatory functions. The next section will therefore examine some of the cellular processes regulating the fate of the cytoplasmic fragment of beta-dystroglycan.

4.4 Nuclear translocation of the cytoplasmic fragment of beta-dystroglycan

4.4.1 The cdβDgFlag is degraded by the proteasome

From DAPT treatment experiments (Figure 4.8) a reduction in the levels of the cytoplasmic fragment of beta-dystroglycan was observed, but there were

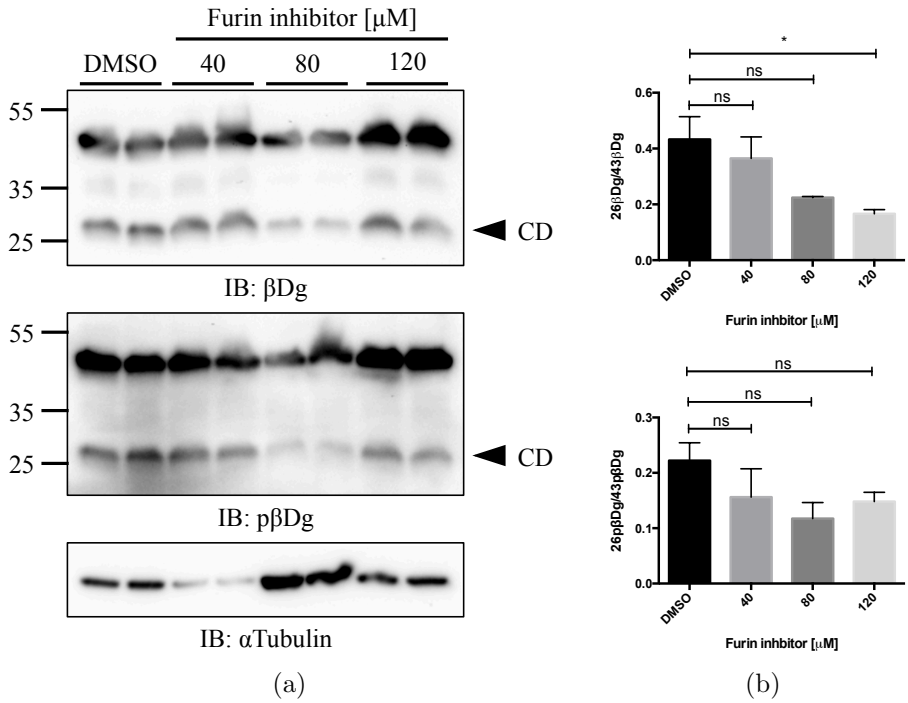

(a) (b)

Figure 4.10: Potential role of furin in the cleavage of beta-dystroglycan. (a) LNCaP cells grown for 24 hours and then treated with Furin inhibitor I at different concentrations. After 24 hours post-treatment, cells were lysed with RIPA buffer and immunoblotted with antibodies anti-βDg and anti-p-βDg. There is a reduction in the amount of the cytoplasmic fragment of beta-dystroglycan upon the increase in the amount of furin inhibitor. Alpha-tubulin is shown as the loading control. (b) The graphs show the normalization of the 26 kDa fragment against the 43 kDa form of phospho- and non-phospho-beta-dystroglycan (means ± SEM, n=3, *p=<0.05).

not any apparent changes in the levels of the transmembrane fragment. This was suggestive of other mechanisms involved in the rapid turnover of these small fragments. From experiments with multiDsk it was observed that beta-dystroglycan is subject to multiple ubiquitination events (see Figure 3.21), indicating a possible involvement of the ubiquitin-proteasomal system.

Inhibition of proteasomal activity with MG132 allowed a great recovery of the transmembrane (TM) and cytoplasmic fragment (CD) of beta-dystroglycan compared with control treatments. Interestingly, the band usually observed between 130 and 250 kDa (HDG) was not detected on cells treated with MG132. The loss was more prominent in immunoblots for non-phosphorylated beta-dystroglycan compared to its phosphorylated counterpart (Figure 4.11).

This leads to the conclusion that, once beta-dystroglycan is subject to proteolytic events mediated by gamma-secretase and furin, both the transmembrane and cytoplasmic fragments are rapidly degraded by the proteasome.

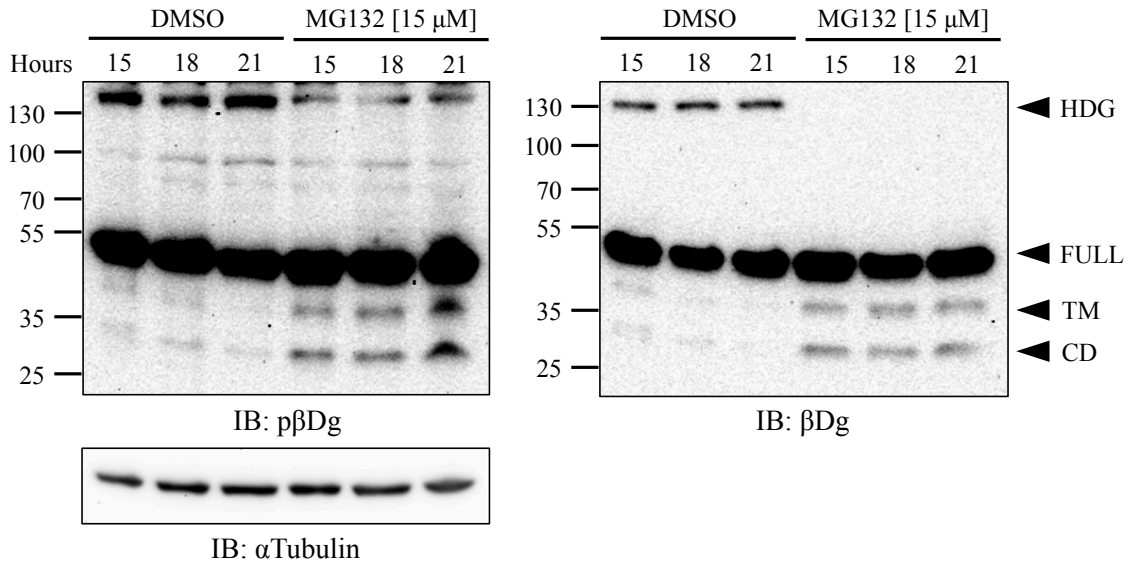

Figure 4.11: Beta-dystroglycan is degraded by the proteasome. After 24 hours growth, LNCaP cells were further treated with MG132 [15 μM] or DMSO (control) for 15, 18 and 21 hours. Cells were collected with RIPA buffer and immunoblotted with anti-βDg and anti-p-βDg antibodies. Treatment of LNCaP cells with MG132 leads to a great recovery of the 31 and 26 kDa forms of beta-dystroglycan compared with the control. The experiment was also performed using different concentrations of MG132 (10, 20 and 30 μM) for 24 hours with the same effect observed with both antibodies (data not shown). Alpha-tubulin is shown as the loading control.

4.4.2 The cdβDgFlag is translocated to the nucleus

If beta-dystroglycan is frequently reduced in cases of muscular dystrophies and cancer then it means that the rate of proteolysis is very high, hence the amount of the cytoplasmic fragment of beta-dystroglycan should be increased. In order to have a better idea about some of the cellular events involved in this situation, it was decided to take advantage of the plasmid expressing recombinant $\alpha\beta$DgFlag and perform some modifications in order to over-express the amino acids encoding the cytoplasmic portion of beta-dystroglycan only (cdβDgFlag)

(Figure 4.12). Besides the Flag tag, it was decided not to introduce any other tags in order to mimic similar conditions to those of the endogenous cleaved cytoplasmic fragment.

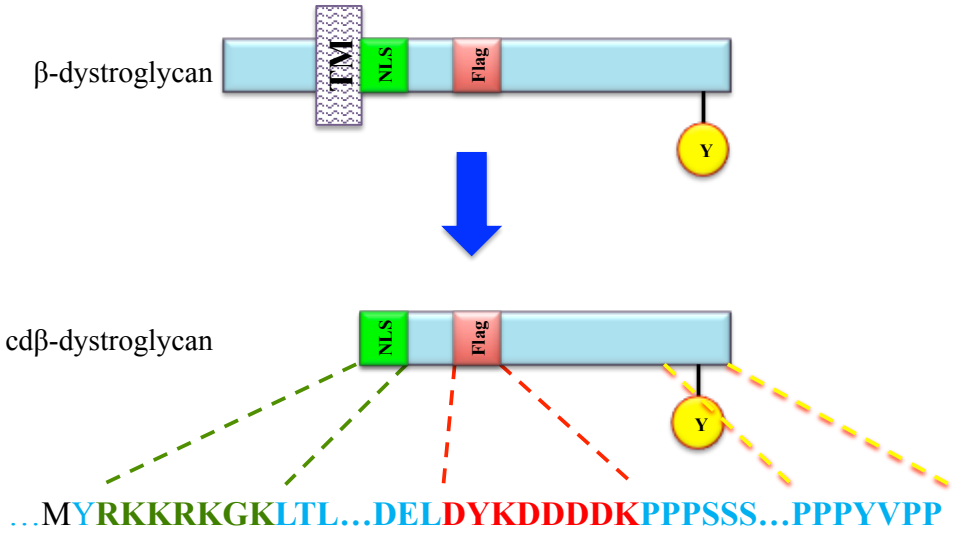

Figure 4.12: Generation of the plasmid pcDNA3.1(+)-cd4βDgFlag. In the schematic is shown the coding sequence of the cytoplasmic fragment of mβDg that was amplified by PCR from the plasmid pcDNA3.1(+)-$\alpha\beta$DgFlag. The forward primer was designed to introduce the starting codon methionine (black) in the 5' end before the codon of Y773 that marks the start of the cytoplasmic fragment of beta-dystroglycan (see material and methods). Following the characterisation by sequencing, the plasmid was purified and transfected in LNCaP cells.

The transfection of LNCaP cells with the plasmid encoding cdβDgFlag followed by co-immunostaining with Mandag2, pyβDG and Flag antibodies showed a clear co-localisation between phospho and non-phospho beta-dystroglycan with Flag-tagged beta-dystroglycan. Importantly, the cytoplasmic fragment was distributed all along the cell but was more concentrated in the nucleus (Figures 4.13a and 4.14a). Additionally, and although it was not quantitatively determined, it was observed that the overexpression of the cytoplasmic fragment of beta-dystroglycan had profound effects in different cellular processes such as (Figures 4.13b and 4.14b):

1. Nucleoli were reduced in number and had an apparent increase in size (may be due to a process of nucleolar fusion)

2. There was an increased number of multinucleated cells.

3. There was an increased number of vesicle-like structures throughout the cytoplasm.

4. Cells were increased in size.

5. There was an increased number of apoptotic-like cells.

All these observations were gathered by comparing the phenotype of transfected cells with their neighbour untransfected counterparts. However more in-depth analysis will be required to further show the implication of the cytoplasmic fragment of beta-dystroglycan in each one of the cellular processes described above.

During the process of characterisation of this recombinant cytoplasmic fragment it was not possible to see its expression by western blotting supporting the idea of a rapid degradation by the proteasome. However, inhibition of proteasomal activity, followed by immunoprecipitation with Flag M2 resin, allowed a substantial recovery of this fragment (Figure 4.15). The detection of a single band is suggestive of a mono-ubiquitinated cytoplasmic fragment and has to be confirmed by other in-depth analysis such as mass spectrometry.

As stated before, full-length beta-dystroglycan co-localized with ubiquitin. In this regard, it was decided to get a better idea about the ubiquitinated status of cdβDgFlag. The immunostaining of cells expressing this fragment revealed its co-localisation with ubiquitin and most importantly, most of the co-localisation was concentrated in the nucleus (Figure 4.16).

The series of experiments shown in this section suggest that the cytoplasmic fragment of beta-dystroglycan is ubiquitinated, translocated to the nucleus and rapidly degraded by the proteasome. The over-expression of the cytoplasmic fragment apparently affected some stages of cell division (abnormal nuclear separation), increased the number of vesicle-like structures in the cell and the number of apoptotic cells (author's own observation) which will require further in-depth analyses to fully understand.

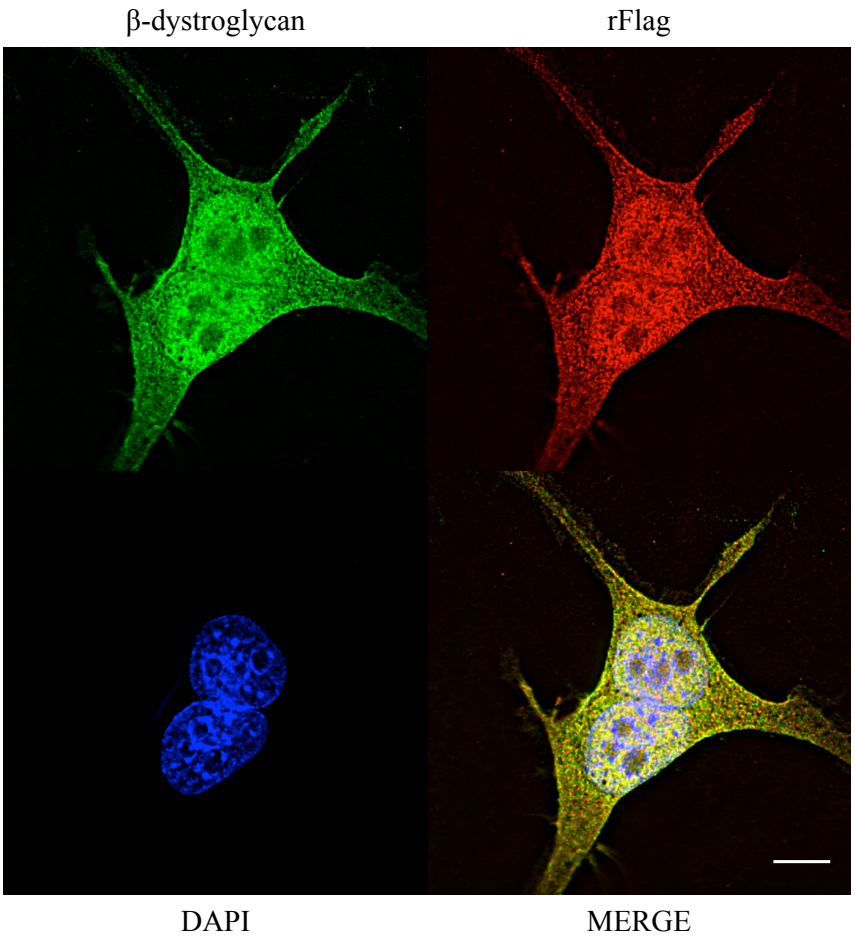

(a)

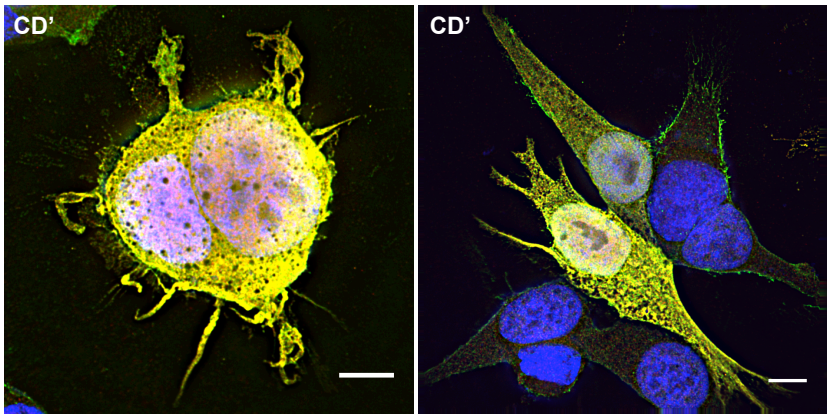

(b)

Figure 4.13: The cdβDgFlag has a preferential nuclear localisation. Transfected LNCaP cells with the plasmid encoding the cytoplasmic fragment of βDgFlag were co-immunostained with anti-βDg (green) and anti-rFlag (red) antibodies. A middle stack section of deconvolved confocal microscopy images shows that a high amount of the exogenous expressed cytoplasmic fragment of βDg is concentrated in the nucleus in addition to some cellular abnormalities (CD'). DAPI is used to counterstain the nucleus. Scale bar = 10 μM.

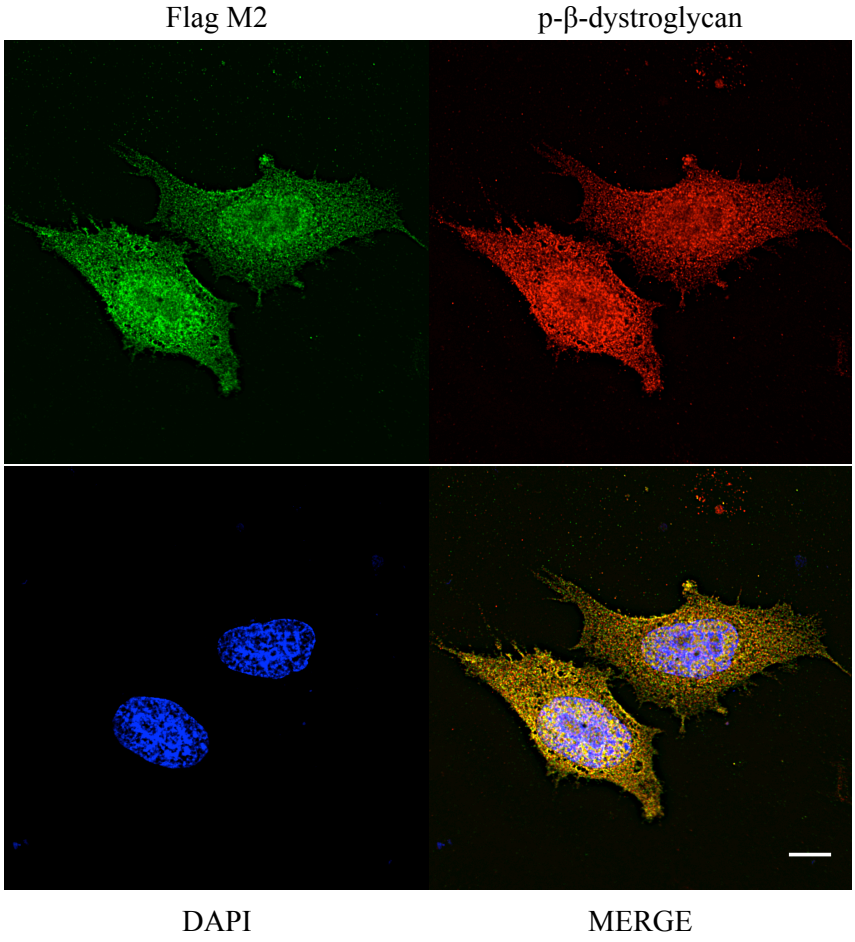

(a)

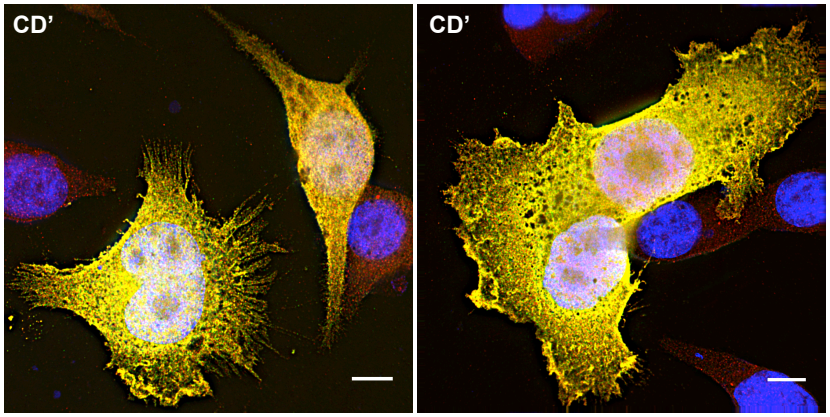

(b)

Figure 4.14: The cdβDgFlag has a preferential nuclear localisation. Transfected LNCaP cells with the plasmid encoding the cytoplasmic fragment of βDgFlag were co-immunostained with anti-p-βDg (red) and anti-Flag M2 (green) antibodies. A middle stack section of deconvolved confocal microscopy images shows that a high amount of the exogenous expressed cytoplasmic fragment of βDg is concentrated in the nucleus in addition to some cellular abnormalities (CD'). DAPI is used to counterstain the nucleus. Scale bar = 10 μM.

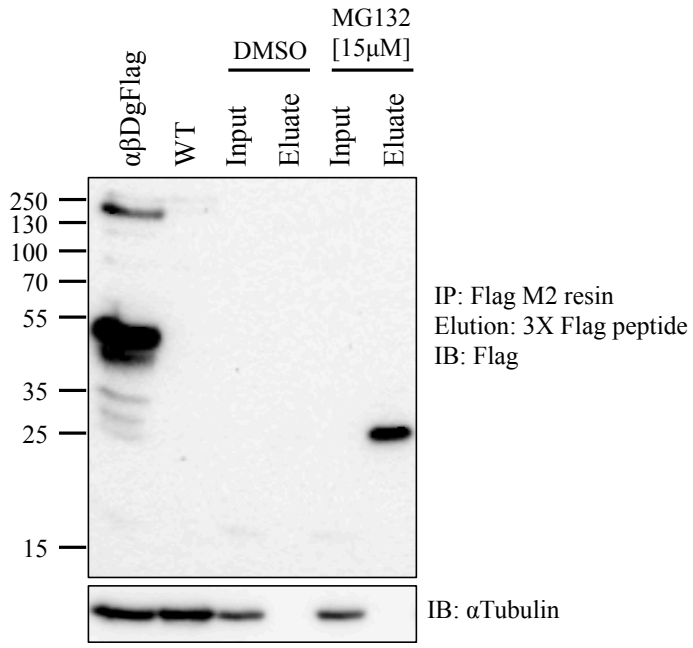

Figure 4.15: The cdβDgFlag is degraded by the proteasome. LNCaP cells were transfected with the cytoplasmic fragment of βDgFlag. 24 hours post-transfection, cells were treated with the proteasomal inhibitor MG132 followed by further immunoprecipitation with the Flag M2 resin. The signal specific to the 26 kDa form of βDg was only detected in cells treated with MG132 followed by immunoprecipitation. Lysates of cells transfected with full-length βDg were included as a reference of the electrophoretic mobility of the exogenous cdβDgFlag. WT lysates helped to discriminate any possible non specificity of the antibody.

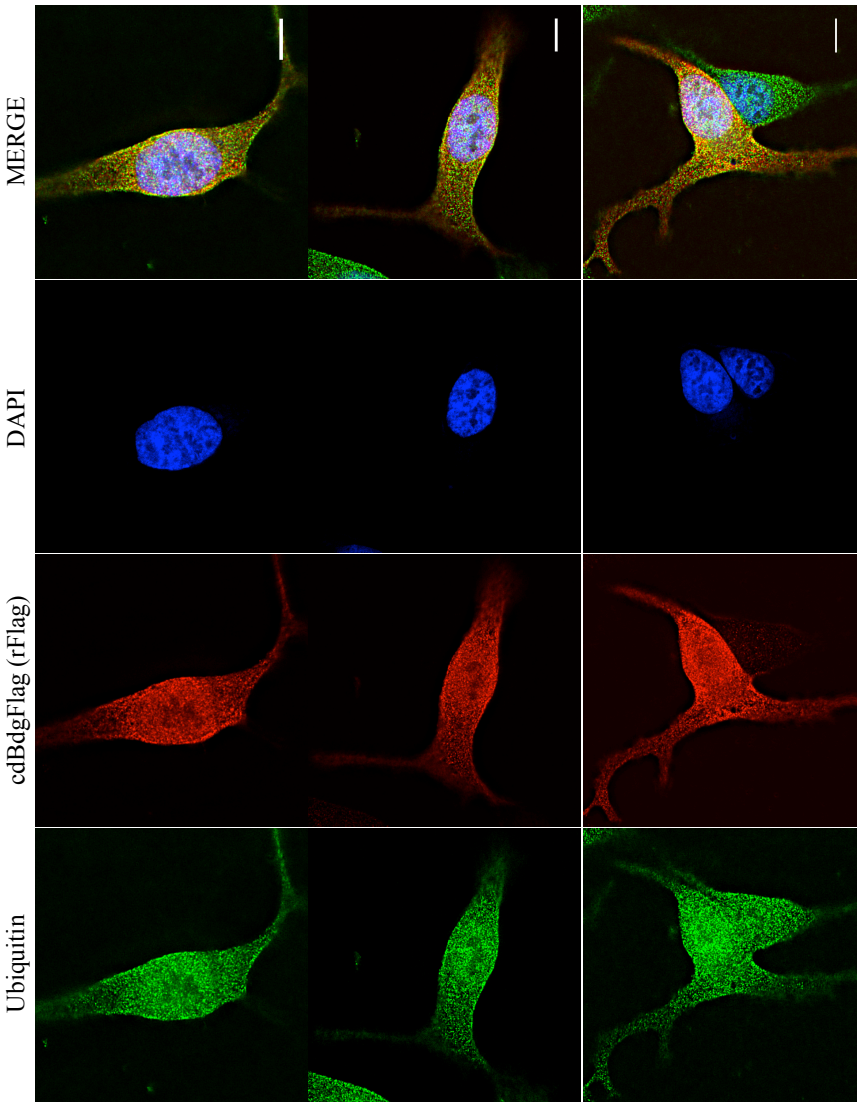

Figure 4.16: Co-localisation between the cdβDgFlag and ubiquitin. The over-expression of exogenous cdβDgFlag leads to its classic nuclear accumulation (red) but also to a predominant co-localisation with ubiquitin (green) in the nucleus of LNCaP cells. DAPI is used to stain the nuclei. Shown are middle stack sections of deconvolved microscopy images (scale bar = 10 μM)

4.4.3 Cleavage site for the generation of cdβDgFlag

The cleavage of beta-dystroglycan, followed by its degradation by the proteasome is a potential pathway for the turnover of this type I transmembrane protein. Importantly, in some muscular dystrophies and forms of cancer these processes are up-regulated. This could be due to an abnormal activity of the proteasome, an increased activity of gamma-secretase and furin, or due to other additional factors, such as glycosylation or the abnormal activity of matrix-metalloproteases. A clear consequence of these abnormal activities could be the increased cleavage of plasma membrane proteins important for the restriction of the abnormal growth of cancerous cells. Additionally, although the cleavage site by MMP-9 has been suggested, there is no knowledge of the functional consequences of the secreted extracellular domains of beta-dystroglycan (Bozzi, Inzitari, et al., 2009).

To distinguish naturally generated cytoplasmic fragments from that originated by trypsin, lysates were subjected to dimethyl labelling. By using this protocol, it is possible to add methyl groups to the free N-terminal sides of proteins by the chemical action of formaldehyde and cyanoborohydride (Shen, Hsu, & Chen, 2007). Therefore, an immunoprecipitation assay was performed using Flag M2 resin from lysates of LNCaP cells transiently transfected with the plasmid $\alpha\beta$DgFlag. Immunoprecipitated material with the Flag M2 resin was separated by SDS-PAGE and then stained with brilliant blue G colloidal dye (Figure 4.17a). Bands corresponding to cytoplasmic fragment and full-length beta-dystroglycan were excised and di-methyl labelled with formaldehyde/cyanoborohydrade or left without any chemical labelling (Figure 4.17b). Following this, the peptides were digested with trypsin and then analysed by tandem mass spectrometry. From this attempt there was a good coverage of beta-dystroglycan (78%), but it was not possible to identify both the sequence corresponding to the extracellular or transmembrane cleavage products of full-length beta-dystroglycan (Figures 4.17c and 4.18).

Figure 4.17: Analysis of the cleavage site of beta-dystroglycan. (a) Immunoprecipitated peptides with anti-Flag M2 resin were reduced, alkylated and resolved by SDS-PAGE. Stained gel with brilliant blue G colloidal dye helped to identify by approximation the areas containing the putative full-length and cytoplasmic forms of βDg. (b) The schematic shows the series of reactions that take place to label free amino terminus of the peptides with dimethyl groups. (c) Shown are the sequences of Flag (black) and mouse alpha- (red) and beta- (blue) dystroglycan. Bold and underlined are the sequences detected by mass spectrometry. Although the mass spectrometer reported a 78% sequence coverage for βDg, the sequence that belongs to the transmembrane domain (green) could not be detected.

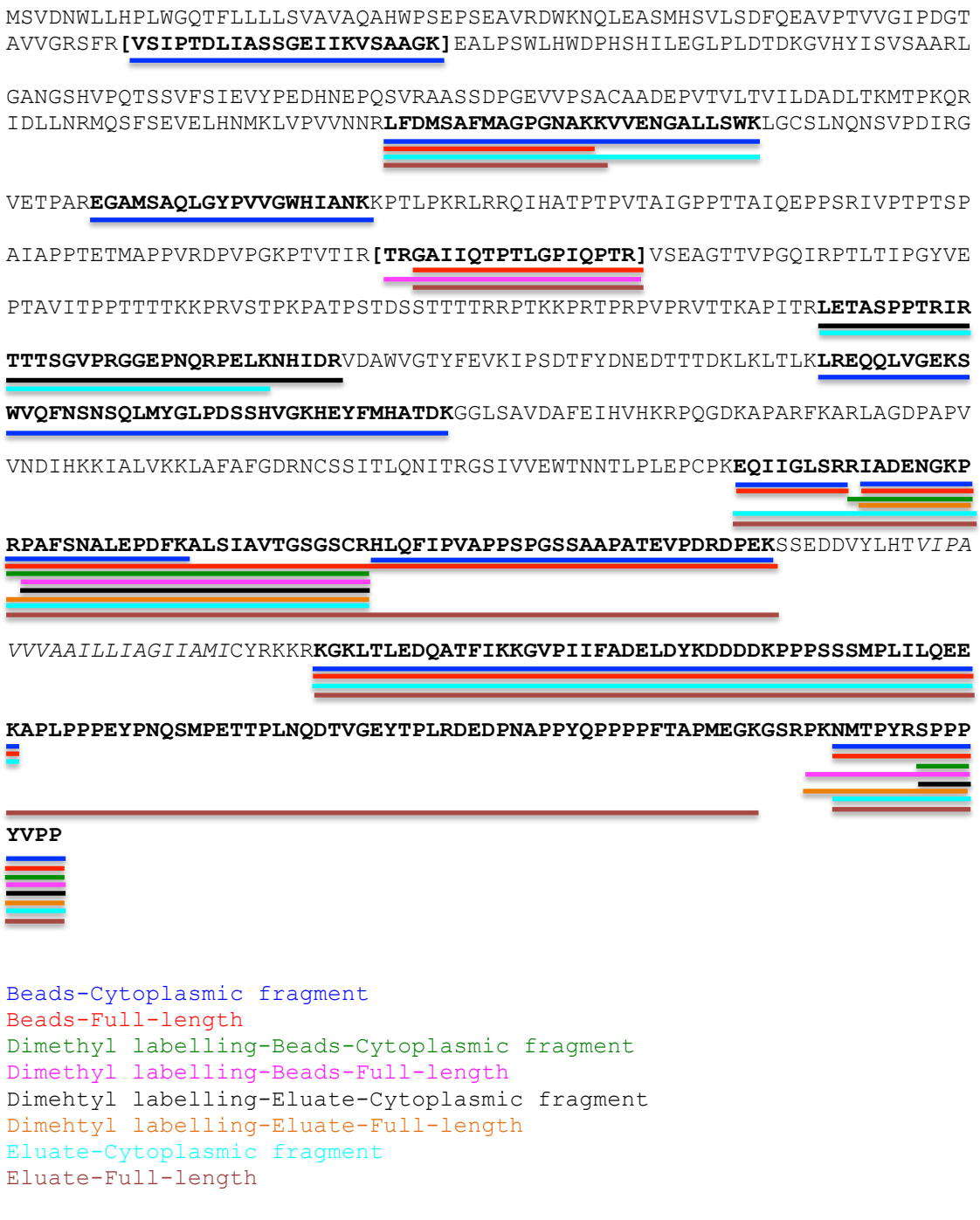

Figure 4.18: Analysis of the cleavage site of beta-dystroglycan. Procedure as in Figure 4.17. Shown are the peptides identified by mass spectrometry in the eluate and bead fractions of the gel slices corresponding to the full-length and cytoplasmic fragment of beta-dystroglycan subject to chemical labelling or left without any treatment.

4.5 The relationship Notch-dystroglycan

During the course of our cell density experiments an apparent increase in the synthesis of beta-dystroglycan was observed. The higher the cell density, the greater the protein levels of full-length beta-dystroglycan (see Figure 4.6). This indicated that cell density could be stimulating the synthesis (or reducing degradation) of beta-dystroglycan through unknown signalling pathways. First, it could be that beta-dystroglycan stimulates its own synthesis through an auto-regulatory mechanism: subsequent increases in the proteolysis of beta-dystroglycan then increases levels of cytoplasmic fragment, its nuclear translocation and its association with nuclear co-factors in order to stimulate its own synthesis. During the course of this project it was observed (in some experiments) that the mutant alpha/beta-dystroglycan-Flag-Y890F, which had reduced levels of the 26 kDa cytoplasmic fragment, had also a reduced expression of full-length beta-dystroglycan compared with wild type alpha/beta-dystroglycan-Flag. This partly supports the hypothesis of beta-dystroglycan auto-regulation, although further, in-depth analysis will be required to show that the cytoplasmic fragment is involved in this auto-regulatory process, as will be discussed later in this chapter.

Second, the increased number of cell contacts generated during high cellular density could be increasing the activation and nuclear translocation of unknown proteins which in turn stimulate the synthesis of beta-dystroglycan. Notch is a protein that is subject to RIP and translocated to the nucleus upon cell-cell contact (Kopan, 2012). In this regard, a previous study has shown the interaction of the DAP complex in *Drosophila* with genes involved in Notch signalling pathway (Kucherenko et al., 2008). More recently, Sirour and colleagues demonstrated that, during skin morphogenesis in *Xenopus laevis*, the transcription of dystroglycan is stimulated upon Notch activation (Sirour et al., 2011). Together, these data support the hypothesis of beta-dystroglycan being subject to transcriptional regulation upon Notch activation during increased cell density.

In order to test this second hypothesis, LNCaP cells were subjected to treatment with the Notch signalling pathway activator resveratrol (Pinchot et al., 2011). The treatment with resveratrol revealed several interesting observations. First, the growth of LNCaP cells was restricted over a period of 72 and 96 hours. Second, cells left untreated confirmed previous findings observed in cell density experiments: that increases in cell confluency led to an up-regulation in beta-dystroglycan protein synthesis. Third, the up-regulation of beta-dystroglycan protein synthesis, was observed at very reduced levels in cells exposed to resveratrol although it is worth noting that even with the very low number of cells at 72 and 96 hours treatment (Figures 4.19a and 4.20a), the levels of full-length and 26 kDa cytoplasmic fragment of beta-dystroglycan had a tendency to increase (Figures 4.19b and 4.20b) and (Figures 4.19c and 4.20c).

Whether dystroglycan protein synthesis is up-regulated as a consequence of its own auto-regulation, or Notch activation, is something that clearly needs further research. It will necessary to link the effects of the over-expression of beta-dystroglycan observed in high cell density experiments, with physiological and disease processes, such as in prostate cancer.

4.6 Discussion

4.6.1 Regulated intramembrane proteolysis of beta-dystroglycan

Regulated intramembrane proteolysis is a mechanism that allows the activation of specific domains within a protein. The mechanism starts with the shedding of the extracellular domain of transmembrane proteins stimulated by different factors such as cell density, phorbol esters, calcium, ligand binding and other unknown stimulants (Jung et al., 2003; Kopan & Ilagan, 2004; Lal & Caplan, 2011), followed by a second cleavage generated by gamma-secretase in the transmembrane domain.

A small 26 kDa cytoplasmic fragment of beta-dystroglycan in addition to

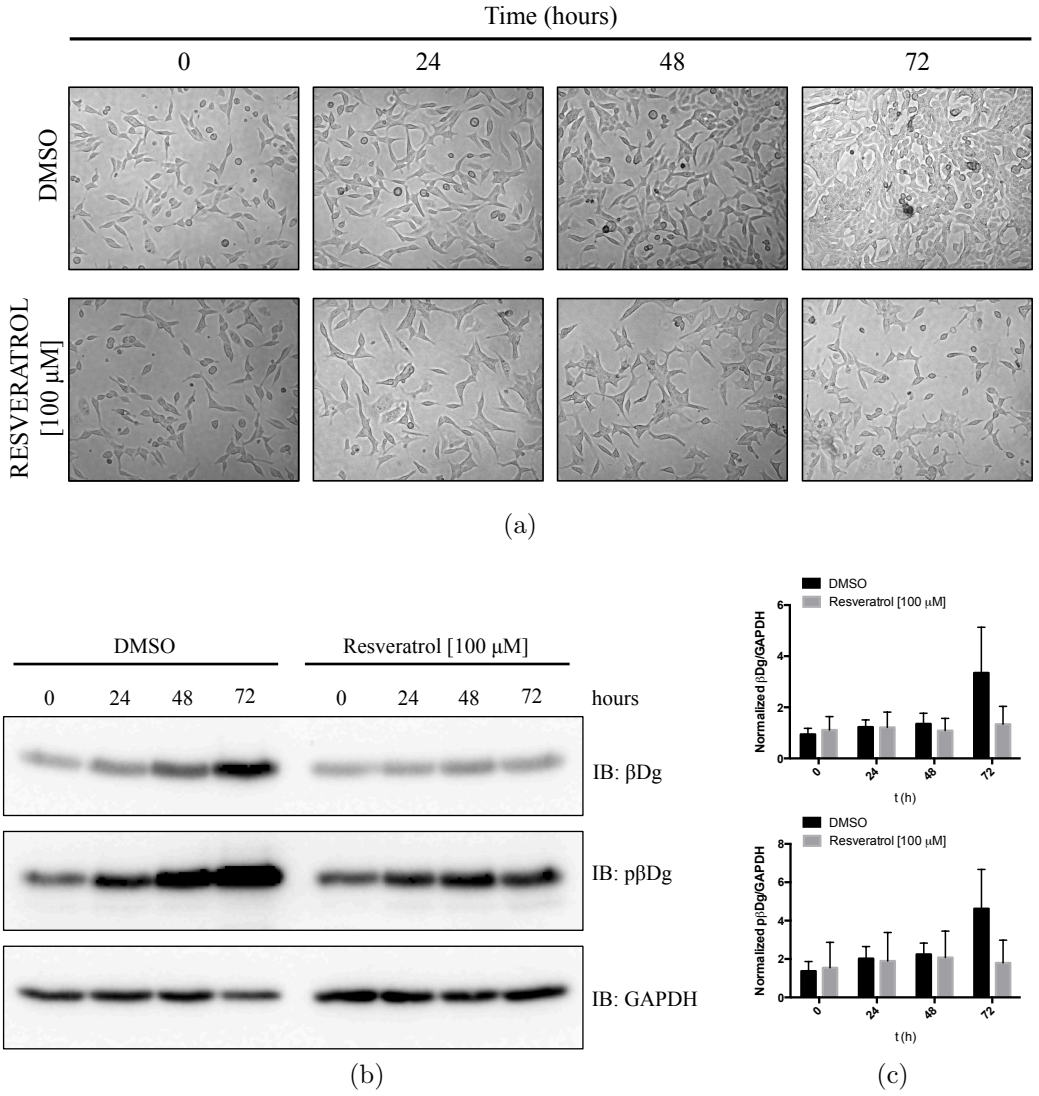

Figure 4.19: Investigating the role of the Notch pathway in the regulation of the synthesis of beta-dystroglycan. (a) LNCaP cells were seeded at a low density and growth for 24 hours before being treated with Resveratrol [100 μM] or the corresponding amount of DMSO for 0, 24, 48 and 72 hours. At every time point, bright-field microscopy images were taken to show the rate of growth of the cells treated against the cells control. (b) Cells collected at the stated times were lysed and the lysates were immunoblotted with antibodies anti-βDg and anti-p-βDg. (c) The band intensity of controls and treatments was quantified and normalized against the loading control GAPDH (means $\pm$ SEM, n = 3). The treatment with resveratrol seems to keep the levels of βDg throughout the 72 hours treatment regardless of the low number of cells as shown in the bright-field microscopy images.

the 43 and 31 kDa forms observed in this and other studies (Mathew et al., 2013; Mitchell et al., 2013; Thompson, 2007), suggests that beta-dystroglycan is subject to a second proteolytic cleavage by gamma-secretase. From the

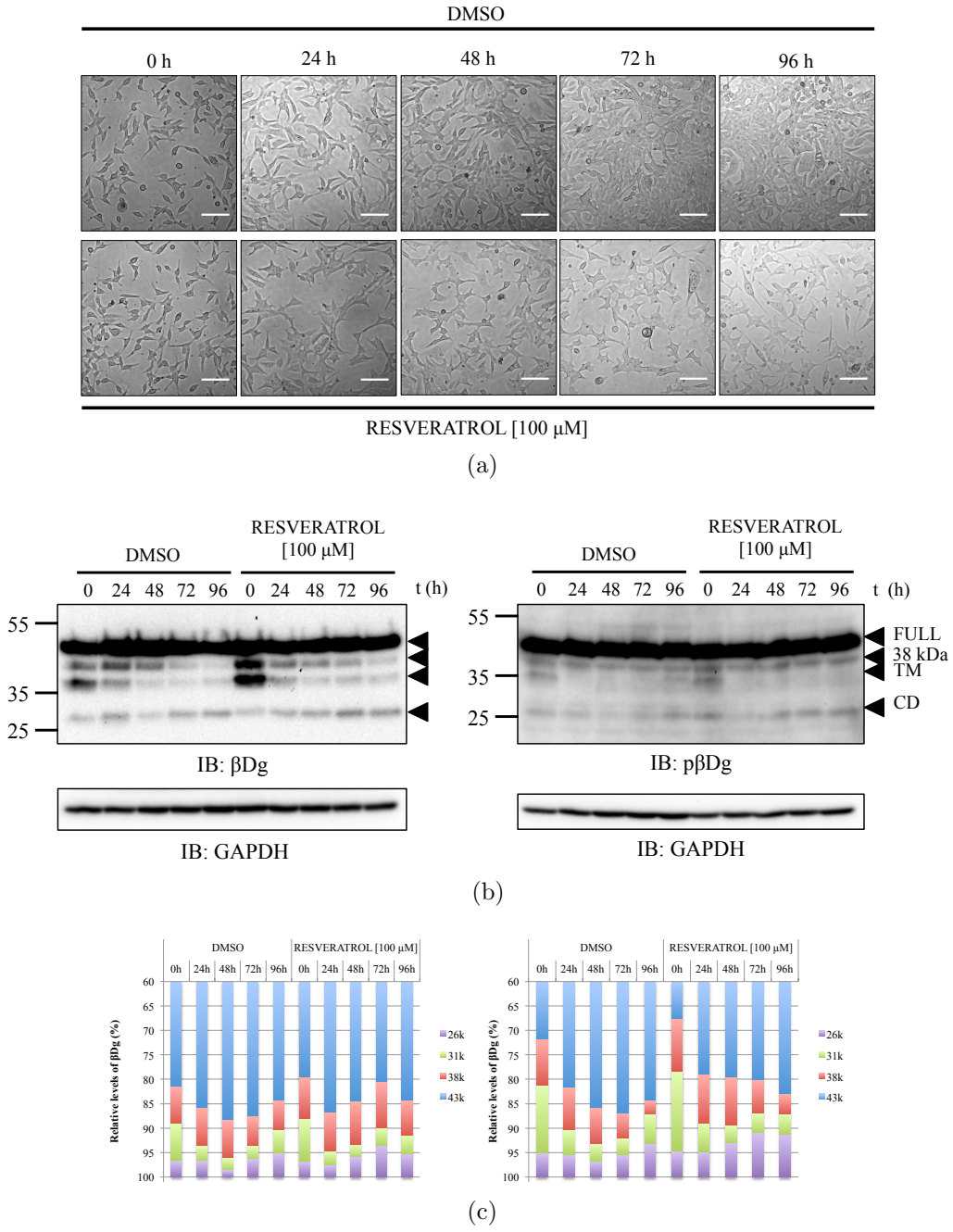

Figure 4.20: Investigating the role of the Notch pathway in the regulation of the proteolysis of beta-dystroglycan. Experiments were performed as in Figure 4.19. In (c), The band intensity of 43 kDa full (FULL), 31 kDa transmembrane (TM), 26 kDa cytoplasmic (CD) and additional 38 kDa (38 kDa) band were quantified and the percentages of each band from two independent experiments are shown. GAPDH is shown as the loading control. The treatment with resveratrol seems to keep increased levels of FULL and CD of βDg throughout the 96 hours treatment regardless of the low number of cells as shown in bright-field microscopy images (scale bar = 100 μm, objective = 10 X).

mechanisms stimulating the proteolysis of plasma membrane proteins, there is evidence that PDBu and cell density are triggering factors for the initial shedding of beta-dystroglycan to the extracellular environment.

The stimulation of LNCaP cells with the PKC activator PDBu, led to an increase in the amount of the 26 kDa cytoplasmic fragment in a time dependent manner, indicating that not only in myoblasts (Thompson, 2007) but also in LNCaP cells, the proteolysis of beta-dystroglycan is stimulated by phorbol esters such as PDBu.

Following phorbol ester stimulation, the cleaved cytoplasmic domains of the p75 neurotrophin receptor and megalin are translocated to the nucleus to perform transcriptional regulatory activities (Jung et al., 2003; Y. Li, Cong, & Biemesderfer, 2008). Stimulation with PDBu increased the levels of the cytoplasmic fragment of beta-dystroglycan in non-nuclear extracts, but not in nuclear extracts as was observed with p75 neurotrophin receptor and megalin. PDBu stimulation produced some phenotypic cellular changes in LNCaP cells such as the formation of ruffles like structures and the re-localisation of beta-dystroglycan to an area surrounding the nucleus. This indicates that, although beta-dystroglycan is prone to proteolysis stimulated by PDBu, the translocation of its cytoplasmic fragment is not triggered by PDBu stimulation.

A previous report has shown that the nuclear translocation of beta-dystroglycan is mediated by the activated F-actin binding protein ezrin in C2C12 muscle derived cells (Vásquez-Limeta et al., 2014). As ezrin is a downstream target of PKC after stimulation with phorbol esters (Ng et al., 2001), it was expected to see increased levels of beta-dystroglycan (either full-length or cytoplasmic fragment) in the nucleus, however this did not happen. As the cytoplasmic fragment of beta-dystroglycan is a sequence that harbours multiple motifs in charge of regulating its interaction with a multitude of proteins (Moore & Winder, 2010), then it is not surprising that the stimulation with PDBu may be promoting its cytoplasmic retention and not its nuclear translocation as might be predicted. In this regard it has been shown that after phorbol ester stimulation, the generated cytoplasmic domain of the ErbB4 receptor is

translocated to the nucleus alone or associated with the transcriptional coactivator YAP, but retained in the cytoplasm as a consequence of its interactions with the tumour suppressor WWOX, associations mainly dictated by the interaction of WW domains with SH2 motifs (Aqeilan et al., 2005). Thus, it may be that the generated cytoplasmic fragment of beta-dystroglycan interacts with proteins containing WW domains through its activated SH2 domains or vice versa, blocking the nuclear translocation regulated by activated ezrin. Further research will be required to determine the protein(s) and cellular conditions modulating the nuclear transport of beta-dystroglycan (or its generated transmembrane and cytoplasmic fragments).

The stimulation with PDBu leads to the shedding of the extracellular domain of beta-dystroglycan leaving a truncated form containing the transmembrane domain (Bozzi, Inzitari, et al., 2009; Yamada et al., 2001). It is possible that this transmembrane fragment is anchored to the nuclear membrane, explaining the strong beta-dystroglycan signal observed around the nucleus. It may be that after the stimulation with PDBu, cleaved beta-dystroglycan is retained at the nuclear envelope in a similar way as the Heparin-binding EGF-like growth factor (HB-EGF) (Hieda et al., 2008) where it exerts its nuclear activities. The detection of full-length and cytoplasmic forms of beta-dystroglycan in the nucleus suggests that if the transmembrane fragment is present in the nucleus it may be in a transitional state, because of its rapid conversion to the 26 kDa cytoplasmic fragment.

So, if PDBu treatment did not result in an apparent increase in the amount of full and cytoplasmic forms of beta-dystroglycan being translocated to the nucleus, what could be another potential mechanism triggering this event? As mentioned above, cell density is another factor that may be able to trigger the proteolysis of plasma membrane proteins and the nuclear translocation of the generated cytoplasmic domains. The growth of LNCaP cells at different densities permitted us to corroborate that beta-dystroglycan is subject to proteolysis in a cell density dependent manner, confirming previous results obtained by Mitchell and colleagues (Mitchell et al., 2013). From cell frac-

tionation assays the nuclear translocation of full-length and cytoplasmic forms of beta-dystroglycan were observed in a cell density dependent manner. One unanticipated finding was the up-regulation of the synthesis of full-length beta-dystroglycan with increasing cell density, a finding that will be discussed later in this section.

From previous reports it is known that cell density could be a triggering factor for the proteolysis and nuclear translocation of activated cytoplasmic domains, as is the case of some protein tyrosine phosphatases (Anders et al., 2006). However the same process can have opposite effects, as has been reported for alpha- adducin (C. L. Chen, Lin, Lai, & Chen, 2011). Increasing cell density leads to an increase in the number of cell-cell contacts suggesting that these are the triggering factor for the cleavage of beta-dystroglycan. However, how these proteolytic events on beta-dystroglycan and its nuclear translocation regulate tumour growth, invasiveness and metastasis, is a question that has to be addressed in order to ascribe a biological role to nuclear beta-dystroglycan under these cellular events.

Different evidence provided by different labs (Cisneros, Muschler and Winder), and cell fractionation experiments performed in this thesis, confirm the nuclear localisation of beta-dystroglycan. In the course of finding an explanation to the nuclear function of beta-dystroglycan the question arose as to whether it provides a structural role to the nuclear lamina, due to an association with components of the nuclear matrix (Fuentes-Mera et al., 2006; Villarreal-Silva et al., 2010), or whether it performs a more dynamic role through the modulation of transcriptional regulatory activities (Mathew et al., 2013; Oppizzi et al., 2008; Sgambato & Brancaccio, 2005). The structural role can be supported by the fact that beta-dystroglycan has a transmembrane domain and its reported association with components of the nuclear lamina (Martínez-Vieyra et al., 2013). On the other hand, the localisation of beta-dystroglycan in the nucleoplasm, detached from the nuclear membrane could be another plausible option as has been observed for some cell surface transmembrane receptors (reviewed in (Carpenter & Liao, 2009)).

From experiments performed in normal and human prostate cancer tissues, and in normal and prostate cancer derived cell lines (Mathew et al., 2013) in addition to experiments performed in this thesis, it is clear that not only the 43 kDa full-length beta-dystroglycan is present in the nucleus as reported by the Cisneros and Muschler labs (Fuentes-Mera et al., 2006; Oppizzi et al., 2008), but also its 31 kDa transmembrane and 26 kDa cytoplasmic fragments. The presence of these three species of beta-dystroglycan in the nucleus could then provide an alternative explanation to the static-dynamic nuclear beta-dystroglycan based on the following analysis.

Oppizzi and colleagues supported the idea of a dynamic 43 kDa beta-dystroglycan that was not restricted to the nuclear envelope based on immunostaining and fluorescence recovery after bleaching (FRAP) experiments. Although these techniques showed the mobility of beta-dystroglycan, they were not sensitive enough to show if the species detected corresponded to its full-length or cytoplasmic forms. Additionally, the biochemical method employed for cell fractionation did not allow them to discriminate if the detected full-length beta-dystroglycan had a nuclear membrane or nucleoplasmic origin (Oppizzi et al., 2008). Then, it may be that the 43 kDa beta-dystroglycan species detected corresponded to the nuclear matrix associated form, whereas the highly dynamic form corresponded to its 26 kDa cytoplasmic species.

If this is the case, are both the 43 and 26 kDa forms of beta-dystroglycan translocated from the cytoplasm to the nucleus? or is full-length beta-dystroglycan translocated from the cytoplasm to the nuclear envelope, and then further processed to generate its 26 kDa species?

Treatment of LNCaP cells with a gamma-secretase inhibitor reduced the levels of the 26 kDa cytoplasmic fragment of beta-dystroglycan in total lysates indicating that the plasma membrane 43 kDa beta-dystroglycan is subject to proteolysis mediated by gamma-secretase. Although the fractionation of cells exposed to the same treatment conditions did not show a reduction in the amount of the 26 kDa cytoplasmic fragment, it did show an increase in the amount of the 31 kDa transmembrane fragment of beta-dystroglycan in non-

nuclear and nuclear fractions. This is suggestive of plasma and nuclear membrane anchored beta-dystroglycan being subject to RIP mediated by gamma-secretase in order to generate a 26 kDa cytoplasmic fragment. The regulation of beta-dystroglycan by proteolysis mediated by gamma-secretase is a mechanism that is present in different cellular models as similar results obtained in this thesis have been reported by mass spectrometry in other cellular models such as HEK and HeLa cells (Hemming et al., 2008).

These findings can be summarised as the following hypothesis: nuclear membrane anchored full-length beta-dystroglycan is subject to a first cleavage on its extracellular domain mediated by MMP-9; the remaining transmembrane fragment is then cleaved by a second proteolytic event performed by gamma-secretase, all this in a similar way to its homologue in the plasma membrane.

As mentioned in the introduction to this chapter, RIP is a process that has been demonstrated for transmembrane proteins found on the plasma membrane, though there is not much evidence of the same process happening for nuclear lamin anchored proteins. If nuclear beta-dystroglycan is subject to RIP, the same elements (or homologues) found on the plasma membrane have to be present in this environment. In this regard, although not direct evidence was gathered in this project, the following elements can be provided in support of the RIP of nuclear beta-dystroglycan:

1. LARGE2, the enzyme responsible for glycosylation of alpha-dystroglycan is not expressed in LNCaP cells. This renders a hypoglycosylated nuclear alpha-dystroglycan susceptible to the cleavage by MMPs (see section 3.5 for more details).

2. In various studies, it has been shown that MMPs, among them MMP-2 and -9, are not only present in the extracellular matrix environment and at the plasma membrane, but also in the nucleus of different cells. Importantly, the nuclear expression of active MMP-9 was correlated with its expression during the S-phase of the cell cycle (Zimowska, Swierczynska,

& Ciemerych, 2013). This could explain the mechanism by which full-length nuclear beta-dystroglycan is being cleaved with the consequent generation of its transmembrane fragment.

3. Presenilin, the core catalytic subunit of the gamma-secretase complex was reported to be associated with components of the nuclear lamina (J. Li, Xu, Zhou, Ma, & Potter, 1997). However, there has not been any complementary reports indicating if this catalytic subunit is functional and, more importantly, if the other components of the complex are present in this nuclear environment.

4. In *Arabidopsis* it has been shown that the transcription factor NTM1 is subject to RIP in the nuclear membrane mediated by calpains, supporting the possibility of the same process happening in mammalian cells (Y. S. Kim et al., 2006).

In-depth research will be required to show that the proteolysis mediated by gamma-secretase is performed in the nuclear boundaries. The employment of strategies such as presenilin-deficient cells or site-directed mutagenesis will be useful to determine the site(s) in where gamma-secretase performs its catalytic activity. Subsequently it would be possible to determine the biological relevance of reduced small cytoplasmic fragments of beta-dystroglycan in cancer and muscular dystrophies.

In an attempt to determine the site where gamma-secretase performs the transmembrane shedding of beta-dystroglycan, mass spectrometry analysis and dimethyl labelling were employed. However, the approach was not successful because the sequence corresponding to the transmembrane domain was not recovered. The sequences retrieved from the mass spectrometer corresponded to the amino-terminus of beta-dystroglycan and the other corresponded to most of its carboxyl terminal half. Interestingly, the sequence reported by the mass spectrometer started on the amino acid lysine 778 (K778), a sequence predicted by in silico analysis as potential furin cleavage site. The inhibition

of the proteolytic activity of furin showed moderate, but consistently reduced levels of the cytoplasmic fragment of beta-dystroglycan.

Additionally, these results need to be interpreted with caution because the stretch of basic amino acids corresponding to the nuclear localisation signal of beta-dystroglycan is susceptible to proteolysis by trypsin, the enzyme used to digest the peptides before mass spectrometry analysis. Also, an analysis in either furin-null or furin-deficient cells will be required to show the specific involvement of furin in the cleavage of beta-dystroglycan.

If gamma-secretase cleaves beta-dystroglycan in its transmembrane domain, how is this domain still susceptible to an extra-cleavage performed by furin a few amino acids downstream of the remnant transmembrane domain? The answer could be a cysteine amino acid located at the interphase between the transmembrane domain of beta-dystroglycan and its nuclear localisation sequence. Palmitoylated cysteines are frequently located in the cytoplasmic side of regions next to transmembrane domains or located inside the hydrophobic environment of the plasma membrane, usually surrounded by hydrophobic and basic amino acids of transmembrane proteins (Aicart-Ramos et al., 2011). A cysteine 772 located within the cytoplasmic fragment of beta-dystroglycan has these characteristics. Indeed, by mass spectrometry analysis it was shown that beta-dystroglycan is subject to palmitoylation in rat embryonic cortical neurons. However, it was not completely reported if the cysteine in the boundaries of the plasma membrane facing the cytosol is the one subject to this PTM (Kang et al., 2008). Further research is necessary to determine if the cysteine immediately below the transmembrane domain of beta-dystroglycan is subject to palmitoylation and facilitates the putative cleavage by furin.

Although the experiments performed in this thesis support the proteolysis of beta-dystroglycan mediated by gamma-secretase and the nuclear localisation of its full and cytoplasmic forms, why did the Cisneros and Muschler groups not detect this small 26 kDa fragment in the nucleus and also, why did they observe a great variability in the levels of full-length nuclear beta-dystroglycan? The answer may be that, although the three species are present

in the nucleus, the 31 kDa transmembrane and 26 kDa cytoplasmic fragments are subject to a rapid turnover in the nucleus as has been reported for other cytoplasmic domains, such as those generated from Notch, EpCAM, Neogenin, APP, among others (Cupers, Orlans, Craessaerts, Annaert, & De Strooper, 2001; Goldschneider et al., 2008; Maetzel et al., 2009).

The first clue was provided by treating LNCaP cells with MG132. Cells in which the proteasomal activity was inhibited had a substantial recovery of the transmembrane and cytoplasmic fragments of beta-dystroglycan indicating that they are subject to a rapid turnover mediated by the proteasome.

To better understand the effects of the cytoplasmic fragment and its cellular localisation, it was decided to transfect LNCaP cells with the DNA coding sequence corresponding to the cytoplasmic fragment of beta-dystroglycan. After many attempts, this cytoplasmic fragment was only recovered when cells were treated with the proteasome inhibitor MG132 followed by further immunoprecipitation. The signal corresponding to this small cytoplasmic fragment was broadly distributed in the cell, but mainly localised to the nucleus. Additional analyses are required to show if the signal detected in the nucleus corresponds to the entire or the degraded cytoplasmic fragment of beta-dystroglycan. Importantly, cells overexpressing this small 26 kDa cytoplasmic fragment presented different phenotypic changes compared with the non-transfected cells, such as an increase in size of the nucleolus, defects in cellular division (nuclear division), and a susceptibility to apoptosis. However, these results require of an in-depth analysis to further show the broad implications of the cytoplasmic fragment of beta-dystroglycan in different cellular processes.

From the the results gathered by the treatment with MG132 it can be suggested that, after the proteolytic events mediated by MMPs and gamma-secretase either on the plasma or nuclear membranes, the cytoplasmic fragment of beta-dystroglycan is rapidly translocated to the nucleus to exert unknown regulatory functions before being degraded by the nuclear proteasome. The degradation of proteins by the nuclear proteasome system has been well established (Rockel et al., 2005; von Mikecz, 2006) and has been demonstrated for

transcription factors such as MyoD (Floyd et al., 2001). Then, it is tempting to speculate that the nucleus is a cellular compartment for the degradation of beta-dystroglycan by the ubiquitin proteasome system. However more evidence will be required to further support this hypothesis or to show that beta-dystroglycan is degraded in other cellular compartments. This will be very important in order to support other therapies aided in restoring the members of DAPC in diseases where the proteolytic activity of the ubiquitin-proteasome system has been shown to be altered.

The proteolysis regulated by gamma-secretase and the degradation mediated by the ubiquitin-proteasome system, could potentially explain the high variability of non-nuclear and nuclear full-length beta dystroglycan observed in tumour tissues (Jing et al., 2004; Sgambato et al., 2007). In these instances, the abnormal function of MMPs and the proteasome, and the presence of a hypo-glycosylated beta-dystroglycan could be the main factors modulating the stability of this important transmembrane protein.

The cytoplasmic fragment of beta-dystroglycan performs most of its interactions with cytoplasmic proteins. Hence, the susceptibility of the full-length protein to frequent proteolytic events mediated by MMPs in cases of muscular dystrophies and cancer could be translated into high levels of the cytoplasmic fragment being secreted into the cytoplasm (or nucleoplasm), leading to the disruption of "normal" interactions, or to the activation/inhibition of signalling pathways involving the cytoplasmic fragment of beta-dystroglycan. Such a scenario has been described where overexpression of a myristoyl-tagged CDβDg construct induced the formation of filopodia at the cell membrane due to recruitment of RhoGEF (Batchelor et al., 2007). Detailed analyses are required to further investigate the consequences of the over-expression of this small fragment.

Cell density regulates not only the proteolysis and nuclear translocation of full and cytoplasmic species of beta-dystroglycan in LNCaP cells, but also the synthesis of full-length protein. It may be that the synthesis of dystroglycan could be subject to cis- or trans-regulation. In a cis-regulation scenario, the

high levels of proteolytic activity during invasion and metastasis of cancerous cells would lead to increased levels of the cytoplasmic fragment of beta-dystroglycan, which would then translocate to the nucleus to regulate its own transcription, a phenomenon similar to that observed for the protein tyrosine phosphatase μ (Gebbink et al., 1995).

The overexpression of beta-dystroglycan may help restrict cell growth through contact inhibition, but in cancerous cells, such as LNCaP cells, this overexpression may be counterbalanced by high levels of MMP activity (Brehmer, Biesterfeld, & Jakse, 2003), which in turn down-regulate the inhibitory activity of beta-dystroglycan. Further experiments involving overexpression of the cytoplasmic fragment of beta-dystroglycan will be required to test this new hypothesis.

With regard to trans-regulation, Notch has been shown to interact with dystroglycan in a drosophila model (Kucherenko et al., 2008) and also to regulate the synthesis of dystroglycan during skin morphogenesis (Sirour et al., 2011). Then the hypothesis of Notch playing a role in the synthesis of beta-dystroglycan as a trans-regulator during cell density experiments could be a reasonable idea. The treatment of LNCaP cells with resveratrol, led to a subtle up-regulation in the expression of beta-dystroglycan in spite of the low number of cells. This may be indicative of NOTCH regulating the transcription and synthesis of beta-dystroglycan, as has been suggested by Sirour and colleagues (Sirour et al., 2011). Further, in-depth analysis will be required to show that cell density is a triggering factor stimulating the activation of Notch, which in turn regulates the transcription and synthesis of beta-dystroglycan. In this model, up-regulated beta-dystroglycan is modulated on the plasma membrane by the proteolytic action of MMPs and gamma-secretase, leading to the generation of a cytoplasmic fragment that is capable of regulating other transcriptional processes. Importantly, future experiments will need to differentiate if the overexpression of beta-dystroglycan is due to a post-transcriptional or post-translational regulation.

4.6.2 Summary

Through the evidence provided in this chapter it can be concluded that:

1. PDBu and cell density are triggering factors for the generation of the 26 kDa cytoplasmic fragment of beta-dystroglycan.

2. The cytoplasmic fragment of beta-dystroglycan is translocated to the nucleus in a cell density dependent manner.

3. Beta-dystroglycan is subject to proteolysis mediated by gamma-secretase and furin.

4. Beta-dystroglycan is transported to the nucleus for its degradation through the ubiquitin proteasome system after performing structural and dynamic nuclear roles.

5. The synthesis of beta-dystroglycan may be regulated by Notch signalling in response to cell-cell contacts.

5

Interactome of beta-dystroglycan

5.1 Introduction

The intricate network of proteins within a cell is indeed complex and exciting, but the understanding of each one of these protein interactions is pivotal in order to unravel the mechanisms that lead to disease. Cancer, the uncontrolled growth of cells, is a clear example wherein most of the signalling pathways are modified in favour of cell survival, invasion and metastasis, some of the hallmarks of cancer (Hanahan & Weinberg, 2011). In this regard, by potentiating cellular interactions with the extracellular matrix and restricting the uncontrolled growth of cells, dystroglycan has been envisaged as a tumour suppressor (Sgambato & Brancaccio, 2005). The role of dystroglycan seems to not to be restricted to cellular interactions with the extracellular matrix, and the following findings support this idea:

- Dystroglycan is ubiquitously expressed in different cellular compartments like the plasma membrane, the cytosol, the nucleus; in a multitude of cells of different systems such as the nervous system, the muscle, the breast, the blood, the prostate, etc.

- Dystroglycan is able to form different complexes (Johnson et al., 2013).

- Dystroglycan is cleaved by gamma-secretase rendering a free fragment with novel unknown functions.

- Different amino acids in the cytoplasmic domain of beta-dystroglycan may be susceptible to different PTMs, such as phosphorylation and ubiquitination. Thus, depending on the triggering signal, different pathways will be switched on, leading to specific cellular events.

- The cytoplasmic fragment of beta-dystroglycan is structurally, highly disordered (Figure 5.1), granting a flexible region that can be shaped according to the type of protein interaction required, possibly with another protein harbouring a highly disordered domain as well, as has been observed for the phosphatase and tensin homologue (PTEN) (Malaney, Pathak, Xue, Uversky, & Davé, 2013).

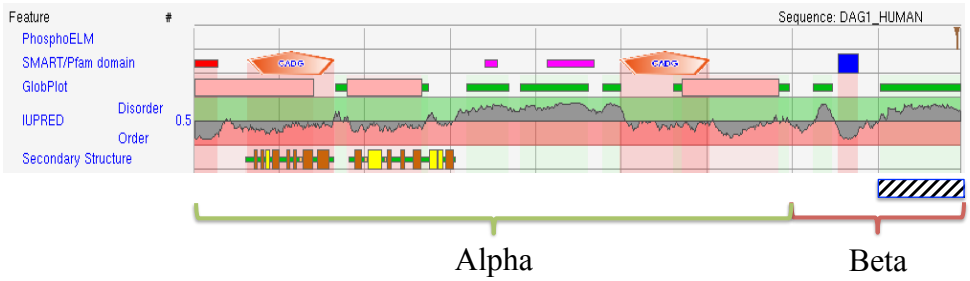

Figure 5.1: The cytoplasmic domain of beta-dystroglycan is highly disordered. ELM (`http://elm.eu.org`) *in silico* analysis of dystroglycan shows that the cytoplasmic domain of beta-dystroglycan (stripped square) is highly disordered with no predicted elements of secondary structure.

The combination of all these characteristics of beta-dystroglycan highlights once more "the complexities of dystroglycan" (Winder, 2001). With the recent discoveries of its nuclear localisation, we asked if there were other proteins interacting with beta-dystroglycan that could explain its functionality beyond the plasma membrane.

Genomic sequence analysis provides us with information about the coding sequence of a protein. However, it does not tell us about other characteristics at the protein level, such as PTMs, protein interactions and subcellular localisation. Therefore, mass spectrometry analysis is an important and highly sensitive tool to investigate and to understand the multitude of protein interactions and post-translational modifications under certain circumstances

(Ahmad & Lamond, 2014; Choudhary & Mann, 2010).

Thus, the objective of this chapter is to determine, by mass spectrometry analysis, other unknown interacting proteins that could provide us with clues about the regulation of beta-dystroglycan throughout the cell cycle, its functions in the nucleus and its regulation by the ubiquitin-proteasome system. Through the set of results presented here, the exquisite multitude of proteins interacting with beta-dystroglycan and the most representative pathways wherein beta-dystroglycan is involved will be shown. Finally, through evidence already provided by other research groups and the results gathered from the mass spectrometry screen analysis, the potential roles that beta-dystroglycan can perform far beyond of those of a simple plasma membrane protein will be highlighted.

5.2 Preparative analysis

The detection of beta-dystroglycan in the nucleus of different cell lines raised the question of its role in this highly regulated compartment. The results obtained in chapter 4, suggest that beta-dystroglycan provides structural integrity to members of the nuclear envelope and is then subjected to proteolytic events, which signal the start of other cellular events, such as a possible co-transcriptional regulation followed by its degradation by the nuclear proteasome.

If dystroglycan (beta or the combination of alpha and beta) is present in the nucleus, it has to perform a function. The possibility of its nuclear translocation solely for degradation is controverted by the great expenditure of energy that the cell has to invest in order to translocate a protein that can be easily degraded in the cytosol (Stewart, 2007). Thus, the main objective of this chapter is to determine if, in addition to the already reported non-nuclear and nuclear components, beta-dystroglycan interacts with proteins that could give an insight about its nuclear function(s) and the way it is further processed.

With this in mind, it was decided to perform fractionation of LNCaP cells in to non-nuclear and nuclear fractions. Because of the relative small size of the nucleus compared with that of the remaining cellular components together (cytosol, mitochondria, endoplasmic reticulum, Golgi apparatus and others), it was therefore required to concentrate this cellular organelle in order to enrich nuclear proteins that could be expressed at relatively low levels, and hence present a low number of interactions with beta-dystroglycan. Consequently, LNCaP cells transiently transfected with the plasmid $\alpha\beta$DgFlag were subjected to cell fractionation by using a sucrose gradient protocol (see appendix A). The reliability of the protocol was tested by immunoblotting the cellular fractions with non-nuclear and nuclear markers such as calnexin and GAPDH, and lamin A/C respectively. Additionally, in order to highlight non-specific signal generated by unspecific binding of Flag antibodies, the same fractions of non-transfected cells were included.

In Figure 5.2, it can be observed that full-length 43 kDa beta-dystroglycan was well distributed between both fractions and importantly, it was accompanied by the 130-250 kDa high molecular weight form, the 31 kDa transmembrane fragment and the 26 kDa cytoplasmic domain (described in chapter 3). Using the conditions mentioned above, it was possible to determine that the protocol used for cell fractionation rendered fractions with minimum cross-contamination between non-nuclear and nuclear fractions and that the antibody Flag M2 had a high level of specificity for Flag-tagged proteins such as beta-dystroglycan (Figure 5.2).

Using these conditions, it was decided to perform mass spectrometry analysis on non-nuclear and nuclear fractions of LNCaP cells transiently transfected with the plasmid $\alpha\beta$DgFlag. The fractions of 4 replicate experiments were subjected to a second screening for cross contamination between non-nuclear and nuclear fractions by using the non-nuclear (GAPDH and calnexin) and nuclear (lamin A/C and fibrillarin) markers. The absence of cross contamination was indicative of fractions suitable for mass spectrometry analysis (Figure 5.3).

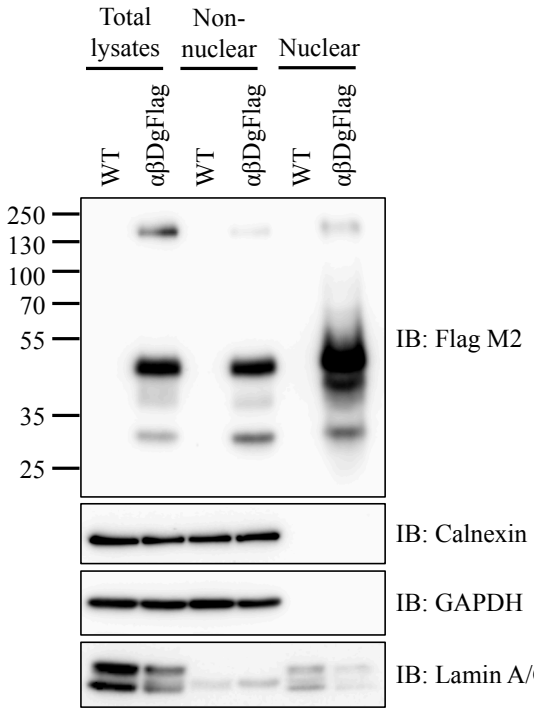

Figure 5.2: Standardization of a protocol for cell fractionation of LNCaP cells. LNCaP cells WT and transiently transfected with the plasmid $\alpha\beta$DgFlag were growth for 36 hours and then collected for total lysates or cell fractionation. Samples were immunoblotted with antibodies anti-Flag. This characterization permitted to evidence the expression of beta-dystroglycan (full length, transmembrane and cytoplasmic) in non-nuclear and nuclear fractions. Calnexin and GAPDH, and Lamin A/C are included as markers and loading controls of non-nuclear and nuclear fractions respectively.

Although the antibody Flag M2 can be highly specific for Flag-tagged proteins, there is the possibility of some proteins binding non specifically with this antibody. Moreover, a high number of proteins can interact non-specifically with agarose beads, the support of the Flag M2 resin (Mellacheruvu et al., 2013). Thus, similar fractions of LNCaP WT cells were included and processed along with the fractions of transfected cells.

Both non-nuclear and nuclear fractions of LNCaP WT and transiently transfected cells with the plasmid $\alpha\beta$DgFlag from 4 biological replicates were immunoprecipitated using the Flag M2 resin following the workflow described in Figure 5.4, and the protocol described in the material and methods chapter (see section 2.1.5.5). Thereafter, eluates after immunoprecipitation were reduced and alkylated, and separated by SDS-PAGE. Subsequently, the gels

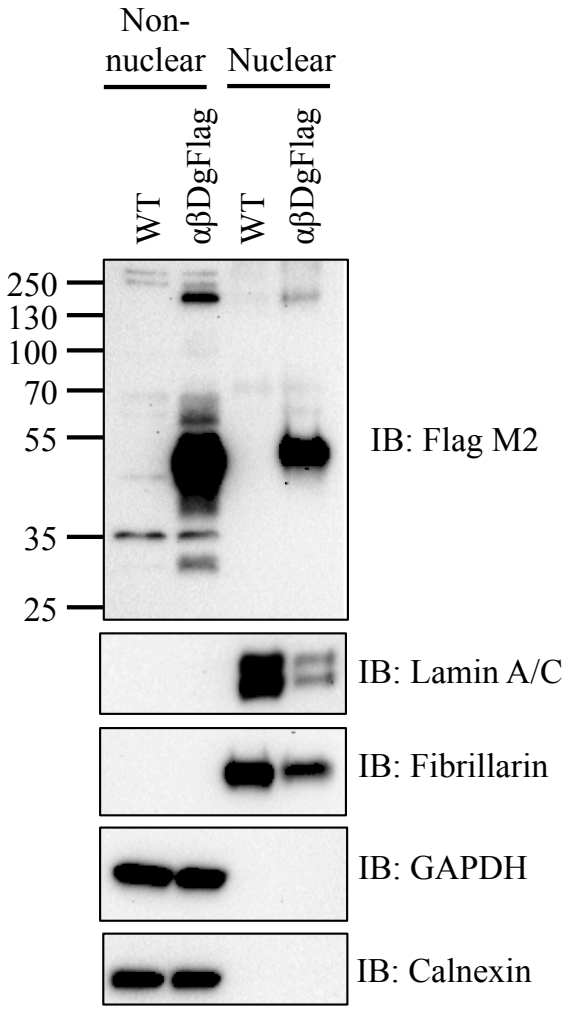

Figure 5.3: Characterization of cellular fractions used for mass spectrometry analysis. Before performing each immunoprecipitation step with the Flag M2 resin, non nuclear and nuclear fractions of LNCaP cells WT or transfected with the plasmid $\alpha\beta$DgFlag were characterized with the controls GAPDH and Calnexin, and Lamin A/C and Fibrillarin, as markers of non nuclear and nuclear fractions respectively. The absence of signal generated by non-nuclear and nuclear markers in the opposite fractions is indicative that if present, the cross contamination between cellular fractions is minimum. Shown is a representative image of 4 independent replicates.

were stained with colloidal Brilliant Blue G followed by further destaining. Destained gels of each corresponding sample were cut in 5 gel slices and then subjected to tryptic digestion. Extracted peptides were subjected to tandem mass spectrometry analysis according to the conditions described in the proteomics techniques in material and methods chapter (see section 2.1.7) (Figure 5.4).

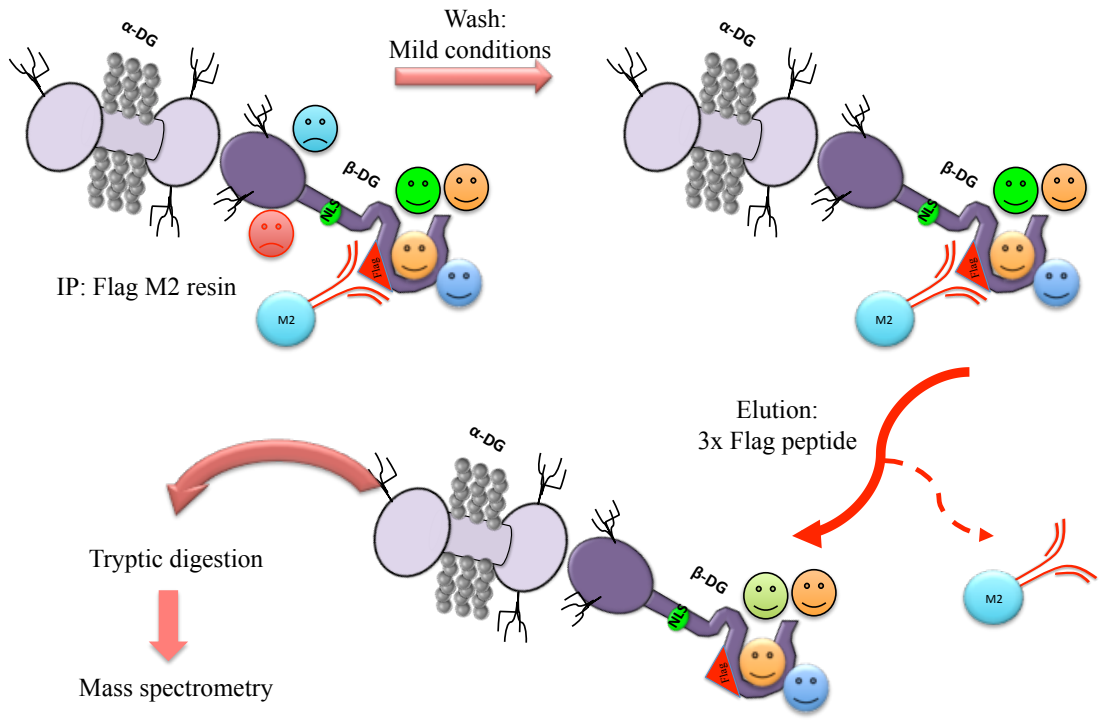

Figure 5.4: Workflow of the interactome of beta-dystroglycan. The schematic shows the strategy used for the identification of proteins interacting with beta-dystroglycan. Briefly, non-nuclear and nuclear fractions of LNCaP cells transfected with the plasmid $\alpha\beta$DgFlag were immunoprecipitated with the Flag M2 resin. Non-specific binding proteins (unhappy faces cartoons) were eliminated by washing the beads under mild conditions with TBS buffer (see appendix A). Following this, beta-dystroglycan Flag and interacting proteins (happy faces cartoons) were eluted from the beads using the 3X Flag peptide. Eluted proteins were reduced, alkylated and separated by SDS-PAGE. Stained gel slices with colloidal Brilliant Blue G were destained and then subjected to tryptic digestion. Extracted peptides were analysed by tandem mass spectrometry to identify proteins interacting with beta-dystroglycan and some possible PTM. The same procedure was followed for cellular fractions of LNCaP WT which were included as a control of non specific interactions with the Flag M2 resin.

5.3 Mass spectrometry results

The results retrieved from the mass spectrometry analysis revealed many proteins, from both non-nuclear and nuclear fractions, that were identified as interacting with Flag M2 resin alone (control) and with Flag tagged beta-dystroglycan (see attached excel file: **1.Interactome beta-dystroglycan**,

"protein groups tab" and Figure 5.5). Overall, non-nuclear fractions had a good protein enrichment in Flag IPs, in contrast to the nuclear fraction where the enrichment was sub-optimal. Therefore, proteins significantly enriched in both non-nuclear and nuclear fractions, and with a peptide count number above 2, were considered for interactome analysis (see section 2.1.7.6 in material and methods chapter, attached excel file (**1.Interactome beta-dystroglycan**, "NN stats and Nuclear stats tabs (proteins highlighted in red)") and Figure 5.5).

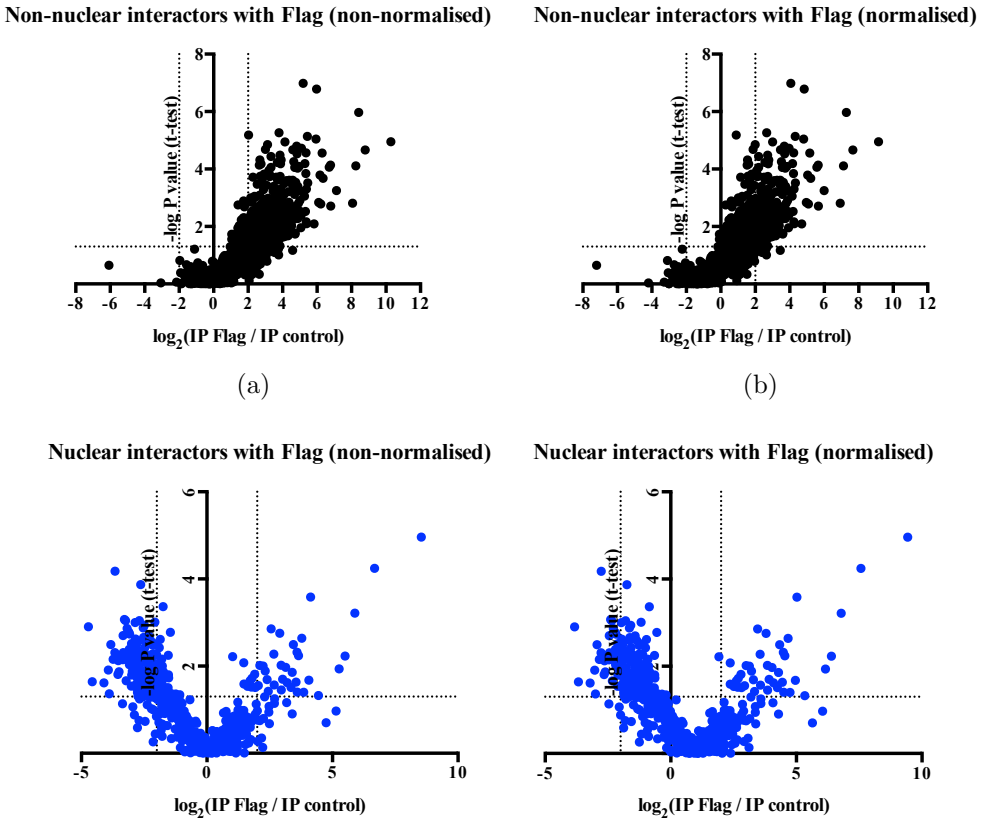

Figure 5.5: Normalisation of proteins detected by mass spectrometry analysis. Volcano plot for proteins identified in control and Flag immunoprecipitations. The x-axis is the $\log_2$ fold change value (IP Flag intensity / IP control intensity) and the y-axis is the corresponding adjusted log P value. The vertical lines represent protein enriched 2 fold changes for control (left side) and Flag (right side) immunoprecipitations, and the horizontal line the P-value cut-off (0.05). a) and c) represent non-normalised data from non-nuclear and nuclear fractions respectively, and b) and c), the normalised counterparts.

5.4 Interactome analysis

Proteins found enriched in Flag IP in both non-nuclear and nuclear fractions are shown in Figure 5.6. Importantly, in both fractions there were proteins found enriched in Flag IPs, but not in control IPs. However, some proteins presented signal in only two replicate experiments and for this reason they were not considered in the list of enriched proteins (Figure 5.7). An important result to highlight is that beta-dystroglycan was highly enriched in both fractions.

Gene names of proteins detected in Flag Ips

Non-nuclear

	TUBA1C	GANAB	PDCD6IP	MTHFD1	SMC1A	RAB6B	HSPA8	PCBP2;PCBP3
Dag1 (mouse)	ANKRD13A	ATP6V0D1	TUBB4A	PPIB	LDHA	CBR3	PSMD6	ACTBL2
CTNNA1	SCAMP3	CTNND1	COPB1	TROVE2	AP1M2	TMED9	UGDH	SEC13
CTNNB1	ATP5B	PDXDC1	EPHX1	SLC25A3	PHGDH	NEDD4L	AP2M1	ERLIN2;ERLIN1
GMPPB	LONP1	HSPA5	RPN1	SLC25A10	SLC25A5	PSMC3	ATP5C1	HADHB
SQSTM1	XPO1	TARS	CSE1L	LRBA	GFPT1	IDH2	EEF2	FLII
TOM1L2	NAPRT1	KPNB1	SLC16A1	GCDH	TFRC	ECHS1	KLK3	GAPDH
CDH1	SFXN1	ATP1A1;ATP1A3	ALDH1B1	CNOT1	MAOA	HSP90AB1	PSMC6	FARSA
SLC3A2	TIMM50	PFKM	ECM29	SPTLC1	QARS	WWC1	CAPZB	CAND1
ETFA	DNM2	MT-CO2	ERGIC1	FADS2	PCBP1	SEC22B	SQRDL	CTTN
SCFD1	ASS1	HSPD1	COMT	ATP6V1A	NIPSNAP1	PSMD2	CD2AP	PRKACB;PRKACA
USP5	HLA-B	PRKCSH	SRPRB	YARS	GOSR1	RDH11	PPP2R1A	RAB5A
ST13	COPG1	ETFB	ATP5A1	PDHB	MRPL11	PSMC2	TUBA4A	DCTN2
SPON2	XPOT	IPO4	GARS	STIP1	APMAP	LMAN1	RUVBL2	RNH1
DAG1 (human)	ATP2B4	ALDH9A1	RAB18	PSMD4	THEM6	KRT18	TUFM	MAT2A
ACADSB	WARS	DPM1	LDHB	HADHA	RHOC;RHOA	ATP5F1	TUBB	AP2B1
ACAA1	STEAP2	RHOA	TLN1	MYO5A	ACADVL	COPE	IMPDH2	PTPRF
LRPPRC	HSD17B4	GBAS	SLC25A6	ARFGEF1	PSMD3	ALDH18A1	HSP90AA1	
ATP1B1	FUBP1	CLU	IPO7	SLC25A1	GNB2L1	COLGALT1	PDIA3	
VDAC1	PYGB	IPO9	ATP2A2	MTCH2	VDAC2	HDLBP	PKM;PKM2	
COPB2	TIMM44	IPO5	HUWE1	PFKL	MON2	CALR	PTPN11	
STAT1	UBB	TUBB2B	ALDH3A2	CNDP2	TUBA1A	ACAT1	RUVBL1	
ATXN10	RNF213	GPD2	FOLH1	PHB2	TMED10	TUBB4B	PDIA6	
DAK	FARSB	CD9	HSP90B1	PYCR1	PFKP	PSMC5	PDIA3	
ARL6IP5	NAMPT	PSMD12	PHB	MCM4	FECH	EPPK1	APRT	
ALDH2	NSF	PCK2	UQCRC2	RAB7A	RAB5C	PSMC4	CPT1A	
TTLL12	GCN1L1	SLC1A5	PSMD8	SEPT11	TARDBP	MCM7	AIMP2	
VPS35	CANX	USO1	MARS	AP1M1	UGGT1	DYNC1H1	PSMD11	
SLC25A11	ACSL1	SRM	GBF1	NPEPPS	DHRS7	HYOU1	EIF4A1	

Nuclear

Dag1 (mouse)
SQSTM1
RARS
DAG1 (human)
EIF3A
HSPD1
CCAR1
DARS;DKFZp781B11202
PHGDH
IGF2R
IARS
EEF1D
EPRS
MTCH2
VDAC1
ANXA6
EPPK1
LARS
ATP5B
GPD2
CKAP4
ATP1A1;ATP1A3

Figure 5.6: Proteins found enriched in Flag IPs. The list shows the gene names of all proteins from non-nuclear and nuclear fractions enriched in Flag IPs compared with control IPs (for a detailed description of each protein, please refer to the attached excel file (**1.Interactome beta-dystroglycan**)).

Gene names of proteins found in 2 replicate experiments in Flag IPs

Non-nuclear

SUMO1	LTA4H	COG1
SH3YL1	ATAD3A	MUT
RBM14	TOM1	ANK3
TMEM205	BAX	LRRFIP1
SSR4	RAB3D	NCAPD2
SEH1L	IPO9	CPT2
ELMOD2	RAB8A	TTC27
CPSF7	DCK	PNPLA6
RPLP2	CECR5	UBE4B
EPT1	SEC63	MYO6
NGLY1	ADCK3	PLIN4
SLFN11	NDUFB10	ARFGEF2
RAB14	IMMT	
PGRMC1	MRPS21	
SEPT7	MYBBP1A	
TMEM238	TBCD	
COPZ1	DSC2	
CD81	ETHE1	
STX8	NUP155	
PSMG1	LETM1	
CYB561	TUBB3	
TMPRSS2	UBA5	
RGPD4;RGPD3	ANKRD13D	
FAHD1	PTGES2	
MAPKAP1	MRPS5	
FKBP11	GCAT	
CLPP	ARCN1	
SMC3	SCO2	
RAB5B	PCDHB5	
MTHFD1L;LOC100996643	RNPEP	
CHCHD2;CHCHD2P9	MYO1B;MYO1A	
PPP1CC	ARHGAP1	
CTNNA2	PYCR2	
C7orf50	FASTKD5	
SEPHS1	SCYL1	
GALK1	LRSAM1	
OS9	TARS2	
CDIPT	NUBP2	
TST	ARMCX3	
TBC1D15	ACBD3	
SAE1	METTL13	
DNM1L	CYP51A1	
CDC37	COG3	
CD276	PELO	
SUN2	THNSL1	
MRPL20	LANCL2	
SNAP23	TM9SF3	
RECQL	PIK3CD	
MGEA5	DIAPH1	
SUCLG1	DHODH	
GCLM	RQCD1	
ELOVL1	IRF2BPL	
RAB3A	COG2	
ASMTL	TANC1	

Nuclear

PRDX6
CCT7
NME1;NME2;NME1-NME2;NME2P1
TUBA4A
SEC22B
EIF3D
EIF3E
EFCAB2
TMED10
DHRS7
ARL6IP5
AIMP2
PRDX4
HSD17B10
COPG1
SLC3A2
QARS
CLU
TMOD3
MLEC
CD2AP
MTMR14
SNX1
XPOT
TOMM70A
CYFIP1;CYFIP2
AKAP11
PIAS1
CHID1
PSIP1
ABCF1
EIF2B4
TNRC6A
GBP1
HECTD1
KTN1

Figure 5.7: Proteins found enriched in Flag IPs in 2 replicate experiments. The list shows the gene names of proteins from non-nuclear and nuclear fractions enriched in two Flag IPs only without any signal in control IPs (for a detailed description of each protein, please refer to the attached excel file **1.Interactome beta-dystroglycan**).

The amount of non-nuclear proteins found enriched in Flag IPs was very high but, contrary to the expected, this was not the case for nuclear proteins. A first analysis performed on nuclear proteins using the GeneMANIA prediction server for biological network integration (`http://www.genemania.org`) and the WEB-based GEne SeT AnaLysis Toolkit (WebGestalt `http://bioinfo.vanderbilt.edu/webgestalt/`) revealed that a large proportion of the enriched proteins in Flag IPs were related to ribosomal-related processes (Figure 5.8). It may be that these proteins represent true interactions with flagged beta-dystroglycan; however non-specific interactions may also be possible.

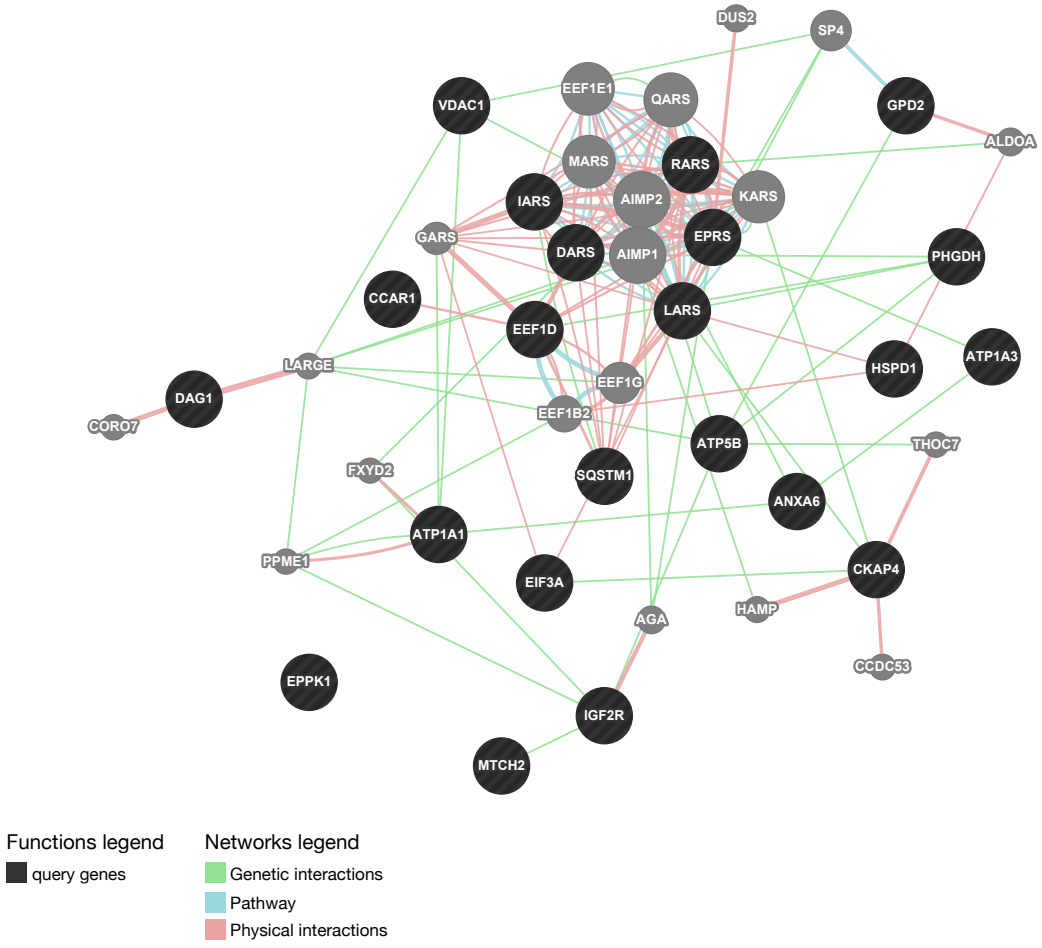

Figure 5.8: Interactome analysis of nuclear proteins found enriched in Flag IPs. A first interactome analysis using GeneMANIA shows that dystroglycan, DAG1, does not have any physical reported interaction with the proteins found in Flag IPs. Additionally, the clustering using the WebGestalt server, shows a random distribution of the proteins in different pathways and none of the pathways retrieved had a particular enrichment of two or more proteins.

The conception of this thesis comes from the idea that, in addition to its function in the plasma membrane, beta-dystroglycan has also a nuclear function. In this regard the type of proteins typically found in the pulldown from the nuclear fraction are not suitable for ascribing a nuclear role to beta-dystroglycan. However, in non-nuclear IPs there were many candidate proteins involved in an immense number of cellular pathways, including some critical nuclear processes (Figure 5.6). Additionally, in both cellular fractions there were proteins significantly enriched but with a peptide count number below two (attached excel file (**1.Interactome beta-dystroglycan**, "NN stats and Nuclear stats tabs (proteins with a "+" sign)"). Furthermore, other interesting candidates in Flag IPs were identified; but they were found in only two replicate experiments (Figure 5.7).

The purpose of this chapter is to find proteins interacting with beta-dystroglycan that could provide us with clues in order to understand the signalling pathways wherein dystroglycan (alpha and beta) has been found to be involved, such as those related to: its interaction with cytoskeletal and extracellular matrix components, its cytoplasmic and nuclear transport, its nuclear function, its degradation, its involvement in the cell cycle, cell division, and other cellular processes. Therefore, when taking into account the identity of proteins significantly enriched but with a low peptide count (attached excel file (**1.Interactome beta-dystroglycan**, "NN stats and Nuclear stats tabs (proteins with a "+" sign)"), proteins found in only two replicate Flag IPs (Figure 5.7) and the purposes pursued in this chapter, it was decided to take into account all these proteins and merge them with the highly enriched proteins of both fractions (Figure 5.6). In this way, through the interaction with intermediate proteins it is expected to find a possible relationship between beta-dystroglycan and cellular processes, such as those related to the nucleus, the cell cycle or the ubiquitin proteasome system.

It is important to emphasize that combining all these proteins could lead to an increase in the background and the number of non-specific interactions, thus caution has to be taken before assuming a direct interaction of beta-

dystroglycan with any reported protein. Importantly, future analyses may be required, such as the corresponding co- and reverse immunoprecipitations to further prove the interactions described here.

The combination of all candidate proteins, as described above, resulted in a total of approximately 721 proteins, which could include some background (attached file **3. Mixed proteins**). Fortunately, a meta-data analysis investigating the identity of contaminant proteins interacting with the Flag M2 immunoprecipitation system has been reported (Mellacheruvu et al., 2013). Hence, all the 721 proteins were subjected to CRAPome analysis (`http://www.crapome.org`). Proteins such as tubulins, histones and GAPDH were the hits with the highest scores, in addition to others, indicating that they are potential background (attached file **2. CRAPome mixed proteins**).

Protein analysis using the WebGestalt database allowed the clustering of proteins by their biological, cellular and molecular characteristics (Figure 5.10). Overall, there was a good distribution of proteins along a great variety of cellular processes from vesicular transport, cancer signalling, cell cycle, DNA replication, actin cytoskeleton regulation to apoptosis and many other processes (Figure 5.11). Dystroglycan is ubiquitously expressed, so it is not surprising to find that it has broad cellular implications. Due to the focus of this thesis on the nuclear function of beta-dystroglycan, the pathways described below will be those related to nuclear functions, cell cycle and the ubiquitin-proteasome system. However, proteins highly enriched in other pathways, will be discussed in the last chapter of this thesis (Chapter 6).

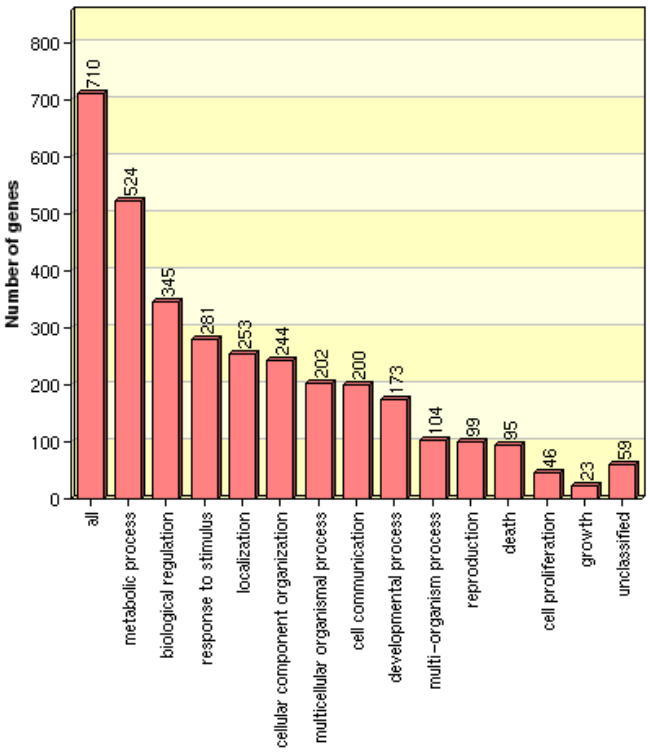

(a)

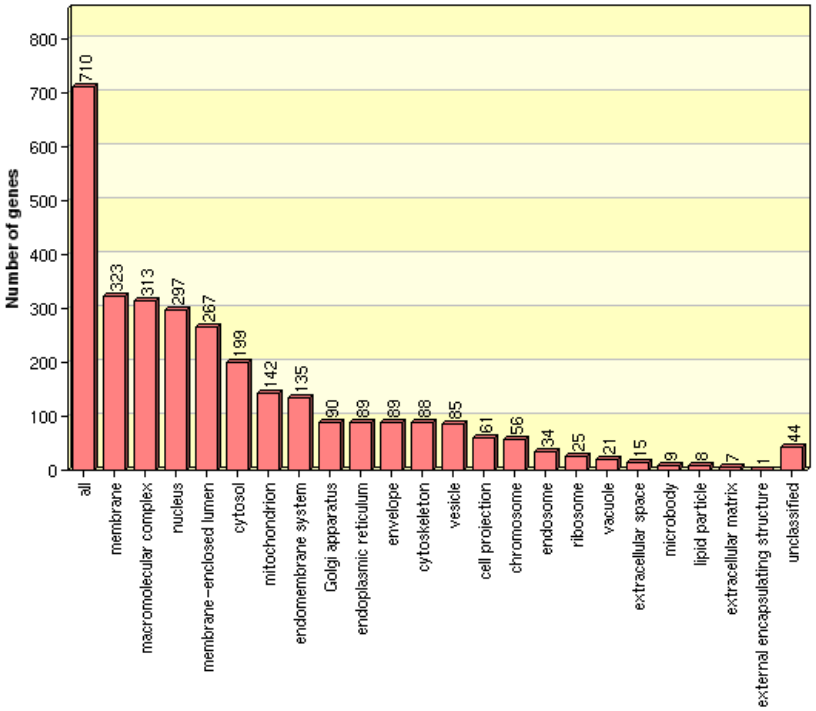

(b)

Figure 5.9: KEGG pathway protein enrichment. Proteins considered for interactome analysis were subject to a KEGG pathway enrichment analysis. Proteins were grouped by their a) biological and b) cellular functions. Proteins have a vast distribution throughout different cellular processes.

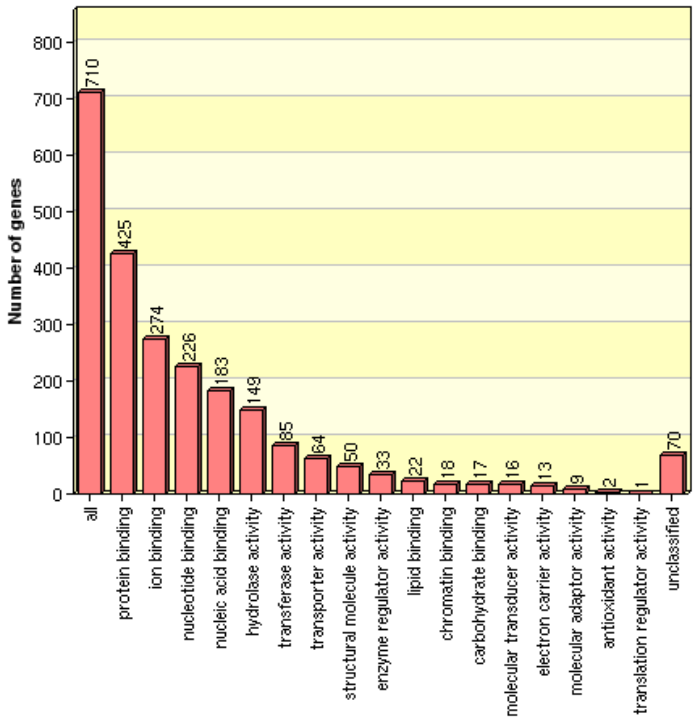

Figure 5.10: KEGG pathway protein enrichment. Proteins considered for interactome analysis were subject to a KEGG pathway enrichment analysis. Proteins were grouped by their molecular functions. Proteins have a vast distribution throughout different cellular processes.

Pathway Name			
Metabolic pathways	Pancreatic secretion	Cell cycle	Protein digestion and absorption
Protein processing in endoplasmic reticulum	PPAR signaling pathway	Glycerolipid metabolism	Progesterone-mediated oocyte maturation
Phagosome	Alzheimer's disease	Glutathione metabolism	Apoptosis
Spliceosome	Fatty acid elongation in mitochondria	Tight junction	Glycine, serine and threonine metabolism
Fatty acid metabolism	mRNA surveillance pathway	Endometrial cancer	NOD-like receptor signaling pathway
Pathogenic Escherichia coli infection	Amino sugar and nucleotide sugar metabolism	Alanine, aspartate and glutamate metabolism	Dilated cardiomyopathy
Valine, leucine and isoleucine degradation	Salivary secretion	Ubiquitin mediated proteolysis	Shigellosis
Huntington's disease	Valine, leucine and isoleucine biosynthesis	Pentose and glucuronate interconversions	Focal adhesion
Propanoate metabolism	Proximal tubule bicarbonate reclamation	Amoebiasis	Neurotrophin signaling pathway
Glycolysis / Gluconeogenesis	Arrhythmogenic right ventricular cardiomyopathy (ARVC)	Vibrio cholerae infection	Colorectal cancer
Proteasome	Adherens junction	DNA replication	Allograft rejection
RNA transport	Pathways in cancer	Prostate cancer	Regulation of actin cytoskeleton
Aminoacyl-tRNA biosynthesis	Calcium signaling pathway	Lysosome	Viral myocarditis
Systemic lupus erythematosus	Galactose metabolism	Biosynthesis of unsaturated fatty acids	Graft-versus-host disease
Pyruvate metabolism	Ascorbate and aldarate metabolism	Epithelial cell signaling in Helicobacter pylori infection	RNA degradation
Arginine and proline metabolism	Pentose phosphate pathway	Adipocytokine signaling pathway	Phenylalanine metabolism
Tryptophan metabolism	Butanoate metabolism	Pyrimidine metabolism	Selenocompound metabolism
beta-Alanine metabolism	Histidine metabolism	Carbohydrate digestion and absorption	One carbon pool by folate
Bacterial invasion of epithelial cells	Citrate cycle (TCA cycle)	Protein export	Glyoxylate and dicarboxylate metabolism
Gap junction	Leukocyte transendothelial migration	Cell adhesion molecules (CAMs)	Steroid biosynthesis
Parkinson's disease	Fructose and mannose metabolism	Hepatitis C	Wnt signaling pathway
Endocytosis	SNARE interactions in vesicular transport	Gastric acid secretion	Small cell lung cancer
Lysine degradation	Cysteine and methionine metabolism	Insulin signaling pathway	Autoimmune thyroid disease
Vasopressin-regulated water reabsorption	Prion diseases	N-Glycan biosynthesis	Toxoplasmosis
Oxidative phosphorylation	Purine metabolism	Cardiac muscle contraction	Fc gamma R-mediated phagocytosis
Ribosome	Aldosterone-regulated sodium reabsorption	Peroxisome	Collecting duct acid secretion
Antigen processing and presentation	Type I diabetes mellitus	Glycerophospholipid metabolism	Arachidonic acid metabolism
Ribosome biogenesis in eukaryotes	Bile secretion	Oocyte meiosis	

Figure 5.11: Pathways enriched by KEGG analysis. Shown are the broad number of KEGG pathways enriched by using the WebGestalt server under the following settings: Organism: *Homo sapiens* (hsapiens); Id Type: gene_symbol; Enrichment analysis: KEGG Analysis; Ref Set: genome; Statistic: Hypergeometric; Significance level: 0.1; Multiple Test Adjustment: BH; Minimum number of genes for a category: 2. Highlighted in green are those pathways further analysed according to the general hypothesis of this thesis.

In the following figures the pathways of proteins recovered by immunoprecipitation with Flag are shown. The sequence of these images is based on mechanisms started on the plasma membrane (cellular interactions), the actin cytoskeleton interactions, to the nuclear compartment, culminating in the integration of some cellular pathways that lead to the generation of cancer, all of which are analysed, in the "Discussion" section of this chapter.

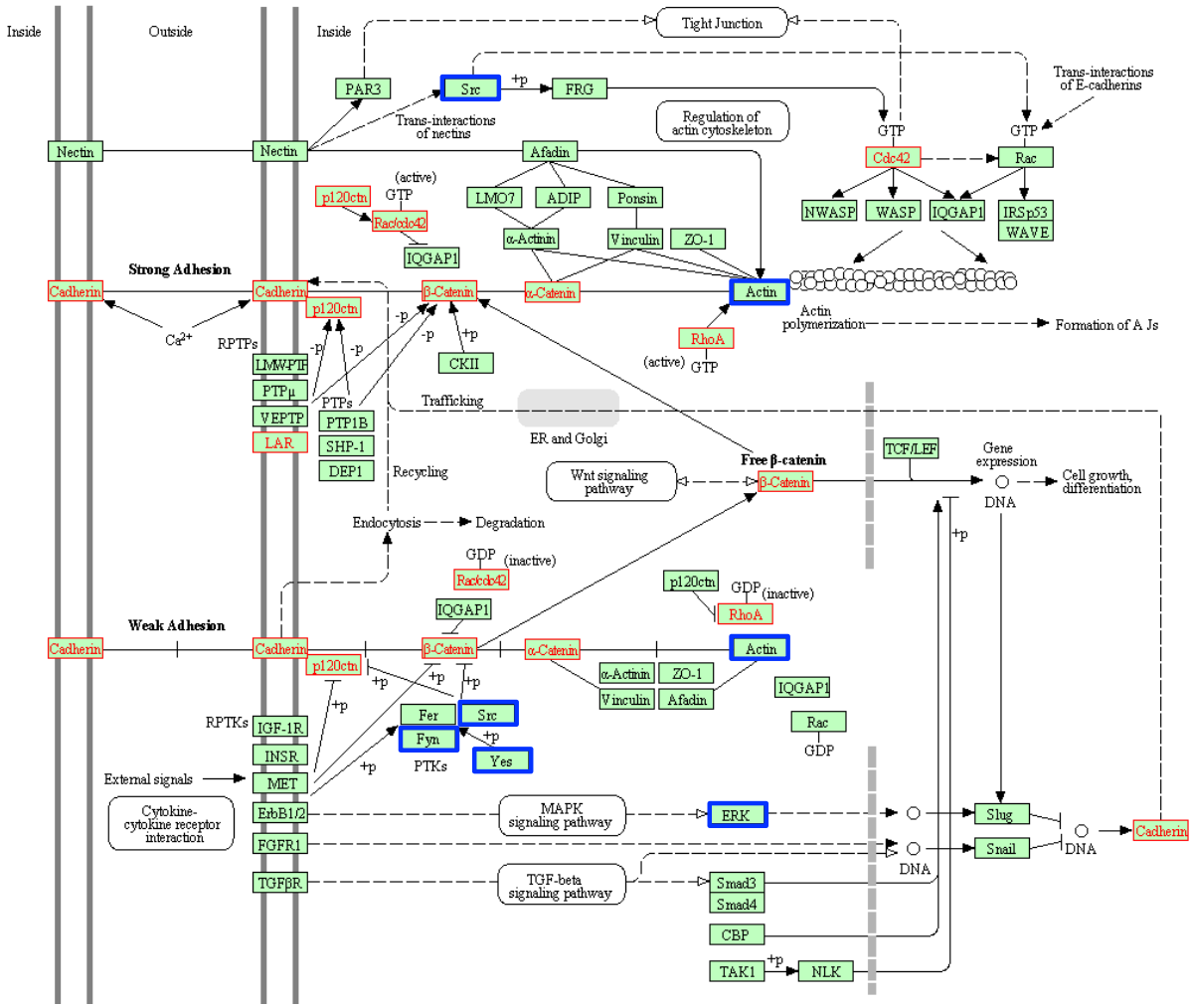

Figure 5.12: Adherens junction. E-cadherin is the main component of cell-cell adherens junctions (AJs) which are important for maintaining tissue architecture, cell polarity, cell movement and proliferation. E-cadherin interacts with β-catenin which in turn binds α-catenin; α-catenin is then able to recruit F-actin. Cadherin may act as a positive or negative regulator of β-catenin. Highlighted in red are the proteins found immunoprecipitating with Flag (Cdc42, RhoA, α/β-catenin, Cadherin, LAR, Rac and p120ctn) and in blue boxes are the already known interacting proteins with dystroglycan (Fyn, Src, Yes, Actin and ERK). Source: `http://www.kegg.jp/dbget-bin/www_bget?pathway+hsa04520`.

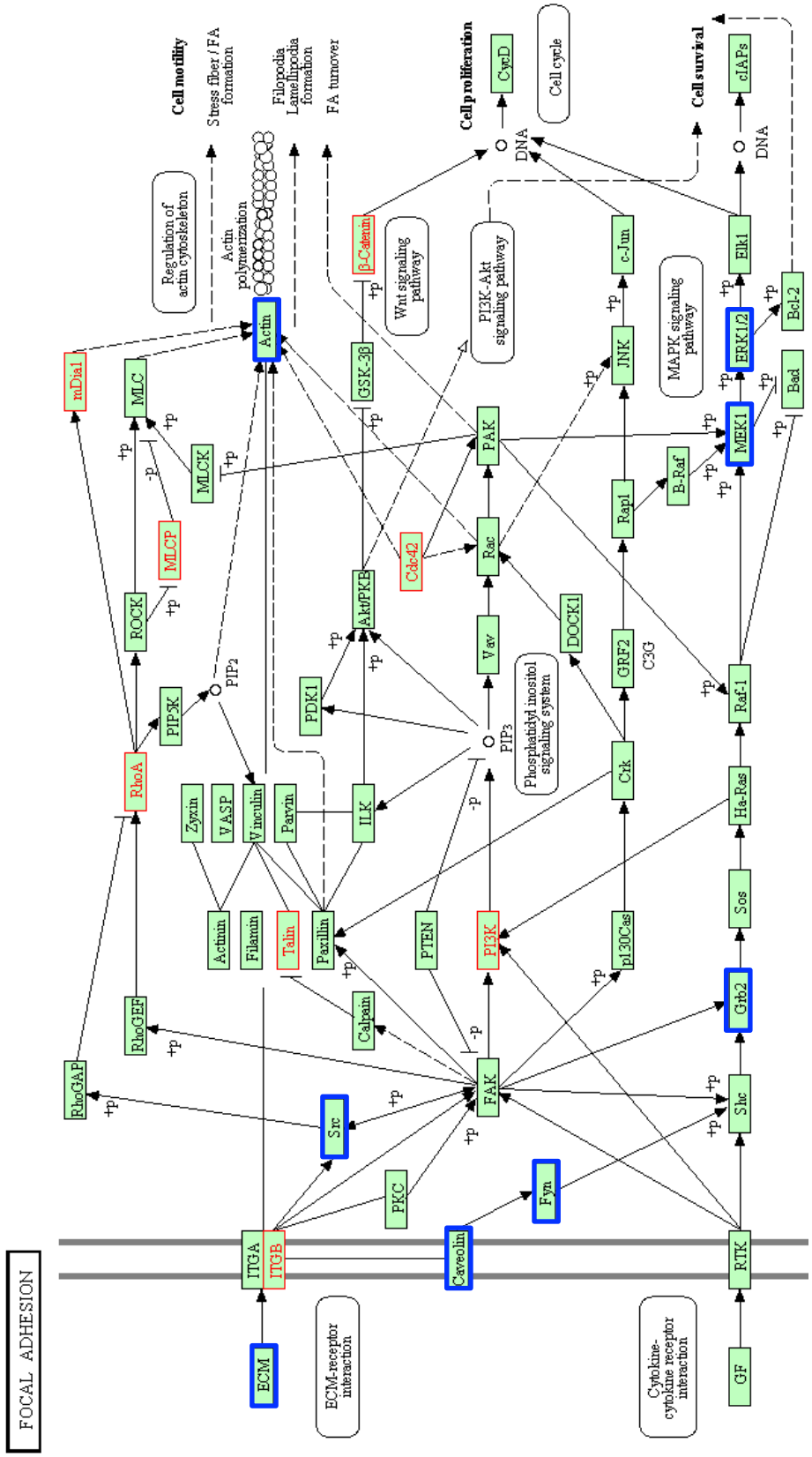

Figure 5.13: Focal adhesion. Focal adhesions are structures formed at the cell-extracellular matrix contact points, and are composed of adaptor proteins implicated in linking the extracellular matrix to the actin cytoskeleton and in cellular signalling. These structures trigger different cellular processes such as the reorganization of the actin cytoskeleton, a requirement in cell motility, cell proliferation, gene regulation, cell survival and others. Highlighted in red are the proteins found immunoprecipitating with Flag (PI3K, ITGB, RhoA, Talin, Cdc42, β-catenin, MLCP and mDia1) and in blue boxes are the already known interacting proteins with dystroglycan (Grb2, Src, MEK1, ERK1/2, Actin, Fyn and Caveolin). Source: `http://www.kegg.jp/dbget-bin/www_bget?pathway+hsa04510`.

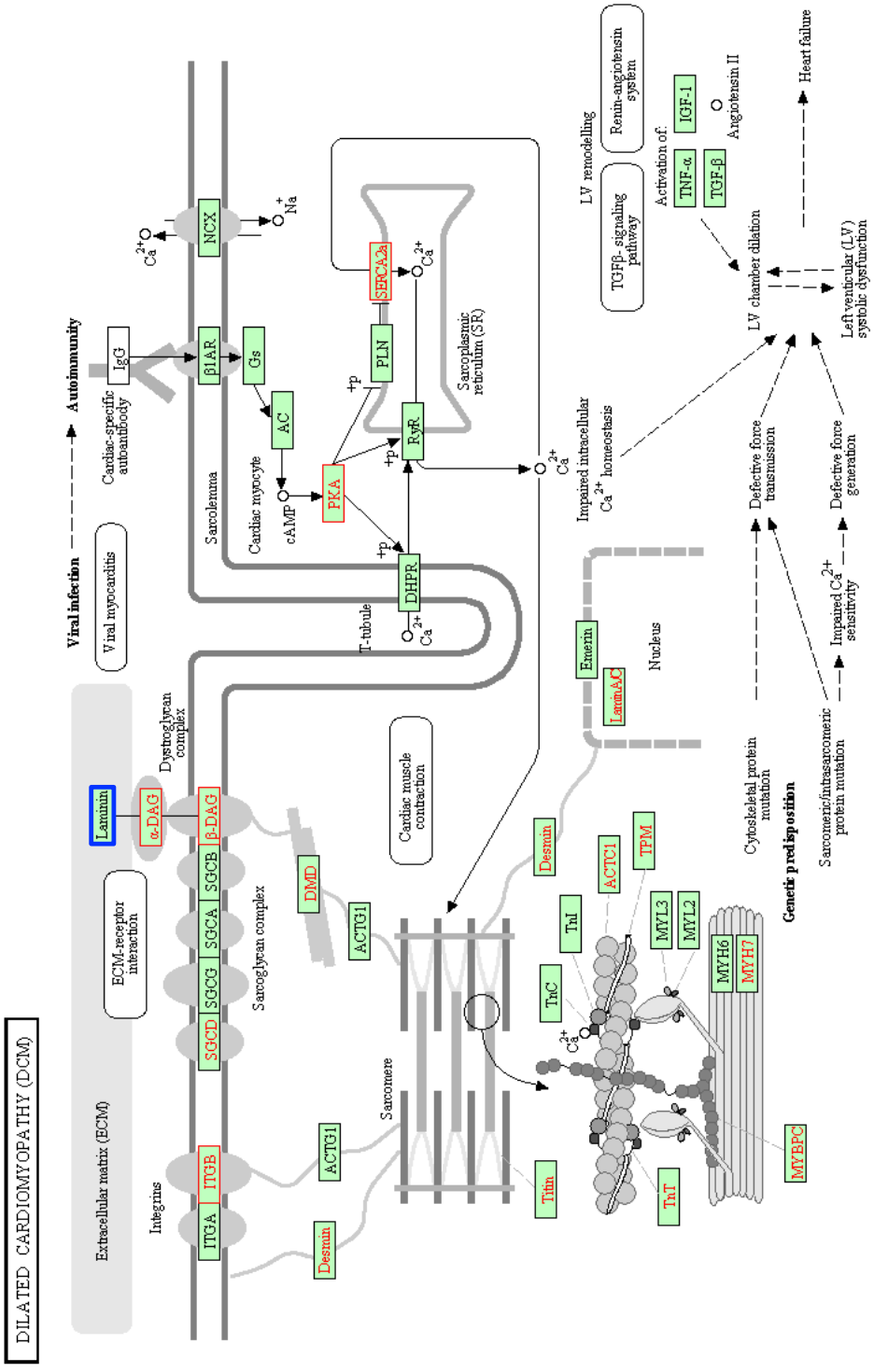

Figure 5.14: Dilated cardiomyopathy. Dilated cardiomyopathy (DCM) is a heart muscle disease characterised by dilation and impaired contraction of the left or both ventricles that results in progressive heart failure and sudden cardiac death from ventricular arrhythmia. It is characterized by defects in force generation and defects in force transmission mediated by the dystrophin associated protein complex. Highlighted in red are the proteins found immunoprecipitating with Flag (ITGB, SGCD, α-DAG and PKA) and in blue boxes are the already known interacting proteins with dystroglycan (Laminin). Source: `http://www.kegg.jp/dbget-bin/www_bget?pathway+hsa05414`.

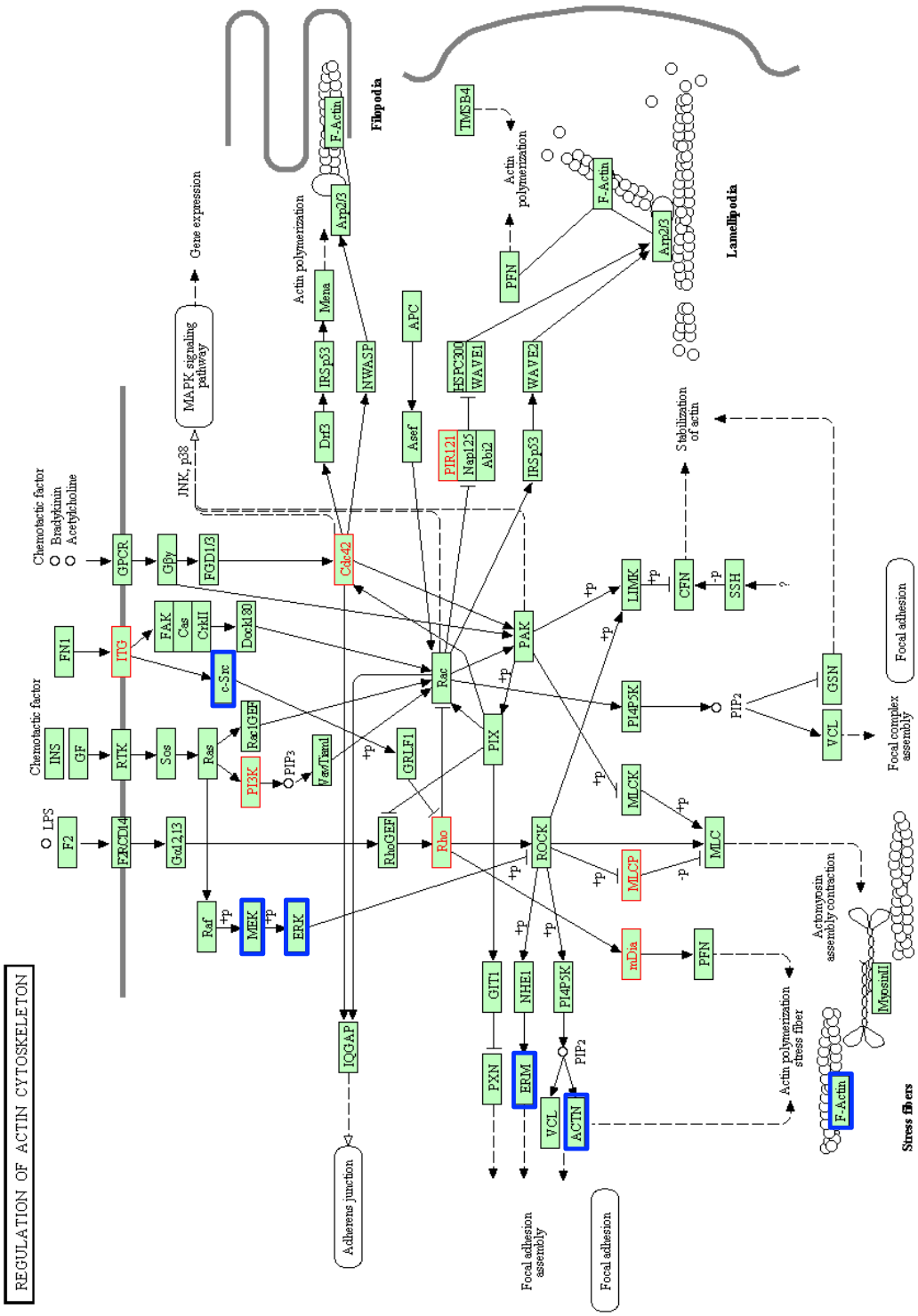

Figure 5.15: Regulation of actin cytoskeleton. Different signals triggered by plasma membrane proteins can result in the actin cytoskeleton reorganization which in turn leads to the formation of lamellipodia and filopodia. Highlighted in red are the proteins found immunoprecipitating with Flag (mDia, MLCP, Rho, PI3K, ITG, Cdc42 and PIR121) and in blue boxes are the already known interacting proteins with dystroglycan (F-actin, Actin, ERM, c-Src, MEK and ERK). Source: `http://www.kegg.jp/dbget-bin/www_bget?pathway+hsa04810`.

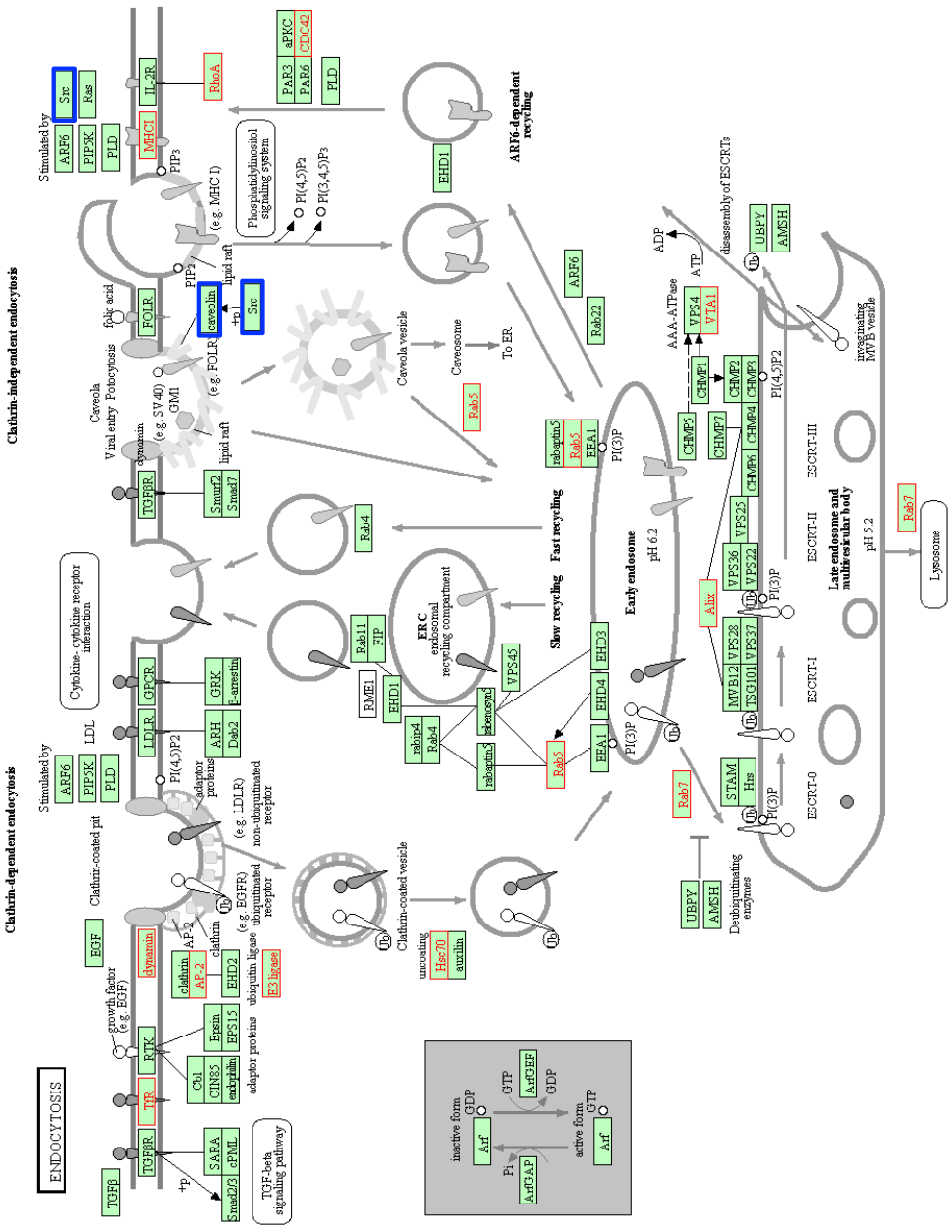

Figure 5.16: Endocytosis. Endocytosis is a mechanism for cells to remove ligands, nutrients, and plasma membrane (PM) proteins, and lipids from the cell surface, bringing them into the cell interior. The removal of PM proteins is achieved by clathrin dependent or independent endocytosis. Cargo proteins are sorted back to the PM, or sorted into intraluminal vesicles. Highlighted in red are the proteins found immunoprecipitating with Flag (TfR, Dynamin, AP2, Hsc70, Rab5/7, CDC42, MHCI, VTA1, E3 ligase and Alix) and in blue boxes are the already known interacting proteins with dystroglycan (Caveolin and Src). Source: `http://www.kegg.jp/dbget-bin/www_bget?pathway+hsa04144`.

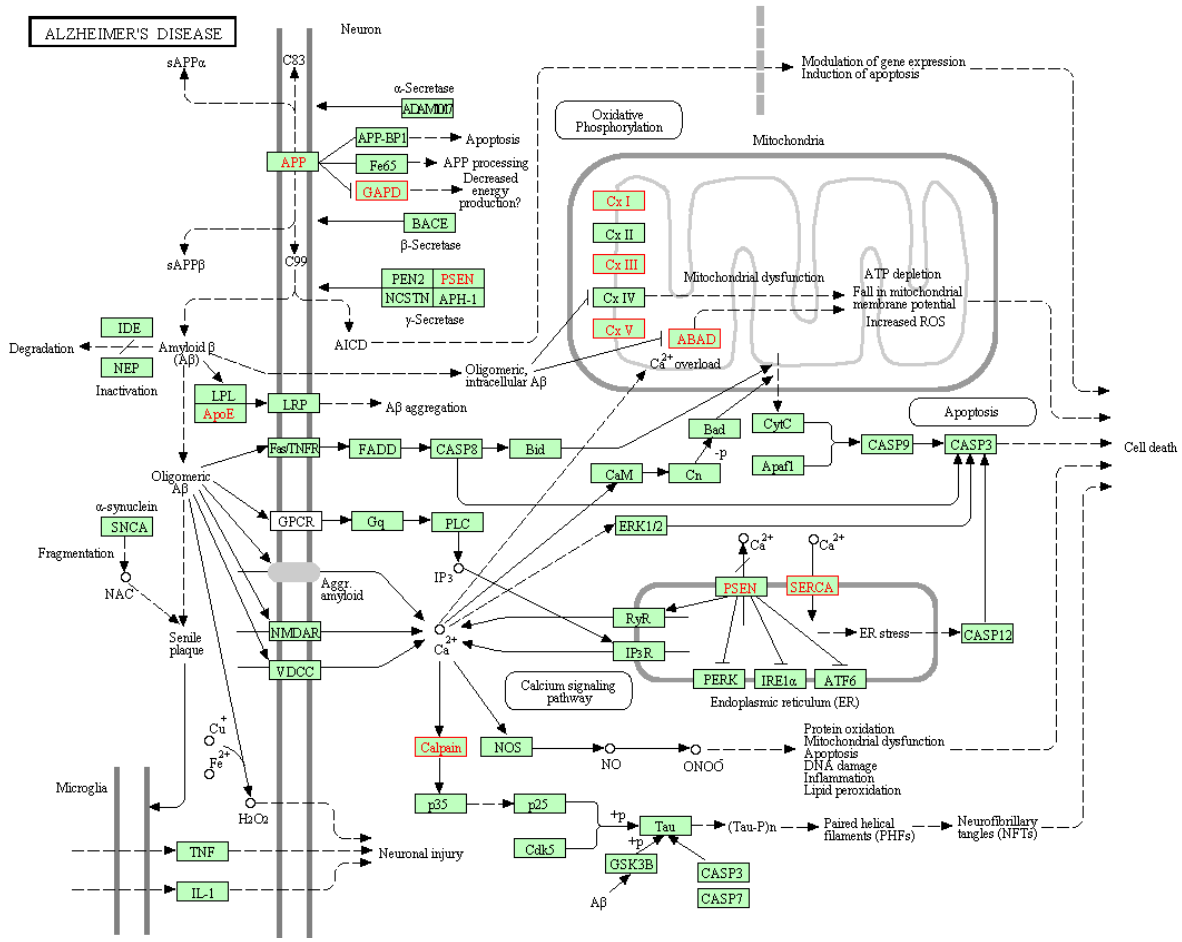

Figure 5.17: Alzheimer's disease. Alzheimer's disease (AD) is associated with senile plaques and neurofibrillary tangles (NFTs). Amyloid-beta (Abeta), a major component of senile plaques, is generated by from the amyloid precursor protein by the consecutive cleavage of different enzymes including the gamma-secretase complex. Highlighted in red are the proteins found immunoprecipitating with Flag (SERCA, Calpain, PSEN, GAPD, ABAD, CX-I, -III and -V) . Source: `http://www.kegg.jp/dbget-bin/www_bget?pathway+hsa05010`.

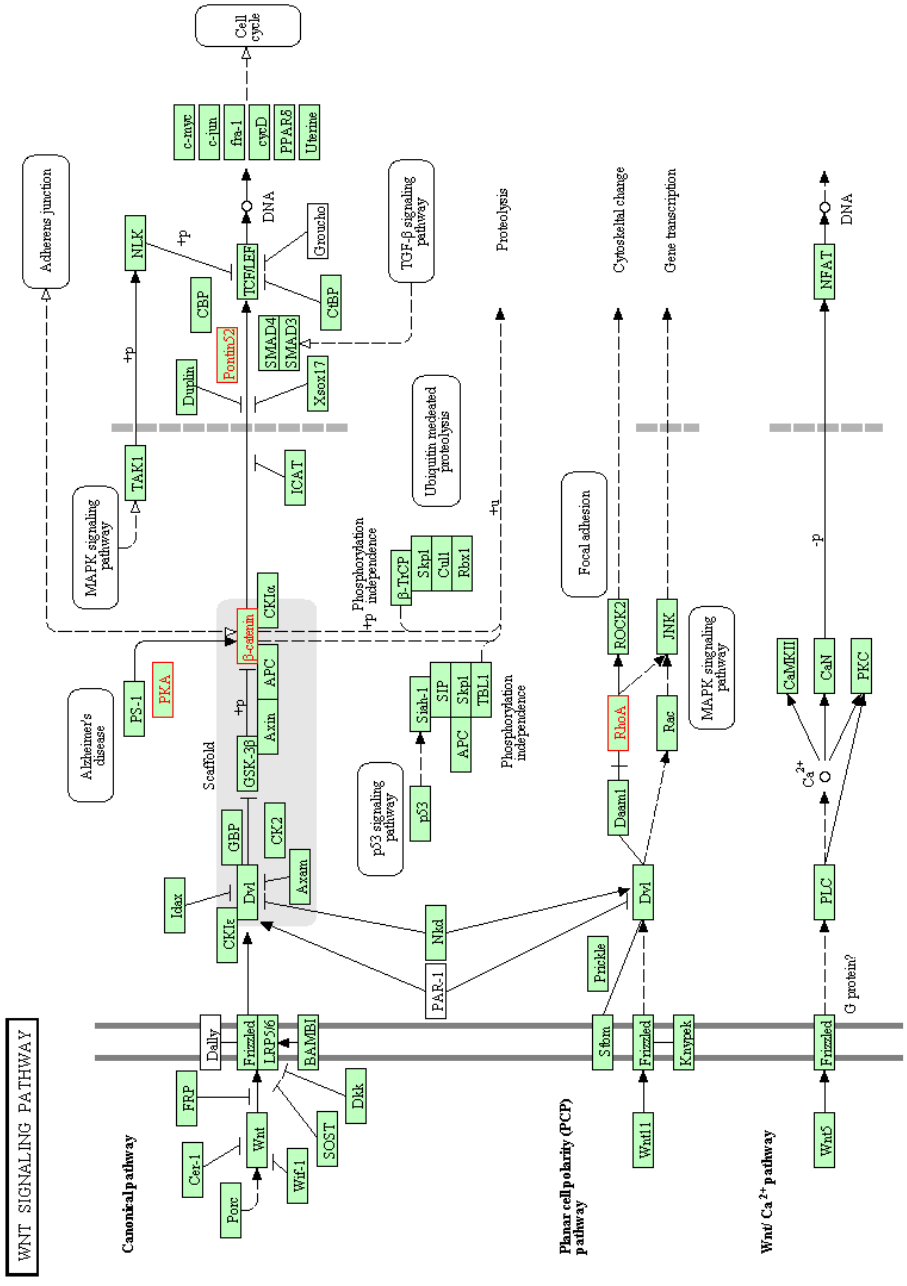

Figure 5.18: WNT signalling pathway. Wnt proteins are secreted morphogens that are required for basic developmental processes, such as cell-fate specification, progenitor-cell proliferation and the control of asymmetric cell division, in many different species and organs. There are at least three different Wnt pathways: the canonical pathway, the planar cell polarity (PCP) pathway and the Wnt/Ca2+ pathway. Highlighted in red are the proteins found immunoprecipitating with Flag (RhoA, PKA, β-catenin and Pontin52). Source: `http://www.kegg.jp/dbget-bin/www_bget?pathway+hsa04310`.

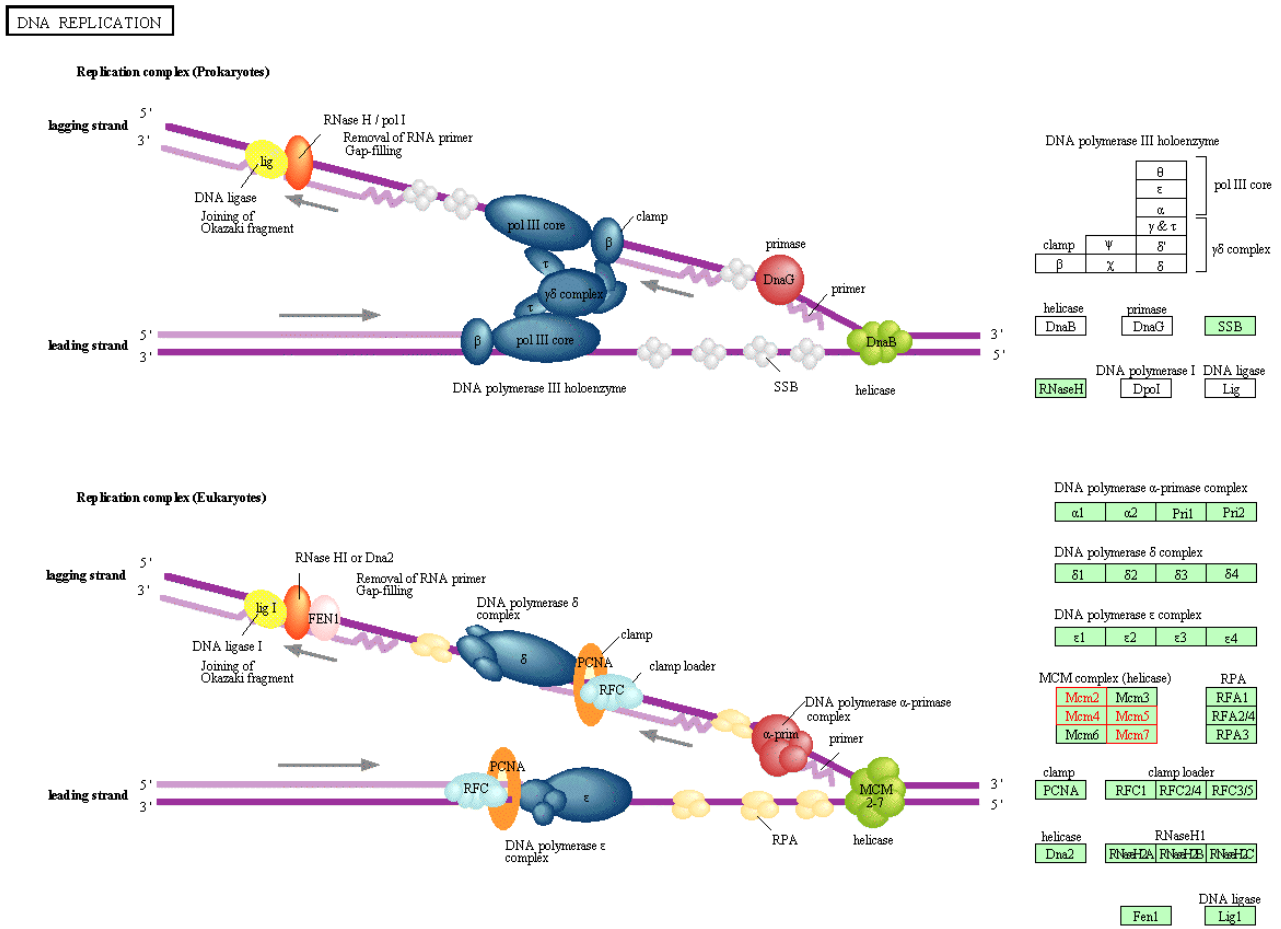

Figure 5.19: DNA replication. A complex network of interacting proteins and enzymes is required for DNA replication. Generally, DNA replication follows a multistep enzymatic pathway. At the DNA replication fork, a DNA helicase (DnaB or MCM complex) precedes the DNA synthetic machinery and unwinds the duplex parental DNA in cooperation with the SSB or RPA. In eukaryotes, three DNA polymerases (alpha, delta, and epsilon) have been identified. Highlighted in red are the proteins found immunoprecipitating with Flag (Mcm-2, -4, -5 and -7). Source: `http://www.kegg.jp/dbget-bin/www_bget?pathway+hsa03030`.

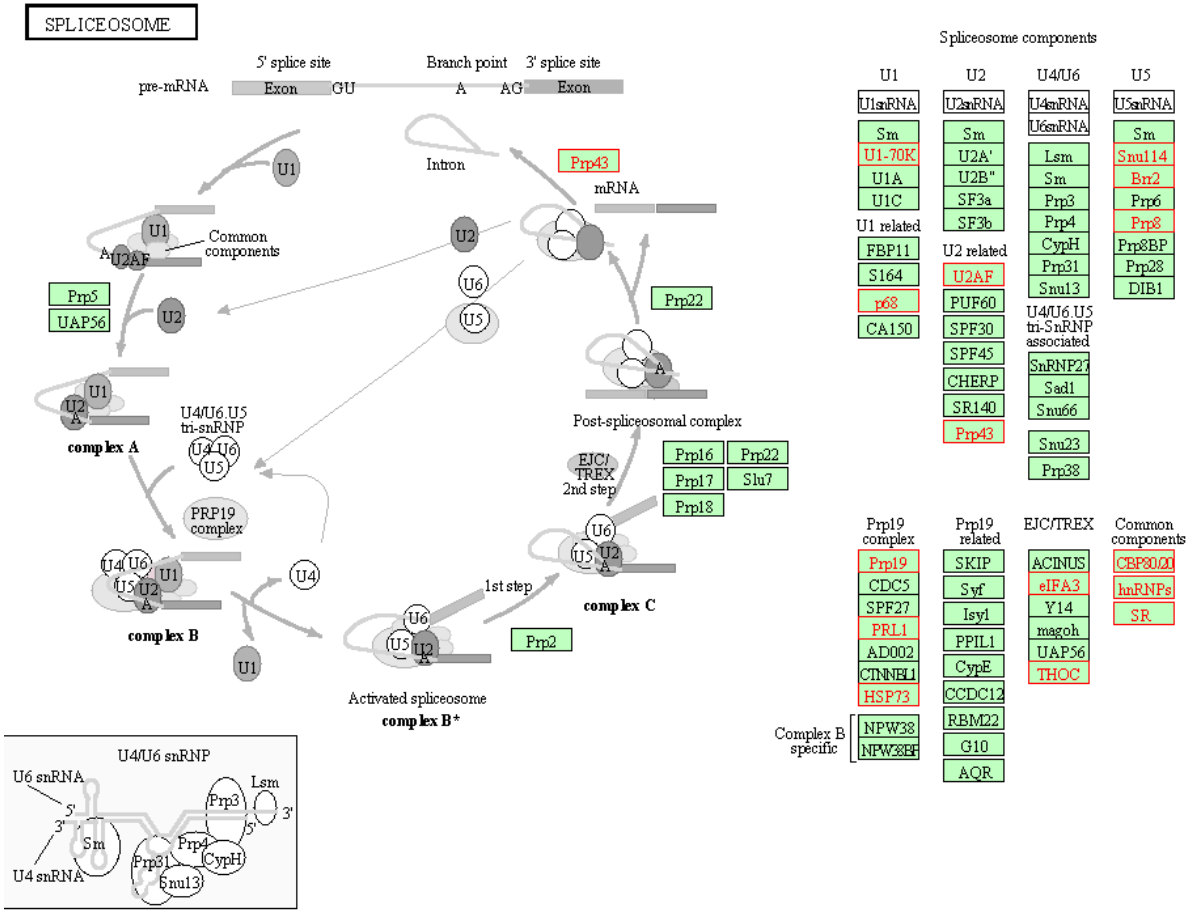

Figure 5.20: Spliceosome. After transcription, eukaryotic mRNA precursors contain protein-coding exons and noncoding introns. In the following splicing, introns are excised and exons are joined by a macromolecular complex, the spliceosome. The standard spliceosome is made up of five small nuclear ribonucleoproteins (snRNPs), U1, U2, U4, U5, and U6 snRNPs, and several spliceosome-associated proteins (SAPs). Various spliceosome forms (e.g. A-, B- and C-complexes) have been identified. Highlighted in red are the proteins found immunoprecipitating with Flag (Prp43, U2AF, Prp8, Brr2, Snu114, U1-70K, p68, Prp19, PRL1, HSP73, EIFA3, THOC, CBP80/20, hnRNPs and SR). Source: `http://www.kegg.jp/dbget-bin/www_bget?pathway+hsa03040`.

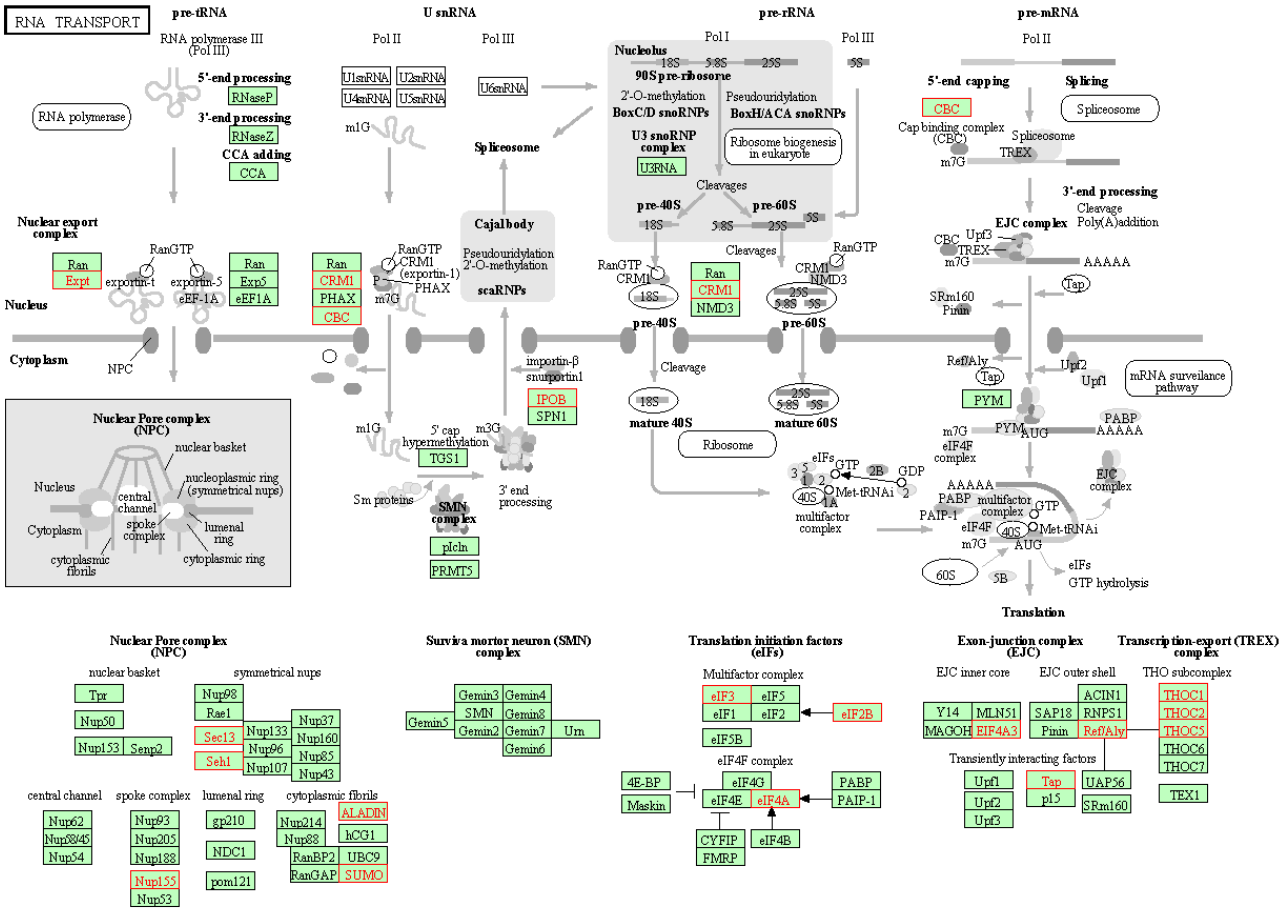

Figure 5.21: RNA transport. RNA transport from the nucleus to the cytoplasm is fundamental for gene expression. The different RNA species that are produced in the nucleus are exported through the nuclear pore complexes (NPCs) via mobile export receptors which belong to the karyopherin-beta family proteins. Nuclear export of mRNAs is functionally coupled to different steps in gene expression processes, such as transcription, splicing, 3'-end formation and even translation. Highlighted in red are the proteins found immunoprecipitating with Flag (Expt, CRM1, CBC, IPOB, Sec13, Seh1, Nup155, ALADIN, SUMO, eIF3, eIF2B, eIF4A, eIF4A3, Tap, Ref/Aly, THC-1, -2 and -5). Source: `http://www.kegg.jp/dbget-bin/www_bget?pathway+hsa03013`.

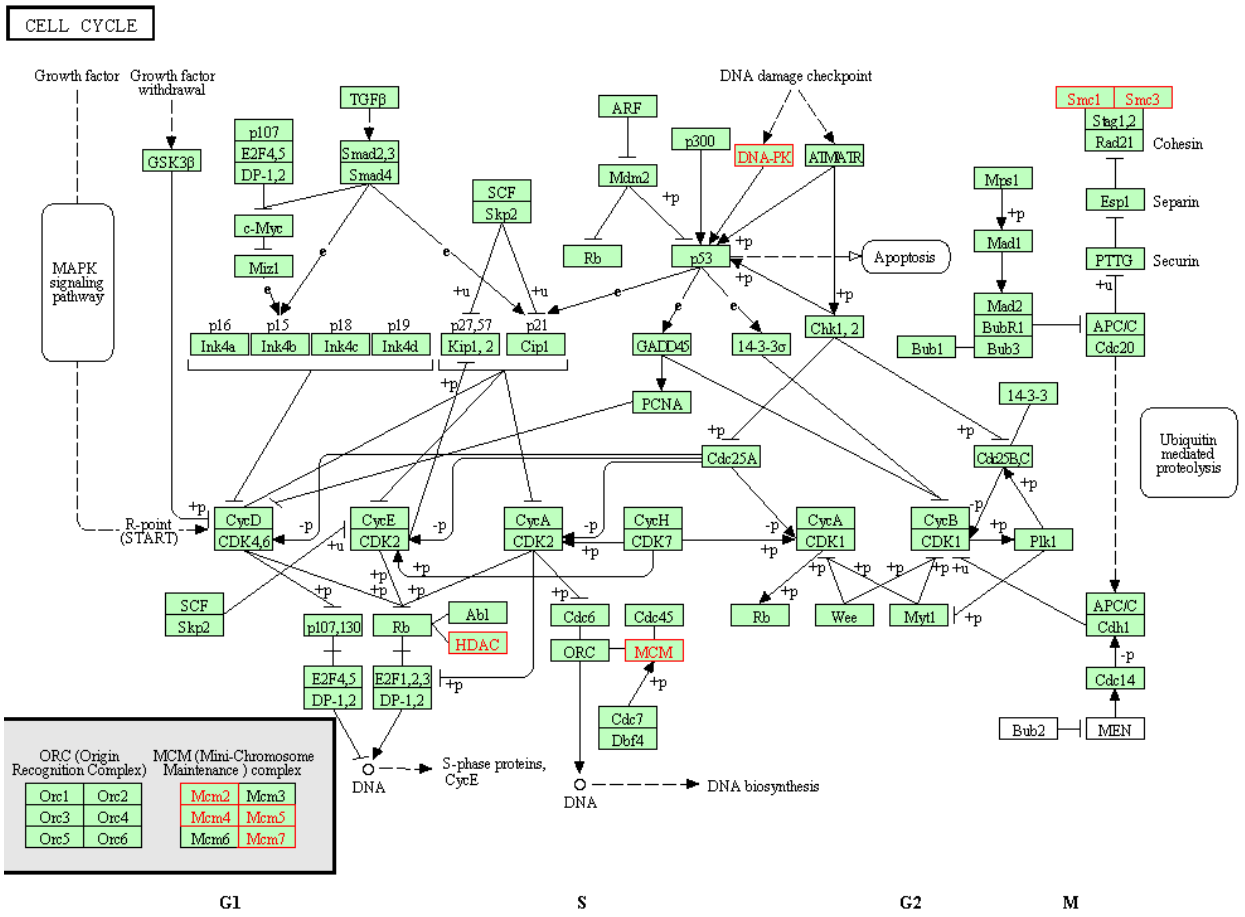

Figure 5.22: Cell cycle. Mitotic cell cycle progression is accomplished through a reproducible sequence of events, DNA replication (S phase) and mitosis (M phase) separated temporally by gaps known as G1 and G2 phases. Cyclin-dependent kinases (CDKs) regulate the cell's progression through the phases of the cell cycle by modulating the activity of key substrates. Eukaryotic cells respond to DNA damage by activating signalling pathways that promote cell cycle arrest and DNA repair. Highlighted in red are the proteins found immunoprecipitating with Flag (Mcm-2, -4, -5 and -7, HDAC, DNA-PK, Smc1 and Smc3). `http://www.kegg.jp/dbget-bin/www_bget?pathway+hsa04110`.

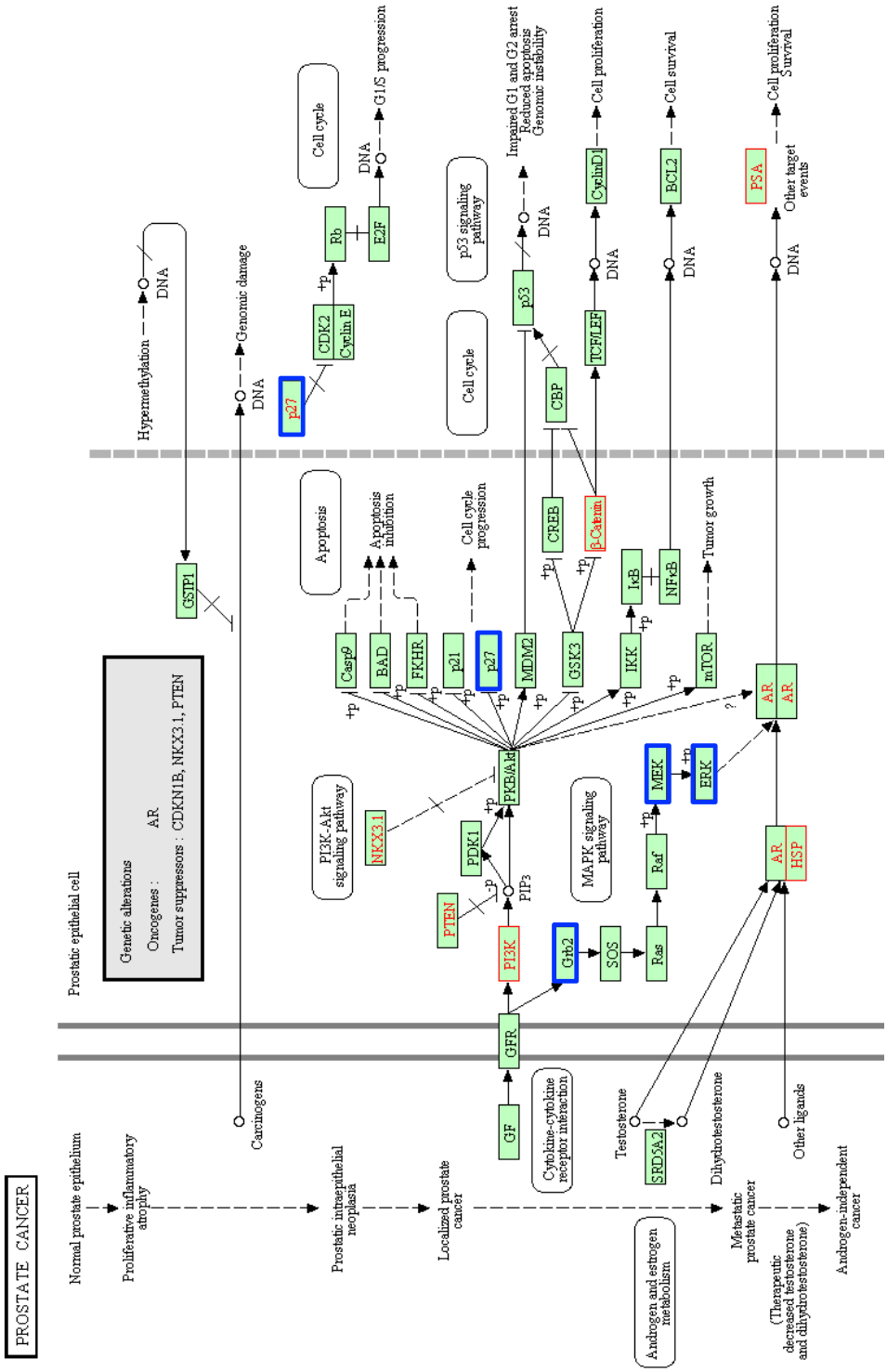

Figure 5.23: Prostate cancer. Prostate cancer is the most frequently diagnosed cancer among men. Inadequate levels of PTEN and NKX3.1, which regulate the growth and survival of prostate cells in the normal prostate, lead to a reduction in p27 levels and to increased proliferation and decreased apoptosis. Androgen receptor (AR) is a transcription factor that is normally activated by its androgen ligand. Highlighted in red are the proteins found immunoprecipitating with Flag (HSP, PSA, β-catenin and PI3K) and in blue boxes are the already known interacting proteins with dystroglycan (MEK, ERK, p27 and Grb2). Source: `http://www.kegg.jp/dbget-bin/www_bget?pathway+hsa05215`.

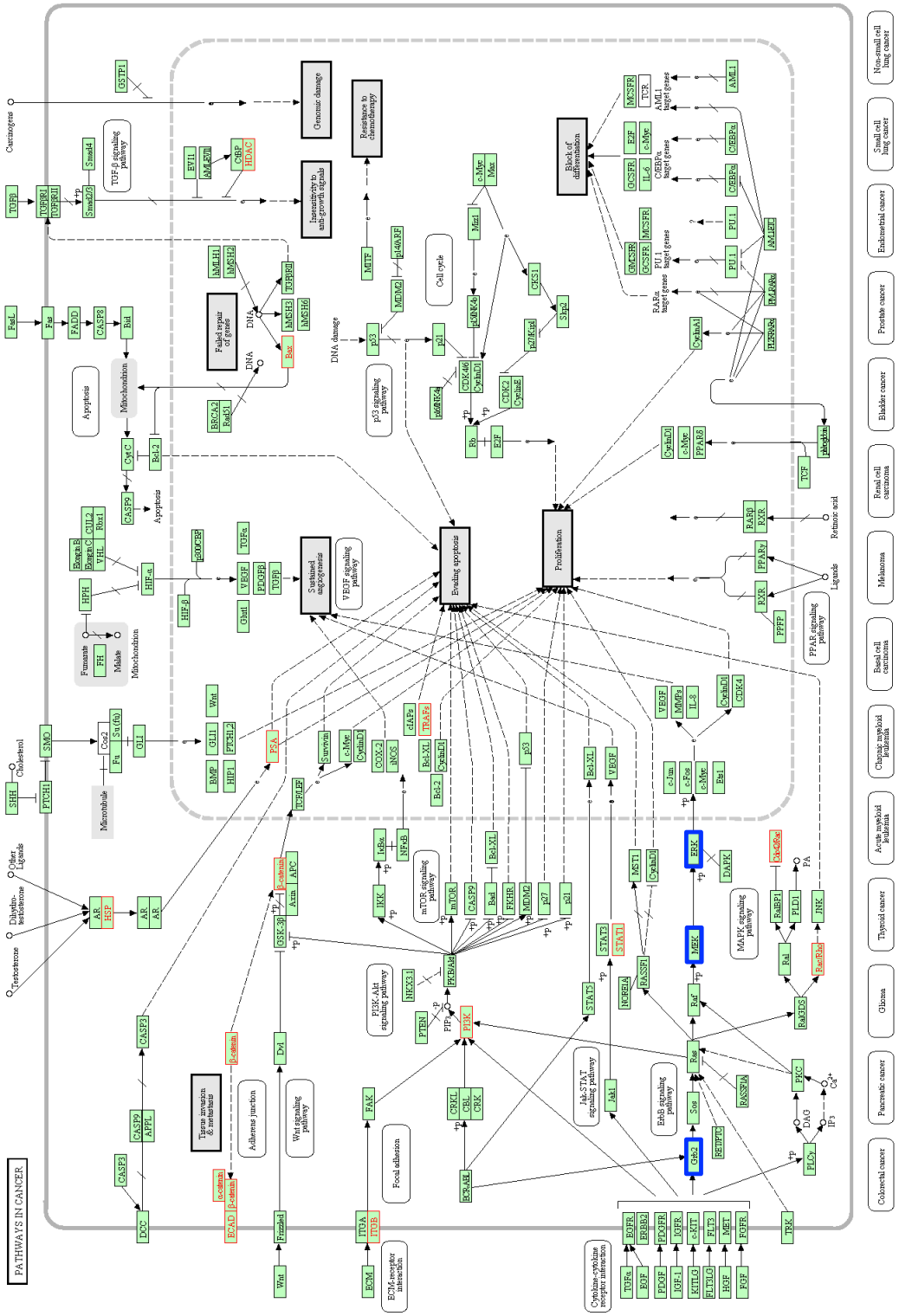

Figure 5.24: Pathways in cancer. The alteration of key cellular events may render cells prone to uncontrolled growth, a hallmark of cancer. There are some pathways that are shared among different types of cancer. Highlighted in red are the proteins found immunoprecipitating with Flag (α/β-catenin, ECAD, ITGB, PI3K, HSP, PSA, Bax, HDAC, TRAFs, STAT1, Rac/Rho and Cdc42/Rac) and in blue boxes are the already known interacting proteins with dystroglycan (Grb2, MEK and ERK). Source: `http://www.kegg.jp/dbget-bin/www_bget?pathway+hsa05200`.

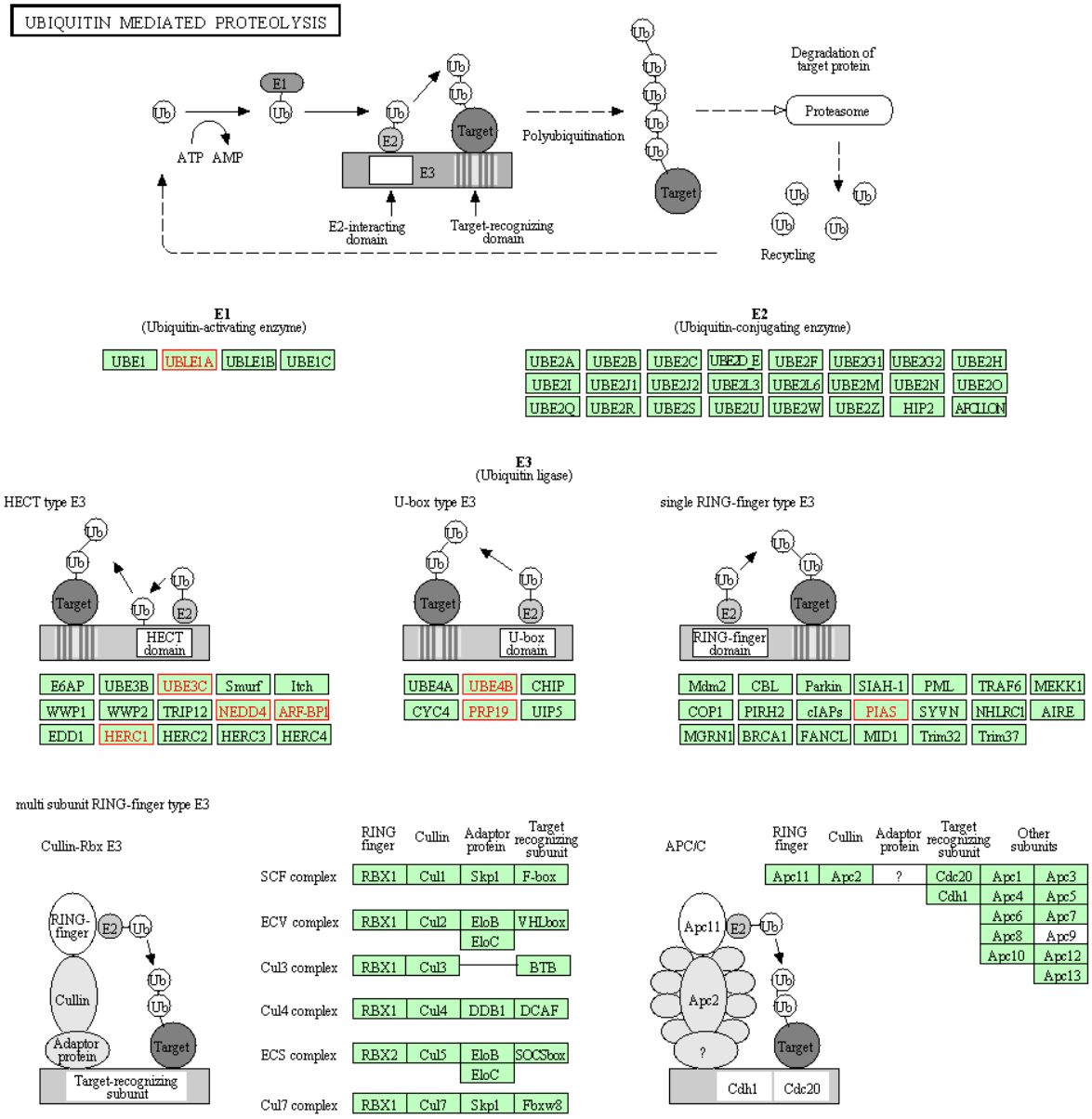

Figure 5.25: Ubiquitin mediated proteolysis. Ubiquitination functions as a signal for 26S proteasome dependent protein degradation and other signalling processes. This PTM is carried out by a process of sequential steps performed by a E1 ubiquitin activating enzyme, a E2 ubiquitin conjugating enzyme, and a E3 ubiquitin ligase. E3 ubiquitin ligases are classified into four groups: HECT type, U-box type, single RING-finger type, and multi-subunit RING-finger type. Highlighted in red are the proteins found immunoprecipitating with Flag (UBLE1A, UBE3C, HERC1, NEDD4, ARF-BP1, UBE4B, PRP19 and PIAS). Source: `http://www.kegg.jp/dbget-bin/www_bget?pathway+hsa04120`.

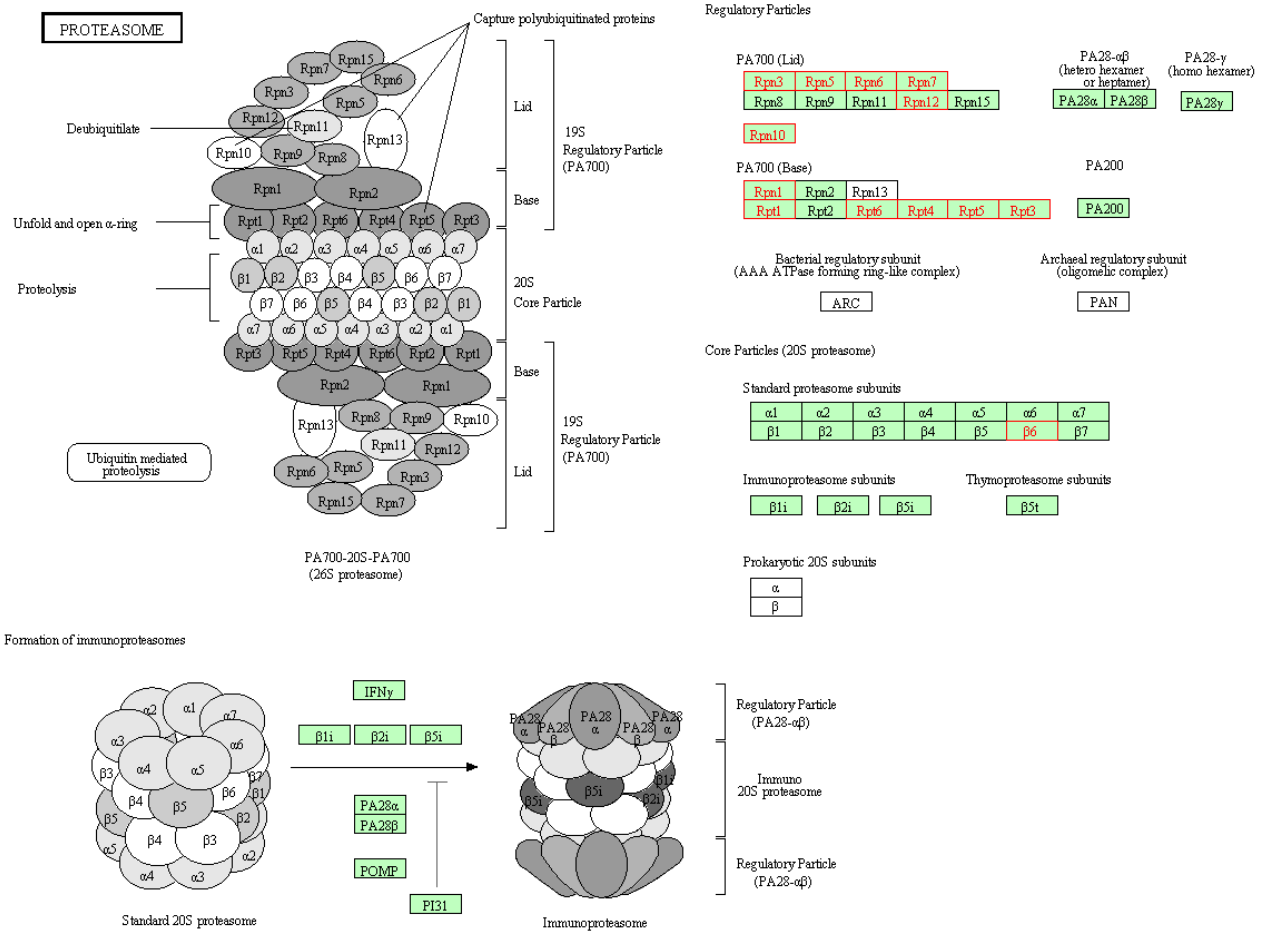

Figure 5.26: Proteasome. The 26S proteasome is a multisubunit protein complex composed of a 20S core particle and two 19S regulatory particles. The proteasome degrades proteins usually modified by ubiquitin groups. This complex has important roles in the regulation of the cell cycle, cell differentiation, signal transduction pathways, antigen processing for appropriate immune responses, stress signalling, inflammatory responses, and apoptosis. Highlighted in red are the proteins found immunoprecipitating with Flag (Rpn-3, -5, -6, -7, -12, -10 and -1, Rpt-1, -6, -4, -5 and -3 and 20Sβ6). Source: `http://www.kegg.jp/dbget-bin/www_bget?pathway+hsa03050`.

5.5 Post-translational modifications of beta-dystroglycan detected by mass spectrometry

The interactome analysis performed with flagged beta-dystroglycan allowed a recovery of a great variety of proteins. In addition to this analysis, samples immunoprecipitated with flag were subjected to a further mass spectrometry analysis in search of PTMs, such as phosphorylation and ubiquitination, that could be present on beta-dystroglycan. Under these conditions it was possible to recover both, a phosphorylated threonine (T790 in human, T788 in mouse) and a ubiquitinated lysine (K794 in human, K792 in mouse) in beta-dystroglycan. Ubiquitinated lysine was found enriched in both fractions, while phosphorylated threonine was found in nuclear fractions only. An *in silico* analysis using the NetPhosK 1.0 server (`http://www.cbs.dtu.dk/services/NetPhosK/`) revealed PKC as the putative kinase responsible for T788 phosphorylation (Figures 5.27 and 5.28, and attached files: **PTM/Phosphorylation and PTM/Ubiquitination**).

5.6 Discussion.

The translation of dystroglycan generates a pro-peptide that is further processed into the alpha- and beta-dystroglycan subunits. Although they are encoded by the same gene, and remain anchored on the plasma membrane, it seems that the critical functions are performed by alpha-dystroglycan, rendering the beta subunit with functions restricted to supporting its counterpart alpha subunit. This is reflected in the content of the published literature to date; most papers are focused on finding the mechanisms that leads to hypoglycosylated alpha-dystroglycan, a core feature of the "dystroglycanopathies". This author's opinion does not intend to dispute the important role of alpha-dystroglycan, but to highlight the fact that beta-dystroglycan is also an impor-

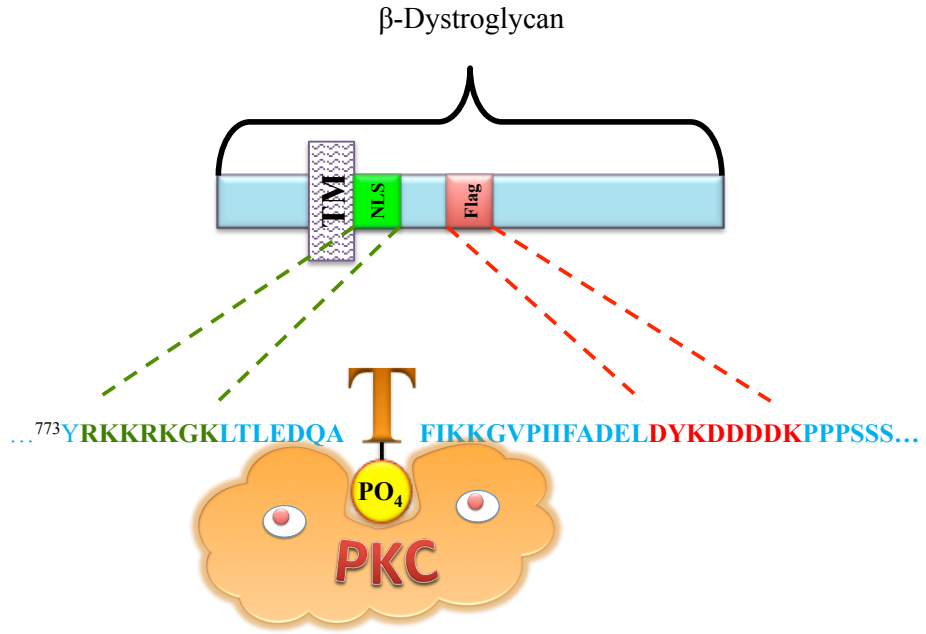

Figure 5.27: Phosphorylation site detected in mouse beta-dystroglycan by mass spectrometry. A schematic of mouse beta-dystroglycan is shown. Highlighted in orange is the relative position of threonine found to be phosphorylated by mass spectrometry. The orange cloud represents PKC phosphorylating T788. The NLS is highlighted in green and the Flag tag in red.

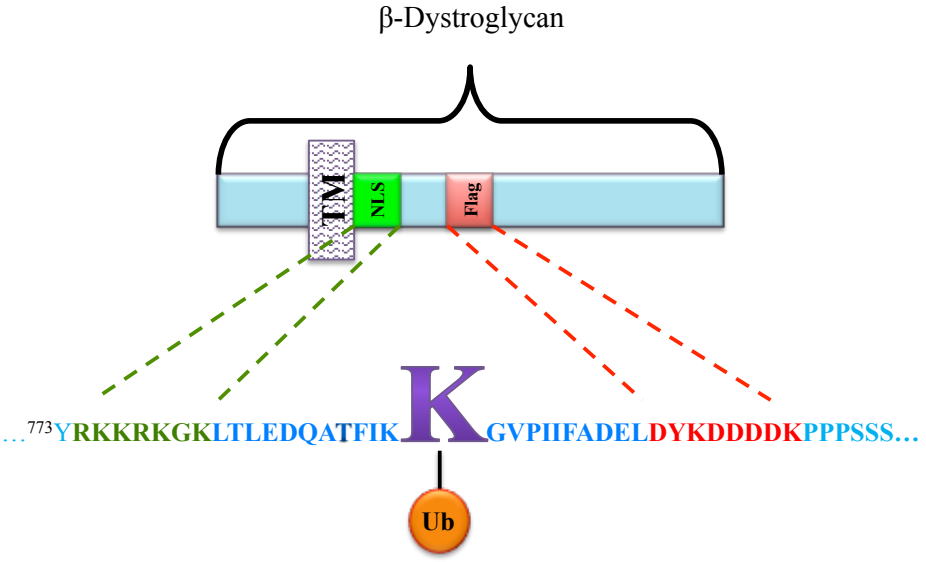

Figure 5.28: Ubiquitination site detected in mouse beta-dystroglycan by mass spectrometry. Ubiquitination site detected in mouse beta-dystroglycan by mass spectrometry. A schematic of mouse beta-dystroglycan is shown. Highlighted in purple is the relative position of lysine found to be ubiquitinated by mass spectrometry. The NLS is highlighted in green and the Flag tag in red.

tant player in the integrity of the dystroglycan complex and that its functions are far beyond a passive protein. This is based on the set of pathways presented above and the discussion below.

5.6.1 The multiple functions of beta-dystroglycan in the plasma membrane and vesicular trafficking

The hydrophobic amino acids found in the transmembrane domain render beta-dystroglycan with the capacity to be inserted in membranous environments. This means that beta-dystroglycan is typically found in two contexts: 1) most of the organelles surrounded by membranes, contain beta-dystroglycan and, 2) every physiological process involving membranes will always implicate, to some extent, beta-dystroglycan. These ideas are represented in pathways such as those related to adherens junctions, focal adhesions, endocytosis, phagosomes, etc. Although an exquisite topic of discussion, pathways in Figures 5.12-5.16 and F.1-F.5, will be further analysed in the discussion section to this thesis.

5.6.2 The Alzheimer's disease and WNT pathways, the missing link in the role of nuclear beta-dystroglycan?

Despite the relatively low peptide count, nicastrin, the adaptor subunit of the gamma-secretase complex (Shah et al., 2005), was identified by mass spectrometry analysis as an interacting protein with Flag-tagged beta-dystroglycan (NCSTN in Figure 5.17, "not highlighted in red"). This subunit, together with presenilin, APH1 and PEN2, is an essential component of the gamma-secretase complex (Hansson et al., 2004). Gamma-secretase cleaves the amyloid precursor protein (APP) in Alzheimer's disease, Notch, EpCAM, CD44 and a myriad of other substrates in order to release active cytoplasmic fragments (De Strooper et al., 1998, 1999; Lammich et al., 2002; Maetzel et al., 2009; Murakami et al., 2003). With the evidence gathered from previous DAPT experiments performed in this thesis (section 4.3.1), and the finding of

nicastrin interacting with beta-dystroglycan, further corroborates that beta-dystroglycan is subject to regulated intramembrane proteolysis mediated by gamma-secretase.

Liberated fragments by RIP are able to perform different biological functions, such as transcriptional regulation (Kopan & Ilagan, 2004), before they are subject to proteasomal degradation. From section 4.4.2, it was shown that the cytoplasmic fragment of beta-dystroglycan has a predominantly nuclear localisation. Furthermore, Mathew and colleagues have shown that beta-dystroglycan translocates to the nucleus in an androgen receptor (AR) dependent manner, and that its cytoplasmic fragment is able to modulate the transcription of several genes, including the ETV1 transcription factor (Mathew et al., 2013). However, based on *in silico* analysis, motifs that allow a DNA interaction have not been clearly identified, with the exception of the BindN algorithm (`http://bioinfo.ggc.org/bindn/`) which clearly states that the NLS in beta-dystroglycan could be a potential DNA binding motif. Nonetheless, no further evidence stands to support this assumption and is therefore likely to be indirect.

If the cytoplasmic fragment of beta-dystroglycan accumulates in the nucleus (either, translocated from the cytoplasm to the nucleus or generated in the nucleus as a a consequence of the cleavage of nuclear full-length beta-dystroglycan) to exert a nuclear (gene) regulation, what is then the mechanism(s) by which this very dynamic fragment orchestrates this new function?

The transmembrane epithelial cell adhesion molecule (EpCAM) is susceptible to RIP, which releases a cytoplasmic fragment that is able to form a complex with beta-catenin and the four and a half LIM domains protein 2 (FHL2), regulating the expression of target genes such as c-myc (Maetzel et al., 2009). From the interactome analysis, the two main proteins significantly enriched were members of the WNT pathway, catenins (alpha and beta) and cadherin-1 (Figures F.1, 5.12 and 5.18). Then the possibility of a signalling mechanism similar to that observed in EpCAM could be plausible.

In high grade prostate cancer, E-cadherin protein levels have been found

to be reduced or absent (Morton, Ewing, Nagafuchi, Tsukita, & Isaacs, 1993; Umbas et al., 1992), a process that clearly mirrors the reduction of full-length beta-dystroglycan in the same disease (Henry et al., 2001; Hetzl, Fávaro, Billis, Ferreira, & Cagnon, 2012; Losasso et al., 2000; Mathew et al., 2013). Thus, the reduction of these two membrane receptors could cause the release of anchored beta-catenin (Kypta & Waxman, 2012) and the increase in the concentration of the cytoplasmic fragment of beta-dystroglycan, which in turn are able to form a complex with FHL2. However, this does not explain the concomitant translocation of beta-dystroglycan following androgen receptor stimulation, nor the mechanism by which this dual translocation regulates the gene expression of ETV1.

AR is able to interact with beta catenin and promote its nuclear translocation (Mulholland, Cheng, Reid, Rennie, & Nelson, 2002; Truica, Byers, & Gelmann, 2000). It has also been shown that, upon ligand stimulation, AR binds the promoter region of ETV1, stimulating its gene expression (Cai et al., 2007). It is therefore likely that such interactions exist among the cytoplasmic fragment of beta-dystroglycan, beta-catenin and the androgen receptor. In this scenario, beta-catenin associated with FHL2 (Wei et al., 2003) serves as a docking protein for the cytoplasmic fragment of beta-dystroglycan. Subsequently, the cytoplasmic fragment enables, together with AR, the nuclear translocation of beta-catenin. In the nucleus, by means of the AR, this complex is able to bind to the TCF/LEF family of co-transcription factors (Behrens et al., 1996; Molenaar et al., 1996), and then to the promoter region of ETV1. However, experiments performed by Chesire and colleagues have shown that the AR competes with the TCF co-transcription factor for its binding to beta-catenin (Chesire & Isaacs, 2002). As a result, external signals may favour the formation of one or another complex. Hence, the interaction of beta-dystroglycan with the complex containing AR and beta-catenin may modulate the interplay between the two pathways (Kypta & Waxman, 2012). Along with the stimulation of ETV1 transcription factor synthesis, this mechanism is a question that clearly requires further research in order to understand the role of beta-

dystroglycan in prostate cancer and other related cancers (Figures 5.23-5.24, and (Cai et al., 2007)).

5.6.3 Beta-dystroglycan, a new player in DNA replication and the cell cycle?

The ability to interact with multiple proteins confers important roles on beta-dystroglycan. From the interactome screening analysis, proteins associated with DNA replication (Figure 5.19), the spliceosome (Figure 5.20), RNA transport (Figure 5.21) and the cell cycle (Figure 5.22) were found immunoprecipitating with Flag-tagged beta-dystroglycan.

A possible function of beta-dystroglycan in the cell cycle has been suggested; however, the mechanisms behind this idea remain unknown. In this regard, the knockdown of dystroglycan led to a delay in S-phase and to an increase in the number of apoptotic cells in Swiss 3T3 cells (Higginson et al., 2008) and HC11 mouse mammary epithelial cells (Sgambato, Di Salvatore, et al., 2006). Importantly, increased protein levels of beta-dystroglycan during the S-phase of the cell cycle have also been observed (Hosokawa et al., 2002; Sgambato, Di Salvatore, et al., 2006).

Of the proteins involved in both DNA replication and the cell cycle, the mini-chromosome maintenance complex (MCM) (MCM2, 4, 5 and 7) and the structural maintenance of chromosome (Smc) (Smc1 and 3) proteins were found to associate with Flag-tagged beta-dystroglycan.

The MCM DNA helicase complex, is a group of proteins implicated in DNA replication. The proteins MCM2-7 are helicases able to interact with each other and, together with other proteins, are recruited in a pre-replicative complex to the initial stages of DNA synthesis, and persist throughout S-phase. The components of this complex, which are assembled during the M-G1 transition phase, are degraded once DNA replication is completed (Aladjem, 2007; Bell & Dutta, 2002; Maiorano, Lutzmann, & Méchali, 2006).

A previous report demonstrated the association of beta-dystroglycan with components of different nuclear compartments; however, an association between beta-dystroglycan and active replication sites was not observed (Martínez-Vieyra et al., 2013). This is in opposition to the interaction of the MCM complex with Flag-tagged beta-dystroglycan observed in the interactome analysis reported in this thesis (Figure 5.19). A possible explanation for this difference could be that beta-dystroglycan associates with the MCM complex during the pre-replication and pre-initiation stages of DNA replication, and then leaves this complex once S-phase proceeds (active DNA synthesis). In favour of this, it has been suggested that during the early stages of S-phase DNA replication is organized in 5-20 foci, and then, as S-phase proceeds, these initiating foci are dispersed in to hundreds of foci throughout the nucleus (Kennedy, Barbie, Classon, Dyson, & Harlow, 2000), a phenotype that is similar to that reported by Martínez and colleagues (Martínez-Vieyra et al., 2013). Focal replication sites co-localize with nuclear lamin A/C structures at early stages of DNA synthesis (Kennedy et al., 2000; Shumaker, Kuczmarski, & Goldman, 2003). Given the reported interaction of beta-dystroglycan with lamin A/C (Martínez-Vieyra et al., 2013), it will be interesting to investigate the presence of this complex (replication foci, Lamin A/C and beta-dystroglycan) during early stages of the S-phase of the cell cycle, as means to establish a role of beta-dystroglycan in DNA replication. This would also explain other reported observations:

1. The increased expression of beta-dystroglycan during the S-phase of the cell cycle and,

2. The delay in the S-phase of cells when dystroglycan levels are reduced.

If increased levels of beta-dystroglycan are required in order to assemble the pre-replication complex and its disruption can be a triggering factor to stop progression into S-phase. Further research aimed to investigate the association of beta-dystroglycan with the MCM complex and their involvement in early stages of the S-phase will provide support to this hypothesis.

Another protein identified as interacting with Flag-tagged beta-dystroglycan was the transcription factor STAT1. Because of its interaction with RNA polymerase II and STAT1, the MCM complex has been ascribed functions related to transcription (Forsburg, 2004; Snyder, He, & Zhang, 2005). This further supports a possible role of beta-dystroglycan in DNA replication and transcription; however, the way in which beta-dystroglycan modulates these two processes and the biological relevance remain unknown.

In light of these findings as a whole, it is clear then that if beta-dystroglycan modulates nuclear processes, such as those related to DNA or RNA, it is not through a direct interaction with nucleic acids, but through an indirect association with adaptor proteins as mentioned above and discussed below.

Proteins involved with the spliceosome complex (Figure 5.20) and RNA transport (Figure 5.21) were also immunoprecipitated with beta-dystroglycan. The existence of these new interactions can be indirectly supported by a previous study reporting the association of beta-dystroglycan with nuclear bodies such as the nucleolus, splicing speckles and Cajal bodies (Martínez-Vieyra et al., 2013).

Each one of these nuclear bodies is composed of different proteins and develops different functions within the nucleus: the nucleolus, composed of ribosome assembly factors, gives rise to the ribosome complex; the nuclear speckles, a complex of pre-mRNA splicing factors, performs the storage and recycling of splicing factors; and the Cajal bodies, of which the main components are coilin and the SMN protein, allow the biogenesis, maturation and recycling of small RNAs (Dundr & Misteli, 2010; Zimber, Nguyen, & Gespach, 2004).

This is really intriguing because the hypothesis stated in this thesis is that beta-dystroglycan, as a co-transcription factor, regulates the transcription of genes involved in cancer progression. However, the interaction with components of the spliceosome suggests nuclear activities beyond gene transcription.

There may be different mechanisms by which beta-dystroglycan could be coupled to the spliceosome machinery and subsequent events until the RNA is

exported to the cytoplasm for its translation. Such mechanisms could involve:

1. Beta dystroglycan functions as a co-transcriptional factor.

2. Beta-dystroglycan modulates actin bridges, hence the positioning of nuclear bodies. The transcriptional activities of actin modulated by its monomeric form are well known (Miralles, Posern, Zaromytidou, & Treisman, 2003). However, the possibility of a polymeric form of nuclear actin (de Lanerolle & Serebryannyy, 2011; Pederson, 2008) has lead to the suggestion of other actin-dependent regulation of gene and nuclear body positioning (Dundr et al., 2007; Visa & Percipalle, 2010). In this scenario, by means of its interaction with nuclear bodies, soluble beta-dystroglycan recruits polymeric actin (Y. J. Chen et al., 2003), which in turn position the DNA sequence to be transcribed.

3. Beta-dystroglycan acts as a scaffolding protein that modulates the transport of nuclear bodies to the target DNA sequences ready to be transcribed. In this regard, it has been shown that the internal nuclear lamina is able to associate and regulate the positioning of the nuclear bodies (Legartová et al., 2014; Shumaker et al., 2003). Additionally, it is known that beta-dystroglycan and other components of the DAPC associate with Lamin A/C, lamin B and Emerin (Fuentes-Mera et al., 2006; Martínez-Vieyra et al., 2013). Thus it is tempting to speculate that beta-dystroglycan, together with the lamins, provides a framework to modulate the location of nuclear bodies.

The idea of an association of beta-dystroglycan with the spliceosome machinery is indeed exciting; however, it has to be shown first that beta-dystroglycan associates with this machinery before the theory can be tested.

Whatever the function of beta-dystroglycan is in the spliceosome complex, if any, it seems that it has to remain anchored to the nascent RNA until it is completely exported, as it is known that the spliceosome machinery is coupled to the RNA export steps (Luo et al., 2001). It is interesting to highlight that

beta-dystroglycan is able to interact with some components of the exportin system such as CRM1 and exportin T. The presence of an NLS within the primary structure of beta-dystroglycan has been well documented (Lara-Chacón et al., 2010; Oppizzi et al., 2008), yet, no DNA binding domains or an NES have been reported so far. A quick *in silico* analysis confirms the lack of NES in beta-dystroglycan; nonetheless, 4 leucines located in the second cadherin like-domain of alpha-dystroglycan may have a potential role as a nuclear export signal (`http://www.cbs.dtu.dk/services/NetNES/`). If this were true, then it could imply that full dystroglycan (alpha and beta) is another mechanism for the nuclear export of nascent RNA. Again, how this complex is assembled, and its relevance within biological systems, is something that requires further research.

It is hard to believe that a plasma membrane protein such as beta-dystroglycan is able to perform such a multitude of functions. When first characterized by Campbell and colleagues, it was thought that dystroglycan was only confined to the plasma membrane for cell adhesion. However, the distribution of beta-dystroglycan within a great variety of organelles, cell types and species, suggests that there are more functions that await discovery.

Microscopy experiments performed by the Winder and Cisneros groups, have shown that beta-dystroglycan is also localised to the cleavage furrow and midbody during cytokinesis (Higginson et al., 2008; Villarreal-Silva et al., 2011), and current research supports both observations. Importantly, recent research findings support a role for beta-dystroglycan in the cell cycle before the final stages of mitosis (note: the author did not perform any experiments to support the following arguments; however, he was aware of the phenotype that will be described below. Additionally, the following discussion will be based on information and images kindly provided by Laura A. Jacobs in the Winder lab). Also, although no further evidence has been gathered, there seems to be a differential distribution between non-phospho and phospho-beta-dystroglycan throughout the different stages of mitosis as described below.

During prophase phospho-beta-dystroglycan is homogeneously distributed

throughout the cytosol. Then, there is a re-distribution to the edges of condensed chromosomes and, interestingly, a pool remains at the very centre of condensed chromosomes. Later, in metaphase, phospho-beta-dystroglycan is found surrounding the lined up chromosomes along the metaphase plate. The most intriguing finding is that during anaphase, phospho-dystroglycan surrounds the separating chromosomes. During telophase it still surrounds the DNA, although the levels of protein are decreased. Finally, at the end of telophase, it is again homogeneously distributed throughout the cytosol, but a little amount remains associated to the midbody.

On the other hand, during prophase, non phospho-beta-dystroglycan is strongly distributed on the plasma membrane and keeps the same association during pro-metaphase, metaphase, anaphase and telophase. During metaphase and anaphase, non phospho-beta-dystroglycan surrounds the aligned chromosomes; however, its levels are low compared to the phosphorylated counterpart. By the time the cell starts dividing in telophase, normal beta-dystroglycan is still strongly concentrated on the plasma membrane and a another pool starts concentrating along the cleavage furrow. Finally, during cytokinesis, the levels of normal beta-dystroglycan are reduced on the plasma membrane, but is strongly concentrated in the midbody. From the observations above, it would seem that beta-dystroglycan is not only present during late mitosis, but has an important role during the condensation, alignment and separation of chromosomes.

So far, we know that beta-dystroglycan is able to interact with F-actin (Y. J. Chen et al., 2003), and, although not completely confirmed, is also able to bind tubulin in human platelets (Cerecedo, Cisneros, Suárez-Sánchez, Hernández-González, & Galván, 2008). Additionally, it has been reported that dystrophin, a direct interacting protein with beta-dystroglycan, is also able to organize microtubules (Prins et al., 2009). Furthermore, beta-dystroglycan is able to interact with ezrin and modulate fillopodia formation (Batchelor et al., 2007; Spence, Chen, et al., 2004).

F-actin is an important player during all the stages of mitosis: it is re-

distributed and localised to the cell cortex and is maintained until cytokinesis (Field & Lénárt, 2011; Kunda & Baum, 2009). Also, through its interaction with actin-binding proteins and moesin, a member of the ERM (Ezrin, Radixin and Moesin) family of actin binding proteins, F-actin is able to modulate cellular events that drive the correct spindle position, facilitating correct chromosome segregation (Fehon, McClatchey, & Bretscher, 2010; Field & Lénárt, 2011; Kunda & Baum, 2009).

Thus, with the role of F-actin and moesin proteins in mitosis, and the confirmed interaction between beta-dystroglycan and F-actin, or beta-dystroglycan and ezrin, it is tempting to formulate a possible explanation for the phenotype observed for beta-dystroglycan. During interphase, a pool of beta-dystroglycan interacts with F-actin leading to a direct regulation of the cytoskeleton (Figure 5.15). Once the cell enters mitosis, beta-dystroglycan is still embedded in the plasma membrane and displays a high affinity for activated ERM proteins which in turn bind F-actin. This results in increased cell stiffness in the rounded cell, which consequently controls the correct positioning of the mitotic spindle. During the separation of the two daughter cells, beta dystroglycan is re-located to the midbody in cytokinesis. In support of this, Notch, whose signalling pathway was believed to be activated after mitosis, has been recently shown to display functions before cell division in neuronal precursor cells (K. M. Bhat, 2014; Pinto-Teixeira & Desplan, 2014). Then, it is possible that, in addition to its anchoring activities, beta-dystroglycan may also be able to modulate signalling events for the proper onset and positioning of the cleavage furrow through its co-transcriptional activities.

This hypothesis fits well with non-phospho-beta-dystroglycan, although the scenario with its phosphorylated counterpart seems to be rather different.

From the mass spectrometry analysis, the structural maintenance of chromosomes (SMC) proteins, Smc1 (significantly enriched) and Smc3 (found in two replicate Flag immunoprecipitations), which are core components of the cohesin complex, and NCAPD2 (found in two replicate Flag experiments), the regulatory subunit of the condensin complex, were found in Flag immunopre-

cipitations (Figure 5.22).

The structural maintenace of chromosome complex includes members of the cohesin, condensin and Smc5/6 complexes. These complexes play important roles in sister chromatids cohesion, chromosome condensation, DNA replication, DNA repair and transcription. Cohesin's function, is to maintain the two sisters chromatides together, once they are generated in S-phase, until they are separated during anaphase. Apparently, the binding of these complexes to DNA does not require DNA binding domains (Jeppsson, Kanno, Shirahige, & Sjögren, 2014; Losada, 2014). The association of phospho-beta-dystroglycan with cohesin and condensin complexes, and the phenotype above described, suggests that beta-dystroglycan participates during the preparative stages of chromosome condensation until they are completely separated in telophase.

Finally, as mentioned above, another plausible option could be the association of phospho-beta-dystroglycan with microtubules. It may be that phospho-beta-dystroglycan binds to microtubules through its interaction with Smc1. This interaction may then provide a strong support to the suggested interaction of Smc1 to the microtubules (Wong & Blobel, 2008).

These hypotheses fit well with the phenotype above described, however, much work needs to be done in order to develop the protein interactions described here, and importantly, the biological relevance of the participation of beta-dystroglycan throughout the cell cycle.

5.6.4 The ubiquitin-proteasome system and beta-dystroglycan

Dystroglycan, a protein with a multitude of functions throughout its lifespan, at some point has to be terminated. Whether it derives from the plasma membrane, the cytosol, the nuclear membrane or the nucleoplasm, dystroglycan has to be subject to protein turnover by one or a combination of different pathways in charge of protein destruction, such as endoplasmic reticulum associated degradation (ERAD), lysosomes and the ubiquitin proteasome system (Vellai & Takács-Vellai, 2010).

Ubiquitination is a multi-step process initiated by an E1 enzyme that activates ubiquitin, followed by the conjugation of the ubiquitin group to a target substrate by an E2 enzyme, and completed by the ligation of the ubiquitin group to the substrate by an E3 ligase (Hochstrasser, 2009; Lecker, Goldberg, & Mitch, 2006). Each group is composed of different enzymes, but particularly E3, which dictates the specificity of the ubiquitin pathway, comprises approximately 600 enzymes divided in to HECT type, U-box type and RING-finger type ligases (Figure 5.25) (Metzger, Hristova, & Weissman, 2012; Rotin & Kumar, 2009). This PTM can enhance or prevent protein interactions, modulating cellular processes such as transcription, signal transduction, membrane-protein trafficking, endocytosis, DNA repair, and proteasomal binding and degradation (Haglund & Dikic, 2012; Hochstrasser, 2009; Lecker et al., 2006).

Given the multiple functions attributable to ubiquitination, the discussion presented here will focus on the ubiquitin-proteasome pathway; however, this does not imply that the ubiquitination of beta-dystroglycan is purely related to degradation. There may be other pathways where the ubiquitination of dystroglycan (alpha and beta) modulates its interaction with other proteins, its role in the cell cycle, localisation or its nuclear function.

In previous chapters it was shown that beta-dystroglycan is ubiquitinated (Figure 3.21) and subject to proteasomal regulation (Figure 3.19 and 4.11), indicating its potential degradation by the ubiquitin proteasome system. From the mass spectrometry analysis, SAE1, an E1 ubiquitin activating enzyme was found to immunoprecipitate with Flag-tagged beta-dystroglycan; however, it was found in only two replicate experiments. Additionally, NEDD4L (also known as NEDD4-2) and ARF-BP1 (also known as HUWE1), members of the HECT type E3 ligases, were highly enriched in Flag IPs. Although there were other protein candidates, they were in the group of significantly enriched proteins with a low peptide count (UBE3C, HERC1), or proteins that were found in only two replicate experiments, interacting specifically with Flag-tagged beta-dystroglycan (PIAS and UBE4B) (Figures 5.6, 5.7, 5.25). Furthermore, other candidate proteins were components of the proteasome. The components

enriched are mainly members of the 19S regulatory particle (lid and base) and only one component of the core regulatory particle was found (Figure 5.26). This all confirms that, in LNCaP cells, the ubiquitin proteasome system may be a pathway in charge of the rapid turnover of beta-dystroglycan.

Dystroglycan (alpha and beta) contains a multitude of lysines in its primary structure that have been predicted to be subject to ubiquitination (`http://www.phosphosite.org`); however, regardless of the potential implication that the ubiquitin proteasome system plays in Duchenne and Becker muscular dystrophies (Bonuccelli et al., 2007; Gazzerro et al., 2010; Winder, Lipscomb, Angela Parkin, & Juusola, 2011) and in cancer (Acharyya et al., 2005; Acharyya & Guttridge, 2007), there are no published studies aimed at understanding the role that ubiquitination and ubiquitin enzymes play in the stability of dystroglycan.

The interaction of SAE1, an E1 ubiquitin activating enzyme, with Flag-tagged beta-dystroglycan could be plausible as there are only two E1 enzymes in charge of activating ubiquitin groups; however, more research will be required to confirm this finding.

The cytoplasmic fragment of beta-dystroglycan has at least two identifiable PY motifs (`http://elm.eu.org`), which could be the motifs interacting with the WW domain in NEDD4L in a similar way to that reported for the epithelial sodium channel (Staub et al., 1996). A recent study suggested that a phosphorylated tyrosine located in a PY motif in the very carboxy-terminus of beta-dystroglycan could be an important signal triggering its proteasomal degradation (Miller et al., 2012), further supporting the interaction of beta-dystroglycan with NEDD4L. However, Pirozzi and colleagues showed that the phosphorylation of a tyrosine within the PY motif prevented its interaction with the WW domain (Pirozzi et al., 1997) and later reported, although not in the context of tyrosine, that the binding of NEDD4L to SMAD7 is not dependent on the phosphorylation of the PY motif (Aragón et al., 2012) which is in contrast to the interaction observed with SMAD3 (Gao et al., 2009). Therefore, it will be important to determine to what extent the phosphorylation of

Y890 in beta-dystroglycan modulates its putative interaction with NEDD4L or HUWE1.

The identification of NEDD4L and ARF-BP1 as potential ubiquitin ligases interacting with beta-dystroglycan leads the author to speculate that they are responsible for the rapid turnover of beta-dystroglycan in cancers where its expression has been shown to be reduced. In this regard, NEDD4L has been ascribed functions such as endocytosis and sorting of transmembrane proteins, whilst ARF-BP1 is associated with neuronal differentiation (by destabilizing N-myc), and the regulation of p53 and Mcl-1 (Rotin & Kumar, 2009). More research will be required in order to understand how these E3 ligases regulate the internalisation, turnover or other cellular events of beta-dystroglycan.

Dystroglycan is a protein that is broadly present in different organelles within the cell (plasma membrane, ER, nucleus), among different tissues (muscle, prostate, brain, breast, etc.), and among different species. Therefore it may be expected that more than one ubiquitin ligase targets dystroglycan for degradation, as dictated by the organelle, cell type and the species. In this regard, it was previously reported by Lee and colleagues that HRD1, a transmembrane RING E3 ubiquitin ligase resident in the endoplasmic reticulum, the main function of which is to degrade misfolded or aberrant proteins (Bays, Gardner, Seelig, Joazeiro, & Hampton, 2001), targets beta-dystroglycan for ubiquitination (K. A. Lee et al., 2011). Another study provided evidence that beta-dystroglycan is able to bind to WWP1 and WWP2 (Pirozzi et al., 1997), and later, although not strictly linked, another study postulated WWP1 as the causative ubiquitin ligase of muscular dystrophy in chickens (Matsumoto et al., 2008). Furthermore, the ubiquitin ligases MAFbx and MuRF1 were correlated to muscle atrophy (Bodine et al., 2001). This all indicates that the ubiquitination of beta-dystroglycan may be mediated by different ubiquitin ligases which may be determined by the cellular context; in the case of prostate cancer ubiquitination is possibly mediated by HUWE1 and NEDD4L.

Further in-depth analysis will be required to show whether the ubiquitination of dystroglycan by NEDD4L and ARF-BP1 has a role in its stability; regu-

lating in this way the amount of dystroglycan on the plasma membrane, which in turn could lead to cancer progression (perhaps potentiating other related processes such as those performed by MMPs). Additionally, having explained the potential role of the co-transcriptional activity of the cytoplasmic fragment of beta-dystroglycan, it will be required to investigate whether NEDD4L and ARF-BP1 have a function regulating post-co-transcriptional events of this fragment.

The mass spectrometry screening performed in this thesis identified K794 in human (K792 in mouse) as a lysine that could potentially be modified by ubiquitination (Figure 5.28). The potential ubiquitination of this lysine was already reported in large-scale mass spectrometry analyses aided to describe ubiquitinated sites in murine tissues (Wagner et al., 2012) and the human ubiquitinome (W. Kim et al., 2011). However, the role that this modified lysine has in the different pathways wherein beta-dystroglycan is implicated, and its relationship with the NEDD4L and ARF-BP1 ligases, is yet to be determined.

The identification of phosphorylated T788 in beta-dystroglycan is intriguing. It may be that its presence modulates the interaction of beta-dystroglycan with the importin complex, as it is located in the middle of the bi-partite NLS. Additionally, it could be possible that this phosphorylated amino acid regulates other PTMs, such as ubiquitination or sumoylation, as it is just three amino acids away from the identified ubiquitinated lysine in this thesis. Furthermore, its location near the plasma membrane could regulate the proteolytic events mediated by Furin and gamma-secretase in beta-dystroglycan described earlier in this thesis.

In the work presented in this thesis a Flag-tagged beta-dystroglycan immunoprecipitation strategy was used to identify possible interacting partners. Interestingly, this strategy did not detect the common components of the DAPC or non-muscle counterparts, such as utrophin, or the beta-syntrophins. The following reasons, although not demonstrated, could explain why this was the case.

It could be that the DAPC members were at a low concentrations compared with the immunoprecipitated proteins, so that they were masked by the most abundant proteins. In this regard, utrophin, a dystrophin homologue and core component of the DAPC in epithelial cells (Nguyen, Le, Blake, Davies, & Morris, 1992), was found at low levels in the mass spectrometry approach. Another possible explanation could be that, due to the conditions used in the immunoprecipitation, other proteins presented a stronger interaction with beta-dystroglycan than the typical DAPC members.

5.6.5 Summary

Through the results and analysis provided in this chapter it can be concluded that:

1. Beta-dystroglycan may be implicated in RNA processing and transport.
2. Beta-dystroglycan may have roles during the S-phase of the cell cycle by modulating DNA replication events.
3. Beta-dystroglycan may perform functional roles from the start of mitosis until the completion of cytokinesis.
4. RIP in beta-dystroglycan may be mediated by the gamma-secretase complex.
5. Beta-dystroglycan may have co-transcriptional properties in partnership with components of the WNT pathway.
6. Beta-dystroglycan is phosphorylated on T788 and ubiquitinated on K792.
7. Beta-dystroglycan is subject to protein turnover by the ubiquitin-proteasome system.

6 Discussion, conclusions and future work

6.1 Discussion

Dystroglycan is a protein subject to several post-translational modifications. These PTMs are important in order to regulate its interaction with other proteins, to control its targeting to different cellular compartments and for its degradation. Therefore, the combination of post-translational modifications with the cellular distribution, confer dystroglycan with properties to regulate different cellular processes.

The data described in this thesis further confirmed that beta-dystroglycan is subject to extensive phosphorylation and ubiquitination. Importantly, it was observed that other post-translational modifications, such as RIP, are also involved in the functionality of beta-dystroglycan. Furthermore, a dystroglycan interactome analysis showed that it may be possible that the interactions of beta-dystroglycan with other proteins extend far beyond those already reported. The main goal in this interactome analysis was to identify co-factors and other proteins that could provide clues about the role of beta-dystroglycan in the nucleus of LNCaP cells. It was exciting to find that, in addition to some potential nuclear candidates, there are other proteins that, together with beta-dystroglycan, may be modulating cellular functions outside of the nucleus. There is still a lot of work that needs to be done in order to understand those potential interactions and the questions that they raise.

This project centred around triggering events on the plasma membrane

that could provide us with a logic explanation for how beta-dystroglycan is transported to the nucleus. For this reason, the project was divided into three main sections:

- Post-translational modifications affecting the integrity of beta-dystroglycan.
- Mechanisms leading to the proteolysis and nuclear translocation of beta-dystroglycan.
- Protein interactions that could explain the function(s) of beta-dystroglycan in the nucleus.

6.1.1 Post-translational modifications of beta-dystroglycan

From data presented in chapter 3 it is clear that beta-dystroglycan may be subject to extensive phosphorylation and ubiquitination. The accumulation of the cytoplasmic fragment of beta-dystroglycan in the nucleus led us to initially propose that it has nuclear functions followed, by its ubiquitination, and then degradation by the nuclear proteasome. Ubiquitination is a post-translational modification that can have two different outcomes. The first is as an additional modification involved in cell cycle, trafficking and nuclear functions. The second one is to flag proteins for degradation by the proteasome (Hochstrasser, 2009; Komander, 2009).

In the first case, this modification could regulate the possible transport and interactions of beta-dystroglycan with other nuclear proteins. Additionally, modification with ubiquitin groups could lead to conformational changes in the highly disordered cytoplasmic fragment of beta-dystroglycan that could cause its activation (see below for discussion) or inactivation. The modifications of beta-dystroglycan in the second scenario represent the final stage of regulation of nuclear beta-dystroglycan. In this regard, once beta-dystroglycan has exerted its functions (whatever they are), the cell does not invest any unnecessary energy by transporting beta-dystroglycan back to the cytoplasm.

Although both are plausible ideas, further research is required in order to identify any other amino acids subject to ubiquitination, how this modification affects the transport of beta-dystroglycan, and if beta-dystroglycan is indeed degraded in the nucleus, or transported back to the cytoplasm.

The nuclear localisation signal of beta-dystroglycan is rich in lysine and arginine amino acids and is strategically located within the sequence contained in the cytoplasmic fragment. Interestingly, the lysine that is shown to be subject to ubiquitination in this project is located in the second stretch of amino acids that belong to the NLS. Thus, it will need to be determined if other lysines within the NLS are modified by ubiquitination (mono or poly) and to what extent this modification affects protein interactions, nuclear transport and the degradation of beta-dystroglycan. This could have several implications as it is also known that this particular motif mediates the interaction with the ERM proteins, rapsyn and ERK, and members of the importin system (see section 1.5.5).

The reason why these questions have to be answered comes from the idea that proteins are regulated differentially depending on whether the modification is mono- or poly-ubiquitination and what type of linkage is involved. Poly-ubiquitinated proteins are usually targeted for proteasomal degradation, whilst mono-ubiquitination serves to target proteins for nuclear transport. In this regard, a similar mechanism has been observed in the enzyme cytidylyltransferase, the enzyme that catalyses the synthesis of the phospholipid phosphatidylcholine. Its transport mediated by the importin system is disrupted by the masking of its nuclear localisation signal by mono-ubiquitination once this enzyme is targeted for lysosomal degradation (B. B. Chen & Mallampalli, 2009).

Additionally, an interesting paper has shown that PTEN (Phosphatase and TENsin homologue) is differentially regulated depending on the type of ubiquitination on its structure. This phosphatase usually antagonises the effects of phosphatidylinositol-3-kinase (PI3K) by converting phosphatidylinositol 3,4,5 phosphate (PIP_3) to phosphatidylinositol 4,5 phosphate (PIP_2) on the

plasma membrane. The subsequent reports of its nuclear localisation led to important discoveries. It was observed that poly-ubiquitination by NEDD4L (NEDD4-1) targeted PTEN to proteasomal degradation. However, the mono-ubiquitination by the same enzyme favoured its nuclear localisation. Additionally, it was suggested that PTEN may had been subject to further deubiquitination to perform its nuclear functions that maintain chromosome integrity (Baker, 2007; Trotman et al., 2007). The opposite regulation by the same PTM has been reported for p53. Mono-ubiquitination of p53 exposes its nuclear export signal, allowing further modification with SUMO groups which in turn enhance nuclear export. The addition of poly-ubiquitin groups retains p53 in the nucleus with its consequent proteasomal degradation (Carter, Bischof, Dejean, & Vousden, 2007).

The cytoplasmic fragment of beta-dystroglycan has other motifs, which combined with ubiquitination, could provide other mechanisms of regulation. A closer view of the primary structure of dystroglycan revealed other interesting regulatory elements within its primary structure. It has five PEST motifs distributed throughout alpha- and beta-dystroglycans (2 in alpha and 3 in beta). These motifs have a low hydrophobicity index indicating that they are exposed and may mediate protein-protein interactions (`http://emboss.bioinformatics.nl/cgi-bin/emboss/epestfind`) (Figure 6.1). The PEST motifs are short sequences of proline (P), aspartic acid (E), serine (S) and threonine (T) residues. These motifs are usually surrounded by lysine (K), arginine (R) or histidine (H) amino acids and are approximately 12 amino acids long. An important characteristic of proteins that have these motifs is that they are, apparently, rapidly and efficiently degraded by the proteasome. It has also been suggested that the presence of additional modifications, such as phosphorylation and changes in the overall conformation of the substrates, increase the turnover of proteins targeted for proteasomal degradation(García-Alai et al., 2006; Rechsteiner & Rogers, 1996).

The presence of these PEST motifs could be the point of convergence between the extensive phosphorylation and ubiquitination present in beta-

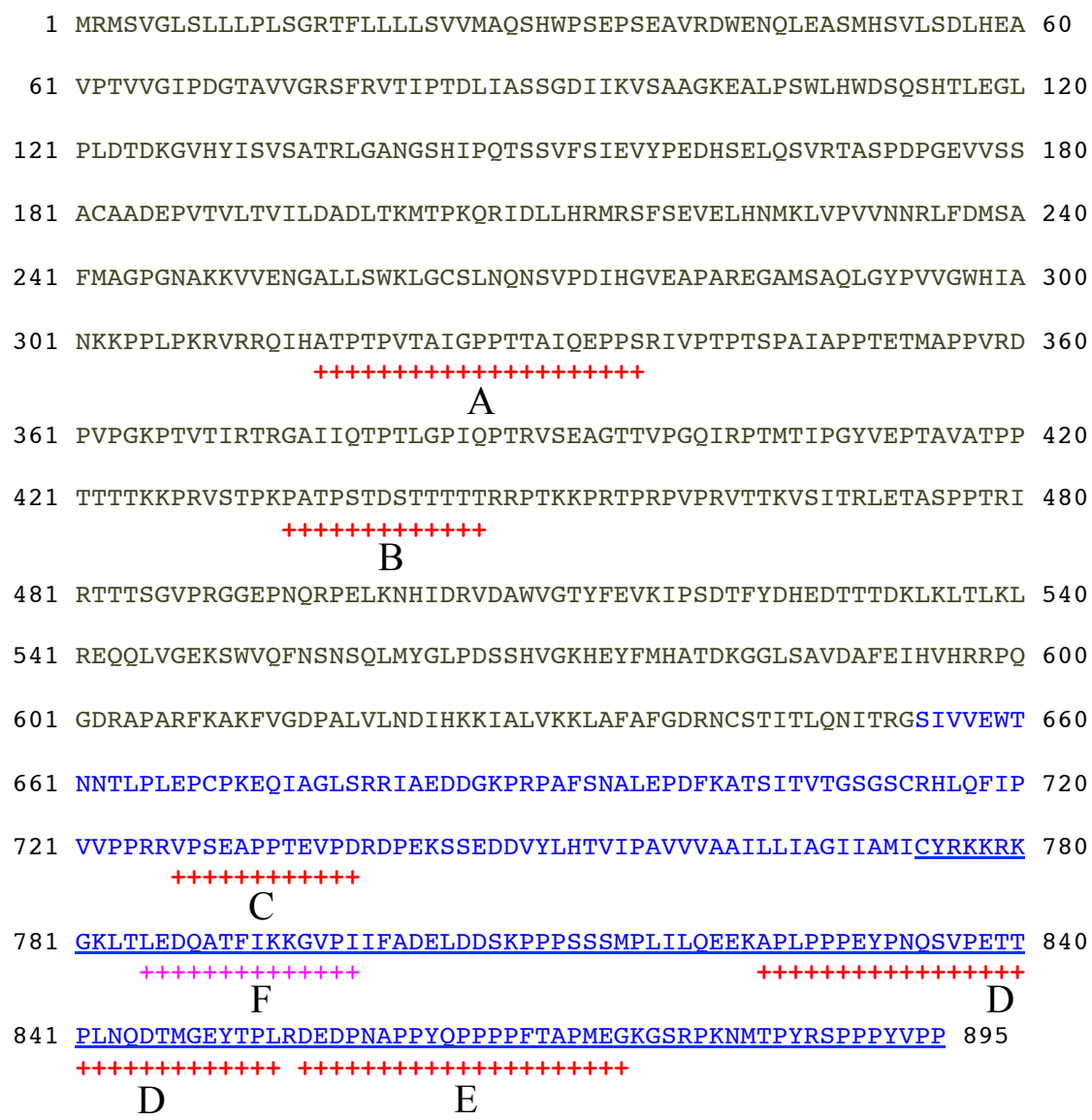

Figure 6.1: Dystroglycan has different potential PEST motifs. The PEST motifs are characterised by short stretches of proline (P), aspartic acid (E), serine (S) and threonine (T) amino acids surrounded by basic residues. Alpha- (dark green) and beta-dystroglycan (blue) have two (A and B) and three (C, D and E) potential PEST motifs (red crosses) respectively. The motif identified by Piggot is highlighted in pink crosses (F) (Piggott, 2014), and the amino acids that belong to the cytoplasmic fragment of beta-dystroglycan are underlined.

dystroglycan. Apparently, the deletion of a PEST motif in human NANOG, a gene that regulates pluripotency of embryonic stem cells, decreased its ubiquitination and extended its half life (Ramakrishna et al., 2011). Furthermore, the phosphorylation of two key serines within a PEST sequence in the vascular endothelial growth factor receptor 2 is important in modulating its ubiquiti-

nation and consequent degradation by the proteasome (Meyer et al., 2011).

Thus, these PEST motifs could correspond to the minimal sequences, the definition of "degrons" (Ravid & Hochstrasser, 2008), that are recognised by the NEDD4L and HUWE1 E3 ligases in order to target beta-dystroglycan for degradation. A speculative idea is that the hydrophilic PEST motifs mediate the interaction of beta-dystroglycan with both ligases, which in turn are able to ubiquitinate adjacent lysines.

Although the idea looks feasible, it seems that this putative interaction is more complicated in reality. In agreement with this thesis, a previous report showed that phosphorylated beta-dystroglycan was subjected to ubiquitination (Piggott, 2014). *In vitro* experiments aimed to identify the E3 ubiquitin ligase responsible for this PTM suggested that the WW1 and WW2 domains of NEDD4L interacted with the LEDQATFIKKGVPI peptide sequence of beta-dystroglycan (see region F in Figure 6.1). However, further *in vivo* characterisation by immunoprecipitation assays was not able to identify any interaction between NEDD4L and beta-dystroglycan in H2K myoblasts (Piggott, 2014). This is contrary to the mass spectrometry results obtained in chapter 5, where NEDD4L was identified as one of the putative ubiquitin ligases interacting with beta-dystroglycan. Because of the characteristics of the sequence previously identified by Piggott, it can be argued that the interaction between NEDD4L and beta-dystroglycan was not detected, because two internal lysines are part of the second stretch of amino acids that conform the nuclear localisation signal in beta-dystroglycan. Thus, it can be speculated that the competitive binding of these amino acids to the importin alpha/beta complex, avoided the subsequent interaction with NEDD4L in the pull-down experiment.

Furthermore, a pull-down assay using the recombinant cytoplasmic fragment of beta-dystroglycan in an importin free system, did not show any binding to the WW1 and WW2 motifs of NEDD4L (Piggott, 2014), indicating that the hypothesis of a possible competition with importins is not feasible. However it is also possible that despite the presence of WW interaction motif in dystroglycan and four WW domains in NEDD4L, that NEDD4L does not in-

teract with beta-dystroglycan via a WW domain interaction. As discussed in chapter 5, it may be that the type of ligases implicated in the ubiquitination of beta-dystroglycan depend on the cellular type. The interaction of NEDD4L with beta-dystroglycan, detected by mass spectrometry analysis in this thesis, has also been observed in other *in vitro* systems (Steve Winder personal communication, and (Piggott, 2014)). Although the interaction between NEDD4L and beta-dystroglycan still has to be confirmed in LNCaP cells, the evidence above suggests a possible indirect interaction.

Investigating the possibility that NEDD4L and HUWE1 are the ubiquitin ligases of beta-dystroglycan is important, because the activity of these ligases could be modulated in order to prevent the pathological loss of beta-dystroglycan from the plasma membrane in certain diseases. Previous studies have used the inhibition of the proteasome as a strategy to restore components of the DAPC to the plasma membrane. However, this strategy has been criticized by the fact that the abolishing of the proteasome activity affects the turnover of proteins that have to be normally degraded by this pathway: it is not "substrate specific", or it fails to improve the dystrophic phenotype of the *mdx* mice (Perkins & Davies, 2012; Selsby, Morris, Morris, & Sweeney, 2012). Therefore, the option of inhibiting these E3 ubiquitin ligases would be a more specific means of preventing the ubiquitination of beta-dystroglycan. In this regard, it is interesting to note that in colorectal cancer the levels of NEDD4L were found to be downregulated at the mRNA and protein levels (Tanksley, Chen, & Coffey, 2013). In prostate cancer, on the other hand, there seemed to be no definite correlation as two independent groups have found increased (Hellwinkel et al., 2011) and also reduced (Hu, Xu, Fu, Yu, & Huang, 2009) levels of NEDD4L.

More research is required in order to determine the way in which the above E3 ubiquitin ligases and beta-dystroglycan interact, either by means of the sequence identified by Piggott or the PEST motifs proposed here. Also, it will be necessary to investigate the role of pY890 and the role of pT788 (which is situated in the middle of the binding sequence identified by Piggott) in this

interaction. These investigations will help develop our understanding of how ubiquitination controls the stability of beta-dystroglycan.

6.1.2 Regulated intramembrane proteolysis of beta-dystroglycan

The results provided in this thesis add more evidence to the modification of beta-dystroglycan by regulated intramembrane proteolysis that occurs by a series of events initiated in the extracellular environment. By combining previous reports with the information gathered in this thesis, a general mechanism of the events initiated on the plasma membrane leading to RIP can be postulated as follows. High cell density and PDBu stimulation are two potential factors that may initiate downstream proteolytic events in beta-dystroglycan. The apparent hypo-glycosylation of alpha-dystroglycan because of decreased expression on LARGE2 and β3GnT1 (Bao et al., 2009; Esser et al., 2013) renders a "naked" protein that is susceptible to a first cleavage by furin (Singh et al., 2004). These events are followed by further proteolytic events by MMP-2 and -9 on the extracellular domain of beta-dystroglycan which in turn generate a membrane-anchored fragment (Yamada et al., 2001). The proteolytic activities mediated by gamma-secretase within the plasma membrane produce a smaller fragment that is still attached to this lipid bi-layer by the palmitoyl modification in a cysteine group immediately below the transmembrane domain (Kang et al., 2008). The final cut at the interface of the plasma membrane and NLS, carried out by furin, releases this small fragment into the cytosol. The released cytoplasmic fragment is then transported to the nucleus by passive diffusion (see section 1.5.4 and Figure 1.7), where it accumulates and regulates gene transcription and is finally degraded by the nuclear ubiquitin-proteasome system (Figure 6.2).

Figure 6.2: Regulation of dystroglycan by proteolysis. Dystroglycan is subject to different proteolytic events. At the extracellular matrix, alpha- and beta-dystroglycan are subject to proteolysis mediated furin and MMP-2 and -9 respectively. Within the plasma membrane, gamma-secretase cleaves a 31 kDa form of beta-dystroglycan followed by another cleavage by furin in the juxtamembrane region. Shown are the approximate MW of the generated products by the proteases.

The localisation in the nucleus of the same key players mediating the proteolysis of beta-dystroglycan on the plasma membrane leads to the hypothesis that the same mechanism could apply in the nucleus. RIP in the nuclear membrane could explain some discrepancies between the pool of beta-dystroglycan anchored to the nuclear membrane and the pool observed moving freely in the nucleoplasm. In this model, full-length beta-dystroglycan is anchored to the nuclear membrane and the released cytoplasmic fragments are free moving in the nucleoplasm. The processing of beta-dystroglycan by RIP may also influence further processing by the nuclear ubiquitin proteasome system. Although the PTMs and the potential nuclear functions of beta-dystroglycan were separated from the RIP mechanisms described in this thesis, all three of these mechanisms have to be thought of as a continuous process.

There are different enzymes with the potential to cleave membrane-anchored proteins: some cleave type II transmembrane proteins, others multi-pass proteins (Lemberg, 2011; Wolfe & Kopan, 2004). However, if nuclear beta-dystroglycan is subject to proteolysis, the question then arises of how this process could be carried out. The possibility of a mechanism mediated by nuclear gamma-secretase (J. Li et al., 1997) was previously discussed in this thesis, but there is still the question of whether other enzymes could perform the same function. In this regard, one of the critical steps in the processing of prelamin A consists of its proteolytic cleavage by the seven transmembrane zinc metalloprotease ZMPSTE24. This protease, which is located in the ER and the inner nuclear membrane, helps with the maturation of lamin A, and is implicated in the Hutchinson-Gilford Progeria Syndrome due to its inability to cleave a mutant form of prelamin A (Davies, Fong, Yang, Coffinier, & Young, 2009).

The processing of prelamin A by ZMPSTE24 teaches us that there could be a similar processing for beta-dystroglycan, as it has been demonstrated that the nucleus is not exempt from proteolytic regulatory activities. In this regard, after being transported to the nucleus and inserted in the plasma membrane, beta-dystroglycan could be cleaved by gamma-secretase or similar

enzymes, such as ZMPSTE24 (Barrowman, Hamblet, George, & Michaelis, 2008; Barrowman, Hamblet, Kane, & Michaelis, 2012). Understanding the way that beta-dystroglycan is processed within the nucleus could explain the possible hypothesis of a liberated cytoplasmic fragment that is able to function as a transcriptional co-factor. It remains to be determined if the purpose of this cleavage is intended to initiate turnover of dystroglycan, if it has a significance in cellular signalling, if it has functions and then it is immediately degraded by the proteasome, or a combination of all three.

The answers to these questions are important because they could influence the design of therapies aimed to prevent the cleavage of beta-dystroglycan. Given the fact that beta-dystroglycan is reduced from the plasma membrane in cancer and in muscular dystrophies via mechanisms that involve the proteasome, PTM and gamma-secretase, a sensible therapeutic strategy could be to inhibit the activity of gamma-secretase. However, like the proteasome, gamma-secretase is not specific to beta-dystroglycan, and it inhibition will inhibit other pathways as a consequence.

By analogy, it is known that the inhibition of the proteasome leads to the restoration of the DAPC components to the plasma membrane. However, this therapeutic strategy has been questioned by the fact that proteins have to be subject to proteasomal degradation as part of normal cell function. Therefore inhibiting proteasomal activity has off-target effects that are potentially harmful, limiting its use as a therapy (Perkins & Davies, 2012).

The same rationale can be applied to the development of therapeutic strategies that inhibit the activity of gamma-secretase in order to stop the cleavage of plasma membrane proteins. Inhibiting gamma-secretase could stop the further processing of beta-dystroglycan, but also of other proteins that have to be cleared because of alterations in their sequences which are potentially harmful to the cell (Selkoe & Wolfe, 2007). In this regard, the development of therapies that are highly specific in preventing the processing of beta-dystroglycan by gamma-secretase could be more useful. Although this could be a sensible strategy, in proteins subject to the same proteolytic events by gamma-

secretase it has been observed that the use of such strategies can lead to other unwanted effects, such as the stimulation of tumourigenesis, alteration of stem cell signalling pathways, and effects associated with the inhibition of the Notch signalling pathway (Purow, 2012). It has to be considered that the proteolytic activation of beta-dystroglycan is merely a consequence of an upstream activation. As mentioned previously, it can be activated under normal conditions or started by defective glycosylation of alpha-dystroglycan followed by the proteolytic cleavages of furin, on alpha- and, subsequently, MMPs on beta-dystroglycan (Figure 6.2). Again, further research is required to show that this process is caused by an event initiated on alpha-dystroglycan and that it is not an independent mechanism concerning beta-dystroglycan alone. If the first scenario is true, then a therapy aimed to restore the glycosylation of alpha-dystroglycan could be enough to restore the components of the DAPC to the plasma membrane. However, if gamma-secretase cleavage is an independent mechanism, other strategies aimed at protecting the cleavage of beta-dystroglycan within the plasma membrane will have to be developed.

So far, the discussion has been focused on the possible consequences of the liberated cytoplasmic fragment of beta-dystroglycan. However, it should not be forgotten that, upon cleavage, alpha- and beta-dystroglycan fragments are released to the extracellular environment. A simple conclusion about these released fragments is that, they are degraded, but the consequences of generated fragments seem to be far more complex than this.

Different research groups have focused their attention on the potential use of released cleaved fragments as biomarkers in neurodegenerative diseases and cancer. By measuring the concentrations of various secreted proteins in cerebrospinal fluid (CSF), Yin and colleagues identified specific secreted proteins that were increased in patients with Alzheimer's and Parkinson diseases. One of the proteins identified was alpha-dystroglycan, and even though the number of patients under study was low, its use as a biomarker of neurodegenerative diseases was suggested (Yin, Lee, Cho, & Suk, 2009). In addition to that study, increased levels of the N-terminal domain of alpha-dystroglycan have

also been observed in the CSF of patients with Lyme neuroborreliosis (Hesse et al., 2011). The secretion of the N-terminal fragment of alpha-dystroglycan has also been reported for various different cell lines (Saito, Saito-Arai, Nakamura, Shimizu, & Matsumura, 2008; Saito et al., 2011).

The other scenario that has to be taken into account is the possibility that the released fragments could be affecting adjacent interactions e.g. by means of the formation of homophilic interactions or by affecting other cellular processes. In this regard, it has been reported that the N-terminal domain of alpha-dystroglycan retains its ability to interact with extracellular matrix components, such as lamins, fibronectin and fibrinogen. Perhaps the most interesting result reported by the authors was the fact that the N-terminal domain was able to induce neurite extension in PC12 cells (Hall, Bozic, Michel, & Hubbell, 2003).

Together, these results highlight the potential use of secreted cleaved fragments of dystroglycan as biomarkers; however, large scale screening is still required to find a correlation between the concentration of extracellular secreted cleaved dystroglycan in body fluids and the onset/progression of muscular dystrophies and cancer. Furthermore, if the cleavage of dystroglycan is a common event in disease, it will be interesting to determine if there are additional cellular events initiated by the liberation of the secreted fragments e.g. by the formation of homophilic interactions.

6.1.3 The function of nuclear dystroglycan

The function of nuclear beta-dystroglycan is an emerging and exciting topic. With its important function on the plasma membrane to protect the sarcolemma from damage during muscle contraction and relaxation, or its role in controlling and co-ordinating the growth of epithelial cells, it is hard to believe that dystroglycan is also present in the nucleus of cells (either alone or accompanied by alpha-dystroglycan) where it has a function within this very controlled environment. In this thesis, evidence indicating that beta-

dystroglycan may have different roles inside the nucleus was found. Some of the information discussed below will be based on the findings gathered in this project, but caution has to be taken as most of the putative functions and interactions of beta-dystroglycan have to be further confirmed.

The localisation of beta-dystroglycan in the nucleus of different cell lines and in human prostate cancer has been well documented. However, there are no studies reporting the nuclear presence of its counterpart, alpha-dystroglycan. This study is the first to show evidence that alpha-dystroglycan is also present in the nucleus. There are several reasons why this observations seems counter-intuitive. Alpha-dystroglycan is a secreted protein, it does not have a nuclear localisation signal, and it does not have a transmembrane domain that could direct its insertion into the nuclear membrane. Furthermore, a previous report using an antibody directed against the glycan groups of alpha-dystroglycan concluded that beta-dystroglycan was the only subunit present in the nucleus (Oppizzi et al., 2008). Also, the only evidence presented thus far corresponds to that of a biochemical cell fractionation of an over-expressed construct presented in this thesis (Chapter 3, Figure 3.10). Although attempts were made in order to detect alpha-dystroglycan by immunofluorescence and western blotting by using antibodies against core and glycosylated alpha-dystroglycan, they were not successful. The idea of nuclear alpha-dystroglycan can not be completely discarded and the following elements provide some insights into how this protein could be transported to the nucleus and its potential roles.

The results shown in section 3.5 correspond to three independent experiments, which, in part, could discard the possibility of an experimental artefact. Also, it is thought that during the biosynthesis of dystroglycan, both alpha- and beta-subunits remain non-covalently attached, suggesting that this interaction could provide a route for the transport of alpha-dystroglycan. Additionally, glycosylation has also been observed to modify the nucleocytoplasmic transport of heat shock proteins-40 and -70 (Zachara et al., 2004), and to confer the properties of a nuclear localisation signal as was observed with BSA (Guinez, Morelle, Michalski, & Lefebvre, 2005; Rondanino, Bousser, Monsigny,

& Roche, 2003; Hart & West, 2009). Furthermore, phosphorylation modulates the glycosylated status of proteins which in turn affects their nuclear transport as has been observed with Tau proteins (Lefebvre et al., 2003). Interestingly, the transport of some glycosylated proteins occurs in a cell cycle-dependent manner (Rondanino et al., 2003) and apparently, this modification, enhances the interaction between some transcription co-factors (Gewinner et al., 2004).

Given the extensive glycosylation of alpha-dystroglycan and the data from the reports cited above, it can be hypothesized that alpha-dystroglycan travels to the nucleus by means of its multiple glycan groups, which mediate unknown nuclear regulations. However, this is contradicted by the fact that in the data reported in this thesis, alpha-dystroglycan was apparently void of glycosylation. Therefore, if alpha-dystroglycan is transported to the nucleus, it has to occur via a novel, glycan-independent mechanism. In support of this, Chuderland and colleagues identified a new motif that is able to translocate cytoplasmic proteins to the nucleus in an importin-independent pathway. This SPS/TPT (Ser-Pro-Ser / Thr-Pro-Thr or S/T-P-S/T) motif, upon phosphorylation and interaction with importin-7, was able to mediate the nuclear transport of the extracellular signal-regulated kinase-2 (ERK-2), SMAD3 and MEK1 (Chuderland, Konson, & Seger, 2008). Thus, in a speculative scenario, hypo-glycosylated alpha-dystroglycan exposes its major TPT domains, which are then phosphorylated, bound by importin-7 and transported to the nucleus. Much research is required to fully characterise the nuclear localisation of alpha-dystroglycan and the significance of this. Some elements have been provided that suggest possible pathways to the nucleus and testing these, with the help of newly developed antibodies (Fortunato et al., 2014; Humphrey et al., 2015), will further support or discard the running hypothesis of a separate pool of nuclear alpha-dystroglycan.

The information provided above, although limited for alpha-dystroglycan, leads to the question of whether the N-glycosylation on the globular domain of beta-dystroglycan could confer additional properties to this subunit, and it may be by modulating its interaction with other proteins in the lumen of the

nuclear envelope.

The nuclear lamina, in addition to the known components lamin-A/C, lamin-B and emerin (a lamin-binding protein), is composed of proteins that are part of the LINC complex (Linker of Nucleoskeleton and Cytoskeleton), which connects the nucleoskeleton to the cytoskeleton (Crisp et al., 2006; Dechat, Adam, Taimen, Shimi, & Goldman, 2010; Starr, 2011; K. L. Wilson & Berk, 2010). The main components of the LINC complex are SUN and KASH proteins. SUN proteins are transmembrane proteins immersed in the inner nuclear membrane, with the N-terminal oriented towards the nucleoplasm and the C-terminal facing the nuclear membrane lumen. On the other hand, KASH proteins span the outer nuclear membrane, with the N-terminal facing towards the cytosol and the C-terminus in the lumenal space of the nuclear membrane. The localisation and the way these two proteins interact resemble a nuclear bridge, able to transmit signals and forces between the nucleoskeleton, the cytoskeleton and the extracellular matrix (Crisp et al., 2006; Hodzic, Yeater, Bengtsson, Otto, & Stahl, 2004; Starr, 2011; Wang et al., 2012)

SUN proteins interact with chromatin-associated proteins, with components of the nuclear lamina in the nucleoplasm, and with KASH proteins in the nuclear membrane lumen. KASH proteins are able to interact with different cytosolic proteins, including actin filaments, microtubules, intermediate filaments and others, and regulate different cellular process in a great variety of organisms. The mutations of KASH proteins have been associated with various diseases, such as Emery-Dreifuss muscular dystrophy, cancer (colorectal, gastrointestinal, ovarian and breast), autism disorders, hearing problems, mental disorders and others (Luxton & Starr, 2014; Starr, 2011; Turgay et al., 2014).

The mass spectrometry analysis identified, SUN2, kinesin, dynein and torsin A (component of the nuclear membrane lumen) as potential binding partners of nuclear beta-dystroglycan. Incorporating these finding with the model suggested by Tadayoni and colleagues (Tadayoni et al., 2012), it is possible to hypothesize that beta-dystroglycan is able to interact with SUN2 and

KASH proteins, which in turn triggers the formation of other complexes in the cytosol, depending on the cellular context. During the development of this thesis and in support of the above hypothesis, SUN1 and emerin nuclear proteins, were found interacting with dystroglycan (Cisneros and Winder labs, Steve Winder personal communication) (Figure 6.3).

Further research is required to confirm the proposed interaction between beta-dystroglycan, SUN and KASH, and its biological and clinical significance. Perhaps this new association will help to explain the molecular basis for the centralised nuclei usually observed in muscular dystrophies, and alterations in the nuclear shape and positioning of the centrosomes which have been reported in different cancers (Gundersen & Worman, 2013).

Figure 6.3: Beta-dystroglycan and the LINC complex. A current hypothesis for nuclear beta-dystroglycan suggests that it is inserted in the inner nuclear membrane with its N-terminal facing towards the perinuclear space (PNS). In the PNS, beta-dystroglycan interacts with SUN, a member of the LINC complex, torsinA, and emerin, although the mechanisms mediating this interaction are still unknown.

6.2 Future perspectives

The broad distribution in cellular organelles of differing tissues and species, confers multiple functions on dystroglycan: whether they are advantageous or disadvantageous, is something that has to be determined. During the course of this thesis there were many questions that arose and these require answers in order to have a better understanding of the effects of phosphorylation-ubiquitination, RIP and the nuclear localisation of dystroglycan, particularly in diseases, such as cancer and muscular dystrophies, and other cellular processes, namely development. Those questions are described in the previous chapters, but the most relevant, are enumerated in the objectives below:

1. To fully characterise the localisation and functionality of alpha-dystroglycan in the nucleus.

2. To determine the effects of the over-expression of the cytoplasmic domain of beta-dystroglycan in heterologous systems. Does it inhibit or stimulate tumour progression?

3. To determine the effects of the extracellular domain of beta-dystroglycan on adjacent and distant cells.

4. To determine the function of beta-dystroglycan in mitosis.

5. To further confirm that NEDD4L and HUWE1 are the ligases implicated in the ubiquitination of beta-dystroglycan.

6. To further characterise the interaction of beta-dystroglycan with members of the LINC complex.

7. To characterise the cross-talk between Notch and dystroglycan signalling pathways.

6.3 Conclusions

This work highlights the possibility that beta-dystroglycan may be subject to multiple phosphorylation and ubiquitination post-translational modifications. It also provides new evidence about another post-translational modification mediated by gamma-secretase, regulated intramembrane proteolysis, that is responsible for the further processing of beta-dystroglycan. The triggering of these three PTM (ubiquitination, phosphorylation and RIP) seems to be initiated by extracellular events affecting the glycosylation of alpha-dystroglycan in disease. The signals initiating these PTM appear to converge on the nucleus, where the cytoplasmic fragment of beta-dystroglycan initiates and regulates downstream events (Figure 6.4).

Although this work has provided more information about the post-translational modifications and interacting partners of beta-dystroglycan, the question still remains: what is the function of nuclear beta-dystroglycan in prostate cancer cells?

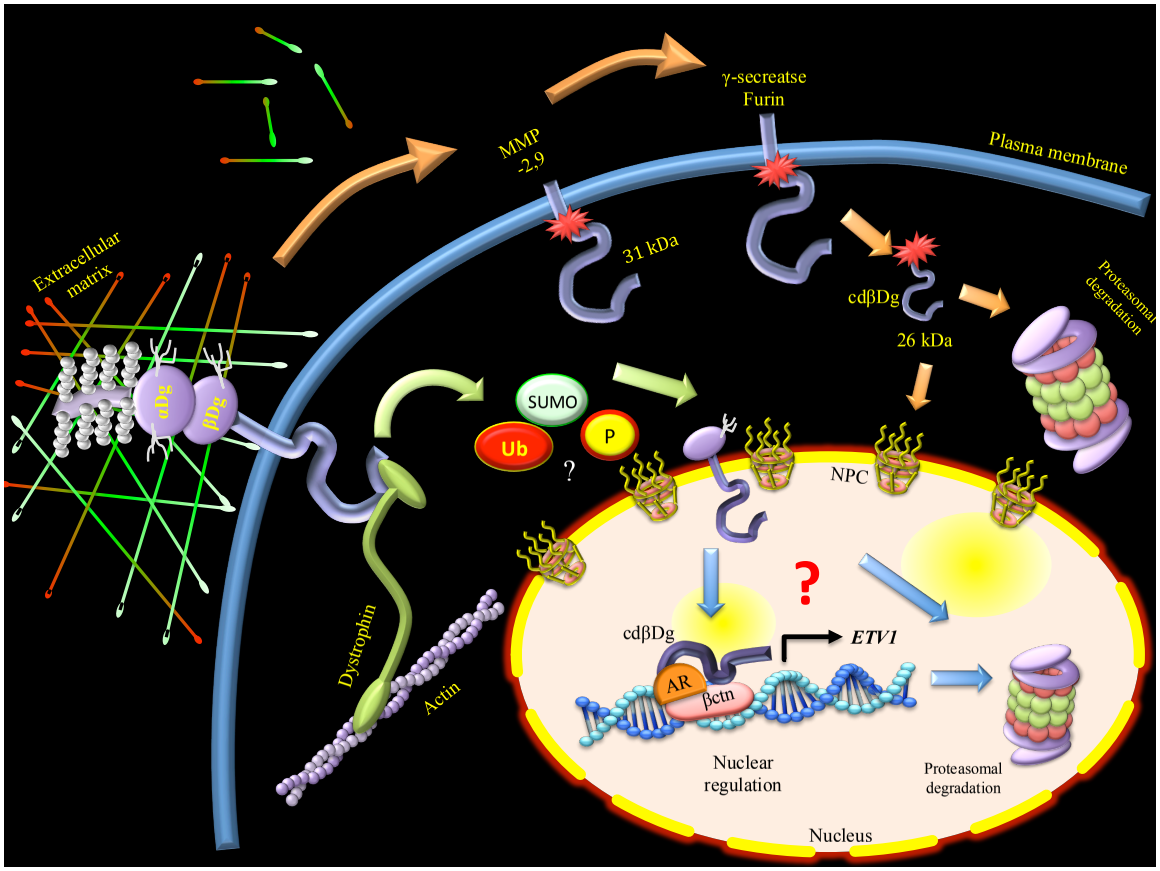

Figure 6.4: The function of nuclear beta-dystroglycan. At the plasma membrane beta-dystroglycan is subject to proteolytic cleavage by different proteases. A 26 kDa cytoplasmic fragment of beta-dystroglycan is then degraded by the proteasome in the cytoplasm (orange arrows). An alternative pathway (green arrows) shows that cytosolic full-length beta-dystroglycan under the regulation of different PTM is transported to the nucleus to provide mechanical support to the nuclear membrane. Nuclear beta-dystroglycan is also subject to proteolysis which in turn releases a cytoplasmic fragment with potential nuclear regulatory activity by means of its interaction with beta-catenin (βctn) and androgen receptor (AR). The cytoplasmic fragment of beta-dystroglycan is finally degraded by the nuclear proteasome (blue arrows).

Appendices

A

Recipes

Buffer	Components		Notes
Acrylamide-bisacrylamide mixture 49.5% T, 3% C	48% (w/v) 1.5% (w/v)	Acrylamide Bisacrylamide	Use to prepare Tris-Tricine gels.
Acrylamide-bisacrylamide mixture 49.5% T, 6% C	46.5% (w/v) 3.0% (w/v)	Acrylamide Bisacrylamide	Use to prepare Tris-Tricine gels.
Anode Buffer	0.2 M	Tris	Adjust the pH to 8.9 with HCl. Use with Tris-Tricine gels.
Bacterial Medium YT (2x)	1% (w/v) 1.6% (w/v) 0.5% (w/v)	Yeast extract Tryptone NaCl	Sterilize by autoclaving.
Blocking Buffer (immunofluorescence)	5% (v/v) 3% (v/v)	FBS BSA	Prepare in PBS pH 7.4
Blocking Buffer (western blotting)	5% (w/v)	Skimmed milk or BSA	Dissolve skimmed milk or BSA in TBST.
Buffer I (cell fractionation)	0.32 M 10 mM 3 mM 2 mM 0.1 mM 0.5% (v/v) 1 mM	Sucrose Tris-HCl pH 8.0 Calcium chloride Magnesium acetate EDTA NP-40 DTT	Add 0.5 mM PMSF fresh before using. Buffer can be supplemented with proteases and phosphatases inhibitors as desired. Filter sterile.
Buffer STE	10 mM 1 mM 100 mM	Tris-HCl pH 8.0 EDTA NaCl	Add proteases inhibitors fresh before using.

Table A.1: Recipes

Buffer	Components		Notes
Buffer II (cell fractionation)	2 M 10 mM 5 mM 0.1 mM 1 mm	Sucrose Tris-HCl pH 8.0 Magnesium acetate EDTA DTT	Add 0.5 mM PMSF fresh before using. Buffer can be supplemented with proteases and phosphatases inhibitors as desired. Filter sterile.
Cathode Buffer	0.1 M 0.1 M 0.1% (w/v)	Tris Tricine SDS	pH is around 8.25, no correction needed. Use with Tris-Tricine gels.
Coomassie Safe Staining	60-80 mg 3 ml	Coomassie brilliant blue G-250 Concentrated hydrocloric acid	Store solution protected from the light.
DNA Loading Buffer	0.25% (v/v) 0.25% (v/v) 30% (w/v)	Bromophenol blue Xylene cyanol FF Glycerol	—
ECL Solution I	100 mM 25 mM 396 μM	Tris-HCl pH 8.5 Luminol p-Coumaric acid	Store at 4°C protected from the light.
ECL Solution II	100 mM 0.02% (v/v)	Tris-HCl pH 8.5 H_2O_2	Store at 4°C protected from the light.
Cell Freezing Medium	20% (v/v) 10% (v/v)	FBS DMSO	Prepare in RPMI-1640 medium.
Laemmli SDS-PAGE Gel Buffer	3 M 0.3% (w/v)	Tris SDS	Adjust the pH to 8.45 with HCl.

Table A.2: Recipes (continued)

Buffer	Components		Notes
Laemmli SDS-PAGE Loading Buffer (2x)	20% (v/v)	Glycerol	Concentrations can be adjusted to prepare a 5x concentrated buffer.
	100 mM	Tris-HCl pH 6.8	
	4% (w/v)	SDS	
	0.2% (w/v)	Bromophenol blue	
	2% (v/v)	2-mercaptoethanol	
Mild Cell Lysis Buffer	50 mM	Tris-HCl pH 7.4	–
	150 mM	NaCl	
	1 mM	EDTA	
	1% (w/v)	Triton X-100	
Mounting Medium	10 ng/ml	DAPI	Dissolve in Hydromount. Store at 4°C protected from the light.
	2.5% (w/v)	Dabco	
Radio Immunoprecipitation Assay Buffer (RIPA)	50 mM	Tris-HCl pH 7.5	Store at RT protected from the light (James et al., 2000).
	150 mM	NaCl	
	1 mM	EGTA	
	1 mM	EDTA	
	1% (v/v)	Triton X-100	
	0.5% (w/v)	Sodium deoxycholate	
	0.1% (w/v)	SDS	
	1 mM	Sodium orthovanadate	
	100 nM	Calyculin	
	1 mM	PMSF	
	10 μM	TPCK	
	10 μM	Leupeptin	
	1 μM	Pepstatin	
	10 μg/ml	Aprotinin	
	1x	Complete protease inhibitor	
	10 mM	Sodium fluoride	

Table A.3: Recipes (continued)

Buffer	Components		Notes
Mild Stripping Buffer (1 L)	15 g 1 g 10 ml	Glycine SDS Tween 20	Adjust the pH to 2.2.
Phosphate Buffered Saline (PBS) (10x)	1.37 M 0.027 M 0.1 M 0.018 M	NaCl KCl Na_2HPO_4 KH_2HPO_4	Adjust the pH to 7.4 with HCl.
Laemmli SDS-PAGE Resolving Buffer	1.5 M 0.4% (w/v)	Tris-HCl pH 8.8 SDS	–
Laemmli SDS Running Buffer (10x)	250 mM 1.92 M	Tris Glycine	–
Laemmli Stacking Buffer	0.5 M 0.4% (w/v)	Tris-HCl pH 6.8 SDS	–
Sucrose (cell fractionation)	1.8 M	Sucrose	Filter sterile.
TAE (1x)	40 mM 1 mM	Tris-Acetate EDTA	–
Tris Buffered Saline Tween (TBST) (1x)	50 mM 150 mM 0.5% (v/v)	Tris-HCl pH 7.4 NaCl Tween 20	–
Towbin Transfer Buffer	25 mM 192 mM 20% (v/v) 0.02-0.1% (w/v)	Tris base Glycine Methanol SDS	The resulting pH is approximately 8.3. Do not adjust the pH (Towbin et al., 1979).
Tris Buffered Saline (TBS) (1x)	50 mM 150 mM	Tris-HCl pH 7.4 NaCl	–

Table A.4: Recipes (continued)

B

List of oligonucleotides

Name	Sequence (5' → 3')	Function
BDGFLAGFWD	TCTTTGCGGATGAGCTGGATTATAAAGATGATGAC-GATAAGCCCCCGCCCTCT	Insertion of Flag tag in the primary sequence of mouse $\alpha\beta$Dg
BDGFLAGREV	AGAGGGCGGGGGCTTATCGTCATCATCTT-TATAATCCAGCTCATCCGCAAAGA	
abDG_F	ATACTAGAATTCATGTCTGTGGACAACTGGCTA	Cloning of the mouse $\alpha\beta$DgFlag DNA sequence into the pcDNA3.1(+) vector
abDG_R	CTATTACTCGAGTTAAGGGGGAACATACGGAGG	
ICDBDG_WTF	ATACTAGAATTCATGTATCGCAAGAAGAGGAAGGGC	Cloning of the cytoplasmic domain of βDgFlag into the pcDNA3.1(+) vector
abDG_R	CTATTACTCGAGTTAAGGGGGAACATACGGAGG	
ICBDGFLAG_Y890F_F	CGATCACCCCCTCCGTTTGTTCCCCCTTAA	Mutation of Y890 to F in the primary sequence of $\alpha\beta$DgFlag
ICBDGFLAG_Y890F_R	TTAAGGGGGAACAAACGGAGGGGGTGATCG	
DG_K806R_F	AGATGATGACGATAGGCCCCCGCCCTCTT	Mutation of K806 to R in the primary sequence of $\alpha\beta$DgFlag
DG_K806R_R	AAGAGGGCGGGGGCCTATCGTCATCATCT	
bGHR primer (source bioscience)	TAGAAGGCACAGTCGAGG	Primer used to sequence the plasmid pcDNA3.1(+) with the coding sequences: $\alpha\beta$DgFlag Y890F, $\alpha\beta$DgFlag K806R and cdβDgFlag
DGSEQ (Winder lab)	CCGAGAAGAGCAGTAGGAC	Primer used to sequence the insertion of Flag tag in the coding sequence of βDg
T7 promoter (F) (source bioscience)	TAATACGACTCACTATAGGG	Primer used for sequencing the insertion of the coding sequence of $\alpha\beta$DgFlag and cdβDgFlag into the plasmid pcDNA3.1(+)

Table B.1: List of oligonucleotides.

C

List of plasmids

Plasmid	Features	Antibiotic resistance	Reference
pcDNA3.1-αDg-myc/hisB	Encodes alpha-dystroglycan with a myc/his tag in its C-ter	Ampicillin	Jane Hewitt, University of Nottingham (unpublished).
pcDNA3.1(+)-$\alpha\beta$Dg-myc/his	Encodes full length $\alpha\beta$Dg with a myc/his tag in its C-ter	Ampicillin	Winder lab (Thompson, 2007).
pcDNA2-$\alpha\beta$Dg	Encodes full length $\alpha\beta$Dg	Ampicillin	Winder lab.
pcDNA2-$\alpha\beta$DgFlag	Encodes full length $\alpha\beta$DgFlag	Ampicillin	This study.
pcDNA3.1(+)-$\alpha\beta$DgFlag	Encodes full length $\alpha\beta$DgFlag	Ampicillin	This study.
pcDNA3.1(+)-cdβDgFlag	Encodes cytoplasmic domain of βDgFlag	Ampicillin	This study.
pcDNA3.1(+)-$\alpha\beta$DgFlag-Y890F	Encodes full length $\alpha\beta$DgFlag with the mutation Y890F	Ampicillin	This study.
pcDNA3.1(+)-$\alpha\beta$DgFlag-K806R	Encodes full length $\alpha\beta$DgFlag with the mutation K806R	Ampicillin	This study.
pGST-MD	Encodes MultiDsk	Ampicillin	(M. D. Wilson et al., 2012).
pKA417	Encodes GST	Ampicillin	Gift from K.R. Ayscough.

Table C.1: List of plasmids

D

Preparation of resolving and stacking gels

	Separating gel (10 ml)				Stacking gel (5 ml)
Concentration	7.5%	10%	12.5%	15%	5%
Acrylamide	2.5	3.35	4.15	5.0	0.8
Gel stock	3.75	3.75	3.75	3.75	0.625
Water	3.65	2.85	2.0	1.2	3.525
TEMED	5 μl	5 μl	5 μl	5 μl	15 μl
10% APS	100 μl	100 μl	100 μl	100 μl	50 μl

Table D.1: Volumes used to prepare Laemmli SDS-PAGE gels (Biorad apparatus).

Solution	**Separating gel**							**Stacking gel**	
Concentration	3%	5%	7.5%	10%	12.5%	15%	20%	3%	5%
Acrylamide	2.5	4.17	6.25	8.3	10.42	12.6	16.7	2	3.32
Gel stock	6.25	6.25	6.25	6.25	6.25	6.25	6.25	5	5
Glycerol 50%	1.4	1.4	1.4	2.8	2.8	2.8	2.0	-	-
Water	14.74	12.95	11.0	7.56	5.44	4.66	-	12.84	11.52
TEMED	12.5 μl	12.5 μl	12.5 μl	12.5 μl	12.5 μl	12.5 μl	12.5 μl	40 μl	40 μl
10% APS	100 μl	100 μl	100 μl	75 μl	75 μl	75 μl	75 μl	120 μl	120 μl
BPB	-	-	-	+	+	+	+	+	+

Table D.2: Volumes used to prepare gradient SDS-PAGE gels (Cambridge apparatus).

Solution	**Stacking gel**	**Spacer gel**	**Separating gel**			
Concentration	4% T, 3% C	10% T, 3% C	10% T, 3% C	16.5% T, 3% C	16.5% T, 6% C	16.5% T, 6% C with 6 M urea
49.5% T, 3% C solution	1 ml	6.1 ml	6.1 ml	10 ml	—	—
49.5% T, 6% C solution	—	—	—	—	10 ml	10 ml
Gel buffer	3.1 ml	10 ml	10 ml	10 ml	10 ml	10 ml
Glycerol (g)	—	—	4	4	4	—
Urea (g)	—	—	—	—	—	10.8
Water to a final volume of	12.5 ml	30 ml	30 ml	30 ml	30 ml	30 ml

Table D.3: Volumes used to prepare Tricine-SDS-PAGE gels.

E

List of antibodies

Name	Concentrations			Epitope	Species	Source
	WB	IF	IP			
pYβDG	1:500	1:200	1:30	Fifteen last amino acids of the C-terminus of beta-dystroglycan with a pY892	Rabbit	In house (Ilsley et al., 2001)
α-tubulin (T5168)	1:4000	–	–	Recognizes an epitope located in the C-terminus end of the α-tubulin isoform	Mouse IgG_1	Sigma
Alexa Fluor 488	–	1:800	–	Anti-mouse IgG Anti-rabbit IgG	Goat Donkey	Life technologies
Alexa Fluor 594	–	1:800	–	Anti-mouse IgG Anti-rabbit IgG	Goat Donkey	Life technologies
c-Myc (9E10	1:700	–	1:20	Amino acids 408-439 within the C-terminus domain of c-Myc of human origin	Mouse mAb IgG_1	Santa Cruz Biotechnology
Calnexin (C5C9)	1:1000	–	–	Total calnexin	Rabbit mAb IgG	Cell signaling technology
Fibrillarin (C13C3)	1:1000	–	–	Synthetic peptide (KHL-coupled) surrounding Thr298 of human fibrillarin	Rabbit mAb IgG	Cell signaling technology
GAPDH (GA1R)	1:8000	–	–	Recombinant GAPDH	Mouse IgG_1	Thermo scientific
GST	1:1000	–	–	Recombinant purified full length GST	Mouse IgG	Thermo fisher scientific
Histone H3 (D1H2)	1:1000	–	–	Total histone H3	Rabbit IgG	Cell signaling technology
HRP anti-mouse (A4416)	1:10000	–	–	Anti-mouse IgG	Goat	Sigma

Table E.1: List of antibodies

Name	Concentrations			Epitope	Species	Source
	WB	IF	IP			
HRP anti-rabbit (A0545)	1:20000	–	–	Anti-rabbit IgG	Goat	Sigma
Lamin A/C (4C11)	1:500-1:1000	1:200	–	Recombinant fragment of human Lamin A protein	Mouse mAb IgG2a/κ	Cell signaling technology
Flag M2 (F3165)	1:2000	1:800	–	DYKDDDDK	Mouse IgG_1	Sigma
Flag M2 resin (A2220)	–	–	40 μl	DYKDDDDK	Mouse IgG_1	Sigma
Mandag2	1:300	1:100	1:20	Beta-dystroglycan (aa 881-895)	Mouse	(Helliwell et al., 1994)
p-p44/42 MAPK Thr202/Tyr204	1:1000	–	–	Detects endogenous levels of activated p44 and p42 MAP Kinase (Erk1 and Erk2) when dually phosphorylated at Thr202 and Tyr204 of Erk1 (Thr185 and Tyr187 of Erk2), and singly phosphorylated at Thr202.	Rabbit IgG	Cell signaling technology
p44/42 MAPK (Erk 1/2)	1:500	–	–	Detects endogenous levels of total p44/42 MAP kinase (Erk1/Erk2) protein.	Rabbit IgG	Cell signaling technology
rFlag (F7425)	1:1000	1:800	–	DYKDDDDK	Rabbit IgG	Sigma
Ubiquitin (P4D1)	1:1000	1:200	–	Recognizes mono- and polyubiquitin protein conjugates, free polyubiquitin chains and free ubiquitin	Mouse IgG_1	Enzo life sciences

Table E.2: List of antibodies (continued)

F

Interactome of beta-dystroglycan

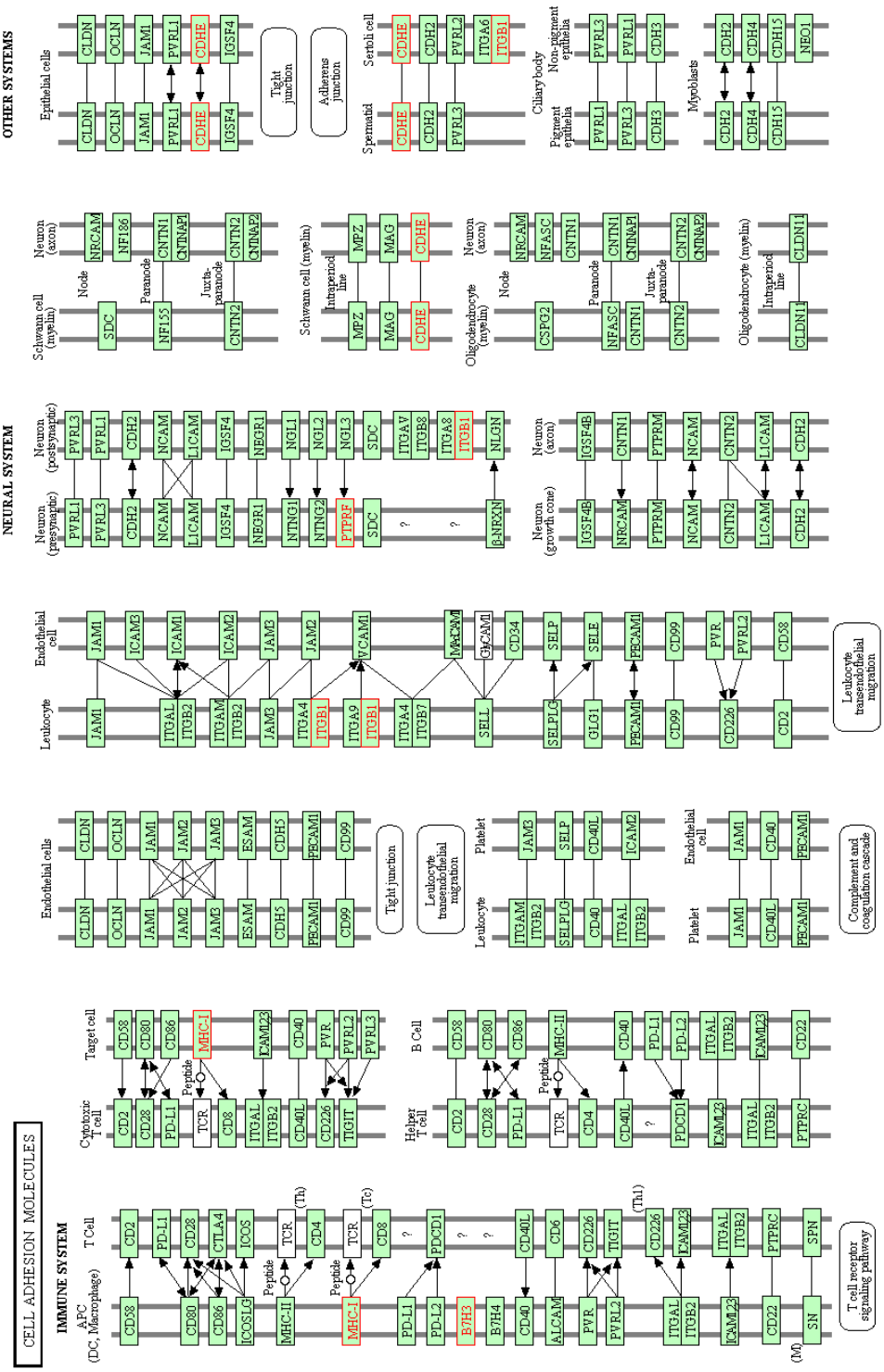

Figure F.1: Cell adhesion molecules. These cell surface proteins are grouped into four main groups: the integrin family, the immunoglobulin superfamily, selectins, and cadherins. They perform different cellular processes that range from immune response, hemostasis, inflammation, embryogeniesis, to development of normal tissue. Highlighted in red are the proteins found immunoprecipitating with Flag (MHC-I, B7H3, ITGB1, PTPRF and CDHE). Source: `http://www.kegg.jp/dbget-bin/www_bget?pathway+hsa04514`.

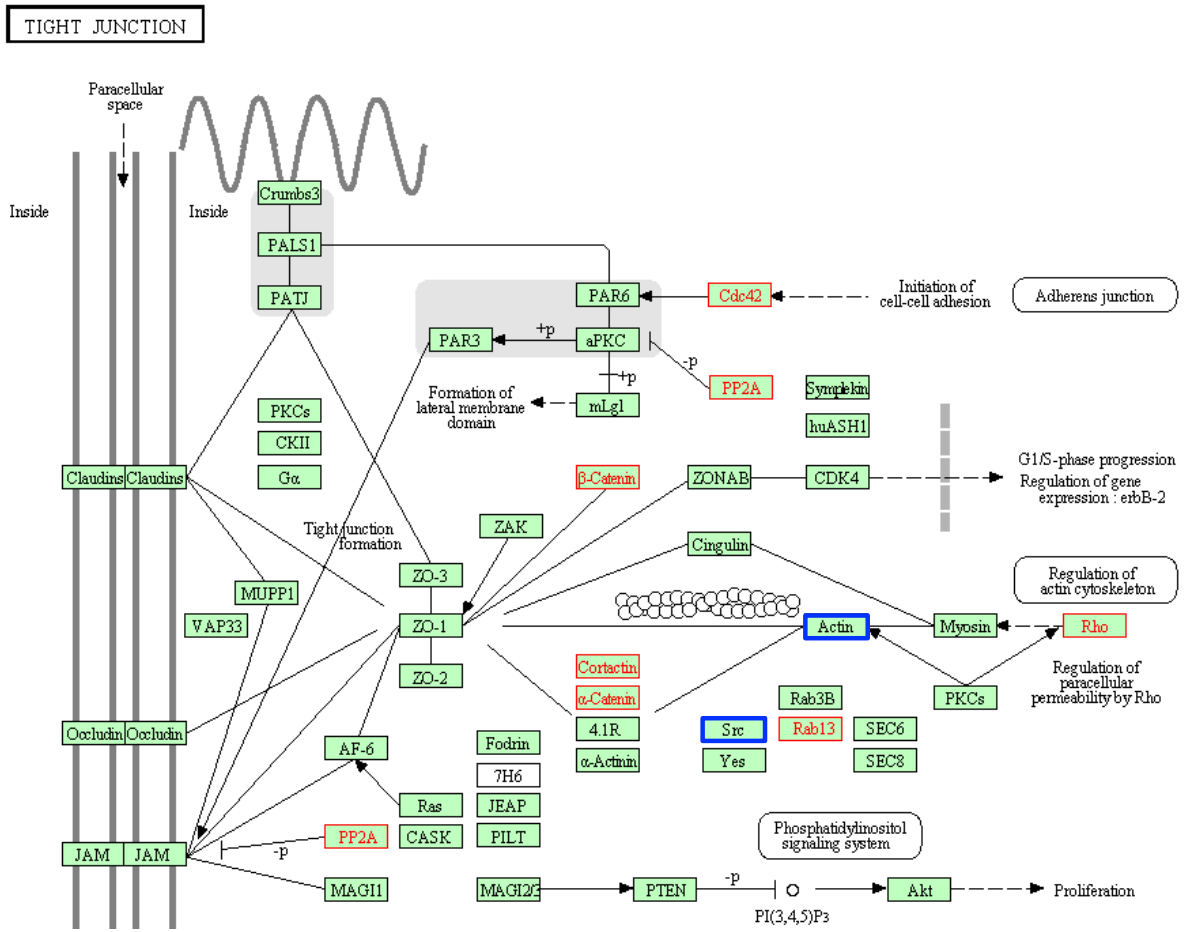

Figure F.2: Tight junctions. Occludin, claudin and junctional adhesion molecules (JAMs) are the main components of the tight junctions. Cell adhesion is regulated by these transmembrane proteins, while its interaction to cytoplasmic proteins is mediated by scaffolding proteins. These proteins are involved in a multitude of pathways such as junction assembly, barrier regulation, gene transcription and others. Highlighted in red are the proteins found immunoprecipitating with Flag (PP2A, α/β-catenin, Cdc42, Cortactin, Rab13 and Rho) and in blue boxes are the already known interacting proteins with dystroglycan (Src and actin). Source: `http://www.kegg.jp/dbget-bin/www_bget?pathway+hsa04530`.

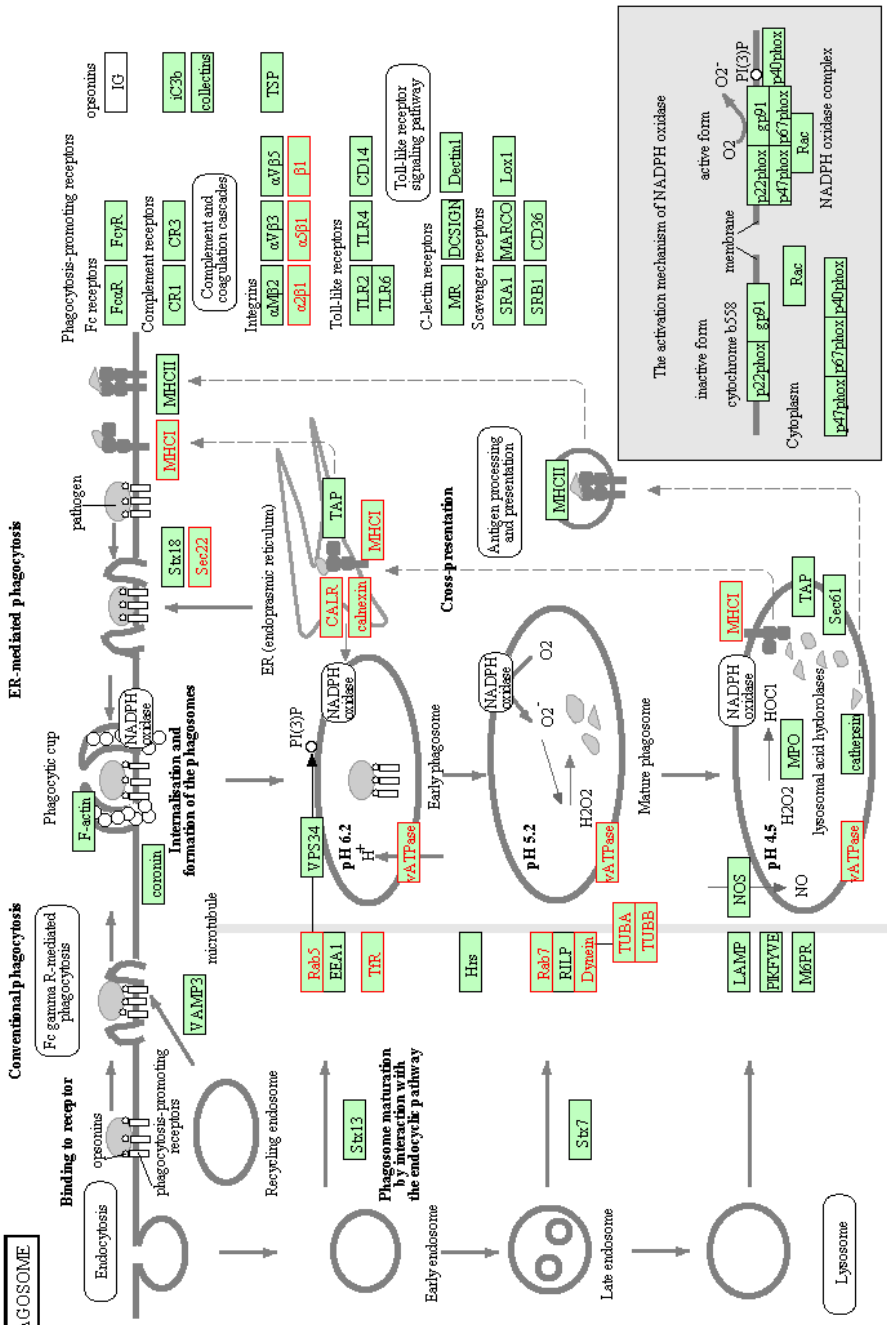

Figure F.3: Phagosome. Phagocytosis is the process of taking in relatively large particles by a cell, and is a central mechanism in the tissue remodelling, inflammation, and defense against infectious agents. A phagosome is formed when the specific receptors on the phagocyte surface recognize ligands on the particle surface. The maturation of phagosomes involves regulated interaction with the other membrane organelles, including recycling endosomes, late endosomes and lysosomes. Highlighted in red are the proteins found immunoprecipitating with Flag. Highlighted in red are the proteins found immunoprecipitating with Flag (Rab5, TfR, Rab7, Dynein, TUBA/B, MHCI, Sec22, CALR, Calnexin, vATPase, Integrin $\alpha 2\beta 1$, $\alpha 5\beta 1$ and $\beta 1$). Source: `http://www.kegg.jp/dbget-bin/www_bget?pathway+hsa04145`.

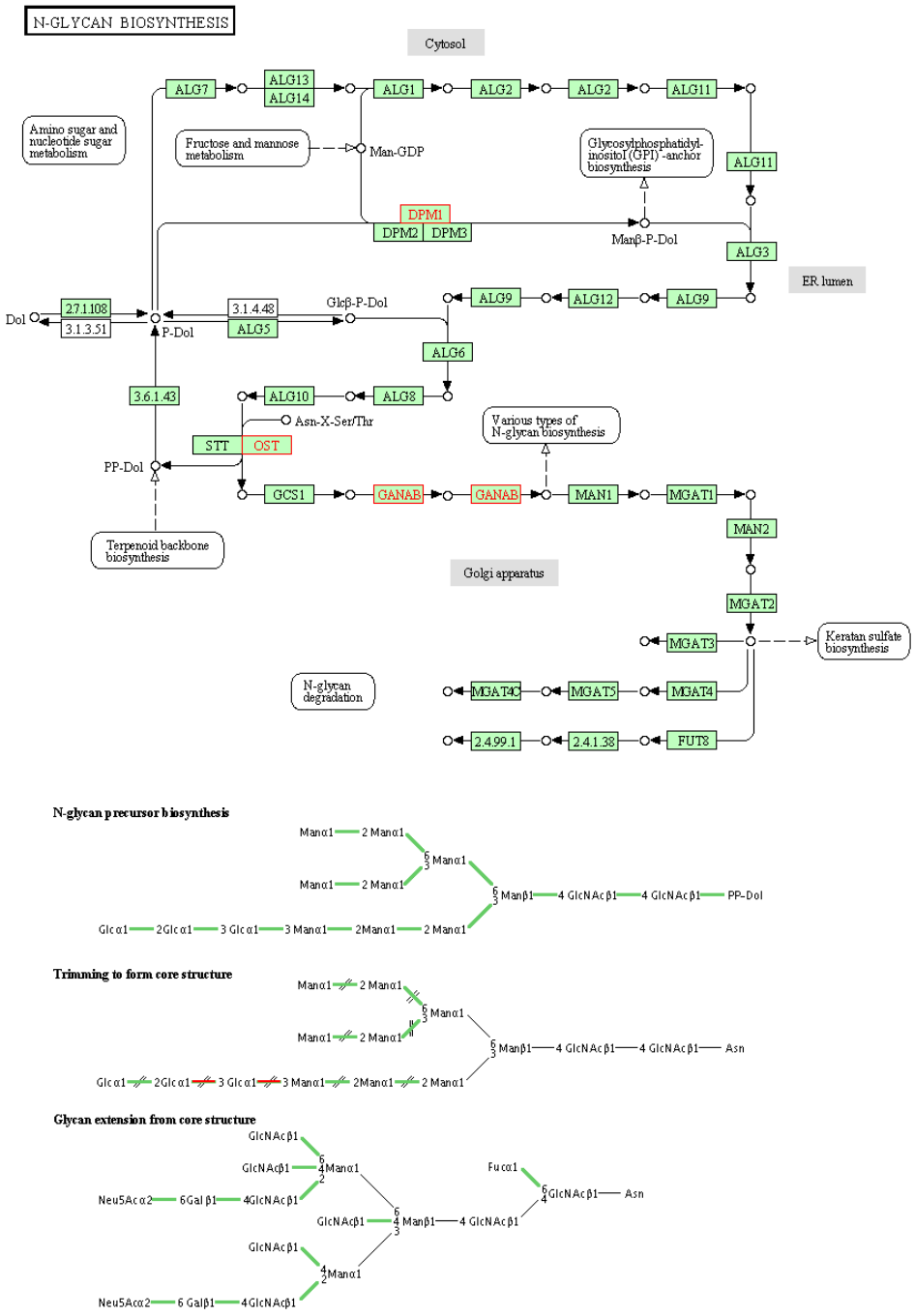

Figure F.4: N-glycan biosynthesis. N-glycans or asparagine-linked glycans are major constituents of glycoproteins in eukaryotes. N-glycans are covalently attached to asparagine with the consensus sequence of Asn-X-Ser/Thr by an N-glycosidic bond, GlcNAc b1- Asn. Highlighted in red are the proteins found immunoprecipitating with Flag (DPM1, OST and GANAB). `http://www.kegg.jp/dbget-bin/www_bget?pathway+hsa00510`.

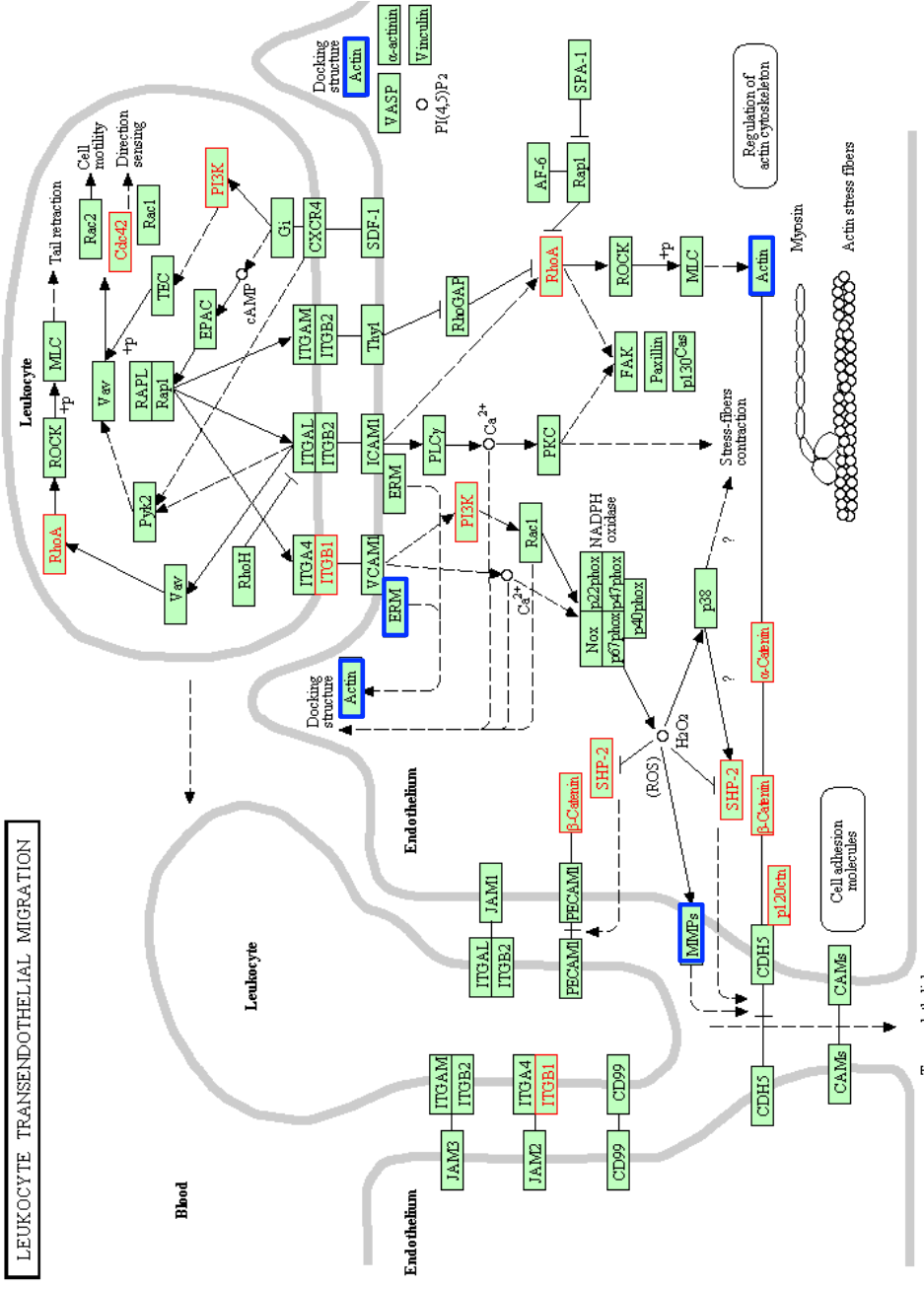

Figure F.5: Leukocyte transendothelial migrations. Leukocyte migration from the blood into tissues is vital for immune surveillance and inflammation. During this diapedesis of leukocytes, the leukocytes bind to endothelial cell adhesion molecules (CAM) and then migrate across the vascular endothelium. This interaction can trigger different pathways that result in the modulation of its own cytoskeleton and that of the endothelial cells. Highlighted in red are the proteins found immunoprecipitating with Flag (ITGB1, α/β-catenin, SHP2, p120ctn, PI3K, RhoA, Cdc42) and in blue boxes are the already known interacting proteins with dystroglycan (Actin, ERM and MMPs). Source: `http://www.kegg.jp/dbget-bin/www_bget?pathway+hsa04670`.

References

Acharyya, S., Butchbach, M. E., Sahenk, Z., Wang, H., Saji, M., Carathers, M., ... Guttridge, D. C. (2005). Dystrophin glycoprotein complex dysfunction: a regulatory link between muscular dystrophy and cancer cachexia. *Cancer Cell*, *8*(5), 421-32.

Acharyya, S., & Guttridge, D. C. (2007). Cancer cachexia signaling pathways continue to emerge yet much still points to the proteasome. *Clin Cancer Res*, *13*(5), 1356-61.

Ahmad, Y., & Lamond, A. I. (2014). A perspective on proteomics in cell biology. *Trends Cell Biol*, *24*(4), 257-64.

Aicart-Ramos, C., Valero, R. A., & Rodriguez-Crespo, I. (2011). Protein palmitoylation and subcellular trafficking. *Biochim Biophys Acta*, *1808*(12), 2981-94.

Akhavan, A., Crivelli, S. N., Singh, M., Lingappa, V. R., & Muschler, J. L. (2008). SEA domain proteolysis determines the functional composition of dystroglycan. *FASEB J*, *22*(2), 612-21.

Akhavan, A., Griffith, O. L., Soroceanu, L., Leonoudakis, D., Luciani-Torres, M. G., Daemen, A., ... Muschler, J. L. (2012). Loss of cell-surface laminin anchoring promotes tumor growth and is associated with poor clinical outcomes. *Cancer Res*, *72*(10), 2578-88.

Aladjem, M. I. (2007). Replication in context: dynamic regulation of DNA replication patterns in metazoans. *Nat Rev Genet*, *8*(8), 588-600.

Alberts, B., Johnson, A., Lewis, J., Raff, M., Roberts, K., & Walter, P. (2008). Molecular biology of the cell, Fifth Edition. *Garland Science, New York*, 1-1268.

Allikian, M. J., & McNally, E. M. (2007). Processing and assembly of the dystrophin glycoprotein complex. *Traffic*, *8*(3), 177-83.

Anders, L., Mertins, P., Lammich, S., Murgia, M., Hartmann, D., Saftig, P., ... Ullrich, A. (2006). Furin-, adam 10-, and gamma-secretase-mediated cleavage of a receptor tyrosine phosphatase and regulation of beta-catenin's transcriptional activity. *Mol Cell Biol*, *26*(10), 3917-34.

Angeloni, D. (2007). Molecular analysis of deletions in human chromosome 3p21 and the role of resident cancer genes in disease. *Brief Funct Genomic Proteomic*, *6*(1), 19-39.

Apel, E. D., Roberds, S. L., Campbell, K. P., & Merlie, J. P. (1995). Rapsyn may function as a link between the acetylcholine receptor and the agrin-binding dystrophin-associated glycoprotein complex. *Neuron*, *15*(1), 115-26.

Aqeilan, R. I., Donati, V., Palamarchuk, A., Trapasso, F., Kaou, M., Pekarsky, Y., ... Croce, C. M. (2005). WW domain-containing proteins, WWOX and YAP, compete for interaction with ErbB-4 and modulate its transcriptional function. *Cancer Res*, *65*(15), 6764-72.

Aragón, E., Goerner, N., Xi, Q., Gomes, T., Gao, S., Massagué, J., & Macias, M. J. (2012). Structural basis for the versatile interactions of Smad7 with regulator WW domains in TGF-β pathways. *Structure*, *20*(10),

1726-36.

Armstrong, S. C., Latham, C. A., & Ganote, C. E. (2003). An ischemic beta-dystroglycan (betaDG) degradation product: correlation with irreversible injury in adult rabbit cardiomyocytes. *Mol Cell Biochem*, *242*(1-2), 71-9.

Assereto, S., Stringara, S., Sotgia, F., Bonuccelli, G., Broccolini, A., Pedemonte, M., ... Minetti, C. (2006). Pharmacological rescue of the dystrophin-glycoprotein complex in Duchenne and Becker skeletal muscle explants by proteasome inhibitor treatment. *Am J Physiol Cell Physiol*, *290*(2), C577-82.

Babst, M. (2014). Quality control: quality control at the plasma membrane: one mechanism does not fit all. *J Cell Biol*, *205*(1), 11-20.

Baker, S. J. (2007). PTEN enters the nuclear age. *Cell*, *128*(1), 25-8.

Balk, S. P., & Knudsen, K. E. (2008). AR, the cell cycle, and prostate cancer. *Nucl Recept Signal*, *6*, e001.

Bao, X., Kobayashi, M., Hatakeyama, S., Angata, K., Gullberg, D., Nakayama, J., ... Fukuda, M. (2009). Tumor suppressor function of laminin-binding alpha-dystroglycan requires a distinct beta3-N-acetylglucosaminyltransferase. *Proc Natl Acad Sci U S A*, *106*(29), 12109-14.

Barresi, R., & Campbell, K. P. (2006). Dystroglycan: from biosynthesis to pathogenesis of human disease. *J Cell Sci*, *119*(2), 199-207.

Barrowman, J., Hamblet, C., George, C. M., & Michaelis, S. (2008). Analysis of prelamin A biogenesis reveals the nucleus to be a CaaX processing compartment. *Mol Biol Cell*, *19*(12), 5398-408.

Barrowman, J., Hamblet, C., Kane, M. S., & Michaelis, S. (2012). Requirements for efficient proteolytic cleavage of prelamin A by ZMPSTE24. *PLoS One*, *7*(2), e32120.

Batchelor, C. L., Higginson, J. R., Chen, Y. J., Vanni, C., Eva, A., & Winder, S. J. (2007). Recruitment of Dbl by ezrin and dystroglycan drives membrane proximal Cdc42 activation and filopodia formation. *Cell Cycle*, *6*(3), 353-63.

Bays, N. W., Gardner, R. G., Seelig, L. P., Joazeiro, C. A., & Hampton, R. Y. (2001). Hrd1p/Der3p is a membrane-anchored ubiquitin ligase required for ER-associated degradation. *Nat Cell Biol*, *3*(1), 24-9.

Behrens, J., von Kries, J. P., Kühl, M., Bruhn, L., Wedlich, D., Grosschedl, R., & Birchmeier, W. (1996). Functional interaction of beta-catenin with the transcription factor LEF-1. *Nature*, *382*(6592), 638-42.

Bell, S. P., & Dutta, A. (2002). DNA replication in eukaryotic cells. *Annu Rev Biochem*, *71*, 333-74.

Bello, V., Moreau, N., Sirour, C., Hidalgo, M., Buisson, N., & Darribère, T. (2015). The dystroglycan: Nestled in an adhesome during embryonic development. *Dev Biol*, *401*(1), 132-42.

Bhat, K. M. (2014). Notch signaling acts before cell division to promote asymmetric cleavage and cell fate of neural precursor cells. *Sci Signal*, *7*(348), ra101.

Bhat, K. P., & Greer, S. F. (2011). Proteolytic and non-proteolytic roles of ubiquitin and the ubiquitin proteasome system in transcriptional regulation. *Biochim Biophys Acta*, *1809*(2), 150-5.

Blanpain, C. (2013). Tracing the cellular origin of cancer. *Nat Cell Biol*, *15*(2), 126-34.

Bodine, S. C., Latres, E., Baumhueter, S., Lai, V. K., Nunez, L., Clarke, B. A., ... Glass, D. J. (2001). Identification of ubiquitin ligases required for skeletal muscle atrophy. *Science*, *294*(5547), 1704-8.

Boffi, A., Bozzi, M., Sciandra, F., Woellner, C., Bigotti, M. G., Ilari, A., & Brancaccio, A. (2001). Plasticity of secondary structure in the N-terminal region of beta-dystroglycan. *Biochim Biophys Acta*, *1546*(1), 114-21.

Bogenrieder, T., & Herlyn, M. (2003). Axis of evil: molecular mechanisms of cancer metastasis. *Oncogene*, *22*(42), 6524-36.

Boland, C. R. (2003). Tumor formation: number of mutations required. *eLS*.

Bonuccelli, G., Sotgia, F., Capozza, F., Gazzerro, E., Minetti, C., & Lisanti, M. P. (2007). Localized treatment with a novel FDA-approved proteasome inhibitor blocks the degradation of dystrophin and dystrophin-associated proteins in mdx mice. *Cell Cycle*, *6*(10), 1242-8.

Bonuccelli, G., Sotgia, F., Schubert, W., Park, D. S., Frank, P. G., Woodman, S. E., ... Lisanti, M. P. (2003). Proteasome inhibitor (MG-132) treatment of mdx mice rescues the expression and membrane localization of dystrophin and dystrophin-associated proteins. *Am J Pathol*, *163*(4), 1663-75.

Bozzi, M., Inzitari, R., Sbardell, D., Monaco, S., Pavoni, E., Gioia, M., ... Coletta, M. (2009). Enzymatic processing of beta-dystroglycan recombinant ectodomain by MMP-9: identification of the main cleavage site. *IUBMB Life*, *61*(12), 1143-52.

Bozzi, M., Morlacchi, S., Bigotti, M. G., Sciandra, F., & Brancaccio, A. (2009). Functional diversity of dystroglycan. *Matrix Biol*, *28*(4), 179-87.

Brancaccio, A. (2012). DAG1, no gene for RNA regulation? *Gene*, *497*(1), 79-82.

Brancaccio, A., Schulthess, T., Gesemann, M., & Engel, J. (1995). Electron microscopic evidence for a mucin-like region in chick muscle alpha-dystroglycan. *FEBS Lett*, *368*(1), 139-42.

Brancaccio, A., Schulthess, T., Gesemann, M., & Engel, J. (1997). The N-terminal region of alpha-dystroglycan is an autonomous globular domain. *Eur J Biochem*, *246*(1), 166-72.

Brehmer, B., Biesterfeld, S., & Jakse, G. (2003). Expression of matrix metalloproteinases (MMP-2 and -9) and their inhibitors (TIMP-1 and -2) in prostate cancer tissue. *Prostate Cancer Prostatic Dis*, *6*(3), 217-22.

Brown, S. C., & Winder, S. J. (2012). Dystroglycan and dystroglycanopathies: report of the 187th ENMC Workshop 11-13 November 2011, Naarden, The Netherlands. *Neuromuscul Disord*, *22*(7), 659-68.

Cai, C., Hsieh, C. L., Omwancha, J., Zheng, Z., Chen, S. Y., Baert, J. L., & Shemshedini, L. (2007). ETV1 is a novel androgen receptor-regulated

gene that mediates prostate cancer cell invasion. *Mol Endocrinol*, *21*(8), 1835-46.

Cao, W., Henry, M. D., Borrow, P., Yamada, H., Elder, J. H., Ravkov, E. V., ... Oldstone, M. B. (1998). Identification of alpha-dystroglycan as a receptor for lymphocytic choriomeningitis virus and Lassa fever virus. *Science*, *282*(5396), 2079-81.

Carmignac, V., Quéré, R., & Durbeej, M. (2011). Proteasome inhibition improves the muscle of laminin α2 chain-deficient mice. *Hum Mol Genet*, *20*(3), 541-52.

Carpenter, G., & Liao, H. J. (2009). Trafficking of receptor tyrosine kinases to the nucleus. *Exp Cell Res*, *315*(9), 1556-66.

Cartaud, A., Coutant, S., Petrucci, T. C., & Cartaud, J. (1998). Evidence for in situ and in vitro association between beta-dystroglycan and the subsynaptic 43K rapsyn protein. consequence for acetylcholine receptor clustering at the synapse. *J Biol Chem*, *273*(18), 11321-6.

Carter, S., Bischof, O., Dejean, A., & Vousden, K. H. (2007). C-terminal modifications regulate MDM2 dissociation and nuclear export of p53. *Nat Cell Biol*, *9*(4), 428-35.

Cavaldesi, M., Macchia, G., Barca, S., Defilippi, P., Tarone, G., & Petrucci, T. C. (1999). Association of the dystroglycan complex isolated from bovine brain synaptosomes with proteins involved in signal transduction. *J Neurochem*, *72*(4), 1648-55.

Cerecedo, D., Cisneros, B., Suárez-Sánchez, R., Hernández-González, E., & Galván, I. (2008). beta-Dystroglycan modulates the interplay between actin and microtubules in human-adhered platelets. *Br J Haematol*, *141*(4), 517-28.

Chen, B. B., & Mallampalli, R. K. (2009). Masking of a nuclear signal motif by monoubiquitination leads to mislocalization and degradation of the regulatory enzyme cytidylyltransferase. *Mol Cell Biol*, *29*(11), 3062-75.

Chen, C. L., Lin, Y. P., Lai, Y. C., & Chen, H. C. (2011). α-Adducin translocates to the nucleus upon loss of cell-cell adhesions. *Traffic*, *12*(10), 1327-40.

Chen, Y. J., Spence, H. J., Cameron, J. M., Jess, T., Ilsley, J. L., & Winder, S. J. (2003). Direct interaction of beta-dystroglycan with F-actin. *Biochem J*, *375*(2), 329-37.

Chesire, D. R., & Isaacs, W. B. (2002). Ligand-dependent inhibition of beta-catenin/TCF signaling by androgen receptor. *Oncogene*, *21*(55), 8453-69.

Choudhary, C., & Mann, M. (2010). Decoding signalling networks by mass spectrometry-based proteomics. *Nat Rev Mol Cell Biol*, *11*(6), 427-39.

Chuderland, D., Konson, A., & Seger, R. (2008). Identification and characterization of a general nuclear translocation signal in signaling proteins. *Mol Cell*, *31*(6), 850-61.

Collins, A. T., & Maitland, N. J. (2006). Prostate cancer stem cells. *Eur J Cancer*, *42*(9), 1213-8.

Constantin, B. (2014). Dystrophin complex functions as a scaffold for signalling

proteins. *Biochim Biophys Acta*, *1838*(2), 635-42.

Crisp, M., Liu, Q., Roux, K., Rattner, J. B., Shanahan, C., Burke, B., ... Hodzic, D. (2006). Coupling of the nucleus and cytoplasm: role of the LINC complex. *J Cell Biol*, *172*(1), 41-53.

Cross, S. S., Lippitt, J., Mitchell, A., Hollingsbury, F., Balasubramanian, S. P., Reed, M. W., ... Winder, S. J. (2008). Expression of beta-dystroglycan is reduced or absent in many human carcinomas. *Histopathology*, *53*(5), 561-6.

Cupers, P., Orlans, I., Craessaerts, K., Annaert, W., & De Strooper, B. (2001). The amyloid precursor protein (APP)-cytoplasmic fragment generated by gamma-secretase is rapidly degraded but distributes partially in a nuclear fraction of neurones in culture. *J Neurochem*, *78*(5), 1168-78.

Davies, B. S., Fong, L. G., Yang, S. H., Coffinier, C., & Young, S. G. (2009). The posttranslational processing of prelamin A and disease. *Annu Rev Genomics Hum Genet*, *10*, 153-74.

de Bernabé, D. B., Inamori, K., Yoshida-Moriguchi, T., Weydert, C. J., Harper, H. A., Willer, T., ... Campbell, K. P. (2009). Loss of alpha-dystroglycan laminin binding in epithelium-derived cancers is caused by silencing of LARGE. *J Biol Chem*, *284*(17), 11279-84.

Dechat, T., Adam, S. A., Taimen, P., Shimi, T., & Goldman, R. D. (2010). Nuclear lamins. *Cold Spring Harb Perspect Biol*, *2*(11), a000547.

de Lanerolle, P., & Serebryannyy, L. (2011). Nuclear actin and myosins: life without filaments. *Nat Cell Biol*, *13*(11), 1282-8.

Deng, W. M., Schneider, M., Frock, R., Castillejo-Lopez, C., Gaman, E. A., Baumgartner, S., & Ruohola-Baker, H. (2003). Dystroglycan is required for polarizing the epithelial cells and the oocyte in Drosophila. *Development*, *130*(1), 173-84.

Deribe, Y. L., Pawson, T., & Dikic, I. (2010). Post-translational modifications in signal integration. *Nat Struct Mol Biol*, *17*(6), 666-72.

De Strooper, B., Annaert, W., Cupers, P., Saftig, P., Craessaerts, K., Mumm, J. S., ... Kopan, R. (1999). A presenilin-1-dependent gamma-secretase-like protease mediates release of Notch intracellular domain. *Nature*, *398*(6727), 518-22.

De Strooper, B., Beullens, M., Contreras, B., Levesque, L., Craessaerts, K., Cordell, B., ... Van Leuven, F. (1997). Phosphorylation, subcellular localization, and membrane orientation of the Alzheimer's disease-associated presenilins. *J Biol Chem*, *272*(6), 3590-8.

De Strooper, B., Saftig, P., Craessaerts, K., Vanderstichele, H., Guhde, G., Annaert, W., ... Van Leuven, F. (1998). Deficiency of presenilin-1 inhibits the normal cleavage of amyloid precursor protein. *Nature*, *391*(6665), 387-90.

Di Stasio, E., Sciandra, F., Maras, B., Di Tommaso, F., Petrucci, T. C., Giardina, B., & Brancaccio, A. (1999). Structural and functional analysis of the N-terminal extracellular region of beta-dystroglycan. *Biochem Biophys Res Commun*, *266*(1), 274-8.

Dong, M., Noguchi, S., Endo, Y., Hayashi, Y. K., Yoshida, S., Nonaka, I.,

& Nishino, I. (2015). DAG1 mutations associated with asymptomatic hyperCKemia and hypoglycosylation of alpha-dystroglycan. *Neurology*, *84*(3), 273-9.

Douville, P. J., Harvey, W. J., & Carbonetto, S. (1988). Isolation and partial characterization of high affinity laminin receptors in neural cells. *J Biol Chem*, *263*(29), 14964-9.

Dovey, H. F., John, V., Anderson, J. P., Chen, L. Z., de Saint Andrieu, P., Fang, L. Y., ... Audia, J. E. (2001). Functional gamma-secretase inhibitors reduce beta-amyloid peptide levels in brain. *J Neurochem*, *76*(1), 173-81.

Dundr, M., & Misteli, T. (2010). Biogenesis of nuclear bodies. *Cold Spring Harb Perspect Biol*, *2*(12), a000711.

Dundr, M., Ospina, J. K., Sung, M. H., John, S., Upender, M., Ried, T., ... Matera, A. G. (2007). Actin-dependent intranuclear repositioning of an active gene locus in vivo. *J Cell Biol*, *179*(6), 1095-103.

Ehmsen, J., Poon, E., & Davies, K. (2002). The dystrophin-associated protein complex. *J Cell Sci*, *115*(14), 2801-3.

Einhauer, A., & Jungbauer, A. (2001). The FLAG peptide, a versatile fusion tag for the purification of recombinant proteins. *J Biochem Biophys Methods*, *49*(1-3), 455-65.

Emery, A. E. (2008). Resistance to infection and the muscular dystrophies–is there a molecular link? *Neuromuscul Disord*, *18*(5), 423-5.

Ervasti, J. M., & Campbell, K. P. (1991). Membrane organization of the dystrophin-glycoprotein complex. *Cell*, *66*(6), 1121-31.

Ervasti, J. M., & Campbell, K. P. (1993). A role for the dystrophin-glycoprotein complex as a transmembrane linker between laminin and actin. *J Cell Biol*, *122*(4), 809-23.

Ervasti, J. M., Ohlendieck, K., Kahl, S. D., Gaver, M. G., & Campbell, K. P. (1990). Deficiency of a glycoprotein component of the dystrophin complex in dystrophic muscle. *Nature*, *345*(6273), 315-9.

Esser, A. K., Miller, M. R., Huang, Q., Meier, M. M., Beltran-Valero de Bernabé, D., Stipp, C. S., ... Henry, M. D. (2013). Loss of LARGE2 disrupts functional glycosylation of α-dystroglycan in prostate cancer. *J Biol Chem*, *288*(4), 2132-42.

Eyermann, C., Czaplinski, K., & Colognato, H. (2012). Dystroglycan promotes filopodial formation and process branching in differentiating oligodendroglia. *J Neurochem*, *120*(6), 928-47.

Fehon, R. G., McClatchey, A. I., & Bretscher, A. (2010). Organizing the cell cortex: the role of ERM proteins. *Nat Rev Mol Cell Biol*, *11*(4), 276-87.

Ferletta, M., Kikkawa, Y., Yu, H., Talts, J. F., Durbeej, M., Sonnenberg, A., ... Genersch, E. (2003). Opposing roles of integrin alpha6Abeta1 and dystroglycan in laminin-mediated extracellular signal-regulated kinase activation. *Mol Biol Cell*, *14*(5), 2088-103.

Fernald, K., & Kurokawa, M. (2013). Evading apoptosis in cancer. *Trends Cell Biol*, *23*(12), 620-33.

Field, C. M., & Lénárt, P. (2011). Bulk cytoplasmic actin and its functions in

meiosis and mitosis. *Curr Biol*, *21*(19), R825-30.

Filtz, T. M., Vogel, W. K., & Leid, M. (2014). Regulation of transcription factor activity by interconnected post-translational modifications. *Trends Pharmacol Sci*, *35*(2), 76-85.

Fincham, V. J., James, M., Frame, M. C., & Winder, S. J. (2000). Active ERK/MAP kinase is targeted to newly forming cell-matrix adhesions by integrin engagement and v-Src. *EMBO J*, *19*(12), 2911-23.

Finn, D. M., & Ohlendieck, K. (1998). Oligomerization of beta-dystroglycan in rabbit diaphragm and brain as revealed by chemical crosslinking. *Biochim Biophys Acta*, *1370*(2), 325-36.

Floyd, Z. E., Trausch-Azar, J. S., Reinstein, E., Ciechanover, A., & Schwartz, A. L. (2001). The nuclear ubiquitin-proteasome system degrades MyoD. *J Biol Chem*, *276*(25), 22468-75.

Forsburg, S. L. (2004). Eukaryotic MCM proteins: beyond replication initiation. *Microbiol Mol Biol Rev*, *68*(1), 109-31.

Fortunato, M. J., Ball, C. E., Hollinger, K., Patel, N. B., Modi, J. N., Rajasekaran, V., ... Beedle, A. M. (2014). Development of rabbit monoclonal antibodies for detection of alpha-dystroglycan in normal and dystrophic tissue. *PLoS One*, *9*(5), e97567.

Frost, A. R., Böhm, S. V., Sewduth, R. N., Josifova, D., Ogilvie, C. M., Izatt, L., & Roberts, R. G. (2010). Heterozygous deletion of a 2-Mb region including the dystroglycan gene in a patient with mild myopathy, facial hypotonia, oral-motor dyspraxia and white matter abnormalities. *Eur J Hum Genet*, *18*(7), 852-5.

Fuentes-Mera, L., Rodríguez-Muñoz, R., González-Ramírez, R., García-Sierra, F., González, E., Mornet, D., & Cisneros, B. (2006). Characterization of a novel Dp71 dystrophin-associated protein complex (DAPC) present in the nucleus of HeLa cells: members of the nuclear DAPC associate with the nuclear matrix. *Exp Cell Res*, *312*(16), 3023-35.

Gao, S., Alarcón, C., Sapkota, G., Rahman, S., Chen, P. Y., Goerner, N., ... Massagué, J. (2009). Ubiquitin ligase Nedd4L targets activated Smad2/3 to limit TGF-beta signaling. *Mol Cell*, *36*(3), 457-68.

García-Alai, M. M., Gallo, M., Salame, M., Wetzler, D. E., McBride, A. A., Paci, M., ... de Prat-Gay, G. (2006). Molecular basis for phosphorylation-dependent, PEST-mediated protein turnover. *Structure*, *14*(2), 309-19.

Gazzerro, E., Assereto, S., Bonetto, A., Sotgia, F., Scarfì, S., Pistorio, A., ... Minetti, C. (2010). Therapeutic potential of proteasome inhibition in Duchenne and Becker muscular dystrophies. *Am J Pathol*, *176*(4), 1863-77.

Gebbink, M. F., Zondag, G. C., Koningstein, G. M., Feiken, E., Wubbolts, R. W., & Moolenaar, W. H. (1995). Cell surface expression of receptor protein tyrosine phosphatase RPTP mu is regulated by cell-cell contact. *J Cell Biol*, *131*(1), 251-60.

Gee, S. H., Blacher, R. W., Douville, P. J., Provost, P. R., Yurchenco, P. D., & Carbonetto, S. (1993). Laminin-binding protein 120 from brain is

closely related to the dystrophin-associated glycoprotein, dystroglycan, and binds with high affinity to the major heparin binding domain of laminin. *J Biol Chem*, *268*(20), 14972-80.

Geis, T., Marquard, K., Rödl, T., Reihle, C., Schirmer, S., von Kalle, T., ... Blankenburg, M. (2013). Homozygous dystroglycan mutation associated with a novel muscle-eye-brain disease-like phenotype with multicystic leucodystrophy. *Neurogenetics*, *14*(3-4), 205-13.

Gewinner, C., Hart, G., Zachara, N., Cole, R., Beisenherz-Huss, C., & Groner, B. (2004). The coactivator of transcription CREB-binding protein interacts preferentially with the glycosylated form of Stat5. *J Biol Chem*, *279*(5), 3563-72.

Godfrey, C., Foley, A. R., Clement, E., & Muntoni, F. (2011). Dystroglycanopathies: coming into focus. *Curr Opin Genet Dev*, *21*(3), 278-85.

Goldschneider, D., Rama, N., Guix, C., & Mehlen, P. (2008). The neogenin intracellular domain regulates gene transcription via nuclear translocation. *Mol Cell Biol*, *28*(12), 4068-79.

González, E., Montañez, C., Ray, P. N., Howard, P. L., García-Sierra, F., Mornet, D., & Cisneros, B. (2000). Alternative splicing regulates the nuclear or cytoplasmic localization of dystrophin Dp71. *FEBS Lett*, *482*(3), 209-14.

González-Ramírez, R., Morales-Lázaro, S. L., Tapia-Ramírez, V., Mornet, D., & Cisneros, B. (2008). Nuclear and nuclear envelope localization of dystrophin Dp71 and dystrophin-associated proteins (DAPs) in the C2C12 muscle cells: DAPs nuclear localization is modulated during myogenesis. *J Cell Biochem*, *105*(3), 735-45.

Gordon, J. A. (1991). Use of vanadate as protein-phosphotyrosine phosphatase inhibitor. *Methods Enzymol*, *201*, 477-82.

Grisoni, K., Martin, E., Gieseler, K., Mariol, M. C., & Ségalat, L. (2002). Genetic evidence for a dystrophin-glycoprotein complex (DGC) in *Caenorhabditis elegans*. *Gene*, *294*(1-2), 77-86.

Guinez, C., Morelle, W., Michalski, J. C., & Lefebvre, T. (2005). O-GlcNAc glycosylation: a signal for the nuclear transport of cytosolic proteins? *Int J Biochem Cell Biol*, *37*(4), 765-74.

Gundersen, G. G., & Worman, H. J. (2013). Nuclear positioning. *Cell*, *152*(6), 1376-89.

Gupta, V., Kawahara, G., Gundry, S. R., Chen, A. T., Lencer, W. I., Zhou, Y., ... Beggs, A. H. (2011). The zebrafish dag1 mutant: a novel genetic model for dystroglycanopathies. *Hum Mol Genet*, *20*(9), 1712-25.

Górecki, D. C., Derry, J. M., & Barnard, E. A. (1994). Dystroglycan: brain localisation and chromosome mapping in the mouse. *Hum Mol Genet*, *3*(9), 1589-97.

Haglund, K., & Dikic, I. (2012). The role of ubiquitylation in receptor endocytosis and endosomal sorting. *J Cell Sci*, *125*(2), 265-75.

Hainaut, P., & Plymoth, A. (2013). Targeting the hallmarks of cancer: towards a rational approach to next-generation cancer therapy. *Curr Opin Oncol*, *25*(1), 50-1.

Hall, H., Bozic, D., Michel, K., & Hubbell, J. A. (2003). N-terminal alpha-dystroglycan binds to different extracellular matrix molecules expressed in regenerating peripheral nerves in a protein-mediated manner and promotes neurite extension of PC12 cells. *Mol Cell Neurosci*, *24*(4), 1062-73.

Hanahan, D., & Weinberg, R. A. (2011). Hallmarks of cancer: the next generation. *Cell*, *144*(5), 646-74.

Hansson, C. A., Frykman, S., Farmery, M. R., Tjernberg, L. O., Nilsberth, C., Pursglove, S. E., ... Ankarcrona, M. (2004). Nicastrin, presenilin, APH-1, and PEN-2 form active gamma-secretase complexes in mitochondria. *J Biol Chem*, *279*(49), 51654-60.

Hara, Y., Balci-Hayta, B., Yoshida-Moriguchi, T., Kanagawa, M., Beltrán-Valero de Bernabé, D., Gündeşli, H., ... Campbell, K. P. (2011). A dystroglycan mutation associated with limb-girdle muscular dystrophy. *N Engl J Med*, *364*(10), 939-46.

Harrison, R., Hitchen, P. G., Panico, M., Morris, H. R., Mekhaiel, D., Pleass, R. J., ... Haslam, S. M. (2012). Glycoproteomic characterization of recombinant mouse α-dystroglycan. *Glycobiology*, *22*(5), 662-75.

Hart, G. W., & West, C. M. (2009). Nucleocytoplasmic glycosylation.

Helliwell, T. R., Nguyen, T. M., & Morris, G. E. (1994). Expression of the 43 kDa dystrophin-associated glycoprotein in human neuromuscular disease. *Neuromuscul Disord*, *4*(2), 101-13.

Hellwinkel, O. J., Asong, L. E., Rogmann, J. P., Sültmann, H., Wagner, C., Schlomm, T., & Eichelberg, C. (2011). Transcription alterations of members of the ubiquitin-proteasome network in prostate carcinoma. *Prostate Cancer Prostatic Dis*, *14*(1), 38-45.

Hemming, M. L., Elias, J. E., Gygi, S. P., & Selkoe, D. J. (2008). Proteomic profiling of gamma-secretase substrates and mapping of substrate requirements. *PLoS Biol*, *6*(10), e257.

Henry, M. D., & Campbell, K. P. (1999). Dystroglycan inside and out. *Curr Opin Cell Biol*, *11*(5), 602-7.

Henry, M. D., Cohen, M. B., & Campbell, K. P. (2001). Reduced expression of dystroglycan in breast and prostate cancer. *Hum Pathol*, *32*(8), 791-5.

Hesse, C., Johansson, I., Mattsson, N., Bremell, D., Andreasson, U., Halim, A., ... Grahn, A. (2011). The N-terminal domain of alpha-dystroglycan, released as a 38 kDa protein, is increased in cerebrospinal fluid in patients with Lyme neuroborreliosis. *Biochem Biophys Res Commun*, *412*(3), 494-9.

Hesson, L. B., Cooper, W. N., & Latif, F. (2007). Evaluation of the 3p21.3 tumour-suppressor gene cluster. *Oncogene*, *26*(52), 7283-301.

Hetzl, A. C., Fávaro, W. J., Billis, A., Ferreira, U., & Cagnon, V. H. (2012). Steroid hormone receptors, matrix metalloproteinases, insulin-like growth factor, and dystroglycans interactions in prostatic diseases in the elderly men. *Microsc Res Tech*, *75*(9), 1197-205.

Hieda, M., Isokane, M., Koizumi, M., Higashi, C., Tachibana, T., Shudou, M., ... Higashiyama, S. (2008). Membrane-anchored growth factor, HB-

EGF, on the cell surface targeted to the inner nuclear membrane. *J Cell Biol*, *180*(4), 763-9.

Higginson, J. R., Thompson, O., & Winder, S. J. (2008). Targeting of dystroglycan to the cleavage furrow and midbody in cytokinesis. *Int J Biochem Cell Biol*, *40*(5), 892-900.

Hochstrasser, M. (2009). Origin and function of ubiquitin-like proteins. *Nature*, *458*(7237), 422-9.

Hodzic, D. M., Yeater, D. B., Bengtsson, L., Otto, H., & Stahl, P. D. (2004). Sun2 is a novel mammalian inner nuclear membrane protein. *J Biol Chem*, *279*(24), 25805-12.

Holt, K. H., Crosbie, R. H., Venzke, D. P., & Campbell, K. P. (2000). Biosynthesis of dystroglycan: processing of a precursor propeptide. *FEBS Lett*, *468*(1), 79-83.

Hood, J. D., & Cheresh, D. A. (2002). Role of integrins in cell invasion and migration. *Nat Rev Cancer*, *2*(2), 91-100.

Horoszewicz, J. S., Leong, S. S., Kawinski, E., Karr, J. P., Rosenthal, H., Chu, T. M., ... Murphy, G. P. (1983). LNCaP model of human prostatic carcinoma. *Cancer Res*, *43*(4), 1809-18.

Hosokawa, H., Ninomiya, H., Kitamura, Y., Fujiwara, K., & Masaki, T. (2002). Vascular endothelial cells that express dystroglycan are involved in angiogenesis. *J Cell Sci*, *115*(7), 1487-96.

Hu, X. Y., Xu, Y. M., Fu, Q., Yu, J. J., & Huang, J. (2009). Nedd4L expression is downregulated in prostate cancer compared to benign prostatic hyperplasia. *Eur J Surg Oncol*, *35*(5), 527-31.

Humphrey, E. L., Lacey, E., Le, L. T., Feng, L., Sciandra, F., Morris, C. R., ... Morris, G. E. (2015). A new monoclonal antibody DAG-6F4 against human alpha-dystroglycan reveals reduced core protein in some, but not all, dystroglycanopathy patients. *Neuromuscul Disord*, *25*(1), 32-42.

Ibraghimov-Beskrovnaya, O., Ervasti, J. M., Leveille, C. J., Slaughter, C. A., Sernett, S. W., & Campbell, K. P. (1992). Primary structure of dystrophin-associated glycoproteins linking dystrophin to the extracellular matrix. *Nature*, *355*(6362), 696-702.

Ibraghimov-Beskrovnaya, O., Milatovich, A., Ozcelik, T., Yang, B., Koepnick, K., Francke, U., & Campbell, K. P. (1993). Human dystroglycan: skeletal muscle cDNA, genomic structure, origin of tissue specific isoforms and chromosomal localization. *Hum Mol Genet*, *2*(10), 1651-7.

Ilsley, J. L., Sudol, M., & Winder, S. J. (2001). The interaction of dystrophin with beta-dystroglycan is regulated by tyrosine phosphorylation. *Cell Signal*, *13*(9), 625-32.

Ilsley, J. L., Sudol, M., & Winder, S. J. (2002). The WW domain: linking cell signalling to the membrane cytoskeleton. *Cell Signal*, *14*(3), 183-9.

Jae, L. T., Raaben, M., Riemersma, M., van Beusekom, E., Blomen, V. A., Velds, A., ... Brummelkamp, T. R. (2013). Deciphering the glycosylome of dystroglycanopathies using haploid screens for lassa virus entry. *Science*, *340*(6131), 479-83.

James, M., Nuttall, A., Ilsley, J. L., Ottersbach, K., Tinsley, J. M., Sudol, M.,

& Winder, S. J. (2000). Adhesion-dependent tyrosine phosphorylation of (beta)-dystroglycan regulates its interaction with utrophin. *J Cell Sci*, *113 (10)*, 1717-26.

Jensen, O. N. (2006). Interpreting the protein language using proteomics. *Nat Rev Mol Cell Biol*, *7*(6), 391-403.

Jeppsson, K., Kanno, T., Shirahige, K., & Sjögren, C. (2014). The maintenance of chromosome structure: positioning and functioning of SMC complexes. *Nat Rev Mol Cell Biol*, *15*(9), 601-14.

Ji, L., Minna, J. D., & Roth, J. A. (2005). 3p21.3 tumor suppressor cluster: prospects for translational applications. *Future Oncol*, *1*(1), 79-92.

Jing, J., Lien, C. F., Sharma, S., Rice, J., Brennan, P. A., & Górecki, D. C. (2004). Aberrant expression, processing and degradation of dystroglycan in squamous cell carcinomas. *Eur J Cancer*, *40*(14), 2143-51.

Johnson, E. K., Li, B., Yoon, J. H., Flanigan, K. M., Martin, P. T., Ervasti, J., & Montanaro, F. (2013). Identification of new dystroglycan complexes in skeletal muscle. *PLoS One*, *8*(8), e73224.

Jung, K. M., Tan, S., Landman, N., Petrova, K., Murray, S., Lewis, R., ... Kim, T. W. (2003). Regulated intramembrane proteolysis of the p75 neurotrophin receptor modulates its association with the TrkA receptor. *J Biol Chem*, *278*(43), 42161-9.

Kanagawa, M., Saito, F., Kunz, S., Yoshida-Moriguchi, T., Barresi, R., Kobayashi, Y. M., ... Campbell, K. P. (2004). Molecular recognition by LARGE is essential for expression of functional dystroglycan. *Cell*, *117*(7), 953-64.

Kang, R., Wan, J., Arstikaitis, P., Takahashi, H., Huang, K., Bailey, A. O., ... El-Husseini, A. (2008). Neural palmitoyl-proteomics reveals dynamic synaptic palmitoylation. *Nature*, *456*(7224), 904-9.

Kau, T. R., Way, J. C., & Silver, P. A. (2004). Nuclear transport and cancer: from mechanism to intervention. *Nat Rev Cancer*, *4*(2), 106-17.

Kelley, L. C., Lohmer, L. L., Hagedorn, E. J., & Sherwood, D. R. (2014). Traversing the basement membrane in vivo: a diversity of strategies. *J Cell Biol*, *204*(3), 291-302.

Kennedy, B. K., Barbie, D. A., Classon, M., Dyson, N., & Harlow, E. (2000). Nuclear organization of DNA replication in primary mammalian cells. *Genes Dev*, *14*(22), 2855-68.

Kim, W., Bennett, E. J., Huttlin, E. L., Guo, A., Li, J., Possemato, A., ... Gygi, S. P. (2011). Systematic and quantitative assessment of the ubiquitin-modified proteome. *Mol Cell*, *44*(2), 325-40.

Kim, Y. S., Kim, S. G., Park, J. E., Park, H. Y., Lim, M. H., Chua, N. H., & Park, C. M. (2006). A membrane-bound NAC transcription factor regulates cell division in Arabidopsis. *Plant Cell*, *18*(11), 3132-44.

Komander, D. (2009). The emerging complexity of protein ubiquitination. *Biochem Soc Trans*, *37*(5), 937-53.

Kopan, R. (2012). Notch signaling. *Cold Spring Harb Perspect Biol*, *4*(10).

Kopan, R., & Ilagan, M. X. (2004). Gamma-secretase: proteasome of the membrane? *Nat Rev Mol Cell Biol*, *5*(6), 499-504.

Kucherenko, M. M., Pantoja, M., Yatsenko, A. S., Shcherbata, H. R., Fischer, K. A., Maksymiv, D. V., ... Ruohola-Baker, H. (2008). Genetic modifier screens reveal new components that interact with the Drosophila dystroglycan-dystrophin complex. *PLoS One*, *3*(6), e2418.

Kumamoto, T., Fujimoto, S., Ito, T., Horinouchi, H., Ueyama, H., & Tsuda, T. (2000). Proteasome expression in the skeletal muscles of patients with muscular dystrophy. *Acta Neuropathol*, *100*(6), 595-602.

Kunda, P., & Baum, B. (2009). The actin cytoskeleton in spindle assembly and positioning. *Trends Cell Biol*, *19*(4), 174-9.

Kunz, S., Rojek, J. M., Kanagawa, M., Spiropoulou, C. F., Barresi, R., Campbell, K. P., & Oldstone, M. B. (2005). Posttranslational modification of alpha-dystroglycan, the cellular receptor for arenaviruses, by the glycosyltransferase LARGE is critical for virus binding. *J Virol*, *79*(22), 14282-96.

Kypta, R. M., & Waxman, J. (2012). Wnt/β-catenin signalling in prostate cancer. *Nat Rev Urol*, *9*(8), 418-28.

Laemmli, U. K. (1970). Cleavage of structural proteins during the assembly of the head of bacteriophage T4. *Nature*, *227*(5259), 680-5.

Lal, M., & Caplan, M. (2011). Regulated intramembrane proteolysis: signaling pathways and biological functions. *Physiology (Bethesda)*, *26*(1), 34-44.

Lammich, S., Okochi, M., Takeda, M., Kaether, C., Capell, A., Zimmer, A. K., ... Haass, C. (2002). Presenilin-dependent intramembrane proteolysis of CD44 leads to the liberation of its intracellular domain and the secretion of an Abeta-like peptide. *J Biol Chem*, *277*(47), 44754-9.

Lara-Chacón, B., de León, M. B., Leocadio, D., Gómez, P., Fuentes-Mera, L., Martínez-Vieyra, I., ... Cisneros, B. (2010). Characterization of an importin alpha/beta-recognized nuclear localization signal in beta-dystroglycan. *J Cell Biochem*, *110*(3), 706-17.

Lazebnik, Y. (2010). What are the hallmarks of cancer? *Nat Rev Cancer*, *10*(4), 232-3.

Lecker, S. H., Goldberg, A. L., & Mitch, W. E. (2006). Protein degradation by the ubiquitin-proteasome pathway in normal and disease states. *J Am Soc Nephrol*, *17*(7), 1807-19.

Lee, H. J., Jung, K. M., Huang, Y. Z., Bennett, L. B., Lee, J. S., Mei, L., & Kim, T. W. (2002). Presenilin-dependent gamma-secretase-like intramembrane cleavage of ErbB4. *J Biol Chem*, *277*(8), 6318-23.

Lee, K. A., Hammerle, L. P., Andrews, P. S., Stokes, M. P., Mustelin, T., Silva, J. C., ... Doedens, J. R. (2011). Ubiquitin ligase substrate identification through quantitative proteomics at both the protein and peptide levels. *J Biol Chem*, *286*(48), 41530-8.

Leeb, T., Neumann, S., Deppe, A., Breen, M., & Brenig, B. (2000). Genomic organization of the dog dystroglycan gene DAG1 locus on chromosome 20q15.1-q15.2. *Genome Res*, *10*(3), 295-301.

Lefebvre, T., Ferreira, S., Dupont-Wallois, L., Bussière, T., Dupire, M. J., Delacourte, A., ... Caillet-Boudin, M. L. (2003). Evidence of a balance between phosphorylation and O-GlcNAc glycosylation of Tau proteins–a

role in nuclear localization. *Biochim Biophys Acta*, *1619*(2), 167-76.

Legartová, S., Stixová, L., Laur, O., Kozubek, S., Sehnalová, P., & Bártová, E. (2014). Nuclear structures surrounding internal lamin invaginations. *J Cell Biochem*, *115*(3), 476-87.

Lemberg, M. K. (2011). Intramembrane proteolysis in regulated protein trafficking. *Traffic*, *12*(9), 1109-18.

Lerman, M. I., & Minna, J. D. (2000). The 630-kb lung cancer homozygous deletion region on human chromosome 3p21.3: identification and evaluation of the resident candidate tumor suppressor genes. The International Lung Cancer Chromosome 3p21.3 Tumor Suppressor Gene Consortium. *Cancer Res*, *60*(21), 6116-33.

Li, J., Xu, M., Zhou, H., Ma, J., & Potter, H. (1997). Alzheimer presenilins in the nuclear membrane, interphase kinetochores, and centrosomes suggest a role in chromosome segregation. *Cell*, *90*(5), 917-27.

Li, Y., Cong, R., & Biemesderfer, D. (2008). The COOH terminus of megalin regulates gene expression in opossum kidney proximal tubule cells. *Am J Physiol Cell Physiol*, *295*(2), C529-37.

Lodish, H., Berk, A., Matsudaira, P., Kaiser, C. A., Krieger, M., Scott, M. P., ... Darnell, J. (2008). Molecular cell biology, Fourth Edition. *W. H. Freeman*, 1-1150.

Losada, A. (2014). Cohesin in cancer: chromosome segregation and beyond. *Nat Rev Cancer*, *14*(6), 389-93.

Losasso, C., Di Tommaso, F., Sgambato, A., Ardito, R., Cittadini, A., Giardina, B., ... Brancaccio, A. (2000). Anomalous dystroglycan in carcinoma cell lines. *FEBS Lett*, *484*(3), 194-8.

Lu, P., Weaver, V. M., & Werb, Z. (2012). The extracellular matrix: a dynamic niche in cancer progression. *J Cell Biol*, *196*(4), 395-406.

Luo, M. L., Zhou, Z., Magni, K., Christoforides, C., Rappsilber, J., Mann, M., & Reed, R. (2001). Pre-mRNA splicing and mRNA export linked by direct interactions between UAP56 and Aly. *Nature*, *413*(6856), 644-7.

Luxton, G. W., & Starr, D. A. (2014). KASHing up with the nucleus: novel functional roles of KASH proteins at the cytoplasmic surface of the nucleus. *Curr Opin Cell Biol*, *28*, 69-75.

Maetzel, D., Denzel, S., Mack, B., Canis, M., Went, P., Benk, M., ... Gires, O. (2009). Nuclear signalling by tumour-associated antigen EpCAM. *Nat Cell Biol*, *11*(2), 162-71.

Maiorano, D., Lutzmann, M., & Méchali, M. (2006). MCM proteins and DNA replication. *Curr Opin Cell Biol*, *18*(2), 130-6.

Malaney, P., Pathak, R. R., Xue, B., Uversky, V. N., & Davé, V. (2013). Intrinsic disorder in PTEN and its interactome confers structural plasticity and functional versatility. *Sci Rep*, *3*, 2035.

Marquez, F. G., Cisneros, B., Garcia, F., Ceja, V., Velázquez, F., Depardón, F., ... Montañez, C. (2003). Differential expression and subcellular distribution of dystrophin Dp71 isoforms during differentiation process. *Neuroscience*, *118*(4), 957-66.

Martin, L. T., Glass, M., Dosunmu, E., & Martin, P. T. (2007). Altered

expression of natively glycosylated alpha-dystroglycan in pediatric solid tumors. *Hum Pathol*, *38*(11), 1657-68.

Martínez-Vieyra, I. A., Vásquez-Limeta, A., González-Ramírez, R., Morales-Lázaro, S. L., Mondragón, M., Mondragón, R., ... Cisneros, B. (2013). A role for beta-dystroglycan in the organization and structure of the nucleus in myoblasts. *Biochim Biophys Acta*, *1833*(3), 698-711.

Mathew, G., Mitchell, A., Down, J. M., Jacobs, L. A., Hamdy, F. C., Eaton, C., ... Winder, S. J. (2013). Nuclear targeting of dystroglycan promotes the expression of androgen regulated transcription factors in prostate cancer. *Sci Rep*, *3*, 2792.

Matsumoto, H., Maruse, H., Inaba, Y., Yoshizawa, K., Sasazaki, S., Fujiwara, A., ... Mannen, H. (2008). The ubiquitin ligase gene (WWP1) is responsible for the chicken muscular dystrophy. *FEBS Lett*, *582*(15), 2212-8.

Matsumura, K., Chiba, A., Yamada, H., Fukuta-Ohi, H., Fujita, S., Endo, T., ... Shimizu, T. (1997). A role of dystroglycan in schwannoma cell adhesion to laminin. *J Biol Chem*, *272*(21), 13904-10.

Matsumura, K., Zhong, D., Saito, F., Arai, K., Adachi, K., Kawai, H., ... Shimizu, T. (2005). Proteolysis of beta-dystroglycan in muscular diseases. *Neuromuscul Disord*, *15*(5), 336-41.

Mellacheruvu, D., Wright, Z., Couzens, A. L., Lambert, J. P., St-Denis, N. A., Li, T., ... Nesvizhskii, A. I. (2013). The CRAPome: a contaminant repository for affinity purification-mass spectrometry data. *Nat Methods*, *10*(8), 730-6.

Mercuri, E., & Muntoni, F. (2013). Muscular dystrophies. *Lancet*, *381*(9869), 845-60.

Merlo, L. M., Pepper, J. W., Reid, B. J., & Maley, C. C. (2006). Cancer as an evolutionary and ecological process. *Nat Rev Cancer*, *6*(12), 924-35.

Metzger, M. B., Hristova, V. A., & Weissman, A. M. (2012). HECT and RING finger families of E3 ubiquitin ligases at a glance. *J Cell Sci*, *125*(3), 531-7.

Meyer, R. D., Srinivasan, S., Singh, A. J., Mahoney, J. E., Gharahassanlou, K. R., & Rahimi, N. (2011). PEST motif serine and tyrosine phosphorylation controls vascular endothelial growth factor receptor 2 stability and downregulation. *Mol Cell Biol*, *31*(10), 2010-25.

Michaluk, P., Kolodziej, L., Mioduszewska, B., Wilczynski, G. M., Dzwonek, J., Jaworski, J., ... Kaczmarek, L. (2007). Beta-dystroglycan as a target for MMP-9, in response to enhanced neuronal activity. *J Biol Chem*, *282*(22), 16036-41.

Michele, D. E., Barresi, R., Kanagawa, M., Saito, F., Cohn, R. D., Satz, J. S., ... Campbell, K. P. (2002). Post-translational disruption of dystroglycan-ligand interactions in congenital muscular dystrophies. *Nature*, *418*(6896), 417-22.

Michele, D. E., & Campbell, K. P. (2003). Dystrophin-glycoprotein complex: post-translational processing and dystroglycan function. *J Biol Chem*, *278*(18), 15457-60.

Miller, G., Moore, C. J., Terry, R., La Riviere, T., Mitchell, A., Piggott, R.,

... Winder, S. J. (2012). Preventing phosphorylation of dystroglycan ameliorates the dystrophic phenotype in mdx mouse. *Hum Mol Genet*, *21*(20), 4508-20.

Miralles, F., Posern, G., Zaromytidou, A. I., & Treisman, R. (2003). Actin dynamics control SRF activity by regulation of its coactivator MAL. *Cell*, *113*(3), 329-42.

Mitchell, A., Mathew, G., Jiang, T., Hamdy, F. C., Cross, S. S., Eaton, C., & Winder, S. J. (2013). Dystroglycan function is a novel determinant of tumor growth and behavior in prostate cancer. *Prostate*, *73*(4), 398-408.

Molenaar, M., van de Wetering, M., Oosterwegel, M., Peterson-Maduro, J., Godsave, S., Korinek, V., ... Clevers, H. (1996). XTcf-3 transcription factor mediates beta-catenin-induced axis formation in Xenopus embryos. *Cell*, *86*(3), 391-9.

Montanaro, F., Lindenbaum, M., & Carbonetto, S. (1999). alpha-Dystroglycan is a laminin receptor involved in extracellular matrix assembly on myotubes and muscle cell viability. *J Cell Biol*, *145*(6), 1325-40.

Moore, C. J., & Winder, S. J. (2010). Dystroglycan versatility in cell adhesion: a tale of multiple motifs. *Cell Commun Signal*, *8*, 3.

Moore, C. J., & Winder, S. J. (2012). The inside and out of dystroglycan post-translational modification. *Neuromuscul Disord*, *22*(11), 959-65.

Moraz, M. L., Pythoud, C., Turk, R., Rothenberger, S., Pasquato, A., Campbell, K. P., & Kunz, S. (2013). Cell entry of Lassa virus induces tyrosine phosphorylation of dystroglycan. *Cell Microbiol*, *15*(5), 689-700.

Morgan, A. R., Han, D. Y., Lam, W. J., Fraser, A. G., & Ferguson, L. R. (2010). Association analysis of 3p21 with Crohn's disease in a New Zealand population. *Hum Immunol*, *71*(6), 602-9.

Morrissey, C., & Vessella, R. L. (2007). The role of tumor microenvironment in prostate cancer bone metastasis. *J Cell Biochem*, *101*(4), 873-86.

Morton, R. A., Ewing, C. M., Nagafuchi, A., Tsukita, S., & Isaacs, W. B. (1993). Reduction of E-cadherin levels and deletion of the alpha-catenin gene in human prostate cancer cells. *Cancer Res*, *53*(15), 3585-90.

Mulholland, D. J., Cheng, H., Reid, K., Rennie, P. S., & Nelson, C. C. (2002). The androgen receptor can promote beta-catenin nuclear translocation independently of adenomatous polyposis coli. *J Biol Chem*, *277*(20), 17933-43.

Mummery, R., Sessay, A., Lai, F. A., & Beesley, P. W. (1996). Beta-dystroglycan: subcellular localisation in rat brain and detection of a novel immunologically related, postsynaptic density-enriched protein. *J Neurochem*, *66*(6), 2455-9.

Murakami, D., Okamoto, I., Nagano, O., Kawano, Y., Tomita, T., Iwatsubo, T., ... Saya, H. (2003). Presenilin-dependent gamma-secretase activity mediates the intramembranous cleavage of CD44. *Oncogene*, *22*(10), 1511-6.

Murphy, D. A., & Courtneidge, S. A. (2011). The 'ins' and 'outs' of podosomes and invadopodia: characteristics, formation and function. *Nat Rev Mol Cell Biol*, *12*(7), 413-26.

Muschler, J., Levy, D., Boudreau, R., Henry, M., Campbell, K., & Bissell, M. J. (2002). A role for dystroglycan in epithelial polarization: loss of function in breast tumor cells. *Cancer Res*, *62*(23), 7102-9.

Ng, T., Parsons, M., Hughes, W. E., Monypenny, J., Zicha, D., Gautreau, A., ... Parker, P. J. (2001). Ezrin is a downstream effector of trafficking PKC-integrin complexes involved in the control of cell motility. *EMBO J*, *20*(11), 2723-41.

Nguyen, T. M., Le, T. T., Blake, D. J., Davies, K. E., & Morris, G. E. (1992). Utrophin, the autosomal homologue of dystrophin, is widely-expressed and membrane-associated in cultured cell lines. *FEBS Lett*, *313*(1), 19-22.

Nilsson, J., Larson, G., & Grahn, A. (2010). Characterization of site-specific O-glycan structures within the mucin-like domain of alpha-dystroglycan from human skeletal muscle. *Glycobiology*, *20*(9), 1160-9.

Oppizzi, M. L., Akhavan, A., Singh, M., Fata, J. E., & Muschler, J. L. (2008). Nuclear translocation of beta-dystroglycan reveals a distinctive trafficking pattern of autoproteolyzed mucins. *Traffic*, *9*(12), 2063-72.

Parberry-Clark, C., Bury, J. P., Cross, S. S., & Winder, S. J. (2011). Loss of dystroglycan function in oesophageal cancer. *Histopathology*, *59*(2), 180-7.

Parsons, M. J., Campos, I., Hirst, E. M., & Stemple, D. L. (2002). Removal of dystroglycan causes severe muscular dystrophy in zebrafish embryos. *Development*, *129*(14), 3505-12.

Pederson, T. (2008). As functional nuclear actin comes into view, is it globular, filamentous, or both? *J Cell Biol*, *180*(6), 1061-4.

Perkins, K. J., & Davies, K. E. (2012). Recent advances in duchenne muscular dystrophy. *Degener Neurol Neuromuscul Dis*, *2*, 141-164.

Petrof, B. J., Shrager, J. B., Stedman, H. H., Kelly, A. M., & Sweeney, H. L. (1993). Dystrophin protects the sarcolemma from stresses developed during muscle contraction. *Proc Natl Acad Sci U S A*, *90*(8), 3710-4.

Piggott, R. (2014). *The regulation of beta-dystroglycan internalization*. Thesis.

Pinchot, S. N., Jaskula-Sztul, R., Ning, L., Peters, N. R., Cook, M. R., Kunnimalaiyaan, M., & Chen, H. (2011). Identification and validation of Notch pathway activating compounds through a novel high-throughput screening method. *Cancer*, *117*(7), 1386-98.

Pinto-Teixeira, F., & Desplan, C. (2014). Notch activity in neural progenitors coordinates cytokinesis and asymmetric differentiation. *Sci Signal*, *7*(348), pe26.

Pirozzi, G., McConnell, S. J., Uveges, A. J., Carter, J. M., Sparks, A. B., Kay, B. K., & Fowlkes, D. M. (1997). Identification of novel human WW domain-containing proteins by cloning of ligand targets. *J Biol Chem*, *272*(23), 14611-6.

Prins, K. W., Humston, J. L., Mehta, A., Tate, V., Ralston, E., & Ervasti, J. M. (2009). Dystrophin is a microtubule-associated protein. *J Cell Biol*, *186*(3), 363-9.

Purow, B. (2012). Notch inhibition as a promising new approach to cancer

therapy. *Adv Exp Med Biol*, *727*, 305-19.

Ramakrishna, S., Suresh, B., Lim, K. H., Cha, B. H., Lee, S. H., Kim, K. S., & Baek, K. H. (2011). PEST motif sequence regulating human NANOG for proteasomal degradation. *Stem Cells Dev*, *20*(9), 1511-9.

Rambukkana, A., Yamada, H., Zanazzi, G., Mathus, T., Salzer, J. L., Yurchenco, P. D., ... Fischetti, V. A. (1998). Role of alpha-dystroglycan as a Schwann cell receptor for Mycobacterium leprae. *Science*, *282*(5396), 2076-9.

Ravid, T., & Hochstrasser, M. (2008). Diversity of degradation signals in the ubiquitin-proteasome system. *Nat Rev Mol Cell Biol*, *9*(9), 679-90.

Rechsteiner, M., & Rogers, S. W. (1996). PEST sequences and regulation by proteolysis. *Trends Biochem Sci*, *21*(7), 267-71.

Rentschler, S., Linn, H., Deininger, K., Bedford, M. T., Espanel, X., & Sudol, M. (1999). The WW domain of dystrophin requires EF-hands region to interact with beta-dystroglycan. *Biol Chem*, *380*(4), 431-42.

Resjö, S., Oknianska, A., Zolnierowicz, S., Manganiello, V., & Degerman, E. (1999). Phosphorylation and activation of phosphodiesterase type 3B (PDE3B) in adipocytes in response to serine/threonine phosphatase inhibitors: deactivation of PDE3B in vitro by protein phosphatase type 2A. *Biochem J*, *341 (3)*, 839-45.

Riemersma, M., Mandel, H., van Beusekom, E., Gazzoli, I., Roscioli, T., Eran, A., ... van Bokhoven, H. (2015). Absence of alpha- and beta-dystroglycan is associated with Walker-Warburg syndrome. *Neurology*.

Rockel, T. D., Stuhlmann, D., & von Mikecz, A. (2005). Proteasomes degrade proteins in focal subdomains of the human cell nucleus. *J Cell Sci*, *118*(22), 5231-42.

Rondanino, C., Bousser, M. T., Monsigny, M., & Roche, A. C. (2003). Sugar-dependent nuclear import of glycosylated proteins in living cells. *Glycobiology*, *13*(7), 509-19.

Rotin, D., & Kumar, S. (2009). Physiological functions of the HECT family of ubiquitin ligases. *Nat Rev Mol Cell Biol*, *10*(6), 398-409.

Ruff, S. J., Chen, K., & Cohen, S. (1997). Peroxovanadate induces tyrosine phosphorylation of multiple signaling proteins in mouse liver and kidney. *J Biol Chem*, *272*(2), 1263-7.

Russell, P. J., & Kingsley, E. A. (2003). Human prostate cancer cell lines. *Methods Mol Med*, *81*, 21-39.

Russo, K., Di Stasio, E., Macchia, G., Rosa, G., Brancaccio, A., & Petrucci, T. C. (2000). Characterization of the beta-dystroglycan-growth factor receptor 2 (Grb2) interaction. *Biochem Biophys Res Commun*, *274*(1), 93-8.

Saito, F., Blank, M., Schröder, J., Manya, H., Shimizu, T., Campbell, K. P., ... Matsumura, K. (2005). Aberrant glycosylation of alpha-dystroglycan causes defective binding of laminin in the muscle of chicken muscular dystrophy. *FEBS Lett*, *579*(11), 2359-63.

Saito, F., Saito-Arai, Y., Nakamura, A., Shimizu, T., & Matsumura, K. (2008). Processing and secretion of the N-terminal domain of alpha-dystroglycan

in cell culture media. *FEBS Lett*, *582*(3), 439-44.

Saito, F., Saito-Arai, Y., Nakamura-Okuma, A., Ikeda, M., Hagiwara, H., Masaki, T., ... Matsumura, K. (2011). Secretion of N-terminal domain of alpha-dystroglycan in cerebrospinal fluid. *Biochem Biophys Res Commun*, *411*(2), 365-9.

Salih, M. A., Sunada, Y., Al-Nasser, M., Ozo, C. O., Al-Turaiki, M. H., Akbar, M., & Campbell, K. P. (1996). Muscular dystrophy associated with beta-dystroglycan deficiency. *Ann Neurol*, *40*(6), 925-8.

Schägger, H., & von Jagow, G. (1987). Tricine-sodium dodecyl sulfate-polyacrylamide gel electrophoresis for the separation of proteins in the range from 1 to 100 kDa. *Anal Biochem*, *166*(2), 368-79.

Sciandra, F., Bozzi, M., Bianchi, M., Pavoni, E., Giardina, B., & Brancaccio, A. (2003). Dystroglycan and muscular dystrophies related to the dystrophin-glycoprotein complex. *Ann Ist Super Sanita*, *39*(2), 173-81.

Selkoe, D. J., & Wolfe, M. S. (2007). Presenilin: running with scissors in the membrane. *Cell*, *131*(2), 215-21.

Selsby, J., Morris, C., Morris, L., & Sweeney, L. (2012). A proteasome inhibitor fails to attenuate dystrophic pathology in mdx mice. *PLoS Curr*, *4*, e4f84a944d8930.

Sgambato, A., & Brancaccio, A. (2005). The dystroglycan complex: from biology to cancer. *J Cell Physiol*, *205*(2), 163-9.

Sgambato, A., De Paola, B., Migaldi, M., Di Salvatore, M., Rettino, A., Rossi, G., ... Cittadini, A. (2007). Dystroglycan expression is reduced during prostate tumorigenesis and is regulated by androgens in prostate cancer cells. *J Cell Physiol*, *213*(2), 528-39.

Sgambato, A., Di Salvatore, M. A., De Paola, B., Rettino, A., Faraglia, B., Boninsegna, A., ... Cittadini, A. (2006). Analysis of dystroglycan regulation and functions in mouse mammary epithelial cells and implications for mammary tumorigenesis. *J Cell Physiol*, *207*(2), 520-9.

Sgambato, A., Migaldi, M., Montanari, M., Camerini, A., Brancaccio, A., Rossi, G., ... Cittadini, A. (2003). Dystroglycan expression is frequently reduced in human breast and colon cancers and is associated with tumor progression. *Am J Pathol*, *162*(3), 849-60.

Sgambato, A., Tarquini, E., Resci, F., De Paola, B., Faraglia, B., Camerini, A., ... Zannoni, G. F. (2006). Aberrant expression of alpha-dystroglycan in cervical and vulvar cancer. *Gynecol Oncol*, *103*(2), 397-404.

Shah, S., Lee, S. F., Tabuchi, K., Hao, Y. H., Yu, C., LaPlant, Q., ... Yu, G. (2005). Nicastrin functions as a gamma-secretase-substrate receptor. *Cell*, *122*(3), 435-47.

Shang, Z. J., Ethunandan, M., Górecki, D. C., & Brennan, P. A. (2008). Aberrant expression of beta-dystroglycan may be due to processing by matrix metalloproteinases-2 and -9 in oral squamous cell carcinoma. *Oral Oncol*, *44*(12), 1139-46.

Shen, P. T., Hsu, J. L., & Chen, S. H. (2007). Dimethyl isotope-coded affinity selection for the analysis of free and blocked n-termini of proteins using LC-MS/MS. *Anal Chem*, *79*(24), 9520-30.

Shimojo, H., Kobayashi, M., Kamigaito, T., Shimojo, Y., Fukuda, M., & Nakayama, J. (2011). Reduced glycosylation of alpha-dystroglycans on carcinoma cells contributes to formation of highly infiltrative histological patterns in prostate cancer. *Prostate*, *71*(11), 1151-7.

Shumaker, D. K., Kuczmarski, E. R., & Goldman, R. D. (2003). The nucleoskeleton: lamins and actin are major players in essential nuclear functions. *Curr Opin Cell Biol*, *15*(3), 358-66.

Singh, J., Itahana, Y., Knight-Krajewski, S., Kanagawa, M., Campbell, K. P., Bissell, M. J., & Muschler, J. (2004). Proteolytic enzymes and altered glycosylation modulate dystroglycan function in carcinoma cells. *Cancer Res*, *64*(17), 6152-9.

Sirour, C., Hidalgo, M., Bello, V., Buisson, N., Darribère, T., & Moreau, N. (2011). Dystroglycan is involved in skin morphogenesis downstream of the Notch signaling pathway. *Mol Biol Cell*, *22*(16), 2957-69.

Smalheiser, N. R., & Kim, E. (1995). Purification of cranin, a laminin binding membrane protein. identity with dystroglycan and reassessment of its carbohydrate moieties. *J Biol Chem*, *270*(25), 15425-33.

Smalheiser, N. R., & Schwartz, N. B. (1987). Cranin: a laminin-binding protein of cell membranes. *Proc Natl Acad Sci U S A*, *84*(18), 6457-61.

Snyder, M., He, W., & Zhang, J. J. (2005). The DNA replication factor MCM5 is essential for Stat1-mediated transcriptional activation. *Proc Natl Acad Sci U S A*, *102*(41), 14539-44.

Sobel, R. E., & Sadar, M. D. (2005). Cell lines used in prostate cancer research: a compendium of old and new lines–part 1. *J Urol*, *173*(2), 342-59.

Sotgia, F., Bonuccelli, G., Bedford, M., Brancaccio, A., Mayer, U., Wilson, M. T., ... Lisanti, M. P. (2003). Localization of phospho-beta-dystroglycan (pY892) to an intracellular vesicular compartment in cultured cells and skeletal muscle fibers in vivo. *Biochemistry*, *42*(23), 7110-23.

Sotgia, F., Lee, H., Bedford, M. T., Petrucci, T., Sudol, M., & Lisanti, M. P. (2001). Tyrosine phosphorylation of beta-dystroglycan at its WW domain binding motif, PPxY, recruits SH2 domain containing proteins. *Biochemistry*, *40*(48), 14585-92.

Sotgia, F., Lee, J. K., Das, K., Bedford, M., Petrucci, T. C., Macioce, P., ... Lisanti, M. P. (2000). Caveolin-3 directly interacts with the C-terminal tail of beta -dystroglycan. identification of a central WW-like domain within caveolin family members [Journal Article]. *J Biol Chem*, *275*(48), 38048-58. Retrieved from `http://www.ncbi.nlm.nih.gov/pubmed/10988290` doi: 10.1074/jbc.M005321200

Spence, H. J., Chen, Y. J., Batchelor, C. L., Higginson, J. R., Suila, H., Carpen, O., & Winder, S. J. (2004). Ezrin-dependent regulation of the actin cytoskeleton by beta-dystroglycan. *Hum Mol Genet*, *13*(15), 1657-68.

Spence, H. J., Dhillon, A. S., James, M., & Winder, S. J. (2004). Dystroglycan, a scaffold for the ERK-MAP kinase cascade. *EMBO Rep*, *5*(5), 484-9.

Stalnaker, S. H., Aoki, K., Lim, J. M., Porterfield, M., Liu, M., Satz, J. S.,

... Wells, L. (2011). Glycomic analyses of mouse models of congenital muscular dystrophy. *J Biol Chem*, *286*(24), 21180-90.

Stalnaker, S. H., Hashmi, S., Lim, J. M., Aoki, K., Porterfield, M., Gutierrez-Sanchez, G., ... Wells, L. (2010). Site mapping and characterization of O-glycan structures on alpha-dystroglycan isolated from rabbit skeletal muscle. *J Biol Chem*, *285*(32), 24882-91.

Starr, D. A. (2011). KASH and SUN proteins. *Curr Biol*, *21*(11), R414-5.

Staub, O., Dho, S., Henry, P., Correa, J., Ishikawa, T., McGlade, J., & Rotin, D. (1996). WW domains of Nedd4 bind to the proline-rich PY motifs in the epithelial Na+ channel deleted in Liddle's syndrome. *EMBO J*, *15*(10), 2371-80.

Steiner, H., Fluhrer, R., & Haass, C. (2008). Intramembrane proteolysis by gamma-secretase. *J Biol Chem*, *283*(44), 29627-31.

Stewart, M. (2007). Molecular mechanism of the nuclear protein import cycle. *Nat Rev Mol Cell Biol*, *8*(3), 195-208.

Tadayoni, R., Rendon, A., Soria-Jasso, L. E., & Cisneros, B. (2012). Dystrophin Dp71: the smallest but multifunctional product of the Duchenne muscular dystrophy gene. *Mol Neurobiol*, *45*(1), 43-60.

Tanksley, J. P., Chen, X., & Coffey, R. J. (2013). NEDD4L is downregulated in colorectal cancer and inhibits canonical WNT signaling. *PLoS One*, *8*(11), e81514.

Tatin, F., Varon, C., Génot, E., & Moreau, V. (2006). A signalling cascade involving PKC, Src and Cdc42 regulates podosome assembly in cultured endothelial cells in response to phorbol ester. *J Cell Sci*, *119*(Pt 4), 769-81.

Thompson, O. (2007). *Role of dystroglycan in myoblast adhesion.* Thesis.

Thompson, O., Kleino, I., Crimaldi, L., Gimona, M., Saksela, K., & Winder, S. J. (2008). Dystroglycan, Tks5 and Src mediated assembly of podosomes in myoblasts. *PLoS One*, *3*(11), e3638.

Thompson, O., Moore, C. J., Hussain, S. A., Kleino, I., Peckham, M., Hohenester, E., ... Winder, S. J. (2010). Modulation of cell spreading and cell-substrate adhesion dynamics by dystroglycan. *J Cell Sci*, *123*(Pt 1), 118-27.

Towbin, H., Staehelin, T., & Gordon, J. (1979). Electrophoretic transfer of proteins from polyacrylamide gels to nitrocellulose sheets: procedure and some applications. *Proc Natl Acad Sci U S A*, *76*(9), 4350-4.

Trotman, L. C., Wang, X., Alimonti, A., Chen, Z., Teruya-Feldstein, J., Yang, H., ... Pandolfi, P. P. (2007). Ubiquitination regulates PTEN nuclear import and tumor suppression. *Cell*, *128*(1), 141-56.

Truica, C. I., Byers, S., & Gelmann, E. P. (2000). Beta-catenin affects androgen receptor transcriptional activity and ligand specificity. *Cancer Res*, *60*(17), 4709-13.

Turgay, Y., Champion, L., Balazs, C., Held, M., Toso, A., Gerlich, D. W., ... Kutay, U. (2014). SUN proteins facilitate the removal of membranes from chromatin during nuclear envelope breakdown. *J Cell Biol*, *204*(7), 1099-109.

Ueda, H., Gohdo, T., & Ohno, S. (1998). Beta-dystroglycan localization in the photoreceptor and Müller cells in the rat retina revealed by immunoelectron microscopy. *J Histochem Cytochem*, *46*(2), 185-91.

Umbas, R., Schalken, J. A., Aalders, T. W., Carter, B. S., Karthaus, H. F., Schaafsma, H. E., ... Isaacs, W. B. (1992). Expression of the cellular adhesion molecule E-cadherin is reduced or absent in high-grade prostate cancer. *Cancer Res*, *52*(18), 5104-9.

Vellai, T., & Takács-Vellai, K. (2010). Regulation of protein turnover by longevity pathways. *Adv Exp Med Biol*, *694*, 69-80.

Villarreal-Silva, M., Centeno-Cruz, F., Suárez-Sánchez, R., Garrido, E., & Cisneros, B. (2011). Knockdown of dystrophin Dp71 impairs PC12 cells cycle: localization in the spindle and cytokinesis structures implies a role for Dp71 in cell division. *PLoS One*, *6*(8), e23504.

Villarreal-Silva, M., Suárez-Sánchez, R., Rodríguez-Muñoz, R., Mornet, D., & Cisneros, B. (2010). Dystrophin Dp71 is critical for stability of the DAPs in the nucleus of PC12 cells. *Neurochem Res*, *35*(3), 366-73.

Visa, N., & Percipalle, P. (2010). Nuclear functions of actin. *Cold Spring Harb Perspect Biol*, *2*(4), a000620.

von Mikecz, A. (2006). The nuclear ubiquitin-proteasome system. *J Cell Sci*, *119*(10), 1977-84.

Vásquez-Limeta, A., Wagstaff, K. M., Ortega, A., Crouch, D. H., Jans, D. A., & Cisneros, B. (2014). Nuclear import of β-dystroglycan is facilitated by ezrin-mediated cytoskeleton reorganization. *PLoS One*, *9*(3), e90629.

Wagner, S. A., Beli, P., Weinert, B. T., Schölz, C., Kelstrup, C. D., Young, C., ... Choudhary, C. (2012). Proteomic analyses reveal divergent ubiquitylation site patterns in murine tissues. *Mol Cell Proteomics*, *11*(12), 1578-85.

Wakabayashi, T., & De Strooper, B. (2008). Presenilins: members of the gamma-secretase quartets, but part-time soloists too. *Physiology (Bethesda)*, *23*, 194-204.

Wang, W., Shi, Z., Jiao, S., Chen, C., Wang, H., Liu, G., ... Zhou, Z. (2012). Structural insights into SUN-KASH complexes across the nuclear envelope. *Cell Res*, *22*(10), 1440-52.

Wei, Y., Renard, C. A., Labalette, C., Wu, Y., Lévy, L., Neuveut, C., ... Buendia, M. A. (2003). Identification of the LIM protein FHL2 as a coactivator of beta-catenin. *J Biol Chem*, *278*(7), 5188-94.

Wente, S. R., & Rout, M. P. (2010). The nuclear pore complex and nuclear transport. *Cold Spring Harb Perspect Biol*, *2*(10), a000562.

White, S. R., Wojcik, K. R., Gruenert, D., Sun, S., & Dorscheid, D. R. (2001). Airway epithelial cell wound repair mediated by alpha-dystroglycan. *Am J Respir Cell Mol Biol*, *24*(2), 179-86.

Whitmore, C., & Morgan, J. (2014). What do mouse models of muscular dystrophy tell us about the DAPC and its components? *Int J Exp Pathol*, *95*(6), 365-77.

Williamson, R. A., Henry, M. D., Daniels, K. J., Hrstka, R. F., Lee, J. C., Sunada, Y., ... Campbell, K. P. (1997). Dystroglycan is essential

for early embryonic development: disruption of Reichert's membrane in Dag1-null mice. *Hum Mol Genet*, *6*(6), 831-41.

Wilson, K. L., & Berk, J. M. (2010). The nuclear envelope at a glance. *J Cell Sci*, *123*(12), 1973-8.

Wilson, M. D., Saponaro, M., Leidl, M. A., & Svejstrup, J. Q. (2012). MultiDsk: a ubiquitin-specific affinity resin. *PLoS One*, *7*(10), e46398.

Winder, S. J. (2001). The complexities of dystroglycan. *Trends Biochem Sci*, *26*(2), 118-24.

Winder, S. J., Lipscomb, L., Angela Parkin, C., & Juusola, M. (2011). The proteasomal inhibitor MG132 prevents muscular dystrophy in zebrafish. *PLoS Curr*, *3*, RRN1286.

Wolfe, M. S., & Kopan, R. (2004). Intramembrane proteolysis: theme and variations. *Science*, *305*(5687), 1119-23.

Wong, R. W., & Blobel, G. (2008). Cohesin subunit SMC1 associates with mitotic microtubules at the spindle pole. *Proc Natl Acad Sci U S A*, *105*(40), 15441-5.

Yamada, H., Saito, F., Fukuta-Ohi, H., Zhong, D., Hase, A., Arai, K., ... Matsumura, K. (2001). Processing of beta-dystroglycan by matrix metalloproteinase disrupts the link between the extracellular matrix and cell membrane via the dystroglycan complex. *Hum Mol Genet*, *10*(15), 1563-9.

Yang, B., Jung, D., Motto, D., Meyer, J., Koretzky, G., & Campbell, K. P. (1995). SH3 domain-mediated interaction of dystroglycan and Grb2. *J Biol Chem*, *270*(20), 11711-4.

Yatsenko, A. S., Kucherenko, M. M., Pantoja, M., Fischer, K. A., Madeoy, J., Deng, W. M., ... Ruohola-Baker, H. (2009). The conserved WW-domain binding sites in Dystroglycan C-terminus are essential but partially redundant for Dystroglycan function. *BMC Dev Biol*, *9*, 18.

Yilmaz, M., Christofori, G., & Lehembre, F. (2007). Distinct mechanisms of tumor invasion and metastasis. *Trends Mol Med*, *13*(12), 535-41.

Yin, G. N., Lee, H. W., Cho, J. Y., & Suk, K. (2009). Neuronal pentraxin receptor in cerebrospinal fluid as a potential biomarker for neurodegenerative diseases. *Brain Res*, *1265*, 158-70.

Yurchenco, P. D. (2011). Basement membranes: cell scaffoldings and signaling platforms. *Cold Spring Harb Perspect Biol*, *3*(2).

Zachara, N. E., O'Donnell, N., Cheung, W. D., Mercer, J. J., Marth, J. D., & Hart, G. W. (2004). Dynamic O-GlcNac modification of nucleocytoplasmic proteins in response to stress. A survival response of mammalian cells. *J Biol Chem*, *279*(29), 30133-42.

Zhong, D., Saito, F., Saito, Y., Nakamura, A., Shimizu, T., & Matsumura, K. (2006). Characterization of the protease activity that cleaves the extracellular domain of beta-dystroglycan. *Biochem Biophys Res Commun*, *345*(2), 867-71.

Zimber, A., Nguyen, Q. D., & Gespach, C. (2004). Nuclear bodies and compartments: functional roles and cellular signalling in health and disease. *Cell Signal*, *16*(10), 1085-104.

Zimowska, M., Swierczynska, M., & Ciemerych, M. A. (2013). Nuclear MMP-9 role in the regulation of rat skeletal myoblasts proliferation. *Biol Cell*, *105*(8), 334-44.